

TALLINN UNIVERSITY OF TECHNOLOGY
DOCTORAL THESIS
36/2020

Quantification of the Reaction of Estonian Beaches to Changing Wave Loads

MARIS EELSALU



TALLINN UNIVERSITY OF TECHNOLOGY

School of Science

Department of Cybernetics

Laboratory of Wave Engineering

This dissertation was accepted for the defence of the degree 27/08/2020

Supervisor:

Prof. Dr. Tarmo Soomere
Department of Cybernetics, School of Science
Tallinn University of Technology
Tallinn, Estonia

Co-supervisor:

Prof. Dr. Artu Ellmann
Department of Engineering and Architecture
School of Engineering
Tallinn University of Technology
Tallinn, Estonia

Opponents:

Prof. Dr. Gerd Masselink
School of Biological and Marine Sciences
Faculty of Science and Engineering
University of Plymouth
Plymouth, United Kingdom

Dr. Luigi Cavaleri
Institute of Marine Sciences (ISMAR-CNR)
Venice, Italy

Defence of the thesis: 05/10/2020, Tallinn

Declaration:

Hereby I declare that this doctoral thesis, my original investigation and achievement, submitted for the doctoral degree at Tallinn University of Technology has not been submitted for doctoral or equivalent academic degree.

Maris Eelsalu

signature



European Union
European Regional
Development Fund



Investing
in your future

Copyright: Maris Eelsalu, 2020

ISSN 2585-6898 (publication)

ISBN 978-9949-83-595-9 (publication)

ISSN 2585-6901 (PDF)

ISBN 978-9949-83-596-6 (PDF)

Printed by Auratrükk

TALLINNA TEHNIKAÜLIKOOL
DOKTORITÖÖ
36/2020

Eesti rannikute reaktsioon muutuvatele lainekoormustele

MARIS EELSALU



Contents

List of publications constituting the thesis.....	6
Author's contribution to the publications	7
Introduction.....	8
Baltic Sea shores	8
Variability in the wave energy flux	11
Extreme water levels in the Baltic Sea.....	12
Quantification of beach evolution	13
The objectives and outline of the thesis.....	14
Approbation of the results	16
1. Wave energy flux in the eastern Baltic Sea	18
1.1. Wave properties in the Baltic Sea	18
1.2. Study area and the converter line.....	21
1.3. Total wave energy resource in the study area	22
1.4. Hot-spots of wave energy	25
1.5. Temporal variability in the wave energy flux	26
1.6. Properties and timing of the wave energy resource	28
2. Extreme water levels in the eastern Baltic Sea	31
2.1. Hindcast and observed water levels	31
2.2. Outliers of water level and the extreme water level distribution.....	33
2.3. Block maxima method.....	34
2.4. Extreme water level projections and local effects	36
2.5. Separation of short-term and long-term variations.....	38
2.6. Spatial variations in the risk of storm surge	40
3. Quantification of beach evolution.....	42
3.1. Study area	42
3.2. Combining airborne and terrestrial laser scanning technologies.....	43
3.3. Subaerial volume changes.....	45
3.4. Underwater changes	46
3.5. Changes in underwater part of the beach profile	47
Conclusions.....	49
Summary of the results	49
Main conclusions proposed to defend	51
Recommendations for further work.....	52
List of figures	53
References.....	55
Acknowledgements	66
Abstract	67
Lühikokkuvõte	68
Appendix: Papers constituting the thesis.....	69
Curriculum Vitae	148
Elulookirjeldus	153

List of publications constituting the thesis

The thesis is based on six academic publications which are referred to in the text as Paper I, Paper II, Paper III, Paper IV, Paper V and Paper VI. All papers are indexed by the ISI Web of Science.

- Paper I Soomere T., **Eelsalu M.** 2014. On the wave energy potential along the eastern Baltic Sea coast. *Renewable Energy*, 71, 221–233, doi: 10.1016/j.renene.2014.05.025.
- Paper II Kovaleva O., **Eelsalu M.**, Soomere T. 2017. Hot-spots of large wave energy resources in relatively sheltered sections of the Baltic Sea coast. *Renewable and Sustainable Energy Reviews*, 74, 424–437, doi: 10.1016/j.rser.2017.02.033.
- Paper III **Eelsalu M.**, Soomere T., Pindsoo K., Lagemaa P. 2013. Ensemble approach for projections of return periods of extreme water levels in Estonian waters. *Continental Shelf Research*, 91, 201–210, doi: 10.1016/j.csr.2014.09.012.
- Paper IV Soomere T., **Eelsalu M.**, Kurkin A., Rybin A. 2015. Separation of the Baltic Sea water level into daily and multi-weekly components. *Continental Shelf Research*, 103, 23–32, doi: 10.1016/j.csr.2015.04.018.
- Paper V Julge K., **Eelsalu M.**, Grünthal E., Talvik S., Ellmann A., Soomere T., Tõnisson H. 2014. Combining airborne and terrestrial laser scanning to monitor coastal processes. 2014 IEEE/OES Baltic International Symposium “Measuring and Modeling of Multi-Scale Interactions in the Marine Environment”, May 26–29, 2014, Tallinn, Estonia. IEEE Conference Proceedings, 10 pp., doi: 10.1109/BALTIC.2014.6887874.
- Paper VI **Eelsalu M.**, Soomere T., Julge K. 2015. Quantification of changes in the beach volume by the application of an inverse of the Bruun Rule and laser scanning technology. *Proceedings of the Estonian Academy of Sciences*, 64(3), 240–248, doi: 10.3176/proc.2015.3.06.

Author's contribution to the publications

Contribution to the papers in this thesis are:

- | | |
|-----------|--|
| Paper I | Contribution to the study plan. Calculations of the wave energy flux. Preparation of the figures and maps. Drafting single parts. |
| Paper II | Contribution to the calculations of the wave energy flux. Analysis and interpretation of the results. Preparation of the figures. Drafting the manuscript and writing single sections. |
| Paper III | Data collection. Data analysis. Drafting single parts of the manuscript. |
| Paper IV | Analyses of the data and preparation of the figures. |
| Paper V | Contribution to repeated field work for data collection. Pre-processing the measured data. Preparation of the figures. Writing the manuscript. |
| Paper VI | Contribution to field work. Pre-processing the data. Preparation of figures. Writing the manuscript. |

Introduction

The coastal zone has been attractive for humans throughout the history due to the dynamically active interaction of the land and the seas and oceans. These regions provide diverse ecosystem services, abundant resources, amenity, and are also of aesthetic value. Consequently, the coastal zones have become heavily populated. They host about 40% of the global population and serve as a location of key infrastructure (Cohen et al., 1997; Adger, 2005; Mentaschi et al., 2018). The gradual increase in human population at the coast creates pressure on the entire nearshore environment. To mitigate this pressure, effective management of the resources and ensuring a sustainable coastal environment is becoming a major challenge.

During the last decades, the general health of the coasts has gradually degraded. This process can to some extent be exemplified by the rate of erosion of sedimentary shores. Sandy beaches are extremely valuable natural resources providing a first line protection against coastal storms by absorbing wind and wave energy (Mentaschi et al., 2018). Approximately 70% of the world's sandy coastline is suffering from degradation (Bird, 2008; Luijendijk et al., 2018).

Climate change is one of the main accelerators of coastal change. The resulting increase in the marine-driven impact on sedimentary coasts will exacerbate the current situation (Nicholls et al., 2007; Ranasinghe, 2016). The changes on the coast are accelerated through global sea-level rise (Cooper and Pilkey, 2004; Chini and Stansby, 2012; Vousdoukas et al., 2020) and through changes in the wave climate and properties of single storms. Changes in the wave approach directions and the increasing presence of more energetic storms may initiate substantial modifications of alongshore sediment transport. These processes have great influence on most of the world's coastlines, in particular, in low-lying areas through frequent inundation and increased erosion during high water events (Ranasinghe, 2016). In the Baltic Sea conditions, such changes may lead to rapid degradation of major landforms such as the Curonian Spit (Viška and Soomere, 2012). In this context, understanding of the functioning of sedimentary beaches and quantification of their long-term evolution become increasingly important in order to manage coastal resources in a sustainable way, and to ensure effective coastal spatial planning and development.

Morphodynamic changes in the coastal environment occur at a wide range of time scales, from short-term changes in a single storm to long-term modifications driven by hydrometeorological conditions over years and decades. Factors such as sediment availability, wave climate, tidal range, storm surges, course of the water level, interaction between nearshore and onshore sedimentary bodies and geological setting of the coastal area, that have significant influence on the evolution of the beaches, vary remarkably at different temporal and spatial scales (Masselink et al., 2011). This variability severely complicates the attempts to quantify the evolution of beaches and gives rise to similar variability of the processes that affect coastal areas and affects the frequency at which coastal changes occur (Kraus et al., 1991; Alexandrakakis and Poulos, 2015).

Baltic Sea shores

The evolution of the beaches in the Baltic Sea is mainly forced by the same factors that drive the beaches on open ocean coasts (Soomere et al., 2017b). The core hydrodynamic drivers include wave impact, water level and nearshore currents. Their influence is modulated by aeolian transport and the presence or absence of sea ice. However, there

are some essential differences in the processes at the shores of this water body in terms of beach evolution. A specific feature of the Baltic Sea is that the amplitude of tides in its interior is very small. It is usually just a few centimetres (Leppäranta and Myrberg, 2009) and reaches up to 25 cm in a few locations in the eastern Gulf of Finland (Medvedev et al., 2016). The development of the Baltic Sea shores is thus mainly controlled by (i) long-term changes in the sea level¹ owing to postglacial uplift, (ii) global sea level rise, (iii) the relatively small seasonal course of the sea level (Hünicke and Zorita, 2008), (iv) much stronger aperiodic variations in the water volume of the entire sea on weekly scales (Lehmann and Post, 2015), and (v) local surges and wave set-up during single storms (Johansson et al., 2001; Suursaar and Sooäär, 2007).

Waves play an important role in shaping the beaches in this microtidal sea. As the Baltic Sea is relatively small, the wave fields are fetch-limited, strong swells are infrequent, and wave properties mainly reflect the local wind climate. Therefore, wave conditions are highly variable. The wave regime in this water body is characterized by relatively infrequent and short high-energy events forced by strong winds on the background of much longer comparatively calm periods (during weak winds or calm times).

The intermittent wave climate in the Baltic Sea gives rise to step-like evolution of the beaches (Soomere and Healy, 2011). Most of wave energy brought to the coast by wind waves is supplied by relatively short and steep wind-seas. Such events are usually responsible for the biggest changes at the coast. The waves during such events are exclusively generated in the Baltic Sea. The typical fetch is 200–300 km with the maximum fetch being about 800 km. The waves generally have relatively short periods (3–6 s, Broman et al., 2006). This means that the Baltic Sea waves are less affected by refraction than long-period open ocean waves and may often approach the shoreline at relatively large angles. Such waves induce more intense alongshore sediment transport than waves of similar height that approach the shore almost shore normal, and thus may be responsible for significant foreshore retreat (Jackson et al., 2002; Ryabchuk et al., 2012).

The conditions which govern the evolution of the Baltic Sea beaches vary substantially depending on the nature of the seabed (bedrock or sediment), sediment availability, location of the beach, and particularly the exposure of the beach to predominant wind directions (Orviku, 2005). The most frequent wind direction in the main basin of the Baltic Sea (Baltic proper) is from the south-west (SW) but occasionally winds from the north-north-west (NNW) may be very strong (Soomere, 2001). The coast of the northern part of Baltic Sea from south-eastern Sweden to the north-eastern Gulf of Finland is dominated by bedrock formations and has only short segments with substantial amounts of fine sediment (Harff and Meyer, 2011; Orviku, 2018). The rocky shores are steady with respect to hydrodynamic driving forces and the coastline changes follow the spatial pattern of relative water level changes.

The southern and eastern margins of the Baltic Sea from the southern tip of Sweden to the Baltic States mainly accommodate sedimentary coasts. A significant part of these coasts is suffering from chronic erosion (Eberhards 2003; Eberhards et al., 2009; Kelpšaitė et al., 2011; Pranzini and Williams, 2013; Soomere and Viška, 2014). This process is enhanced by climatically controlled sea-level rise (Harff and Meyer, 2011) and

¹ I use the notion “sea level” to denote offshore sea level that is formed by global or basin-wide processes and “water level” to denote the height of water surface at the shore.

gradual subsidence in the southern part of this domain. Their joint impact is currently causing an increase in the relative sea-level in the southern Baltic Sea (Dailidienė et al., 2006; Vestøl et al., 2019). The affected shores are sensitive to adverse changes in the hydrodynamic loads. Some beaches of this region may be heavily damaged in certain storms (Zaromskis and Gulbinskas, 2010).

The most significant erosion events occur if long-lasting winds directed towards the coast drive high waves and extensive storm surge during ice-free times (Orviku et al., 2003). During such events waves may reach unprotected sediment on upper sections of the coastal profile. Recent studies of coastal processes in the eastern Baltic Sea have revealed several extreme erosion events. Some segments of the eastern coast of the Gulf of Finland have shown migration (both regression and progression) rates from 2 m/yr to 5 m/yr (Ryabchuk et al., 2011; Sergeev et al., 2018). During the last 60 years significant shoreline retreat, about 50–60 m, has occurred along several sections of the coast of Latvia (Eberhards et al., 2009). An increase in the intensity of coastal processes has been observed in Estonia during the last 20–30 years in spite of isostatic and neotectonic uplift (Orviku et al., 2003). Until today land uplift compensates global sea level rise on most Estonian beaches (Rosentau et al., 2007). Further sea level increase will eventually override the current postglacial uplift for all Estonian coasts and the risk posed by erosion will increase (cf. Johansson et al., 2014).

Climate change projections signal that the relative sea level rise in the eastern Baltic Sea will be at least 60 cm by the end of the century (Grinsted, 2015; Pellikka et al., 2018). The frequency and intensity of storms is expected to increase in many parts of the world (IPCC, 2013). The changes may have different patterns in different locations. The storminess and overall wind speed have not systematically increased during the last century in the Baltic Sea region (Hünicke et al., 2015). However, weather patterns that drive elevated water levels of the entire sea or the Gulf of Riga have become more persistent (Soomere and Pindsoo, 2016; Männikus et al., 2019), and the directional structure of strong winds that cause storm surges or high wave set-up (in the Gulf of Finland, Pindsoo and Soomere, 2015) has experienced certain changes.

These changes have led to a substantial increase in the extreme water levels in the eastern Baltic Sea (Pindsoo and Soomere, 2020). It is thus likely that many coastal areas will suffer from flooding and a higher rate of coastal erosion in the future. It is therefore essential to describe in more detail the properties and potential impact of various drivers responsible for shaping the coasts in the Baltic Sea and to better understand how the shore reacts to the joint impact of these drivers. This knowledge is essential for determining mitigation measures of existing and future marine-driven impacts and for the sustainable management of the coastal zone.

The focus of this thesis is on understanding the long-term evolution of the beaches in the eastern part of the Baltic Sea from the viewpoint of wave impact. This part of the coast is exposed to two predominant wind directions from SW and NNW and has beaches comprised of fine sediment. These features define it as one of the most vulnerable sections with respect to possible changes of extreme hydrodynamics events in the Baltic Sea. An adequate understanding and forecast of the evolution of sandy shores requires first of all extensive knowledge of the main drivers of processes affecting coastal systems.

Variability in the wave energy flux

Wind waves are the predominant source of energy along most sea and ocean. This energy source is ultimately the driving force behind most morphological changes at the coast (Masselink et al., 2011). The distribution of wave energy along the coastline largely controls many aspects of coastal dynamics, such as the spatial variability of the intensity of coastal processes, the nature and width of the equilibrium beach profile, and intensity of alongshore sediment transport (Dean and Dalrymple, 2002). To a first approximation, the sediment volume transported along the coast is usually assumed to be roughly proportional to the amount of wave energy flux that reaches the nearshore (USACE, 2002). Even though the actual patterns of transport depend on many other features and may be highly variable (Roelvink and Reniers, 2011), estimates of the magnitude of wave energy flux that arrives the shore give a first insight into the intensity of coastal processes at the site of interest.

Several studies have attempted to link the distribution of wave energy flux with the spatial variability of erosion (Benumof et al., 2000; Murray and Ashton, 2013; Jones et al., 2018). The vulnerability of a single coastal section with respect to erosion depends additionally to the wave climate and geological composition of the shore on the orientation and location (exposedness) of the coastline. The segments that are widely open towards the predominant wave directions are usually more exposed to incoming waves and greater energies (Carter et al., 1990; Limber et al., 2014). The properties of waves that arrive at the coast also define the evolution cycle of the beach.

The classic cut-and-fill concept (e.g., Brenninkmeyer, 1982) assumes that most energetic steep waves induce beach erosion and transport of sediment to the deeper part of the shore whereas sandbar formation, transport of sediment onshore and accretion of the same beach appears during calmer (constructive swell) wave conditions with less energy and longer wave periods. Changes on the beach thus primarily follow the incident wave energy level (Masselink and Pattiaratchi, 2001). This cycle is much less significant in the Baltic Sea where the wave regime is highly intermittent (~30% of the annual energy flux arrives during the 3–4 most stormy days; Paper I) and contains very small proportion of low intensity constructive long swell waves (Broman et al., 2006; Soomere et al., 2012). In such conditions, as in other relatively small semi-enclosed seas, alongshore, rather than on/offshore, sediment transport prevails and the classic cut-and-fill cycle of beach change is modulated by alongshore movement of sediment. As waves often arrive at the shores of the Baltic Sea under a relatively large angle, alongshore transport plays a much larger role in the semi-enclosed Baltic Sea than on open ocean beaches. As a consequence, natural beach recovery is often slow or missing.

The first task in the understanding of the functioning of the Baltic Sea beaches is thus the quantification of the wave energy flux towards different coastal sections. This task is even more important in terms of mitigation of climate change by exploiting renewable energy sources. Ocean waves serve as one of the largest untapped and very attractive renewable energy resources. Wave energy stems ultimately from solar power, is relatively well predictable and presents an opportunity to generate significant quantities of grid power. Wave energy harvesting is associated with low levels of pollution and CO₂ release, and side effects like shifting of ship navigation routes (Jacobson, 2009) are minor.

Several properties of the Baltic Sea wave climate, first of all large variation of the wave energy flux in time, are not favourable for the use of wave energy resources for grid energy production (Paper I). Solutions that involve wave energy harvesting may still

provide suitable protection against climate change induced erosion and provide an option for reducing wave loads to heavily populated coastal zones. Vulnerable locations can be protected against high waves by suitably located wave energy converters (WEC). WECs extract part of energy from the approaching wave fields and thus reduce (significant) wave height and weaken erosion accordingly (Abanades et al., 2015, 2018). Such converters can be easily adapted to changing water levels (Abanades et al., 2014).

Extreme water levels in the Baltic Sea

Low-lying coastal areas are particularly vulnerable to flooding and erosion. The main drivers of these processes are elevated water level and high waves. As mentioned above, the most extensive erosion events occur when large waves attack unprotected sediment higher on the shore during strong storm events that have created excessive surge (Kirshen et al., 2008). The projected sea-level rise together with possibly increasing storm frequency in Estonia (Orviku et al., 2003) and decreasing periods of winter ice and snow cover (Jaagus, 2006; Rimkus et al., 2018) in the Baltic Sea region will probably increase the extent of flooding and erosion during the twenty-first century. The combinations of these drivers have a different nature in different parts of the Baltic Sea. Along the Swedish coast high waves usually occur during low water levels (Hanson and Larson, 2008) while in the eastern part of the basin high waves most often coincide with elevated water levels (Pindsoo and Soomere, 2015).

Ideally, the joint probability of simultaneous occurrence of extreme water levels and high waves would provide adequate input in assessing these risks. This technique has been widely studied for different coastal areas (see Hanson and Larson, 2008; Hawkes, 2008; Mazas and Hamm, 2017 and references therein). In the Baltic Sea, this approach is infrequently applied because of specific features of the generation of extreme water levels.

Elevated water levels responsible for coastal flooding are usually created by the joint impact of multitude drivers. The inverted barometric effect and wind-driven surge (together called storm surge; Dean and Dalrymple, 2002) together with high, periodic, astronomic tides are usually responsible for extreme still water levels on the shores of the open ocean. In contrast, the microtidal Baltic Sea, having almost no tides, experiences substantial aperiodic water level variations (Leppäranta and Myrberg, 2009). The water volume of the entire Baltic Sea can change extensively. Persistent westerly winds can block the outflow of surface water through the narrow Danish straits and strong winds may push water into this sea. Specific sequences of storm cyclones may increase the water level by up to 1 m in the entire basin over a few weeks (Franck and Matthäus, 1992; Post and Kõuts, 2014; Lehmann and Post, 2015). Very high overall sea level (60–80 cm higher than the long-term mean) can persist for several weeks (Leppäranta and Myrberg, 2009) or even several months (Soomere and Pindsoo, 2016). Extremely dangerous water levels in single coastal segments are often driven by the contribution of local storm surge to the already high basin-scale sea level.

Wave induced set-up may remarkably contribute to the local water level at the waterline (Dean and Bender, 2006). The resulting increase in the water level is sensitive to the approach angle of the waves. Waves that arrive to the coast almost perpendicularly to the shoreline have the strongest impact (Soomere and Pindsoo, 2015).

As the coastline of the Baltic Sea is irregular, some sections are much more vulnerable to storm surges. The highest local water levels are usually present in relatively shallow bayheads. The highest maximum water level has exceeded 4 m in the eastern end of the

Gulf of Finland and has reached close to 3 m in the Gulf of Riga at Pärnu and near Riga (Averkiev and Klevanny, 2010).

Better understanding of the formation and properties of extreme water levels is thus essential in the context of the evolution of the beaches in the eastern Baltic Sea. Progress in this direction makes it possible to more adequately quantify the destructive force of waves higher on the shore. Moreover, high waves may contribute significantly to the increase in the total water level. The effect of set-up extends the reach of high waves and may lead to flooding and erosion farther inland. This information identifying sensitive areas under different conditions is extremely valuable for coastal planning and management, and for local governments.

The predictions of the high water level in the Baltic Sea have to take into account that dangerous water levels are formed by the joint impact of differently generated components. Additional complexity is added due to the irregular coastline along the eastern part of the Baltic Sea. In this thesis, I shed light onto these problems using an ensemble approach for long-term projections of extreme water levels and their return periods (Paper III) and make an attempt to separate components responsible for extreme water levels (Paper IV).

Quantification of beach evolution

Changes in coastal systems are apparently currently accelerating (Wright and Nichols, 2018) even though some evidence and interpretations are controversial (Vousdoukas et al., 2020). Sandy beaches with limited sediment volume are particularly vulnerable to modifications by human activities like sand mining, construction of coastal protection structures, or tourism. Climate change and human stressors at the coast are adding a new dimension to these modifications, altering erosion rates, sediment transport patterns and the general cycle of the beach (Torres et al., 2017; McLachlan and Defeo, 2018; Rangel-Buitrago et al., 2015, 2018).

Hard coastal protection structures may be constructed to control erosion at specific sites. Many such structures have been built with little or no understanding of their impact on neighbouring areas (Rangel-Buitrago et al., 2015, 2018). Such structures can have negative impact and some of them may cause more extensive erosion (Rodríguez-Ramírez et al., 2008; 2018; Flor-Blanco et al., 2015). More generally, inadequate knowledge of the functioning of beaches combined with limited data coverage, spatially or temporally, often leads to poor coastal management practice.

Climate change is often associated with increasing pressure on the coastal area via sea level rise and changing patterns of storminess. These changes may increase the amount of sediment eroded from the beaches during sequences of strong storms (Dodet et al., 2019) and substantially increase the duration of the recovery phase of the beaches. This shift in the ratio of beach erosion and recovery may destroy the present quasi-equilibrium cycle of sediment at many shores and may eventually lead to the complete removal of sediment from beaches (Alexandrakis and Poulos, 2015; Wright and Nichols, 2018; Vousdoukas et al., 2020).

Predictions of beach evolution are core inputs for sustainable coastal management on the background of changing climate and the increasing intensity of human activities in coastal areas (Short and Jackson, 2013). Although there are many models available for this purpose (Roelvink and Reniers, 2011), data-driven understanding of beach evolution and beach cycles remains lacking.

Individual short but strong storms generally result in a dramatic reaction of the coast. Their impact on the coast is relatively easy to define. It becomes evident as shoreline erosion, flattening of dunes, and sometimes damage to coastal vegetation. Rapid changes to the coast are usually followed by short-term accretion. This cycle often leads to negligible net change over time scale of few weeks, months (Wright and Nichols, 2018). Often on Baltic Sea beaches, however, the sediment deficit persists for a long period of time due to the dominance of alongshore sediment transport. It is often accompanied by anthropogenically driven reduction of fluvial sediment supply to the coast (Orviku, 2018) that may enhance chronic erosion (Ranasinghe et al., 2019). Identifying long-term variations in the sediment budget during such longer periods of slow evolution under sediment deficit is thus essential for quantifying the development and stability of coastal systems.

Quantification of long-term beach evolution is often a complicated task. Long-term data sets usually have a poor temporal resolution. Historically, the acquisition of shoreline and cross-shore profile data has been a laborious and expensive task. The existing long-term data sets generally rely on a single proxy of the beach volume. Such proxies may include the shoreline location, relocation of the dune toe or single elevation contours, or single or very few cross-section profiles for larger beach areas. They are usually interpreted as being representative of certain sections of the beach.

The situation is particularly complicated in the Baltic Sea where many small local sources contribute to the sediment budget and the changes to the coast are highly intermittent. The quantification of the resulting volume changes over the subaerial beach requires high-resolution measurement techniques.

The use of remotely gathered data (e.g., by satellites for the estimations of the shoreline changes) has become the most feasible solution of this problem (Luijendijk et al., 2018). Comparison of the shoreline position in different years is a great tool for identifying the eroding areas and to determine the speed and scale of retreat. Large-scale data from satellites provides adequate results for wide and mostly homogenous sandy beaches where the rate of the changes is comparable or larger than the image pixels (Hagenaars et al., 2018; Vos et al., 2019a, 2019b). This technique is not always applicable for beaches of the eastern Baltic Sea that often have a small volume of sand and are relatively narrow (Orviku, 2003; Harff et al., 2017).

Medium-range remote sensing technologies like terrestrial laser scanning (TLS) and airborne laser scanning (ALS) provide a reasonable alternative. If applied together, they make it possible to quantify beach evolution in relatively large coastal areas with complicated geometry and highly intermittent wave regime. In this thesis I address the possibilities of a combination of results of terrestrial and airborne laser scanning with the concept of the equilibrium beach profile (EBP) to quantify the changes in the total sand volume of a typical almost equilibrium beach in Tallinn Bay, Estonia (Papers V–VI).

The objectives and outline of the thesis

The coast of the eastern Baltic Sea suffers from the deficit of fine sediment and is exposed to the predominant wind and wave directions. These features define this region as the most sensitive in the Baltic Sea to extreme hydrodynamic events and prone to possible large-scale erosion in the future. Many coastal sections of this part of the Baltic Sea have been studied in detail from this viewpoint. Studies into wave-driven sediment transport patterns (Soomere et al., 2011; Soomere and Viška, 2014) and scenarios reflecting the vulnerability of the coastal systems in terms of possible structural changes in response

to changes in the wind fields (Viška and Soomere, 2012) have made clear how fragile the entire system is. Studies that focus on single coastal sections provide valuable information about the rate and intensity of coastal processes at particular sites (Tõnisson et al., 2014; Orviku, 2018, among others). Still, there is no systematic understanding of the properties of core drivers of the evolution of beaches in the eastern part of the Baltic Sea from the viewpoint of wave impact and water levels.

This thesis is targeted at the analysis of the properties of the main drivers responsible for the biggest changes on the coast and their impact on the evolution of the beaches in the eastern Baltic Sea. This task includes the need to quantify the long-term evolution of sandy beaches. The main objectives of this thesis are to:

- quantify the approaching wave energy flux to the coast and its spatial and -temporal variability in the eastern Baltic Sea;
- adequately estimate the properties of high water level events and their return periods in different coastline segments;
- identify the components of extreme water levels and their specific drivers;
- combine high-resolution beach measurements with the theory of sandy beaches to reach a better quantification of long-term beach evolution.

To fulfil these objectives, Chapter I addresses wave energy flux (wave power) in the eastern Baltic Sea. The properties of wave energy that arrives at the coast help understand the intensity and course of coastal processes in the study area. For the analysis I employ long-term time series of nearshore wave properties calculated by Dr. A. Räämet using the WAM model driven by adjusted geostrophic winds for 1970–2007. The results, first of all, highlight extensive temporal and spatial variability of the instantaneous wave energy flux in the study area and make it possible to provide basic estimates of the spatial and temporal distribution and the overall usability of the wave energy resource in the eastern Baltic Sea.

Chapter II focuses on the course of water levels in the Baltic Sea. It aims at clarifying in which occasions and/or locations high water levels may significantly contribute to rapid changes in the coastal zone. The analysis and projections of extreme water levels in the eastern Baltic Sea is a complicated task because such events are jointly driven by several mechanisms. Moreover, different coastal regions may need different statistical models to properly replicate extreme events (Soomere et al., 2018). Chapter II builds an ensemble of projections for extreme water levels and their return periods. The analysis employs offshore sea level time series numerically reconstructed using the RCO (Rossby Center, Swedish Meteorological and Hydrological Institute) ocean model for 1961–2005 and observed water levels from four tide gauges. A cluster of projections of extreme water level is constructed using different extreme value distributions and methods for evaluation of their parameters. The feasibility of the ensemble approach in different locations of the coastline of Estonia is discussed based on Paper III. Another look into this problem is provided by means of a separation of nearshore water level time series into components with different time scales. While storm surges develop and relax at a daily scale, the water volume of the entire Baltic Sea varies at a weekly or even longer time scale (Johansson and Kahma, 2016). A separation of components of water level on these time scales is possible using different filtering techniques (Paper IV). The two components obey different statistical distributions.

Chapter III explores the potential of a laser scanning technique to quantify detailed changes in the sand volume of beaches during their slow phase of evolution. The terrestrial laser scanning technique is combined with airborne laser scanning to

minimize inconsistencies in the vertical accuracy between different data sets (Paper V). The changes to the underwater beach volume are approximately estimated by the application of an inverse Bruun Rule and the concept of the equilibrium beach profile. The aim is to deliver a feasible solution how to evaluate the long-term changes in sand volume in semi-sheltered sea areas (Paper VI).

Approbation of the results

The basic results described in this thesis have been presented by the author at the following international conferences:

Eelsalu M., Soomere T. 2018. Quantification of changes in the beach volume by the application of an inverse of the Bruun Rule and laser scanning technology. Oral presentation at the *3rd LatWaves Conference* (18–20 November 2018, Medellin, Colombia).

Eelsalu M., Soomere T., Julge K. 2016. Combining remote sensing with an inverse Bruun Rule for the analysis and management of almost equilibrium beaches. Poster presentation at the *European Geosciences Union General Assembly 2016* (17–22 April 2016, Vienna, Austria).

Eelsalu M., Soomere T. 2015. Laineenergia ja selle kasutamise perspektiividest Läänemeres (Perspectives of wave energy harvesting in the eastern Baltic Sea). Oral presentation (in Estonian) at the *METOBS 150, Eesti geofüüsika konverents* (Geophysics in Estonia) (2–3 December 2015, Tõravere, Estonia).

Eelsalu M., Soomere T., Pindsoo K., Lagemaa P. 2015. Ensemble approach for the projections of extreme water levels reveals bias in water level observations. Oral presentation at the *10th Baltic Sea Science Congress: Science and innovation for future of the Baltic and the European regional seas* (15–19 June 2015, Riga, Latvia).

Eelsalu M., Soomere T. 2015. Võimalusi rannikuprotsesside kvantifitseerimiseks poolsuletud merealadel (On the possibilities to quantify beach processes in semi-enclosed seas). Oral presentation (in Estonian) at the conference *Eesti veeteaduse horisondid* (Horizons of water resources research in Estonia) (28 April 2015, Limnoloogiakeskus, Estonia).

Eelsalu M., Soomere T. 2015. Quantification of changes in the beach volume by applying an inverse Bruun's Rule and laser scanning technology in Pirita Beach, Tallinn Bay. Poster presentation at the *International seminar Climate modelling and impacts: From the Global to the Regional to the Urban scale* (10 March 2015, Hamburg, Germany).

Eelsalu M., Julge K., Grünthal E., Ellmann A., Soomere T. 2014. Laser scanning reveals detailed spatial structure of sandy beaches. Poster presentation and oral introduction at the *IUTAM Symposium on Complexity of Nonlinear Waves* (08–12 September 2014, Tallinn, Estonia).

Eelsalu M., Soomere T. 2014. Intermittency of the wave energy flux in the eastern Baltic Sea. Oral presentation at the *1st International Conference on Mathematics and Engineering in Marine and Earth Problems* (22–25 July 2014, Aveiro, Portugal).

Eelsalu M., Soomere T., Julge K., Grünthal E., Ellmann A. 2014. Combining airborne and terrestrial laser scanning to monitor coastal processes. Oral presentation at the *1st International Conference on Mathematics and Engineering in Marine and Earth Problems* (22–25 July 2014, Aveiro, Portugal).

Eelsalu M., Soomere T. 2014. On spatio-temporal variations of the wave energy potential along the eastern Baltic Sea coast. Oral presentation at the *2nd International Conference Climate Change–The environmental and socio-economic response in the southern Baltic region* (12–15 May 2014, Szczecin, Poland).

Eelsalu M., Soomere T., Org M. 2014. Visually observed wave climate in the Gulf of Riga. Oral presentation at the *2014 IEEE/OES Baltic International Symposium* (May 26–29, 2014, Tallinn, Estonia).

Julge K., **Eelsalu M.**, Grünthal E., Talvik S., Ellmann A., Soomere T., Tõnisson H. 2014. Combining airborne and terrestrial laser scanning to monitor coastal processes. Oral presentation at the *2014 IEEE/OES Baltic International Symposium* (May 26–29, 2014, Tallinn, Estonia).

Eelsalu M., Julge K., Soomere T., Grünthal E. 2014. Quantification of the evolution of a small beach applying laser scanning technology. Poster presentation at the *Baltic Earth Workshop on Natural hazards and extreme events in the Baltic Sea region* (30–31 January 2014, Helsinki, Finland).

Eelsalu M., Ellmann A., Julge K., Märdla S., Soomere T. 2014. Rannaprotsesside anatoomia laserskaneerimise skalpelliga (Laser scanning of beach processes). Oral presentation (in Estonian) at the conference *Kaugseire Eestis* (Remote Sensing in Estonia, October 2014, Tõravere Observatoorium).

Eelsalu M., Soomere T. 2013. Wave energy potential in the north-eastern Baltic Sea. Oral presentation at the *9th Baltic Sea Science Congress* (26–30 August 2013, Klaipėda, Lithuania).

Eelsalu M., Soomere T. 2013. Closure depth along the north-eastern coast of the Baltic Sea. Poster presentation at the *9th Baltic Sea Science Congress* (26–30 August 2013, Klaipėda, Lithuania).

Eelsalu M., Soomere T. 2012. Wave energy potential in the north-eastern Baltic Sea and Estonian coastal waters. Oral presentation at the *6th International student conference “Aquatic environmental research”* (17–19 October 2013, Palanga, Lithuania).

1. Wave energy flux in the eastern Baltic Sea

The wave climate of the Baltic Sea is generally unfavourable from the viewpoint of wave energy harvesting. Wave heights in extreme storms are relatively large (Björkqvist et al., 2017) but waves are comparatively short (Broman et al., 2006) and thus provide less usable energy than longer waves with the same height typically found on open ocean coasts. The wave heights and periods in the Baltic Sea are highly intermittent in both time and space (Soomere and Räämet, 2011). These properties have led to the conjecture that the production of energy from waves is non-profitable in the Baltic Sea (Cruz, 2008). This was also one of the main conclusions in Paper I.

The development of new wave energy converters (Blazauskas et al., 2015) and the increasing need for energy production from renewable sources has reinforced the interest in wave energy in semi-sheltered sea areas. In this context, viable detailed estimations of wave energy resources at various locations are essential (Berins and Petrichenko, 2019; Nilsson et al., 2019). Paper II indicates that several seemingly sheltered nearshore segments receive relatively large amounts of wave energy and may serve as feasible locations for wave energy converters.

In this Chapter wave energy potential is systematically analysed in the eastern part of the Baltic Sea. The focus is on an almost 1400 km long nearshore stretch from the Sambian (Samland) Peninsula to the eastern Gulf of Finland, including the Gulf of Riga and Bay of Gdańsk (Fig. 1). The analysis of wave energy flux includes i) evaluation of total power of waves in terms of the onshore energy flux, ii) quantification of spatial variability of the wave energy flux, iii) identification of hot-spots of wave energy flux, iv) quantification of temporal intermittency of wave energy flux, v) estimates of theoretically available wave energy in the contemporary wave climate.

1.1. Wave properties in the Baltic Sea

Wave energy levels are highly variable along the coasts of the world. The most promising sections for wave-generated power comprise only 2% of the shoreline, but they may provide up to 480 GW of power output (Arinaga and Cheung, 2013). The areas with largest wave energy density are located at latitudes 40–50 where the atmospheric forcing generates relatively high swells all year long (Cruz, 2008, Arinaga and Cheung, 2013).

The wave energy potential is generally less in semi-enclosed seas and inland water bodies (Cruz, 2008). The main implicit limiter for harvesting energy from the Baltic Sea waves is the small size of the sea (Fig. 1). It restricts the growth of waves and thus the atmospheric energy that can be converted into wave energy. The wave fields are fetch-limited, that is, their properties are largely dictated by the size of the water body.

Some areas in semi-enclosed seas may be suitable for wave energy production (Stopa et al., 2013). The obvious candidates for wave energy harvesting are downwind sea areas. The Baltic Sea wind and wave climates are strongly anisotropic. The predominant wind and wave directions are from SW or NNW (Soomere and Keevallik, 2003; Jönsson et al., 2003). Accordingly, the highest concentration of wave energy is found in the nearshore of the eastern Baltic Sea. The coasts with the longest fetches for these winds are the Bay of Gdańsk, sea areas near the Finnish archipelago and the eastern Gulf of Finland.

On average, the wave climate of the Baltic Sea is relatively mild but highly intermittent (Schmager et al., 2008; Soomere and Räämet, 2011; Tuomi et al., 2011; Hünicke et al., 2015). The long-term significant wave height H_S slightly exceeds 1 m in the open part of the Baltic proper. The wave climate is even milder, with H_S around 0.6–0.8 m in semi-sheltered sub-basins such as the Gulf of Finland (Soomere et al., 2010) or Gulf of Riga.

The Baltic Sea has, however, occasionally very strong wave storms. The largest instrumentally measured significant wave height is $H_S = 8.2$ m in the northern Baltic proper (Tuomi et al., 2011). The significant wave height may reach almost 10 m in the nearshore of the Western Estonian Archipelago (Soomere et al., 2008) and along some parts of the Latvian coast (Schmager et al., 2008). The probability of significant wave height exceeding 1 m varies from about 90% in November to about 10% in May (Soomere and Räämet, 2011) whilst most of the time the significant wave height is below 0.5 m.

Regular long-period swells are usually the best source for energy harvesting (Cruz, 2008). Such wave systems are infrequent in the Baltic Sea (Broman et al., 2006; Soomere and Räämet, 2011; Soomere, 2016). As characteristic in semi-sheltered water bodies, the predominant wave periods are considerably shorter in the Baltic Sea than in the

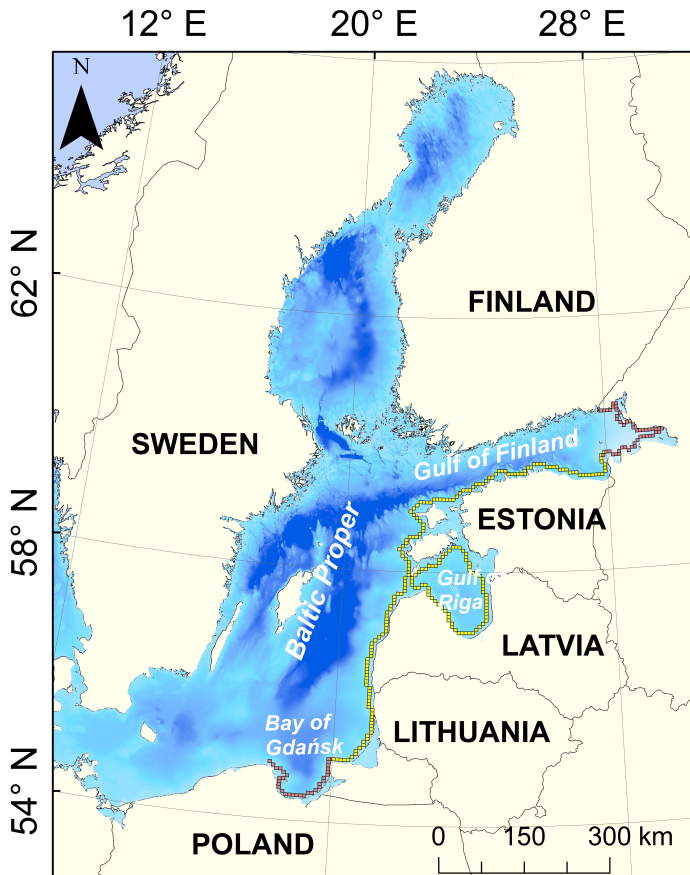


Figure 1. The Baltic Sea. Yellow nearshore squares: study area in Paper I, orange squares: study areas in Paper II.

neighbouring North Sea or the North Atlantic. Usually waves with periods of 4–6 s predominate in the Baltic proper (where periods up to 7–8 s also often occur). The typical periods are even smaller, about 3–4 s in more sheltered coastal regions (Hünicke et al., 2015; Soomere, 2016).

The analysis of wave energy flux and its spatio-temporal variations in the eastern Baltic Sea in Papers I and II relies on numerically simulated instantaneous wave fields over 38 years 1970–2007. Time series of wave properties in the study area in the eastern Baltic Sea (Fig. 1) were extracted from the wave model WAM (Komen et al., 1994). The model was run in finite-depth mode for the entire Baltic Sea to the east of the Danish straits on a regular rectangular grid with a spatial resolution of 3' along latitudes and 6' along longitudes (about 3×3 nautical miles, 11 545 sea grid-points) (Räämet and Soomere, 2010). The wave energy flux from the North Sea through the Danish straits is very small (Jönsson et al., 2003; Soomere, 2003) and was ignored in the calculations.

The input for the wave model was near-surface wind at the 10 m level derived from the Swedish Meteorological and Hydrological Institute (SMHI) geostrophic wind database with a spatial and temporal resolution of $1^\circ \times 1^\circ$ and 3 h, respectively (6 h prior to September 1977). The geostrophic wind speed was multiplied by 0.6 and the wind direction was turned counter-clockwise by 15° (Räämet and Soomere, 2010). This approximation, although neglecting many details of the wind fields, is often used in studies in the Baltic Sea region (e.g., Myrberg et al., 2010; Höglund and Meier, 2012).

The directional resolution of calculations was 15° (24 equally spaced directions). The lowest frequency was 0.042 Hz (wave period 23.9 s) as in the standard set-up of the WAM model for open ocean conditions (Komen et al., 1994). The frequencies of wave components were arranged in a geometrical progression with an increment of 1.1. The calculations were performed in an extended frequency range up to about 2 Hz using 42 frequency bins reflecting wave periods down to 0.5 s. Such an extension ensures realistic wave growth rates in low wind conditions after calm situations (Soomere, 2005) and an adequate reproduction of the high-frequency part of the wave fields (Soomere et al., 2012). The output, saved once in hour, comprised 333 096 single values of wave height, period and direction at each grid cell during the simulation interval. Significant wave height, peak period and wave approach direction for 38 years (1970–2007) are used in Papers I and II for the calculations of wave energy flux (Fig. 1).

The accuracy and reliability of the simulated wave data is analysed in Räämet (2010) and Soomere et al. (2011) by means of comparison of the outcome of simulations with historical wave records. The model underestimates the long-term average wave height by about 10%. The main statistical properties such as the distribution of the occurrence of wave conditions with different height and period satisfactory match the measured data (Soomere et al., 2011). The largest discrepancies occur during extreme wave events and the model underestimates wave height in short storms. The presence of ice is not taken into account. This approach is generally acceptable for the southern part of the study area and apparently also in the mostly ice-free future climates. The results presented in Paper I and Paper II, however, may overestimate the overall wave energy resource in the northern Baltic proper and especially in the Gulf of Riga and Gulf of Finland in the current wave climate. These shortcomings do not change the key messages of the analysis.

1.2. Study area and the converter line

As waves rapidly lose their energy in shallow water (Ardhuin et al., 2003), the largest wave energy resource is available in reasonably deep nearshore regions where interactions with the seabed do not yet considerably reduce the wave energy. As the average depth in the Baltic Sea is only 54 m (Leppäranta and Myrberg, 2009), it is not rational to limit the study to the truly deep-water areas. As Baltic Sea waves are often fetch-limited, their energy tends to increase almost until the coast. A reasonable depth for wave energy harvesting in the Baltic Sea is estimated in Paper I based on the linear wave theory and properties of approaching waves.

As typical wave periods in the Baltic Sea are shorter than in the open ocean, the intensity of wave-bottom interaction is weaker in this water body. The difference can be expressed from the linear wave theory in terms of the parameter kd , where k is the wave number and d is the water depth. The intermediate-depth dispersion relation for water waves is $\omega = \sqrt{gk \tanh(kd)}$, where $\omega = 2\pi / T$ is the angular frequency, T is the wave period and g is acceleration due to gravity. Relatively long Baltic Sea waves with $T = 7$ s correspond to the same value $kd \approx 1.5$ at a depth of $d = 16.5$ m as relatively common ocean swells with a period of $T = 12$ s at a depth of $d = 50$ m.

This difference is even larger in terms of the maximum near-bottom orbital velocity. Swells with periods of 12 to 15 s lose part of their energy starting from a depth of 50–60 m (Ardhuin et al., 2003). A typical Baltic Sea wave with the same height but with a period of $T = 5.5$ s develops the same near-bottom orbital velocity as the above swells at a depth of about 17 m. It is therefore natural to assume that the WAM model (that performs well for depths >50 m along the open ocean coasts, Ardhuin et al., 2003) works well until depths of 10–15 m for the wave fields that are common in the Baltic Sea.

Based on the presented estimates, the wave power in Paper I and Paper II (Fig. 1) is calculated for grid cells of the wave model located at the distance of a few kilometres from the eastern coast of the Baltic Sea. The average water depth in those grid cells is 18 m and varies in the range of 7 to 48 m. Only the onshore wave energy flux is taken into account (see Section 1.3). The cells used in Paper I are ordered along an about 1400 km long piecewise straight line called converter line below. It consists of 222 about 6 km long sections (Fig. 2).

The line starts from the Sambian Peninsula (20°E, 55°N) and extends to the eastern Gulf of Finland to Russia (28°E, 59°51'N). It covers the entire nearshore of Lithuania, Latvia, and Estonia and includes the Gulf of Riga. About 950 km (154 sections, Fig. 2) of this line follows the coast of the Baltic proper and Gulf of Finland and about 450 km (68 sections, Fig. 2) is in the Gulf of Riga. In Paper II this line was extended to the Bay of Gdańsk and towards the eastern end of the Gulf of Finland.

The approaching wave power is estimated in units of power per unit of length of the shoreline (Paper I–II). The converter line may have different length in different grid cells (Fig. 3). The length of sections oriented in the North–South direction (e.g., L_{73} in Fig. 3) is 3 nautical miles (about 5.5 km). Depending on the mutual location of the neighbouring cells, the relevant section may be by $\sqrt{2}$ times or by $\sqrt{5}/2$ times the grid size (Fig. 3). The length of sections oriented along latitudes follow the length of the relevant latitude circle and can vary to some extent. The difference in the length of the North–South and East–West oriented sections is the largest at the latitude 55°N in the southernmost part of the study area and vanishes close to the latitude 60°N in the Gulf of Finland. The length of each converter line segment was calculated using the ArcMap software.

The wave properties (significant wave height $H_{s,ij}$, peak period $T_{s,ij}$) during the i -th sequential ($1 < i < 333\,096$) hourly interval in 1970–2007 along the j -th section ($1 < j < 222$ in Paper I, $1 < j < 75$ in Paper II) of the converter line are set equal to the modelled wave properties at these wave model cells where this j -th section is located (Fig. 2).

1.3. Total wave energy resource in the study area

The total energy density of a wave field in terms of significant wave height H_s is:

$$E = \frac{1}{16} \rho g H_s^2, \quad (1)$$

where ρ is the water density. The magnitude of energy flux (wave power) $P = E c_g$ is the product of wave energy density and group speed c_g . The contribution P_{ij} of an instantaneous wave field approaching the j -th section of the converter line during the i -th hourly interval into the total energy flux is thus



Figure 2. Nearshore grid cells of the wave model along the eastern Baltic Sea coast and in the Gulf of Riga. Four selected points (24, 73, 147 and 194), used to characterise wave energy resources at single locations, are marked by black squares. Coloured segments indicate the total wave power over the coastal section. Adapted from Paper I.

$$P_{ij} = E_{ij}c_{g,ij} = \frac{1}{16}\rho g H_{S,ij}^2 c_{g,ij}. \quad (2)$$

Technically, this contribution is equal to the energy flux of sine waves with the height of $H_{S,ij}/\sqrt{2}$ and group speed $c_{g,ij}$.

As the Baltic Sea is relatively shallow, it is necessary to describe the wave properties, including the group speed

$$c_g = \frac{\omega}{2k} \left(1 + \frac{2kd}{\sinh 2kd} \right), \quad (3)$$

using the intermediate-depth dispersion relation $\omega = \sqrt{gk \tanh(kd)}$. The dispersion relation was solved for the wave number k_{ij} for each section of the converter line (using water depth d_j in the relevant cell of the wave model, Fig. 3) for each modelled value of the wave angular frequency ω_{ij} and period $T_{ij} = 2\pi/\omega_{ij}$. The resulting values of k_{ij} were used to calculate the group speed $c_{g,ij}$ of waves after Eq. (3).

The wave energy flux is a vector $\vec{P} = E\vec{c}_g$ aligned with the wave propagation direction. Baltic Sea waves often approach the coast at large angles (Viška and Soomere, 2012). During offshore-directed winds wave energy may even propagate, on average, in the offshore direction. The theoretically available (onshore-propagating) wave energy resource is expressed by the component of the wave energy flux normal to the relevant segment of the coastline. The density of this flux P_{ijn} (per unit of length of the converter line) is

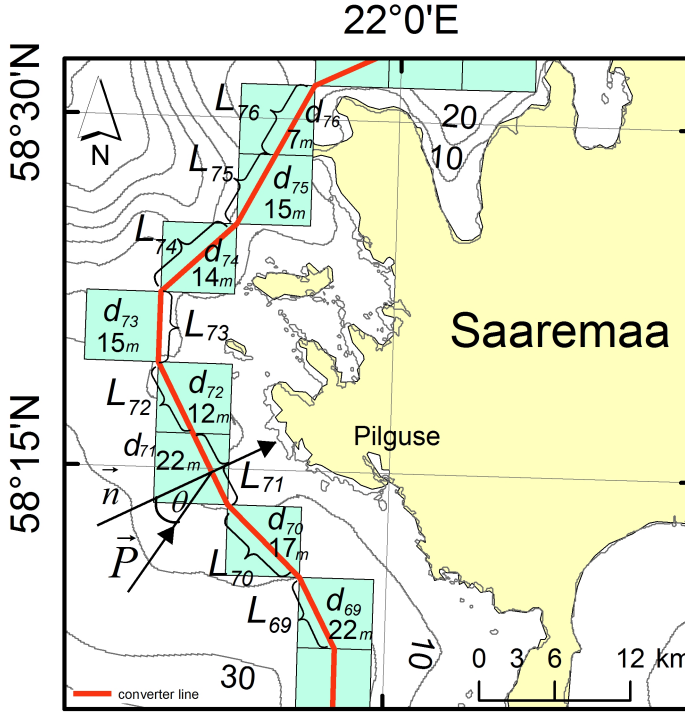


Figure 3. The location of the converter line through wave model grid cells near the western tip of the island of Saaremaa, Estonia. Adapted from Paper I.

$$P_{ijn} = P_{ij} \cos \theta_{ij} \text{ [W/m]}, \quad (4)$$

where θ_{ij} is the angle between the wave energy flux vector approaching the j -th segment of the converter line and its onshore-directed normal (Fig. 3) within the i -th hourly time interval. We assume that the energy of waves propagating along the converter line or to the offshore is not useable; thus we set $P_{ijn} = 0$ when $\theta_{ij} > 90^\circ$.

The total instantaneous onshore wave energy flux P_{ijn}^h , theoretically available for real converters mounted along a particular (j -th) section of the converter line of a length of L_j (Fig. 3) during the i -th hourly time interval, is

$$P_{ijn}^h = P_{ijn} L_j \text{ [W]}. \quad (5)$$

Waves approaching the study area in the eastern Baltic Sea could theoretically provide, on average 1.5 GW of wave power at the converter line (Fig. 2, Paper I). The regional variations in the wave energy resource (Fig. 4) are highlighted for four regions. The entire coast of Lithuania and Latvia contributes about 600 MW to the total power of the study area. Western Estonia provides in total almost 400 MW. Wave power at the southern coast of the Gulf of Finland is about 220 MW and thus much smaller,

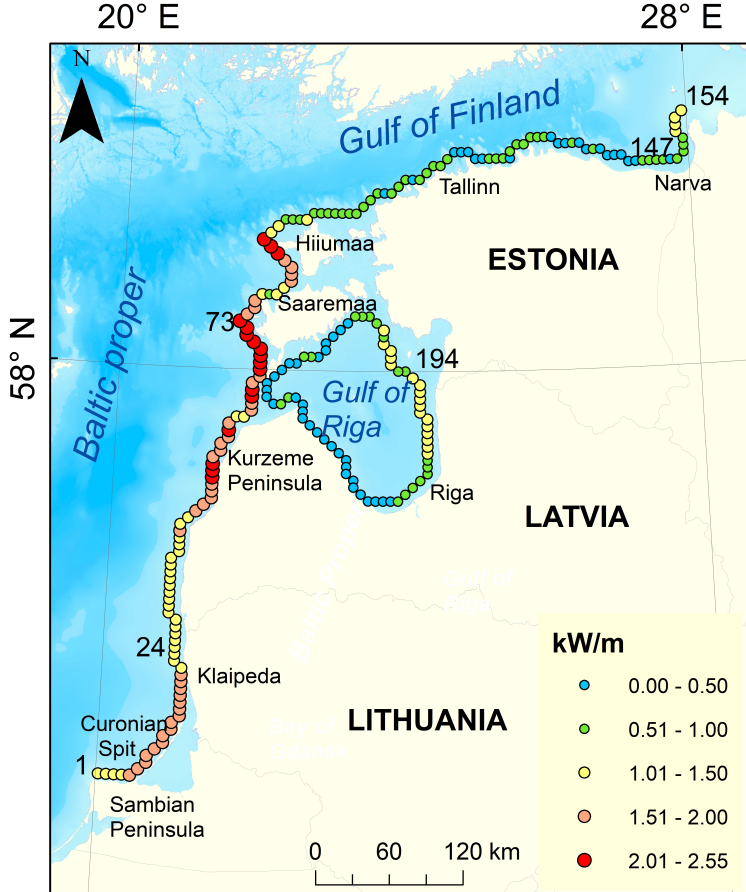


Figure 4. Long-term average wave energy flux along the coasts of the eastern Baltic proper, Gulf of Finland and Gulf of Riga in 1970–2007. Adapted from Paper I.

considering the length of the coastline. The wave energy resource in the entire coastal area of the Gulf of Riga is about 280 MW (Paper I).

The average long-term onshore wave energy flux per unit length of the coastline varies markedly along the study area (Fig. 4). It reaches its highest values (1.5–2.55 kW/m) along the open coast of the Baltic proper of Latvia and in the nearshore of the Western Estonian Archipelago. The largest average wave energy flux 2.55 kW/m reaches the nearshore of Saaremaa (Fig. 4, grid cell 73). Similar levels of energy flux occur in the northern part of the Kurzeme Peninsula (to the north of 57°N), in the nearshore of the Sõrve Peninsula (the southernmost part of Saaremaa) and in the SW and western nearshore of the island of Hiiumaa (Fig. 4). The average energy flux is 1.5–2 kW/m along the coastline of the Kaliningrad District and Lithuania and along the southern part of the Latvian coastline.

The spatial pattern of long-term energy flux mirrors the well-known anisotropy of moderate and strong winds in the northern Baltic proper (Soomere, 2003). The described alongshore variations in this flux signal that waves from SW reach their maximum height in the nearshore of Western Estonia and north of the Kurzeme Peninsula providing the highest onshore wave energy flux to the study area.

The average wave energy flux in sub-basins of the Baltic Sea is much smaller than in the open part of the water body (Fig. 4). This flux decreases rapidly to the east of the Kõpu Peninsula (the westernmost part of Hiiumaa) and is mostly well below 1 kW/m in the interior of the Gulf of Finland. In the Gulf of Riga, values over 1 kW/m are represented along its eastern coast and remain below 0.5 kW/m along its western coast. Part of this difference stems from relatively short wave periods in these gulfs. The southern part of the Gulf of Finland and the western shore of the Gulf of Riga are also sheltered against the predominant wave directions and wave growth in the Gulf of Riga is limited by short fetch.

1.4. Hot-spots of wave energy

Some locations in the Bay of Gdańsk and in the easternmost Gulf of Finland have attractive potential locations 'hot-spots' for wave energy harvesting (Paper II). These nearshore areas have a long fetch for one of the predominating wind directions (Fig. 1). The Bay of Gdańsk is fully open to the waves that approach from the North and NNW. Strong winds from these directions over the northern Baltic proper (Soomere, 2001) may drive most severe wave conditions in the vicinity of this bay (Schmager et al., 2008). The eastern Gulf of Finland is occasionally affected by long waves produced by strong western or west-south-western winds (Soomere and Keevallik, 2003).

These two regions (the easternmost Gulf of Finland and the vicinity of the Bay of Gdańsk, Fig. 5) host in total about 450 MW of average onshore wave energy flux. Up to 280 MW reaches the nearshore of the Bay of Gdańsk and about 170 MW is carried by waves to the eastern Gulf of Finland (Fig. 5).

Both of these areas also exhibit extensive alongshore variation in the long-term average wave energy flux (Fig. 5). The largest values of wave energy flux are 1.79 kW/m on the coast of Sambian Peninsula and 1.61 kW/m between Saint Petersburg and Vyborg. These hot-spots of wave energy flux are located in coastal sections that are fully open to waves approaching from the most frequent strong wind directions (Fig. 5, sections 18–21 and 31–33 in the Bay of Gdańsk and sections 61–62 and 66–67 in the Gulf of Finland).

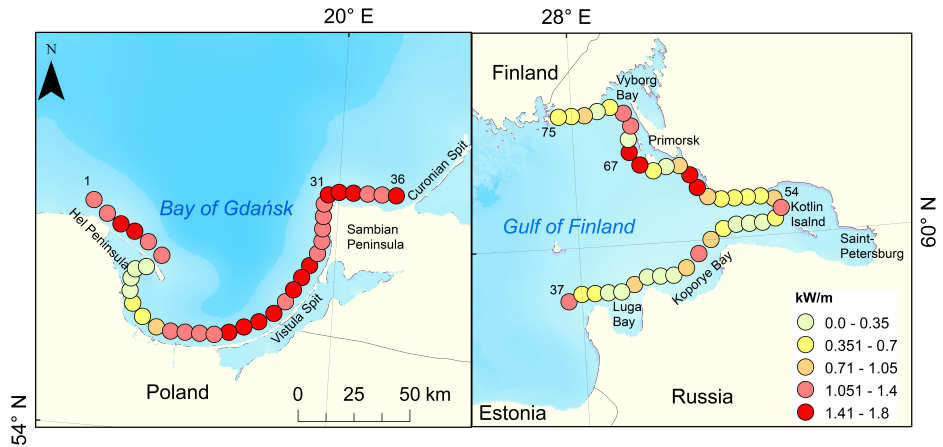


Figure 5. Long-term average wave energy flux along the Bay of Gdańsk (left panel) and the eastern Gulf of Finland (right panel) in 1970–2007. Adapted from Paper II.

The alongshore variations in the wave energy flux are minor in the open part of the Bay of Gdańsk, along the northern coast of the Hel Peninsula and Sambia Peninsula. Low levels of energy are found in the sheltered western Bay of Gdańsk. The alongshore variations in the eastern Gulf of Finland are more complicated. The southern coast of this area and shores of Neva Bight receive a very limited amount of wave energy. Substantial amounts of wave energy may penetrate to the vicinity of the island of Kotlin. An approximately 10 km long section with large wave energy flux is found around Primorsk on the north-eastern coast of the Gulf of Finland (Fig. 5).

1.5. Temporal variability in the wave energy flux

The typical average values of wave energy flux in the prospective areas of the open ocean coast for energy harvesting are in the range 30–50 kW/m (Alcorn, 2014). In such areas, ocean swells are consistently present and provide a relatively steady energy resource. The instantaneous wave energy flux can exceed the average values by one or two order of magnitudes depending on the location. There are locations and seasons when rough sea conditions can produce 1000–2000 kW/m (Cruz, 2008). This variability highlights the difficulties that the production of energy from the ocean waves must face. A suitable device must be efficient at converting the typical wave conditions but it also must withstand the most severe wave conditions applied to the converter (Alcorn, 2014).

In semi-sheltered sea areas, wave energy flux is usually not as intense as on the open ocean shores but it is much more intermittent. Although maximum wave heights in the Baltic Sea are less than half of those in the open ocean, the limited size of the sea dictates that wave fields have short memory and persist only a few hours after wind has ceased (Soomere, 2005). As wave energy flux behaves roughly as $H_s^{2.5}$ in shallow water, even modest variations in the wave height may lead to significant variations in the wave energy flux. The wave field is also very sensitive with respect to the wind direction.

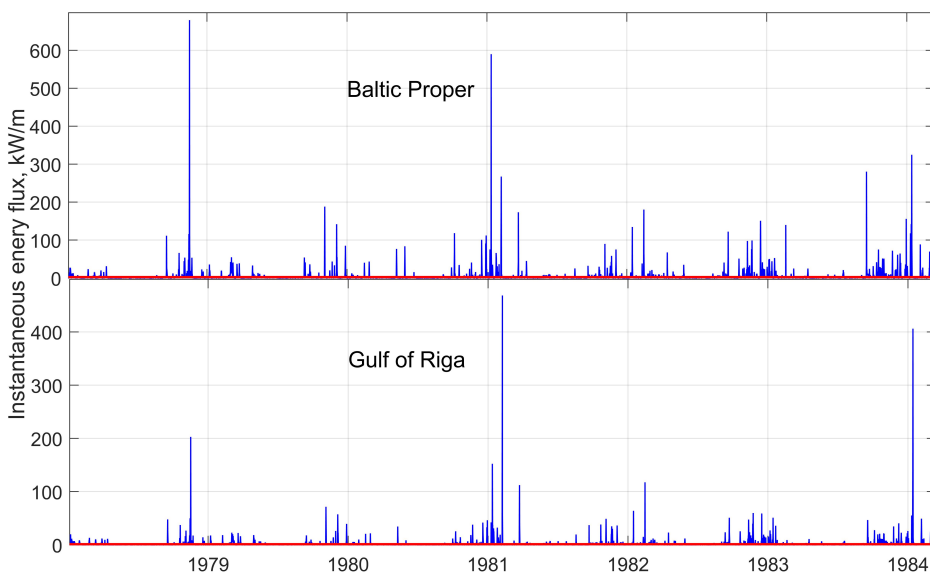


Figure 6. Instantaneous onshore wave energy flux at grid cells No 73 and 194 (see Fig. 2) in the nearshore of Saaremaa in the north-eastern Baltic proper and in the eastern Gulf of Riga in selected 5 years. The red horizontal line indicates the average wave energy flux for the location.

The maximum levels of instantaneous wave energy flux during 38 years of simulations (Fig. 6) exceed the long-term average levels by more than 100 times. The wave power maximum reaches 680 kW/m near Saaremaa in the nearshore of Baltic proper, about 400 kW/m in the eastern Gulf of Riga and almost 300 kW/m along the coast of Lithuania and Latvia (Paper I). The intermittency has the same level in the Bay of Gdańsk and

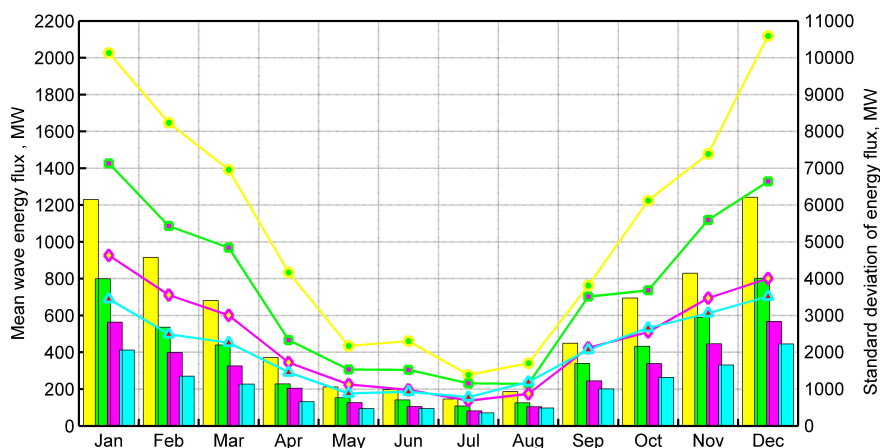


Figure 7. Seasonal course of the monthly onshore wave energy flux (bars) and the monthly standard deviation of single values (lines) summarised for the coastal stretches from the Sambian Peninsula to the Irbe Strait (Kurzeme, yellow), Western Estonia (green), Gulf of Riga (magenta) and Gulf of Finland (cyan).

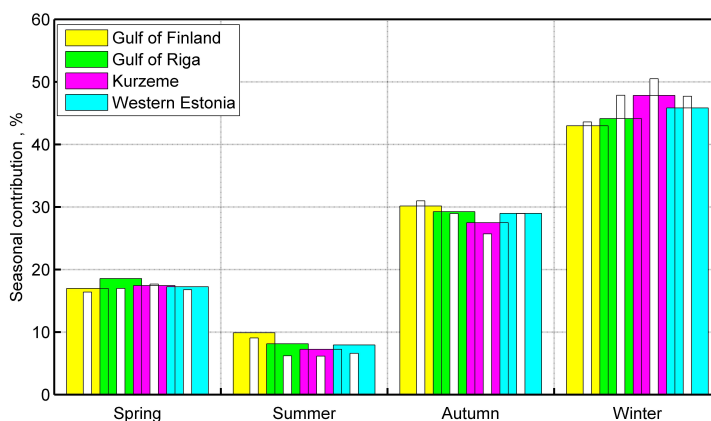


Figure 8. The proportion of the average wave energy flux in different seasons over longer coastal stretches in (wide bars) and in grid cells Nos. 24, 73, 147 and 194 in Fig. 2 (narrow white bars).

eastern Gulf of Finland (Paper II). Therefore, such extreme intermittency of wave energy flux is inherent for this water body.

The wave energy flux also has strong seasonal variability (Fig. 7). The standard deviation of single hourly values for entire coastal sections exceeds the monthly value by 8–10 times (Papers I and II). The highest difference between the average and single values occurs in the stormiest months from November until February. The variations are much smaller from April to August.

Almost half of the annual wave energy flux arrives in winter (December–January–February) and less than 10 % in summer months (June–July–August, Fig. 8). The total contribution to energy flux in spring and summer months remains usually under 25%. The proportions are roughly the same along the entire study area. In essence, they mirror seasonal patterns of wind speed and wave climate in the region.

The onshore wave energy flux in single seasons can vary significantly between different years (Paper I). For example, in 1986 the wintertime energy flux contributed only 20% to the annual total power but up to 70% during severe winters such as in 2005/2006.

1.6. Properties and timing of the wave energy resource

It is rational to optimise wave energy converters to match the parameters of waves that provide the largest contribution to the wave energy flux at the selected site. The combinations of heights and periods of wave fields with the largest wave energy resource can be estimated using combined scatter and energy diagrams (Fig. 9). The greatest contribution to the wave power is provided by wave conditions with significant wave height of 1.5–2.5 m and the peak period of 5–8 s. The typical instantaneous energy flux of waves with these parameters is about 10 kW/m (Paper I). Much higher wave energy flux may at times occur (see Fig. 6). Wave energy fluxes >100 kW/m have occurred, according to our calculations, for about 1 h/yr in the Gulf of Finland and about 15 h/yr near Saaremaa (Paper I). The converter must withstand such wave conditions.

In the nearshore of the Estonian Archipelago, the best resource of energy is concentrated in a narrow range of wave heights and wave periods (Fig. 9). The properties

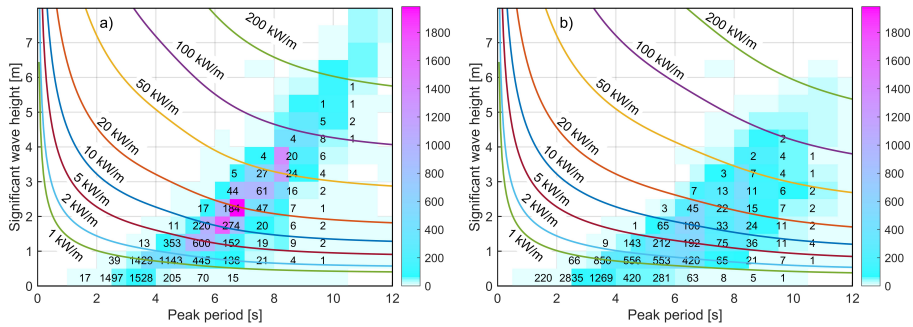


Figure 9. Combined scatter and energy diagram for two selected wave model grid cells: (a) point 73 near Saaremaa in Fig. 2, b) point 21 in Fig 5, nearshore of Bay of Gdańsk. The numbers show the annual average of hours with the relevant wave conditions with a resolution of 0.5 m in wave heights and 1 s in wave periods for 1970–2007. The colour scale shows the annual bulk energy resource [kW·h/m] carried onshore by wave fields with the relevant wave properties with a resolution of 0.5 m in wave heights and 0.5 s for waves with periods less than 7 s and 1 s for waves with periods longer than 7 s. Solid blue lines present isolines of instantaneous energy flux.

of waves suitable for energy harvesting are much more variable in the nearshore of the Bay of Gdańsk.

The analysis in Paper I reveals that a substantial amount of the wave energy in the Baltic Sea is concentrated into relatively short time periods (Fig. 10). A few severe wave storms with total duration of about 2 days contribute up to 20% of the annual wave energy flux (Fig. 10). About 60 % of the annual energy arrives to the nearshore within 18 stormiest days and 75% of it arrives in five weeks. More than 90% of the entire annual energy arrives during the 3 windiest months. The contribution of the roughest seas to the total annual energy flux is practically the same for the entire study area (insert in Fig. 10).

On many calmer days almost no onshore energy flux is available in the entire study area (Fig. 10). The calmest 93.8 days provide, on average, only 1% of the total annual

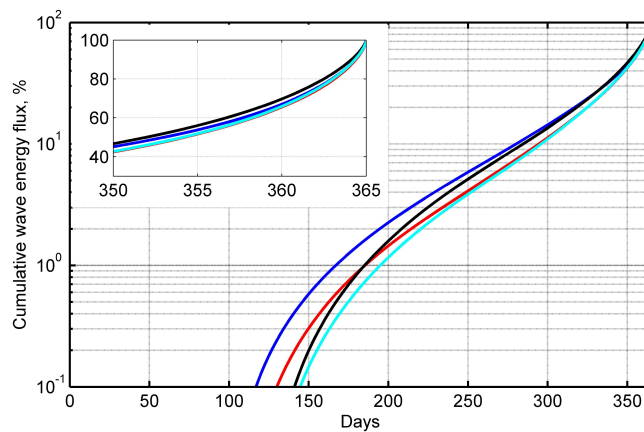


Figure 10. Cumulative annual energy flux at four selected points in the study area (Fig. 2) Blue: the border between Latvia and Lithuania, red: western coast of Saaremaa, black: eastern Gulf of Finland, cyan: eastern Gulf of Riga. The inset reflects the contribution of the most intense wave fields for 360 h (15 days) a year (Paper I)

energy flux in the southern Baltic Sea. The same amount is provided on the 102.7 calmest days in the nearshore of Saaremaa. In semi-sheltered sub-basins the time intervals with less than 1% of the annual onshore energy flux are even longer, about 118–119 days/yr in the eastern Gulf of Finland and Gulf of Riga (Fig. 10).

Additional to the demonstrated high intermittency of wave energy flux, there are other limiters for energy production in the study area. Although some wave energy converters (see Paper II and references therein) are apparently able to catch as much as 80% of the total wave energy, losses in the conversion and transmission into the grid are still considerable. The realistic output into the electricity grid hardly exceeds 50% of the theoretically available energy (Bernhoff et al., 2006).

The practical use of this resource is limited by the presence of numerous marine protected and Natura areas that cover 46% of the study area. The theoretically available wave power in coastal stretches with no environmental restrictions is about 840 MW for the entire study area (Paper I). A realistic upper limit for the total wave energy contribution to the grid is thus 300–400 MW (Paper I).

Even though wave energy harvesting in the Baltic Sea is generally thought to be economically not beneficial, wave energy farms can serve as preventive solutions for environmental management of coastal sections affected by erosion (Martinelli, 2011, Abanades et al., 2015, Abanades et al., 2018). They act similarly to detached breakwaters that partially shelter vulnerable shore sections against strong waves (Vaidya et al., 2015). The study area contains long coastal sections with fine sediment (Fig. 2; Paper II). The majority of beaches in this area suffer from sediment deficit (Harff et al., 2017b) and many coastal segments are prone to erosion (Pranzini and Williams, 2013). The situation is particularly complicated in the eastern Gulf of Finland (Ryabchuk et al., 2011) where high waves may approach at large angles with respect to the coastline and give rise to instability of the entire coastal system (Ashton et al., 2001; Murray and Ashton, 2013). The presence of hot-spots of wave energy highlighted in Paper II signals that much more intense coastal processes than previously thought based on the classic wave statistics may occur in single coastal sections. The use of suitably placed wave energy converters would reduce wave intensity and thus mitigate erosion of the affected coastal sections.

2. Extreme water levels in the eastern Baltic Sea

The most intense erosion usually occurs when large waves attack unprotected sediment higher on the shore. Such events happen relatively frequently in the “downwind” areas of the eastern Baltic Sea during strong western storms that often create high surge and generate severe wave conditions. Therefore, estimations of properties and projections of future extreme water levels are necessary to properly interpret the wave impact on the coast (Chapter I). In particular, understanding the joint effect of strong waves and high water level plays an essential role in the perception of the threats to, and complicated analyses of the evolution of the beaches.

Paper III constructs a projection of extreme water levels and their return periods for selected locations of the eastern Baltic Sea. It uses a simple approach for building an ensemble of projections based on the block maximum method of seasonal and annual maximum water levels. This approach is tested at four locations on the Estonian coast.

Paper IV explores the mechanisms that drive extreme water levels in the eastern Baltic Sea. The contribution of some mechanisms to the total water level is determined by a simple use of a running average. The analysis reveals that single components of water level are not only driven by processes at different time scales but also follow different statistical distributions. The analysis in Papers III and IV employs numerically simulated water level time series from the Rossby Centre Ocean (RCO) model for 1961–2005 and observed water level data from four tide gauges (Fig. 11).

2.1. Hindcast and observed water levels

The analysis of extreme water levels and their return periods in Paper III relies on the data from simulations of the water level and measurements from four Estonian coastal sites (Fig. 11). The tide gauge at Ristna characterizes processes on a relatively straight coastal section that is exposed to high waves from the open Baltic Sea. The tide gauge in Tallinn Harbour portrays a semi-enclosed coastal segment with relatively deep water and complicated geometry. The measurement site in Narva Bay (Narva River mouth) represents a bay that is widely open to the west and north that is vulnerable to storm surges driven by western winds. The location of the tide gauge in Pärnu Bay is vulnerable to high storm surges driven by SW winds.

Measurements of water level at these sites have been taken for many decades, and some data are available from the end of the 19th century. Regular observations started in the middle of the 20th century, two or four times per day. Later, the records exist for every hour. The frequency of observations has been variable and none of the time series is completely homogeneous. The recordings used in Papers III and IV are presented in the Baltic Height System BK77 that was used in Estonia until 2018.

The numerically modelled data used in Papers III and IV were selected from grid cells located at the distance of a few kilometres from the shoreline (Fig 11). This choice was made to avoid insufficient spatial resolution of the model bathymetry and geometry in nearshore areas. The water level time series at chosen grid cells were extracted from the output of two circulation models. The Rossby Center Ocean (RCO) model was developed and implemented by the Swedish Meteorological and Hydrological Institute (SMHI). The output information has a temporal resolution of 6 hours. The RCA4-NEMO model provides hourly water level time series. Both models were run with the same set-up but with a slightly different start time.

Simulations by the RCO model were run from May 1961 to May 2005. The grid cells used were 2×2 nautical miles. The water column was split into 41 vertical layers. This model was forced with high-resolution meteorological information from a regionalization of the ERA-40 re-analyses over Europe with a horizontal resolution of 22 nautical miles.

The undisturbed water level of the RCO model is related to the stationary topography of the model (so-called Warnemünde topography, Seifert et al., 2001) that does not take into account postglacial uplift. As the bathymetry has been compiled from several maps with different base elevation systems, the RCO model is not linked to any particular height. This approach is acceptable in the study area where the global sea level rise in recent decades (Cazenave et al., 2014) is compensated by land uplift. The detailed set-up for the RCO model has been thoroughly described in Meier et al., (2003) and Meier and Höglund (2013). The quality of numerically replicated water level data has been analysed in Meier et al. (2004).



Figure 11. Observations sites at Tallinn, Pärnu, Ristna and Narva-Jõesuu (red circles) and the locations of offshore grid cells of the RCO model (black squares) used in Paper III, and the locations of the RCO grid cells used in Paper IV.

In the context of extreme water levels and their return periods a systematic bias between the modelled and measured values is immaterial as long as both the modelled and measured extreme values are determined from the long-term mean water level. For this reason the modelled water levels were de-meaned and described as hindcast data in Paper III.

The modelled data represents open sea water level conditions. The records at the observation sites are likely also affected by local effects such as wave set-up. Therefore, the mixed use of these data sets is not justified. To make the data comparable, an alternative semi-synthetic data set was created in Paper III by transforming the measured water levels to offshore conditions with the use of the hindcast of the High-Resolution Operational Model for the Baltic Sea (HIROMB) with an output resolution of 1 nautical mile. The transformation was accomplished using the HIROMB model and linear regression. The new locations were at a distance of 10 km from Tallinn, 15 km from Pärnu, 20 km from Ristna, and 40 km from Narva-Jõesuu. The suitability of this method was estimated using Pearson correlation coefficients. These coefficients R were >0.99 for all sites. For brevity, the resulting transformed values are called observed data in Paper III.

2.2. Outliers of water level and the extreme water level distribution

Typically, the empirical probability (density) distributions of water level resemble a Gaussian distribution in the eastern Baltic Sea (Johansson et al., 2001). They are usually slightly asymmetric, being skewed towards the high water levels. The empirical distribution of simulated water levels in Tallinn Bay also mainly follows a Gaussian distribution (Fig. 12). Its skewness is 1.23 and kurtosis 3.09. These parameters are 0 and 3, respectively, for Gaussian distributions. Therefore, the probability of very large values insignificantly differs from this probability for the Gaussian distributed data set.

Figure 12 shows that on top of almost Gaussian distributed water levels, occasional very high water levels (called outliers below) may occur. The presence of outliers is typical for the eastern Baltic Sea (Suursaar and Sooäär, 2007). This feature may substantially affect the parameters of the associated extreme value distribution and projections of return periods of very high water levels (Fig. 12). The outliers of extreme

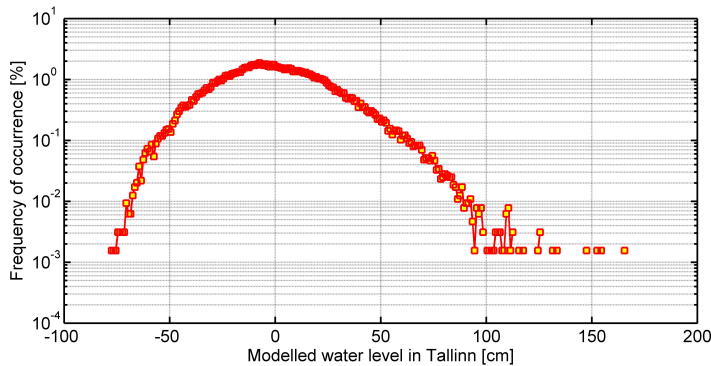


Figure 12. Frequency of occurrence of deviations of the water level from the long-term mean in the RCO simulations near Tallinn (6-h values from 1961–2005).

water levels often do not obey the classic Generalised Extreme Value (GEV) distribution or its particular realisations – Fréchet, three-parameter Weibull, or Gumbel distribution (Coles, 2001). Even slightly different methods may lead to significantly different predictions of extreme water levels and their return periods (Suursaar and Sooäär, 2007).

A feasible way of employing various projections to obtain the most credible outcome is the use of an ensemble of estimates of extreme water levels and their return periods. Paper III explores a simple approach of creating an ensemble based on the existing data and commonly used extreme value distributions. The core of the approach is a GEV distribution with the cumulative distribution function

$$G(y) = \exp \left\{ - \left[1 + \xi \left(\frac{y - \mu}{\sigma} \right) \right]^{-\frac{1}{\xi}} \right\}. \quad (6)$$

Here y has the meaning of block maxima (e.g., annual maximum water levels) and μ , σ , and ξ are the location, scale and shape parameters, respectively (Coles, 2001).

For $\xi \rightarrow 0$ the GEV distribution reduces to the Gumbel distribution with a cumulative distribution function $\Lambda(y) \sim \exp\{-\exp(-y)\}$. For $\xi < 0$ it represents a three-parameter (reversed) Weibull distribution and for the case $\xi > 0$ it represents a Fréchet distribution. The three-parameter Weibull distribution describes extremes of so-called light-tailed (very rapidly decaying) distributions. The Fréchet distribution is the limiting one of those which have polynomially (that is, relatively slowly) decaying tails. The Gumbel distribution is suitable for the description of extremes of processes that have an exponential tail such as the Gaussian distribution. In many applications also, the two-parameter Weibull distribution is used to estimate the threshold that is exceeded once during a certain time interval.

The return period $T(\hat{y})$ for a certain value \hat{y} is given by the $[1 - 1/T(\hat{y})]$ -th percentile of $G(y)$:

$$T(\hat{y}) = \frac{1}{1 - G(\hat{y})}. \quad (7)$$

The core idea of Paper III was to apply these three extreme value distributions (the GEV distribution, the Gumbel distribution and a 2-parameter Weibull distribution) and the different data sets described in Section 2.1 to build a cluster of projections of extreme water levels and their return periods. Even though the Gumbel distribution is a particular case of the GEV family, in many applications the validity of the condition $\xi = 0$ is not evaluated. This approach employed in Paper III implicitly assumes that the processes that drive extreme water levels are statistically stationary (cf. Kudryavtseva et al., 2018) and that the errors of different projections are randomly distributed. Under these conditions it is likely that the average over all projections of the ensemble provides a plausible vision of future extreme water levels and their return periods.

2.3. Block maxima method

The use of extreme value distributions from the GEV family and the block maxima method (e.g., Haigh et al. 2014; Arns et al., 2013) requires that the single extremes used in projections must be identically distributed and uncorrelated (Coles, 2001). Even though some outliers of water level seem to represent a different population (Suursaar and Sooäär, 2007), single values of water level apparently represent the same Gaussian-like distribution (Fig. 12).

A common practice is to use water level maxima over single months or calendar years as the set of block maxima (e.g., Lagemaat et al., 2013, Ribeiro et al., 2014). In the Baltic Sea, monthly maximum water levels are often correlated and daily maxima converge to a 2-parameter Weibull distribution (Särkkä et al., 2017). Water volume in the Baltic Sea has a relatively long reaction time to the atmospheric forcing that is responsible for substantial variations in the water volume of the entire sea (Lehmann and Post, 2015; Lehmann et al., 2017). Events of elevated water levels may last several weeks (Leppäranta and Myrberg, 2009) or even months (Soomere and Pindsoo, 2016). Consequently, the water level responsible for the annual maxima that occurred in December of one year and the next year annual maximum that occurred in January of the subsequent year may be caused by the same cluster of storms.

For the listed reasons the analysis in Paper III additionally employs another method for the selection of (block) maxima over certain time intervals. The calendar year maxima are used as one set of maxima. The alternative set of block maxima represents water level maxima over the relatively stormy season from August to March. As during the calm spring and summer period coastal areas in the Baltic Sea do not experience high water level events (Johansson et al., 2001, Suursaar et al., 2002; Jaagus and Suursaar, 2013), single maxima in this set (called stormy season maxima) are uncorrelated.

The differences between the single values of these sets are minor. However, even such minor differences play an important role in projections of the extreme water levels and their return periods (Fig. 13). The predictions based on the stormy season maxima

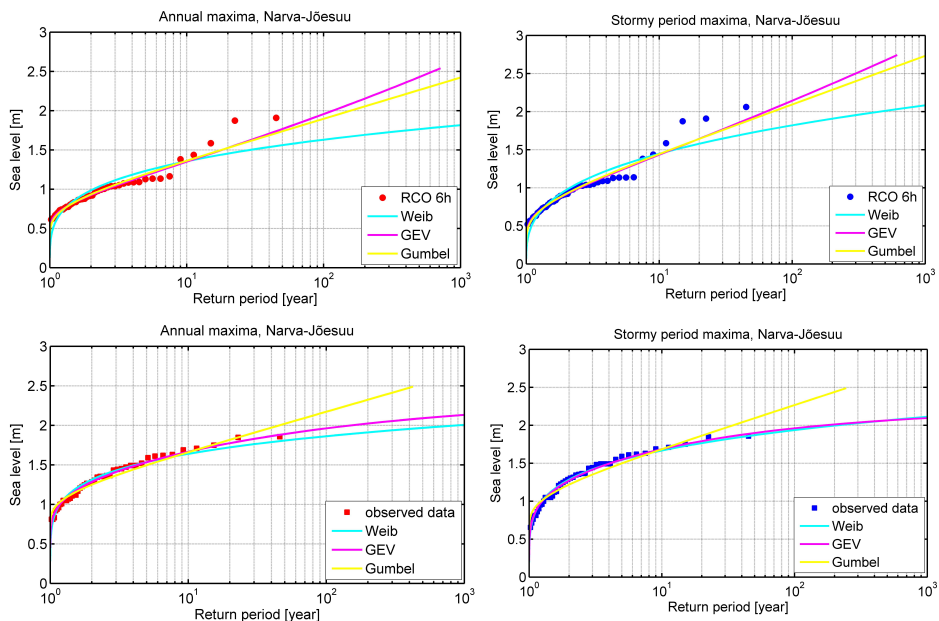


Figure 13. Return periods of extreme water levels at Narva-Jõesuu calculated from the results of the 6-h RCO data (upper panels) and the observed 1-h data set (lower panels, a semi-synthetic data set obtained based on observations and the output of the HIROMB model). The panels on the left correspond to projections based on annual maxima, the panels on the right – to projections based on maxima over stormy seasons. Markers represent single block maxima.

are usually higher for the Estonian coastal waters than those based on the annual maxima. A similar difference also becomes evident in modelled data. Predictions of extreme water levels for a 50 year return period based on modelled stormy season maxima are by 20 cm higher than those calculated using calendar year maxima. The difference is about 10 cm for the observed data (Fig. 13).

2.4. Extreme water level projections and local effects

The demonstrated extensive variability of different projections calls for the use of another approach to improve the results. The core idea in Paper III is that (i) an average of many projections reflects relatively well the true value and (ii) the differences between single different projections provide information about the uncertainty of single estimates. The approach in Paper III used six sets of block maxima (both annual and stormy season maxima) for three data sets (RCO 6 h, RCA4-NEMO 1 h and observed data) to evaluate the parameters of the GEV, Gumbel and 2-parameter Weibull distributions and for subsequent construction of an ensemble of 18 projections at each particular site.

As expected from the basic properties of the employed distributions, the Gumbel fit (that represents exponentially decaying processes such as the ones following a Gaussian distribution) almost always projects higher water levels for longer return periods than the Weibull fit. This is natural as the Weibull fit, in essence, estimates the threshold that is exceeded once during a certain time interval but does not predict the extreme water level itself. A GEV fit (Fréchet or 3-parameter Weibull distribution depending on the particular location; see Soomere et al., 2018) usually provides intermediate values (Fig. 14). Furthermore, different sets of block maxima sometimes match a 2-parameter Weibull and sometimes a Gumbel fit. In general, all projections based on different extreme value distributions largely follow the observed and modelled water level maxima.

The overall appearance of the ensemble of projections is different at single measurement sites. The ensemble, Narva-Jõesuu contains two clusters for return periods of 2 to 10 years (Fig. 14). The estimations based on observed values exceed those based on hindcasts typically by up to 50 cm. It is likely that this difference reflects the local features of the measurement site. The tide gauge is located a few hundred meters upstream of the Narva River mouth. The river flow is occasionally restricted by a sand bar (Laanearu et al., 2007). The sandy seabed is gently sloping and the river mouth is open to one of the predominant wave propagation directions. These are favourable conditions for the formation of local wind driven surge and wave set-up. These phenomena probably quite often contribute to the observed water levels. General circulation models like the RCO model do not resolve these local features.

Starting from the 30-year return period, the two clusters merge and the projections within the ensemble are more or less uniformly distributed. The spread for the return period of 100 years is about 60 cm and reaches about 100 cm for return periods of about 500 years.

The coastal area of Pärnu has one of largest water level variations in the Baltic Sea (Averkiev and Klevanny, 2010) with the highest storm surge, 2.75 m, recorded in 2005 (Suursaar et al., 2006). The outliers of extreme water levels measured in 1953 and 2005 markedly affect the Gumbel and GEV fit while the 2-parameter Weibull fit seems to be largely governed by the rest of the block maxima (Fig. 14). Similar to Narva-Jõesuu, the ensemble for Pärnu has two different “populations” of projections. They deviate by 20 cm for the return period of 15 years and up to 30 cm for the return period of 22 years.

The centres of projections of different clusters coincide for the return period of 30 years. The spread of projections for this return period is about 40 cm. The spread increases up to 150 cm for the return period of 500 years. The different projections are relatively uniformly spread within the ensemble.

The projections for Tallinn are relatively close to each other. The spread of the ensemble is smaller than at Narva-Jõesuu and Pärnu: about 25 cm for the return period of 20 years, 50 cm for 100 years and about 80 cm for 1000 years. This signals consistency of the underlying data and suggests that the middle value of the ensemble is a good estimate for the future extreme water levels at this location.

The ensemble of projections is substantially different at Ristna. The projections based on measured and hindcast block maxima differ radically. The average difference is from 30 cm for the return period of 2 years up to almost 90 cm for the return period of 45 years. The spread of projections within each cluster is fairly limited (below 10 cm) until return periods of about 25 years, and increases to 25–30 cm for return periods of 100 years and to 40–60 cm for return periods of 500 years. The two clusters do not overlap even for the return period of 1000 years. This appearance signals that the modelled and measured maxima may be affected by different factors. The analysis in Paper III provides several arguments in favour of a strong contribution of wave set-up to

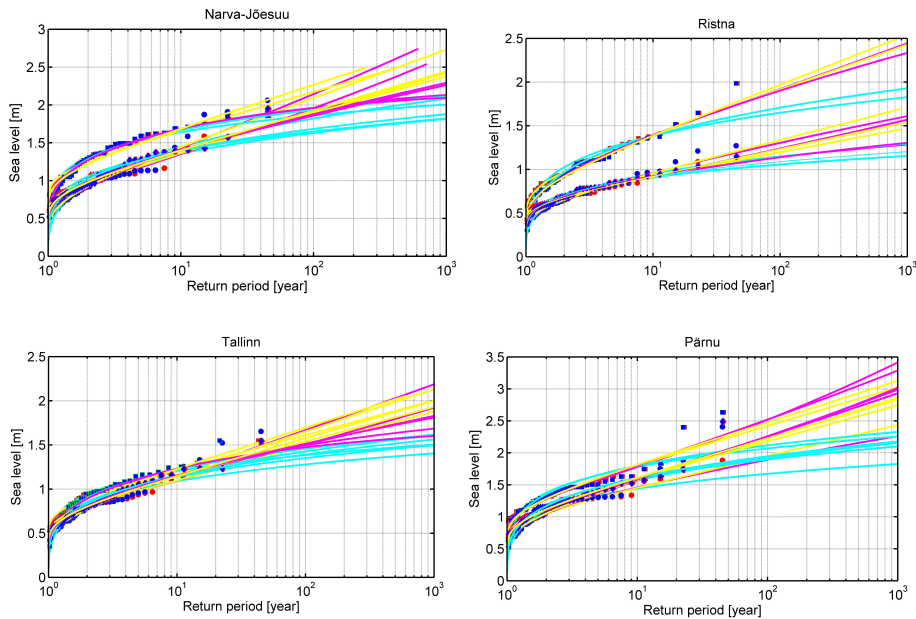


Figure 14. Return periods of extreme water levels calculated from different projections at Narva-Jõesuu, Ristna, Tallinn and Pärnu. Block maxima: red circles – annual maxima of the RCO 6-h data, blue circles – stormy season maxima of the RCO 6-h data; red rhombi – annual maxima of the RCO 1-h data, blue rhombi – stormy season maxima of the RCO 1-h data; red squares – annual maxima of the observed data set; blue squares – stormy season maxima of the observed data set. The markers showing the block maxima derived from the 1-h RCO data almost coincide with those for the RCO 6-h data set. Yellow lines: projections using the Gumbel distribution, magenta – GEV distribution; cyan – 2-parameter Weibull distribution. The difference between the observed and hindcast block maxima corresponding to the calendar years (red) or to stormy seasons (blue) does not become evident at the scale of the image but considerably impacts the relevant projections starting from return periods of about 20 yr (Paper III).

measured water levels at this location. Large waves created by SW storms reach the immediate vicinity of the harbour. Waves with significant wave height >4 m may occur relatively often in this area (Tuomi et al., 2011). Therefore, in ideal conditions, wave set-up may add up to 1 m to the water level at the tide gauge (Dean and Bender, 2006).

The main conclusion of Paper III is that none of the commonly used extreme value distributions is able to perfectly replicate extreme water levels along the coast of Estonia. This conclusion is reinforced in (Soomere et al., 2018). The ensemble approach apparently provides plausible projections for the southern shore of the Gulf of Finland which is geometrically sheltered for the predominant SW wind direction. The results for Pärnu have a relatively large spread apparently because of the presence of “statistically almost impossible outliers” (in the words of Suursaar and Sooäär, 2007) in the water level time series.

The analysis also highlights an unexpected use of ensemble approach for the identification of coastal areas where local effects (in particular, wave set-up) play a significant role in the formation of extreme water levels. The existence of multiple clusters of projections in such locations may help to quantify the proportion of local effects at a particular site (Paper III).

2.5. Separation of short-term and long-term variations

Further analysis of the properties of water level is performed in Paper IV for the nearshore of the eastern Baltic Sea (Fig. 11) and relies on the water level time series produced by the RCO model and described in the Section 2.2.

Dangerous water levels in the eastern Baltic Sea are usually formed by the joint impact of several drivers that generally have different time scales. The temporal course of the Baltic Sea water level has no typical period (Paper IV). Only tidal cycle can be distinguished (Medvedev et al., 2016). As the resulting water level variations are generally aperiodic, standard tools used in the analysis of periodic signals such as spectral (Fourier) analysis are not applicable for the separation of different processes from the time series.

The amplitudes of Fourier components with periods shorter than about 3 weeks decay rapidly. Components that have periods less than about 5–7 days have amplitudes about 1/10 of the typical values of the components with period of about one month (Paper IV). This feature provides a clue for the separation of water level components with different time scales. Namely, it is possible to distinguish variations which are longer than about one week from the more frequent. The weekly-scale components are singled out of the water level time series using a smoothing procedure (running or moving average) in Paper IV. The residual represents relatively short-term water level variations that can be considered as a proxy of single storms. This approach allows the separate analysis of the contribution to extreme water levels of variations in the water volume of the entire Baltic Sea and the impact of single (local) storms.

The outcome of the separation procedure depends on the length T_A of the averaging interval of the smoothing procedure. For short averaging intervals (about 2 days) the resulting smoothed time series contain a few positive outliers. They disappear for $T_A > 3$ days. For $T_A > 10$ days the smoothed water level substantially deviates from the overall course of the water level and apparently is not usable for the separation of single storms from events of elevated water levels of the entire sea.

The appearance of the empirical distribution of the residual also substantially depends on the length of the averaging interval T_A . For intervals less than 3 days both branches of this distribution (for negative and positive surges) are concave in the log-linear plot. For longer averaging intervals (over 10 days) both branches have a convex shape. Both cases can be approximated using a quadratic function.

The coefficient at the leading term of such an approximation vanishes if $T_A \approx 8$ days (Fig. 15). In this case the probabilities for both for low and high storm-driven water levels decay linearly in the log-linear plot (Fig. 16) for a certain range of water levels. In other words, the relevant empirical probability distribution follows the classic exponential distribution $\exp(-\lambda x)$, where x is the water level. The best match of this distribution with the empirical distribution of the residual occurs when $T_A = 8.25$ days (Fig. 16). This value is used in Paper IV for the further analysis.

The running average (equivalently, the weekly-scale component of water level) reasonably replicates the average water level in the entire Baltic Sea. Its largest values reach almost 1 m, that is, about 60% of the extreme water levels (Fig. 16). This estimate is consistent with the fact that the changes in the entire Baltic Sea water volume may be up to 1 m and may substantially contribute to extreme water levels (Leppäranta and Myrberg, 2009). The distribution of the running average largely follows a Gaussian distribution and does not contain any outliers for $T_A > 4$ days. Therefore, probabilities of a substantial contribution of this component into the total water level obtained using $T_A = 8.25$ days can be reasonably quantified using classical Gaussian statistics.

The described separation process thus associates all outliers with the residual signal (that is, with local storms) and indicates that storm-driven variations contribute about 40% to the total water level extremes (Fig. 16). This component of the water level reveals an asymmetry of the high and low water levels and contains numerous positive outliers.

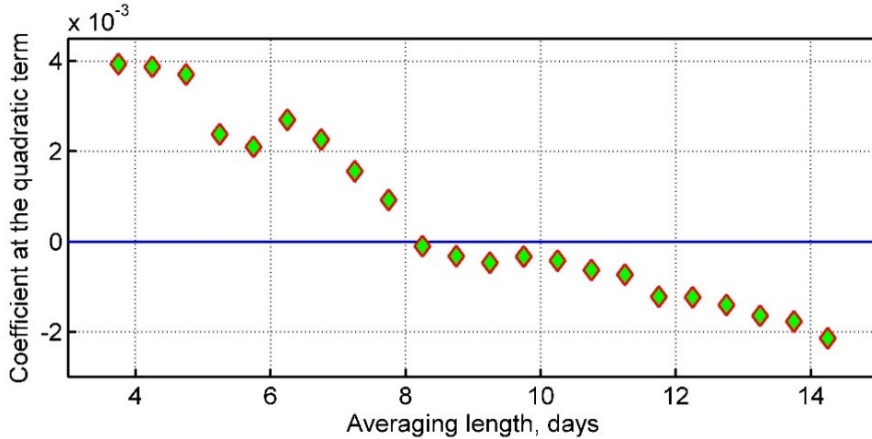


Figure 15. The dependence of the coefficient at the quadratic term in the exponent of the distribution of the positive residual water level variations (positive storm-driven surges) on the length of the averaging interval. The data are the same as in Fig. 16). The quadratic equation is fitted to the interval from 3% down to 0.01% of the probability of occurrence.

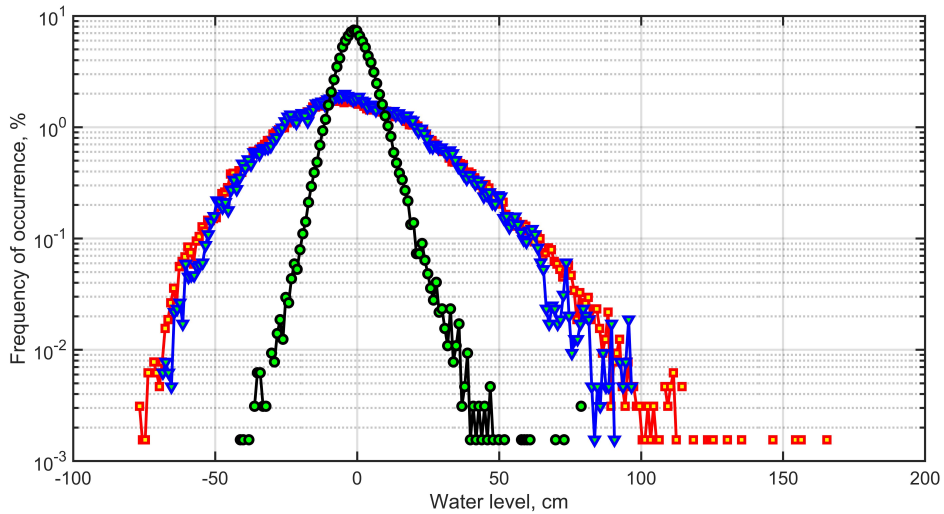


Figure 16. Frequency of occurrence of water levels near Tallinn with the averaging interval of 8 days. Squares: full water level, diamonds: running average of water level (low-frequency variations mimicking the water volume in the Baltic Sea), circles: the residual (that mimics storm-driven variations).

2.6. Spatial variations in the risk of storm surge

The analysis in Paper IV identified that the distribution of the storm driven component almost exactly matches an exponential distribution with the probability density function $\sim \exp(\lambda x)$ for averaging intervals with a length of about 8 days (Fig. 16). This kind of distribution describes *inter alia* that the time between events is a Poisson process. The described separation and the basic properties of the distributions of both water level components are valid for the entire eastern Baltic Sea, including the observed water levels (Paper IV).

This feature makes it possible to quantify to some extent the probability of having very high local storm surges for any location of the study area using just one parameter – the exponent of this distribution λ . The spatial variations of this probability along the study area are conveniently described with the use of the associated scale parameter $-1/\lambda$. Negative values of this parameter characterise negative surges and positive ones – storm-driven high water levels (Fig. 17). This quantification is, in essence, a version of an express method as it ignores the presence of outliers and is only applicable for a limited range of the total water level.

The spatial distribution of the scale parameter of the negative branches of the exponential distribution varies significantly along the eastern Baltic Sea coast (Fig. 17) from absolute values 2.1 up to 5.6. The lowest storm-driven water levels are more likely to occur in the interior of the semi-enclosed sub-basins in the Gulf of Riga and Gulf of Finland. The water levels well below the average are less frequent along the coast of the Baltic proper.

The scale parameters of the distribution of storm-driven positive surges mirror a similar pattern for low water levels in the eastern Baltic Sea. The absolute values of the scale parameter for storm surges are generally larger but less variable along the study

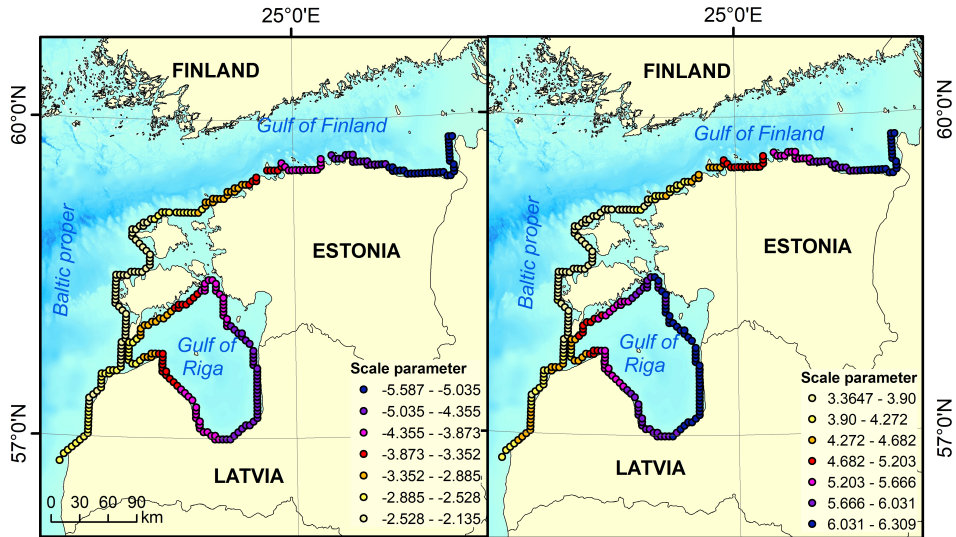


Figure 17. The scale parameter of the exponential distribution of the frequency of occurrence of negative (left panel) and positive (right panel) storm-driven surges in the eastern Baltic Sea.

area (Fig. 17) than those for negative surges. The smallest values are found, as expected, along the coast of Baltic proper and the largest values occur in the interior of the Gulf of Riga and in the eastern Gulf of Finland.

3. Quantification of beach evolution

The development of the beaches in the eastern Baltic Sea is governed by the combination of several hydrodynamic drivers and site-specific peculiarities. The classic cut-and-fill cycle model is not generally applicable for the Baltic Sea beaches. The main reasons are that the highly intermittent wave regime contains a very small proportion of low intensity constructive long swell waves (Broman et al., 2006; Soomere et al., 2012) and the high angle of wave approach that causes intense alongshore sediment transport. Many local conditions such as substantially varying water level, ice conditions, and the geometry of the coastline contribute to the formation of the sediment budget. The beaches often develop in a step-like manner where rapid changes during single severe wave storms are separated by long periods of slow evolution. In particular, the quantification of both short- and long-term variations in the sediment budget during calm seasons is complicated.

High-resolution measurements are the core input for reasonable estimations of the long-term beach evolution in such situations. Papers V and VI describe the technology and outcome of such measurements carried out at Pirita Beach at the south-eastern bayhead of Tallinn Bay. Paper V provides a detailed description of a combination of terrestrial and airborne laser scanning techniques to quantify the changes in the subaerial sand volume of slowly evolving beaches. The quantification of changes in the sand volume is expanded for the entire beach profile using the classical concept of the equilibrium beach with an application of an inverse Bruun's Rule in Paper VI.

3.1. Study area

A combined method of airborne and terrestrial laser scanning together the use of a classic beach theory was tested on a 200 m long section (Fig. 18) of Tallinn Bay (Paper V and VI). The test area, Pirita Beach, is a typical small, embayed beach (Fig. 18). The sandy part of the beach is about 2 km long. The beach suffers from a sand deficit, active foredunes are missing and ancient dunes dominate the landscape further from the shoreline (Orviku, 2018).

The local wave climate in Tallinn Bay is mild (Soomere, 2005) and the overall intensity of the coastal processes is low. The maximum height of the erosion scarp at the edge of the coastal forest is 1.5 m (Orviku, 2018). The shore of the study area is stabilised to some extent by postglacial uplift (about 2 mm/yr, Kall et al., 2014) and by sediment supply from the Pirita River. The stability of the beach is today threatened by an increase in global sea level rise and by the reduction of natural sediment supplies (Soomere and Healy, 2011; Orviku, 2018).

The volume of natural sediment supplied by the Pirita River has substantially decreased since the construction of Pirita Harbour in 1980. This has led to a substantial decrease in the subaerial sand volume between the waterline and coastal scarp (Orviku and Granö, 1992). The beach has suffered from periods of severe destruction due to single storms from unfavourable directions that have created exceptional water levels in the 2000s (Orviku et al., 2003; Soomere et al., 2007; Soomere and Healy, 2011). Approximately 50% of Pirita Beach, mostly its central and northern sections, suffers from damages at times (Soomere et al., 2008).



Figure 18. The study area in Tallinn Bay. The inset shows the location of the test section (blue polygon) and the reference surface (parking lot, green square). Adapted from Paper V.

The most vulnerable part of the Pirita Beach is its approximately 1 km long northern section. The coastal scarp has receded up to 5 m in the northernmost section of the beach. The southern part of the beach is the most stable. It has an about 100 m wide sandy section with an elevation up to 2 m above mean water level near the northern mole of the Pirita River. The central part of Pirita Beach (where the test section is located, Papers V and VI) is in an approximately equilibrium state and has a variable sediment transport direction (Soomere et al., 2011).

3.2. Combining airborne and terrestrial laser scanning technologies

The analysis in Paper V relies on high-resolution measurements using different laser scanning technologies that are combined into a vertically homogenised data set. Laser scanning is a remote sensing method which utilizes laser pulses to measure distances to objects. A basic advantage of this method is its ability to almost instantaneously gather accurate and high-resolution data over the entire surface of the beach. The outcome of the rectification process provides a three-dimensional representation of measured objects in terms of a cloud of surface points.

Terrestrial laser scanning (TLS) is used to acquire higher-resolution spatial data about objects with an accuracy of about 1 cm or even better (Dorninger et al., 2011) and at a vertical resolution of up to a few mm. Airborne laser scanning (ALS) technology is cost-effective in applications where one has to cover large areas. Usually the scanning device is mounted on an aircraft or unmanned aerial vehicle. The density of the point cloud is much lower compared to the clouds generated using the TLS and varies usually

in the range of 0.1–20 points/m². Acquiring high-resolution data requires more flight hours and is therefore more expensive.

The use of repeated ALS surveys makes it possible to create sequences of three-dimensional representations of the beach to assess the dynamics of coastal structures driven by the impacts of storms and the subsequent recovery processes (Dorninger et al., 2011; Grünthal et al., 2014; Johnson et al., 2020). The Estonian Land Board has performed repeated ALS measurements over the Estonian land and coastal areas regularly since 2008, once or twice a year. For the analysis in Papers V and VI the elevation data from Pirita Beach from 2008 to 2013 was retrieved from the database of ALS measurements measured and pre-processed by the Estonian Land Board. Only points classified as 'ground' were used. These ALS data sets were measured from an altitude of 2400 m and with an average density of 0.45 points/m².

A problem with the direct use of this data is that elevation maps in subsequent years usually contain systematic elevation errors. The ALS method involves many parameters that need to be determined for the accurate calculations of coordinates and height of each point in the cloud. In order to determine the position and orientation of the aircraft at any instant, a Global Navigation Satellite System (GNSS) receiver and an Inertial Measurement Unit (IMU) are used. The GNSS receiver records the position and the IMU pitch, roll and yaw of the aircraft. Because of possible errors introduced via calculations of these parameters, the accuracy of results of ALS is less than that of TLS. In favourable conditions the estimated accuracy is usually in the range of 2–15 cm. A large part of deviations from the true value form systematic elevation errors. These can be corrected using local high-precision scanning.

A combination of ALS and TLS techniques was used for the estimations of the changes in sand volume on the subaerial beach at the test section at Pirita Beach (Fig. 19, Papers



Figure 19. Test area at Pirita Beach and the parking lot (reference surface) nearby. Yellow circles: reference points, blue triangles: TLS stations. Reference points were measured with the geodetic accuracy of a GNSS receiver. Adapted from Paper VI.

V and VI). For reliable estimations of the changes in the subaerial beach, the ALS data sets were complemented with TLS measurements with a much higher resolution (about 2×2 cm) measured at Pirita Beach in 2013 and 2014. These high-resolution measurements enabled the reduction of all ALS surfaces to the reference surface using corrections derived from the exact elevation of a large car park near Pirita Beach (Fig. 19). The parking lot has remained unchanged since the first flight in 2008. It was measured using the TLS technology in December 2013 and linked to the measurements on the beach (Paper V). The resulting digital elevation models of the beach were suitable for estimations of the changes in the absolute height of the beach and sediment volume on the subaerial beach.

3.3. Subaerial volume changes

The comparison of digital elevation models from different years reveal a spatial structure of sand accumulation and motion patterns over the years 2008–2010 (Fig. 20, left panel). Loss of sand in those years was almost negligible and occurred only in a few spots. The entire subaerial beach on the test section (Fig. 20) gained about 500 m^3 of sand per year (Table 1). The average increase in the height of the subaerial beach was 20–30 cm (Paper VI).

The processes on the beach between 2010 and May 2014 showed an almost totally opposite pattern (Fig. 20, right panels). The subaerial beach mostly lost sand in an amount almost equal to the total gain in 2008–2010. The total loss of sand was almost 1200 m^3 (Table 1). The changes in the beach height were largest on the upper part of the subaerial beach where most of the sand was lost.

The described changes in the sand volume are consistent with the changing pattern of storms over the period 2008–2013 (Paper V). On the one hand, the wave climate was relatively mild during the years 2008–2010 in the Tallinn Bay area. A relatively large proportion of swells during these years was favourable for beach sand accumulation. On the other hand, the autumn and winter of 2011/2012 and 2012/2013 were

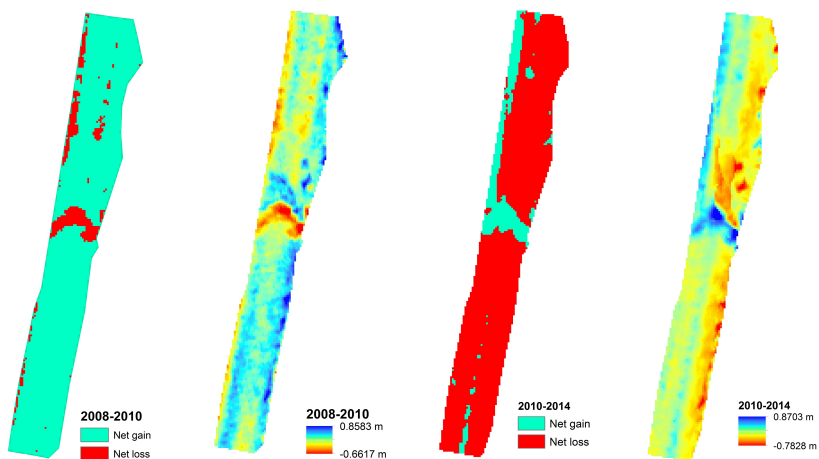


Figure 20. Changes in the beach height in 2008–2010 and 2010–2014. The scale shows the differences in the beach height (m, right) and the relevant erosion (red) and accumulation (blue) areas.

comparatively stormy. The Pirita Beach was frequently impacted by severe wave conditions accompanied by elevated water levels.

The overall pattern of changes in sand volume suggests that a multi-year cycle of erosion and accumulation, with the recovery time of a few years, have occurred at the Pirita Beach similar to the one described in (Dodet et al., 2019). It is likely that the common seasonal “cut and fill” cycle of sandy beaches also occurred in the years in question. Both cycles involve two phases but have different duration. Under severe wave conditions and high water levels waves erode unprotected sediment from the upper part of the beach. The eroded material is mostly deposited within the equilibrium beach profile (EBP). This material is brought back to the vicinity of the waterline either by the onshore motion of sandbars or by regular swells.

Another explanation of the identified patterns is the alongshore motion of sand. As discussed above, the Baltic Sea storm waves often approach the beaches under relatively large angles. However, the Pirita Beach is a pocket beach and thus the transport of large amounts of sand alongshore is not possible. Still it is likely that sand was moved back and forth over the Pirita Beach. This conjecture is some extent supported by earlier simulations that demonstrate a relatively large variability in the direction of the alongshore transport at the Pirita Beach (Soomere et al., 2008).

The overall changes in the sand volume of the subaerial beach during six years 2008 to 2014 were fairly minor (Table I). The changes in the beach height in 2008–2014 are predominantly less than ± 12.5 cm with a total change only of about 300 m³ for the entire subaerial beach.

3.4. Underwater changes

The analysis of the changes in the sand volume on the subaerial part of the beach (Paper V) is extended for the entire active beach profile in Paper VI. A first approximation of the estimations of changes in the sand volume in the underwater part of beach is obtained using the theory of the equilibrium beach profile (EBP) (Dean, 1991) and an application of the so-called Bruun Rule (Bruun, 1962).

For many decades the Bruun Rule has been used to theoretically evaluate the impact of the global sea level rise on sedimentary beaches in terms of a possible retreat of the shoreline. This simple application has provided a useful (albeit not particularly reliable) method for interpreting changes to the beach and for designing beach stabilization projects (Rosati et al., 2013). Approximate methods such as the Bruun Rule continue to be applied in global applications (Vousdoukas et al., 2020) despite being widely criticised (Cooper and Pilkey; 2004; Le Cozannet et al., 2016).

In Paper VI an extension (inversion) of the Bruun Rule was applied to evaluate the changes in the underwater part of the beach profile from the associated shift of the shoreline Δy and closure depth h^* . The change in the volume ΔV over the EBP is expressed as (Kask et al., 2009):

$$\Delta V_{\Sigma} = \int_0^{x_d} h^*(x) \Delta y(x) dx, \quad (8)$$

where the x -axis is directed alongshore, the y -axis is perpendicular to the shoreline and the integral is taken from the shoreline to the location where the water depth reaches the closure depth. This approximation is only reasonable for small values (a few metres) of the shift of the shoreline Δy . The closure depth along the entire Pirita Beach varies

insignificantly (2.4–2.6 m, Kask et al., 2009; Soomere et al., 2017a). For this reason, in Paper VI the closure depth is considered as constant 2.5 m for the test area (Fig. 19). The shift of the shoreline Δy is retrieved from the location of the shoreline evaluated from laser scanned data in 2008–2014.

The analysis relies on the widely used shape of the EBP that corresponds to the uniform wave energy dissipation per unit water volume in the surf zone (Dean and Dalrymple, 2002). On such occasions the water depth at the distance y from the waterline down to the closure depth is expressed as $h(y) = Ay^{2/3}$. The profile scale factor A (which depends on the predominant grain size) is immaterial for the quantification of volume changes in Eq. (8) (Kask et al., 2009).

The approach in Paper VI is to some extent controversial as it combines an extremely reliable and accurate way of measuring changes in the subaerial beach using laser scanning with a very coarse application of the Bruun Rule and the EBP theory, both of which have been critically reviewed in the literature (Cooper and Pilkey, 2004). Strictly speaking, this approach based on the Bruun Rule is applicable only in coastal segments where the EBP is clearly evident and the seabed rapidly deepens starting from the closure depth. This is the case for the sandy part of Piritä Beach (Soomere et al., 2007). Existing observations, and simulations for Piritä Beach and in other locations of the Estonian nearshore (Soomere et al., 2007; Kartau et al., 2011; Soomere and Healy, 2011) suggest that both the concept of EBP and the inversion of the Bruun Rule provide an acceptable description of the phenomena in question.

However, the existing laboratory and field studies have not convincingly demonstrated the validity of the Bruun Rule (Stive, 2004). Even though much uncertainty may arise from noise in the data (Pilkey and Davis, 1987; Bruun, 1988; List et al., 1997), the quantitative estimates in Paper VI should be interpreted with care as long there is no alternative verification of the outcome.

3.5. Changes in underwater part of the beach profile

Paper VI makes an attempt to roughly estimate the underwater volumetric changes for the short test section at Piritä Beach (Fig. 19). As described above, the estimates are performed using a simple application of the Bruun Rule. Equation (9) suggests that the change in the underwater sediment volume over the EBP is, to a first approximation, proportional to the gain or loss of the dry beach area. The shape of the beach in the vicinity of the waterline and the location of the waterline itself may be subject to rapid and essentially random variations and thus are not always representative of the changes in the underwater sand volume. The appearance of the beach between the landward end of the swash zone and foredunes is often much more homogeneous and representative (Smith and Bryan, 2007).

The analysis in Paper VI considered the shift of various height isolines between 0.3–0.7 m with a step of 0.1 m. Changes in the position of four isolines representing the heights 0.4–0.7 m in different years were highly coherent along the test area (Fig. 21). The average shifts of these isolines in different years were used to represent the shift of the waterline in Eq. (8).

The gain in dry beach area in 2008–2010, estimated from the shift of these isolines, was about 1172 m² (Paper VI). In 2010–2014 these isolines moved towards the shore. The estimated loss of land was about 873 m². The changes over entire period from 2008–2014 were relatively small, about 581 m².



Figure 21. Changes in the position of the isolines (0.5 m and 0.6 m) in 2008–2010.

Consequently, about 2930 m³ of sand was added to the underwater part of the beach in 2008–2010 (Table 1). The total gain of sand for the entire EBP was thus 4444 m³. The amount of sand lost in 2010–2014 was comparable with the gain in previous years (3400 m³). The subaerial part lost about 1200 m³ and the underwater profile about 2200 m³. These estimates suggest that the classic cut and fill model could be only conditionally applied to the Pirita Beach as the total volume of sand in dry and underwater parts of the beach varies considerably.

The results, albeit containing a large uncertainty for the underwater section, indicate that changes in the sediment volume from the waterline to the closure depth (about 2.5 m for the test area at Pirita Beach) are much (by a factor of 2–2.5) larger than similar changes in the subaerial part of the beach. Although this feature may reflect the small amount of contemporary marine sand in the subaerial part of the test area, it still suggests that underwater processes in the nearshore may actually predominate the evolution and fate of almost equilibrium beaches of the north-eastern Baltic Sea.

Table 1. Changes in sand volume (m³) over the subaerial beach and down to the closure depth in the test area in 2008–2014.

Time interval	Subaerial beach	Underwater profile	Total
2008-2010	1514	2930	4444
2010-2014	–1188	–2183	–3371
2008-2014	302	1453	1755

Conclusions

Summary of the results

The presented studies focus on the properties of drivers of the long-term evolution of beaches in the eastern Baltic Sea and on methods to assist in the quantification of the sediment budget on these beaches. Large parts of this coastal area are exposed to the predominant wind directions from SW and NNW. Many coastal segments consist of easily erodible sediments and are thus vulnerable to strong waves and high water levels.

The central objectives were to: (i) quantify the approaching wave energy flux to the coast and its spatio-temporal variability in the eastern Baltic Sea (ii) adequately project extreme water level events and their return periods in different coastline segments, (iii) identify the components of the extreme water levels and their contribution to the total water level, (iv) develop an express method for the quantification of long-term beach evolution using a combination of the high-resolution measurements and a theory of sandy beaches.

An estimate of spatio-temporal variations in the intensity of coastal processes in the eastern Baltic Sea was established in terms of the onshore wave energy flux. The calculations relied on a wave hindcast for the entire Baltic Sea for 1970–2007.

The calculations provided the first systematic quantification of wave energy potential in Estonian coastal waters. The estimated onshore wave energy flux (also called wave power) reveals substantial spatial variability. On average, it is about 1.5 kW/m and reaches up to 2.55 kW/m in selected locations of the north-eastern Baltic proper. The wave energy resources are much smaller, normally around 0.6–0.7 kW/m, in the interior of the Gulf of Finland and in the Gulf of Riga. The theoretical total wave energy flux for the eastern Baltic Sea shore from the Sambian Peninsula until the eastern part of Gulf of Finland is about 1.5 GW.

Several locations in the Bay of Gdańsk and eastern Gulf of Finland have much larger resources of wave energy than other areas. This peculiarity is apparently caused by the match of certain predominant wind directions with the shape and orientation of the Baltic Proper and the Gulf of Finland.

The greatest limiter for the practical use of wave energy in the Baltic Sea is high temporal intermittency of the wave energy flux. During the roughest sea conditions, instantaneous onshore wave energy flux may exceed the long-term average flux by two orders of magnitude. The strongest storms in a year bring most of the annual available wave energy to the shore. Around 90% of wave energy arrives within the three stormiest weeks in a year. Most of the energy is transported to the shore by wave fields with a significant wave height about 2–4 m and a peak period about 6–9 s.

Rapid evolution of fine sediment beaches in the eastern Baltic Sea occurs when high waves reach the unprotected coast simultaneously with an elevated water level. The development of reliable projections of extreme water levels in the eastern Baltic Sea is a complicated task because periods of very high elevated water levels are driven by the joint impact of several mechanisms. The possibilities and challenges for solving this task by means of building an ensemble of projections for extreme water levels and their return periods are analysed using observed water levels from four tide gauges, offshore sea level time series numerically reconstructed using the RCO (Rossby Center, Swedish Meteorological and Hydrological Institute) ocean model for 1961–2005, and classic extreme value distributions. This approach provides a reasonably spread cluster of projections for extreme water levels and their return periods for two locations

(Narva-Jõesuu, Tallinn) on the southern coast of the Gulf of Finland. The projections for Pärnu in the Gulf of Riga in south-eastern Estonia have a relatively large spread but the ensemble average provides a consistent projection for the future water levels. The use of this approach revealed major mismatch for projections based on modelled and measured values at Ristna. The most probable reason for this mismatch is the impact of local effects (e.g., wave set-up) that play a significant role in the formation of extreme water levels. Based on this observation, the use of multiple clusters of projections in the ensemble approach as an indicator of the important proportion of local effects at a particular site is recommended.

Extreme water levels in the Baltic Sea are usually caused by several components that are driven by different mechanisms that have different spatial and temporal scales. The contribution of these components is explored by means of splitting the water level time series into two components using a running average. The average over about a week approximately follows a Gaussian distribution and reflects the water level of the entire Baltic Sea whereas the residual is a proxy of the local storm surge. If the running average is applied over 8.25 days, the short-term component almost exactly follows an exponential distribution. The slopes of the positive and negative branches of this distribution (for low- and high-water levels, respectively) provide a useful express method for the quantification of the range of local flooding heights in different coastal areas. As expected, this method predicts the highest local storm surges to occur in the interior of the semi-enclosed gulfs in the eastern Gulf of Riga and Gulf of Finland.

An attempt is made to quantify the evolution in the sandy beaches in the Baltic Sea using a combined data set from high-resolution airborne and terrestrial laser scanning measurements. This technology is able to reveal many details of the evolution of sandy beaches as demonstrated in a test section of Pirita Beach in Tallinn Bay on the southern coast of the Gulf of Finland. The changes in the sand volume in the subaerial beach, quantified by a comparison of digital elevation models in different years, show large temporal variations but very moderate changes over 6–7 years. The changes in the underwater part of the beach profile are approximately estimated using an inverse of the Bruun Rule applied within the concept of equilibrium beach profile. The estimated changes in the underwater sand volume are much larger than in the subaerial beach.

Main conclusions proposed to defend

1. Wave energy flux is calculated for the eastern Baltic Sea coast. The total wave power from the Sambian Peninsula to the eastern part of the Gulf of Finland is 1500 MW. The Bay of Gdańsk and the interior of the eastern part of Gulf of Finland may provide up to 450 MW of total wave power.
2. Wave energy flux has extensive spatio-temporal variability in the Baltic Sea. The long-term average energy flux along the coast of eastern Baltic Sea varies from 0.5 kW/m up to 2.55 kW/m. Instantaneous wave energy flux during strong storms may exceed the long-term average by two orders of magnitude.
3. The few strongest storms in the year are responsible for most of the annual energy arriving to the coast. About 30% of the annual energy arrives at the coast within 3–4 days. The waves with a significant wave height of 2–4 m and a peak period of 6–9 s transport the largest amount of energy to the coast.
4. The ensemble approach provides reasonable estimations for projections of future extreme water levels and their return periods in the eastern Baltic Sea. It also provides a tool for identifying the coastal areas where local effects contribute substantially to extreme water levels.
5. A method is developed to split the water level time series in the Baltic Sea into two components that reflect storm surges and the water volume of the entire Baltic Sea, using a running average. For an averaging length of about 8 days the distribution of the proxy for local storm surges follows the exponential distribution and contains all outliers. An express quantification of the risk of local flooding in different coastal sections is developed based on the exponent of the exponential distribution.
6. A method for the quantification of changes to the beach during its slow evolution phase is developed by combining airborne and terrestrial laser scanning technology. This method is applied to estimate interannual changes in the sand volume of Pirita Beach.
7. An express method to estimate the volume changes over the entire beach profile is suggested by jointly using laser scanning measurements and the equilibrium beach theory. This method shows that changes in the underwater section of the beach may be considerably larger than changes on the subaerial beach.

Recommendations for further work

- In the light of presented results of the systematic wide-scale calculations of wave energy flux and the developed method for the estimation of extreme water levels for the eastern Baltic Sea, the natural next step is to identify the coastal areas where the combined effect of high waves and extreme water levels is more likely to occur, which possibly contributes to possible large-scale coastal erosion. This allows more detailed and more useful studies of coastal processes, to more exactly determine the extent of flooding and wave impact on the affected coastal areas, and to identify both vulnerable and resilient coastal segments.
- From the viewpoint of gaining more detailed understanding and knowledge of coastal processes on the Baltic Sea coast, it makes sense to study more deeply the coastal areas that have specific peculiarities of hydrometeorological forcing. Driving forces of coastal processes are highly variable along this geometrically diverse coast. The techniques of determining the properties and impacts of single factors make it possible to separately analyse the conditions when a specific driver is governing coastal evolution at a certain location. This approach could be realised using the methods presented in Papers V–VI together with hydrometeorological data.
- It is essential to continue with the analyses of sand volume changes on subaerial beaches (based on the laser scanner data that are regularly surveyed by the Estonian Land Board). It is equally important to carry out physical measurements of the underwater beach profile for estimations of the sediment volume changes over the entire beach profile. This work is urgently needed to improve and/or validate the sediment flux modelling results obtained in the eastern Baltic Sea beaches. It would also be an inherent component of, e.g., planning of beach nourishment activities. Extensive empirical measurements may also result in important modifications of the widely used equations for estimations of sediment fluxes for the Baltic Sea coasts.
- The Baltic Sea is a suitable place to test the proposed approach presented in Paper VI of using the inverse Bruun Rule for sand volume estimations on the underwater part of the beach profile. The uplifting coasts of the Baltic Sea are suitable test locations where the equilibrium beach profile apparently often exists and the seabed deepens rapidly seaward of the closure depth. The adequacy of the outcome of this approach can be evaluated, for example, in locations where the natural alongshore sediment transport has been blocked by a large coastal engineering structure.
- Most of the future climate change scenarios suggest an increase in coastal erosion and more frequent and severe coastal flooding. Even though wave energy conversion into grid electricity might not be economically viable, further studies of the potential of the wave energy converters from the viewpoint of coastal protection are worth investigating. Such converters may serve as a viable alternative for breakwaters in some locations, slowing littoral flow of sediments to benefit coastal stretches that suffer from erosion, or to partially protect open landing places against high waves.
- Finally, the further development of the ensemble approach technique has the potential to lead to the most reasonable projections of extreme water levels in coastal areas in Baltic Sea, and also to identify shortcomings of new circulation and water level models.

List of figures

Figure 1. The Baltic Sea. Yellow nearshore squares: study area in Paper I, orange squares: study areas in Paper II.	19
Figure 2. Nearshore grid cells of the wave model along the eastern Baltic Sea coast and in the Gulf of Riga. Four selected points (24, 73, 147 and 194), used to characterise wave energy resources at single locations, are marked by black squares. Coloured segments indicate the total wave power over the coastal section. Adapted from Paper I.	22
Figure 3. The location of the converter line through wave model grid cells near the western tip of the island of Saaremaa, Estonia. Adapted from Paper I.	23
Figure 4. Long-term average wave energy flux along the coasts of the eastern Baltic proper, Gulf of Finland and Gulf of Riga in 1970–2007. Adapted from Paper I.	24
Figure 5. Long-term average wave energy flux along the Bay of Gdańsk (left panel) and the eastern Gulf of Finland (right panel) in 1970–2007. Adapted from Paper II.	26
Figure 6. Instantaneous onshore wave energy flux at grid cells No 73 and 194 (see Fig. 2) in the nearshore of Saaremaa in the north-eastern Baltic proper and in the eastern Gulf of Riga in selected 5 years. The red horizontal line indicates the average wave energy flux for the location.	27
Figure 7. Seasonal course of the monthly onshore wave energy flux (bars) and the monthly standard deviation of single values (lines) summarised for the coastal stretches from the Sambian Peninsula to the Irbe Strait (Kurzeme, yellow), Western Estonia (green), Gulf of Riga (magenta) and Gulf of Finland (cyan).	27
Figure 8. The proportion of the average wave energy flux in different seasons over longer coastal stretches in (wide bars) and in grid cells Nos. 24, 73, 147 and 194 in Fig. 2 (narrow white bars).	28
Figure 9. Combined scatter and energy diagram for two selected wave model grid cells: (a) point 73 near Saaremaa in Fig. 2, b) point 21 in Fig 5, nearshore of Bay of Gdańsk. The numbers show the annual average of hours with the relevant wave conditions with a resolution of 0.5 m in wave heights and 1 s in wave periods for 1970–2007. The colour scale shows the annual bulk energy resource [kW·h/m] carried onshore by wave fields with the relevant wave properties with a resolution of 0.5 m in wave heights and 0.5 s for waves with periods less than 7 s and 1 s for waves with periods longer than 7 s. Solid blue lines present isolines of instantaneous energy flux.	29
Figure 10. Cumulative annual energy flux at four selected points in the study area (Fig. 2) Blue: the border between Latvia and Lithuania, red: western coast of Saaremaa, black: eastern Gulf of Finland, cyan: eastern Gulf of Riga. The inset reflects the contribution of the most intense wave fields for 360 h (15 days) a year (Paper I).	29
Figure 11. Observations sites at Tallinn, Pärnu, Ristna and Narva-Jõesuu (red circles) and the locations of offshore grid cells of the RCO model (black squares) used in Paper III, and the locations of the RCO grid cells used in Paper IV.	32
Figure 12. Frequency of occurrence of deviations of the water level from the long-term mean in the RCO simulations near Tallinn (6-h values from 1961–2005).	33

Figure 13. Return periods of extreme water levels at Narva-Jõesuu calculated from the results of the 6-h RCO data (upper panels) and the observed 1-h data set (lower panels, a semi-synthetic data set obtained based on observations and the output of the HIROMB model). The panels on the left correspond to projections based on annual maxima, the panels on the right – to projections based on maxima over stormy seasons. Markers represent single block maxima. 35

Figure 14. Return periods of extreme water levels calculated from different projections at Narva-Jõesuu, Ristna, Tallinn and Pärnu. Block maxima: red circles – annual maxima of the RCO 6-h data, blue circles – stormy season maxima of the RCO 6-h data; red rhombi – annual maxima of the RCO 1-h data, blue rhombi – stormy season maxima of the RCO 1-h data; red squares – annual maxima of the observed data set; blue squares – stormy season maxima of the observed data set. The markers showing the block maxima derived from the 1-h RCO data almost coincide with those for the RCO 6-h data set. Yellow lines: projections using the Gumbel distribution, magenta – GEV distribution; cyan – 2-parameter Weibull distribution. The difference between the observed and hindcast block maxima corresponding to the calendar years (red) or to stormy seasons (blue) does not become evident at the scale of the image but considerably impacts the relevant projections starting from return periods of about 20 yr (Paper III). 37

Figure 15. The dependence of the coefficient at the quadratic term in the exponent of the distribution of the positive residual water level variations (positive storm-driven surges) on the length of the averaging interval. The data are the same as in Fig. 16). The quadratic equation is fitted to the interval from 3% down to 0.01% of the probability of occurrence. 39

Figure 16. Frequency of occurrence of water levels near Tallinn with the averaging interval of 8 days. Squares: full water level, diamonds: running average of water level (low-frequency variations mimicking the water volume in the Baltic Sea), circles: the residual (that mimics storm-driven variations). 40

Figure 17. The scale parameter of the exponential distribution of the frequency of occurrence of negative (left panel) and positive (right panel) storm-driven surges in the eastern Baltic Sea. 41

Figure 18. The study area in Tallinn Bay. The inset shows the location of the test section (blue polygon) and the reference surface (parking lot, green square). Adapted from Paper V. 43

Figure 19. Test area at Pirita Beach and the parking lot (reference surface) nearby. Yellow circles: reference points, blue triangles: TLS stations. Reference points were measured with the geodetic accuracy of a GNSS receiver. Adapted from Paper VI. 44

Figure 20. Changes in the beach height in 2008–2010 and 2010–2014. The scale shows the differences in the beach height (m, right) and the relevant erosion (red) and accumulation (blue) areas. 45

Figure 21. Changes in the position of the isolines (0.5 m and 0.6 m) in 2008–2010. 48

References

- Abanades J., Greaves D., Iglesias G. 2014. Coastal defence through wave farms. *Coastal Engineering*, 91, 299–307, doi: 10.1016/j.coastaleng.2014.06.009.
- Abanades J., Greaves D., Iglesias G. 2015. Coastal defence using wave farms: the role of farm-to-coast distance. *Renewable Energy*, 75, 572–582, doi: 10.1016/j.renene.2014.10.048.
- Abanades J., Flor-Blanco G., Flor G., Iglesias G. 2018. Dual wave farms for energy production and coastal protection. *Ocean & Coastal Management*, 160, 18–29, doi: 10.1016/j.ocecoaman.2018.03.038.
- Adger W.N., Hughes T.P., Folke C., Carpenter S.R., Rockström J. 2005. Social-ecological resilience to coastal disasters. *Science*, 309, 1036–1039, doi: 10.1126/science.1112122.
- Alcorn R. 2014. Wave Energy. In: Letcher T.M. (ed.), *Future Energy* (2nd ed.). Improved, Sustainable and Clean Options for our Planet, 357–382, doi: 10.1016/B978-0-08-099424-6.00017-X.
- Alexandrakis G., Poulos S.E. 2015. A holistic approach to beach erosion vulnerability assessment. *Scientific Reports*, 4, 6078, doi: 10.1038/srep06078.
- Ardhuin F, O'Reilly W.C., Herbers T.H.C., Jessen P.F. 2003. Swell transformation across the continental shelf. Part I: attenuation and directional broadening. *Journal of Physical Oceanography*, 33, 1921–1939, doi: 10.1175/1520-0485(2003)033<1921:STATCS>2.0.CO;2.
- Arinaga R.A., Cheung K.F. 2013. Atlas of global wave energy from 10 years of reanalysis and hindcast data. *Renewable Energy*, 39(1), 49–64, doi: 10.1016/j.renene.2011.06.039.
- Arns A., Wahl T., Haigh I.D., Jensen J., Pattiaratchi C. 2013. Estimating extreme water level probabilities: a comparison of the direct methods and recommendations for best practise. *Journal of Coastal Engineering*, 81, 51–66, doi: 10.1016/j.coastaleng.2013.07.003.
- Ashton A., Murray A., Arnault O. 2001. Formation of coastline features by large-scale instabilities induced by high-angle waves. *Nature*, 414(6861), 296–300.
- Averkiev A.S., Klevanny K.A. 2010. A case study of the impact of cyclonic trajectories on sea-level extremes in the Gulf of Finland. *Continental Shelf Research*, 30(6), 707–714, doi: 10.1016/j.csr.2009.10.010.
- Benumof B., Storlazzi C., Seymour R., Griggs G. 2000. The relationship between incident wave energy and seacliff erosion rates: San Diego County, California. *Journal of Coastal Research*, 16, 1162–1178.
- Berins J., Petrichenko L. 2019. Economical valuation of wave power plant in the Baltic Sea region at pre-flexibility stage. *Latvian Journal of Physics and Technical Sciences*, 56(6), 32–46, doi: 10.2478/lpts-2019-0033.
- Bernhoff H., Sjostedt E., Leijon M. 2006. Wave energy resources in sheltered sea areas: a case study of the Baltic Sea. *Renewable Energy*, 31(13), 2164–2170, doi: 10.1016/j.renene.2005.10.016.
- Bird E.C.F. 2008. *Coastal Geomorphology: An Introduction* (2nd edn.), Wiley and Sons, Chichester, 436 pp.

- Björkqvist J.V., Tuomi L., Tollman N., Kangas A., Pettersson H., Marjamaa R., Jokinen H., Fortelius C. 2017. Characteristic properties of extreme wave events observed in the northern Baltic Proper, Baltic Sea. *Natural Hazards and Earth System Sciences*, 17(9), 1653–1658, doi: 10.5194/nhess-17-1653-2017.
- Blazauskas N., Pasilis A., Knolis A. 2015. Potential applications for small scale wave energy installations. *Renewable & Sustainable Energy Reviews*, 49, 297–305, doi: 10.1016/j.rser.2015.04.122.
- Brenninkmeyer B.M. 1982. Cut and fill. In: *Beaches and Coastal Geology*. Encyclopedia of Earth Science. Springer, Boston, MA, doi: 10.1007/0-387-30843-1.
- Broman B., Hammarklint T., Rannat K., Soomere T., Valdmann A. 2006. Trends and extremes of wave fields in the north–eastern part of the Baltic Proper, *Oceanologia*, 48(S), 165–184.
- Bruun P. 1962. Sea level rise as a cause of erosion. *Journal of the Waterways and Harbors Division – ASCE*, 88(1), 117–133.
- Bruun P. 1988. The Bruun Rule of erosion by sea level rise: a discussion on large-scale two- and three-dimensional usages. *Journal of Coastal Research*, 4, 627–648.
- Carter R.W.G., Jennings S.C., Orford J.D. 1990. Headland erosion by waves. *Journal of Coastal Research*, 6(3), 517–529.
- Cazenave A., Dieng H-B., Meyssignac B., von Schuckmann K., Decharme B., Berthier E. 2014. The rate of sea-level rise. *Nature Climate Change*, 4, 358–361, doi: 10.1038/nclimate2159, 2014.
- Chini N., Stansby P.K. 2012. Extreme values of coastal wave overtopping accounting for climate change and sea level rise. *Coastal Engineering*, 65, 27–37, doi: 10.1016/j.coastaleng.2012.02.009.
- Cohen J.E., Small C., Mellinger A., Gallup J., Sachs J. 1997. Estimates of coastal populations. *Science*, 278, 1211–1212, doi: 10.1126/science.278.5341.1209c.
- Coles S. 2001. *An Introduction to Statistical Modeling of Extreme Values*. Springer, London, doi: 10.1007/978-1-4471-3675-0.
- Cooper J.A.G., Pilkey O.H. 2004. Sea-level rise and shoreline retreat: time to abandon the Bruun Rule. *Global and Planetary Change*, 43, 157–171, doi:10.1016/j.gloplacha.2004.07.001.
- Cruz J. (ed.). 2008. *Ocean Wave Energy: Current Status and Future Perspectives*. Green Energy and Technology. Springer: Berlin, 431 pp.
- Dailidiene I., Davulienė L., Stankevičius A., Myrberg K. 2006. Sea level variability at the Lithuanian coast of the Baltic Sea. *Boreal Environment Research*, 11, 109–121.
- Dean R.G. 1991. Equilibrium beach profiles: characteristics and applications. *Journal of Coastal Research*, 7, 53–84.
- Dean R.G., Bender C.J. 2006. Static wave set-up with emphasis on damping effects by vegetation and bottom friction. *Coastal Engineering*, 53, 149–165, doi: 10.1016/j.coastaleng.2005.10.005.
- Dean R.G., Dalrymple R.A. 2002. *Coastal Processes with Engineering Applications*. Cambridge University Press, Cambridge, 475 pp, doi: 10.1017/CBO9780511754500.

- Dodet G., Castelle B., Masselink G., Scott T., Davidson M., Floc'h. F., Jackson D., Suanes S. 2019. Beach recovery from extreme storm activity during the 2013-14 winter along the Atlantic coast of Europe. *Earth Surface Processes and Landforms*, 44(1), 393–401, doi: 10.1002/esp.4500.
- Dorninger P., Szekely B., Zamolyi A., Roncat, A. 2011. Automated detection and interpretation of geomorphic features in LiDAR point clouds. *Vermessung & Geoinformation*, 2, 60–69.
- Eberhards G. 2003. The Sea Coast of Latvia (Morphology. Structure. Coastal Processes. Risk Zones. Forecast. Coastal protection and monitoring). University of Latvia, Riga, 292 pp. (in Latvian).
- Eberhards G.I., Lapinskis J., Purgalis I., Salupe B., Torklere A. 2009. Changes in Latvia's seacoast (1935–2007). *Baltica*, 22(1), 11–22.
- Eelsalu M., Soomere T., Julge K. 2015. Quantification of changes in the beach volume by the application of an inverse of the Bruun Rule and laser scanning technology. *Proceedings of the Estonian Academy of Sciences*, 64(3), 240–248 doi: 10.3176/proc.2015.3.06.
- Flor-Blanco G., Pando L., Morales J.A., Flor G. 2015. Evolution of beach–dune fields systems following the construction of jetties in estuarine mouths (Cantabrian coast, NW Spain). *Environmental Earth Sciences*, 73(3), 1317–1330.
- Franck H., Matthäus W. 1992. The absence of effective major inflows and the present changes in the hydrographic conditions of the central Baltic deep water. *Proceedings of the 12th Baltic Marine Biologists Symposium, Helsingør, Denmark, 25–30 August 1991, Olsen & Olsen*, 53–60.
- Grinsted A. 2015. Projected change–Sea level. In: BACC II Author Team, Second assessment of climate change for the Baltic Sea basin, 253–263. London: Springer.
- Grünthal E., Gruno A., Ellmann A. 2014. Monitoring of coastal processes by using airborne laser scanning data. In Cygas D. (ed.), Selected papers of the 9th International Conference on Environmental Engineering, Vilnius, Lithuania, 22–23, May, 2014. Vilnius: Vilnius Gediminas Technical University Press “Technika”, 7 pp.
- Hagenaars G., de Vries S., Luijendijk A.P., de Boer W.P., Reniers J.H.M. 2018. On the accuracy of automated shoreline detection derived from satellite imagery: a case study of the sand motor mega-scale nourishment. *Journal of Coastal Engineering*, 133, 113–125, doi: 10.1016/j.coastaleng.2017.12.011.
- Haigh I.D., Wijeratne E.M.S., MacPherson L.R., Pattiaratchi C.B., Mason M.S., Crompton R.P., George S. 2014. Estimating present day extreme water level exceedance probabilities around the coastline of Australia: tides, extra-tropical storm surges and mean sea level. *Journal of Climate Dynamics*, 42, 121–138, doi:10.1007/s00382-012-1652-1.
- Hanson H., Larson M. 2008. Implications of extreme waves and water levels in the southern Baltic Sea. *Journal of Hydraulic Research*, 46(sup2), 292–302, doi: 10.1080/00221686.2008.9521962.
- Harff J., Meyer M. 2011. Coastlines of the Baltic Sea – zones of competition between geological processes and a changing climate: examples from the southern Baltic. In: Harff J., Björck S., Hoth P. (eds.) *The Baltic Sea Basin*, Springer, Berlin/Heidelberg, 149–164.

- Harff J., Furmańczyk K., von Storch H. (eds.) 2017. Coastline Changes of the Baltic Sea from South to East: Past and Future Projection, Springer, Coastal Research Library, 386 pp, doi: 10.1007/978-3-319-49894-2.
- Hawkes P.J. 2008. Joint probability analysis for estimation of extremes. *Journal of Hydraulic Research*, 246–256, doi: 10.1080/00221686.2008.9521958.
- Höglund A., Meier H.E.M. 2012. Environmentally safe areas and routes in the Baltic Proper using Eulerian tracers. *Marine Pollution Bulletin*, 64, 1375–1385, doi: 10.1016/j.marpolbul.2012.04.021.
- Hughes M.G., Heap A.D. 2010. National-scale wave energy resource assessment for Australia. *Renewable Energy*, 35, 1783–1791, doi: 10.1016/j.renene.2009.11.001.
- Hünicke B., Zorita E. 2008. Trends in the amplitude of Baltic Sea level annual cycle. *Tellus A*, 60(1), 154–164, doi: 10.1111/j.1600-0870.2007.00277.x.
- Hünicke B., Zorita E., Soomere T., Madsen K.S., Johansson M., Suursaar Ü. 2015. Recent Change – Sea Level and Wind Waves. In: The BACC II Author Team, Second Assessment of Climate Change for the Baltic Sea Basin, Regional Climate Studies, Springer, 155–185, doi: 10.1007/978-3-319-16006-1_9.
- IPCC 2013. Climate Change 2013: The Physical Science Basis. Contribution of Working Group I to the Fifth Assessment Report of the Intergovernmental Panel on Climate Change [Stocker T.F., Qin D., Plattner G.-K., Tignor M., Allen S.K., Boschung J., Nauels A., Xia Y., Bex V., Midgley P.M. (eds.)]. Cambridge University Press, Cambridge, United Kingdom and New York, NY, USA, 1535 pp, doi: 10.1017/CBO9781107415324.
- Jaagus J. 2006. Trends in sea ice conditions on the Baltic Sea near the Estonian coast during the period 1949/50–2003/04 and their relationships to large-scale atmospheric circulation. *Boreal Environment Research*, 11(3), 169–183.
- Jaagus J., Suursaar U. 2013. Long-term storminess and sea level variations on the Estonian coast of the Baltic Sea in relation to large-scale atmospheric circulation. *Estonian Journal of Earth Sciences*, 62(2), 73–92, doi: 10.3176/earth.2013.07.
- Jackson N.L., Nordstrom K.F., Eliot I., Masselink G. 2002. ‘Low energy’ sandy beaches in marine and estuarine environments: a review. *Geomorphology*, 48, 147–162, doi: 10.1016/S0169-555X(02)00179-4.
- Jacobson M.Z. 2009. Review of solutions to global warming, air pollution, and energy security. *Energy & Environmental Science*, 21, 48–73, doi: 10.1039/B809990C.
- Johansson M.M., Kahma K.K. 2016. On the statistical relationship between the geostrophic wind and sea level variations in the Baltic Sea. *Boreal Environment Research*, 21(1–2), 25–43, 2016.
- Johansson M., Boman H., Kahma K., Launiainen J. 2001. Trends in sea level variability in the Baltic Sea. *Boreal Environment Research*, 6, 159–179.
- Johansson M., Pellikka H., Kahma K., Ruosteenoja K. 2014. Global sea level rise scenarios adapted to the Finnish coast. *Journal of Marine Systems*, 129, 35–46.
- Johnson L., Chen Q., Ozdemir C.E. 2020. Lidar time-series analysis of a rapidly transgressing low-lying mainland barrier (Caminada Headlands, Louisiana, USA). *Geomorphology*, 352, 106979, doi: 10.1016/j.geomorph.2019.106979.
- Jönsson A., Broman B., Rahm L. 2003. Variations in the Baltic Sea wave fields. *Ocean Engineering*, 30, 107–126, doi.org/10.1016/S0029-8018(01)00103-2.

- Kall T., Oja T., Tänavsuo K. 2014. Postglacial land uplift in Estonia based on four precise levelings. *Journal of Tectonophysics*, 610, 25–38.
- Kartau K., Soomere T., Tõnisson H. 2011. Quantification of sediment loss from semi-sheltered beaches: a case study for Valgerand Beach, Pärnu Bay, the Baltic Sea. *Journal of Coastal Research*, 2011, Special Issue 64, 100–104.
- Kask A., Soomere T., Healy T.R., Delpeche N. 2009. Rapid estimates of sediment loss for “almost equilibrium” beaches. *Journal of Coastal Research*, Special Issue 56, 971–975.
- Kelpšaitė L., Dailidienė I., Soomere T. 2011. Changes in wave dynamics at the south-eastern coast of the Baltic Proper during 1993–2008. *Boreal Environment Research*, 16, 220–232.
- Komen G.J., Cavaleri L., Donelan M., Hasselmann K., Hasselmann S., Janssen P.A.E.M. 1994. Dynamics and Modelling of Ocean Waves. Cambridge University Press, 532 pp.
- Kirshen P., Watson C., Douglas E., Gontz A., Lee J., Tian Y. 2008. Coastal flooding in the Northeastern United States due to climate change. *Journal of Mitigation and Adaptation Strategies for Global Change*, 13(5), 437–451, doi: 10.1007/s11027-007-9130-5.
- Kraus N.C., Larson M., Kriebel D.L. 1991. Evaluation of beach erosion and accretion predictors. In: *Proceeding Coastal Sediments '91 ASCE, New York*, 572–587.
- Kudryavtseva N., Pindsoo K., Soomere T. 2018. Non-stationary modeling of trends in extreme water level changes along the Baltic Sea Coast. *Journal of Coastal Research*, Special Issue 85, 586–590, doi: 10.2112/SI85-118.1.
- Laanearu J., Koppel T., Soomere T., Davies P.A. 2007. Joint influence of river stream, water level and wind waves on the height of sand bar in a river mouth. *Nordic Hydrology*, 38(3), 287–302. doi:10.2166/nh.2007.012.
- Lagemaa P., Raudsepp U., Kõuts T., Allik A., Elken J. 2013. Tallinna linna Haabersti, Põhja-Tallinna ja Kakumäe linnaosade meretasemete stsenaariumite modelleerimine (Modelling of water level scenarios for City of Tallinn). Research report, Marine Systems Institute at Tallinn University of Technology, Tallinn, 29 pp. [In Estonian].
- Le Cozannet G., Oliveros C., Castelle B., Garcin M., Idier D., Pedreros R., Rohmer J. 2016. Uncertainties in sandy shorelines evolution under the Bruun Rule assumption. *Frontiers in Marine Science*, 3, Art. No. 49, doi: 10.3389/fmars.2016.00049
- Lehmann A., Post P. 2015. Variability of atmospheric circulation patterns associated with large volume changes of the Baltic Sea. *Journal of Advanced Science and Research*, 12, 219–225, doi: 10.5194/asr-12-219-2015.
- Lehmann A., Höflich K., Post P., Myrberg K. 2017. Pathways of deep cyclones associated with large volume changes (LVCs) and major Baltic inflows (MBIs). *Journal of Marine Systems*, 167, 11–18, doi: 10.1016/j.jmarsys.2016.10.014.
- Leppäranta M., Myrberg K. 2009. The Physical Oceanography of the Baltic Sea. Springer, Berlin, 378 pp.
- Limber P.W., Murray A.B., Adams P.N., Goldstein E.B. 2014. Unraveling the dynamics that scale cross-shore headland relief on rocky coastlines: 1. Model development. *Journal of Geophysical Research-Earth Surface*, 119(4), 854–873, doi: 10.1002/2013JF002950.

- List J.H., Sallenger A.H., Hansen M.E., Jaffee B.E. 1997. Accelerated relative sea-level rise and rapid coastal erosion: testing a causal relationship for the Louisiana barrier islands. *Marine Geology*, 140, 347–363, doi: 10.1016/S0025-3227(97)00035-2.
- Luijendijk A., Hagenaars G., Ranasinghe R., Baart F., Donchyts G., Aarninkhof S. 2018. The state of the world's beaches. *Scientific Reports*, 8, 6641, doi: 10.1038/s41598-018-24630-6.
- Martinelli L. 2011. Wave energy converters under mild wave climates. In: *OCEANS'11 MTS/IEEE KONA, 19–22 Sept 2011, Waikoloa, Hawaii, USA, IEEE*, 1362, 9 pp., doi: 10.23919/OCEANS.2011.6107322.
- Masselink G., Pattiaratchi G.B. 2001. Seasonal changes in beach morphology along the sheltered coastline of Perth, Western Australia. *Marine Geology*, 172(3–4), 243–263, doi: 10.1016/S0025-3227(00)00128-6.
- Masselink G., Hughes M., Knight J. 2011. *Introduction to Coastal Processes and Geomorphology* (2nd Edition). Hodder Education, 416 pp.
- Mazas F., Hamm L. 2017. An event-based approach for extreme joint probabilities of waves and sealevels. *Coastal Engineering*, 122, 44–59, doi: 10.1016/j.coastaleng.2017.02.003.
- McLachlan A., Defeo O. (eds.). 2018. *The Ecology of Sandy Shores*, 3rd Edition, Academic Press, London, 572 pp.
- Medvedev I.P., Rabinovich A.B., Kulikov E.A., Shirshov P., Fedorov R. 2016. Tides in Three Enclosed Basins: The Baltic, Black, and Caspian Seas. *Frontiers in Marine Science*, 3, Art. No. UNSP 46, doi: 10.3389/fmars.2016.00046.
- Meier H.E.M., Döscher R., Faxén T. 2003. A multiprocessor coupled ice-ocean model for the Baltic Sea: application to salt inflow. *Journal of Geophysical Research: Oceans*, 108(C8), 32–73.
- Meier H.E.M., Broman B., Kjellström E. 2004. Simulated sea level in past and future climates of the Baltic Sea. *Journal of Climate Research*, 27(1), 59–75, doi: 10.3354/cr027059.
- Meier H.E.M., Höglund A. 2013. Studying the Baltic Sea circulation with Eulerian tracers. In: Soomere T., Quak E. (eds.), *Preventive Methods for Coastal Protection*, Springer, 101–129, doi: 10.1007/978-3-319-00440-2_4.
- Mentaschi L., Voudoudoukas M.I., Pekel J.F., Voukouvalas E., Feyen L. 2018. Global long-term observations of coastal erosion and accretion. *Scientific Reports*, 8, 12876, doi.org/10.1038/s41598-018-30904-w.
- Murray A.B., Ashton A.D. 2013. Instability and finite-amplitude self-organization of large-scale coastline shapes. *Philosophic Transactions of the Royal Society A-Mathematical and Engineering Sciences*, 371, Art. No. 20120363, doi: 10.1098/rsta.2012.0363.
- Männikus R., Soomere T., Kudryavtseva N. 2019. Identification of mechanisms that drive water level extremes from in situ measurements in the Gulf of Riga during 1961–2017. *Continental Shelf Research*, 182, 22–36, doi: 10.1016/j.csr.2019.05.014.
- Myrberg K., Ryabchenko V., Isaev A., Vankevich R., Andrejev O., Bendtsen J., Erichsen A., Funkquist L., Inkala A., Neelov I.A., Rasmus K., Rodríguez Medina M., Raudsepp U., Passenko J., Söderkvist J., Sokolov A., Kuosa H., Anderson T.R., Lehmann A., Skogen M.D. 2010. Validation of three-dimensional hydrodynamic models in the Gulf of Finland based on a statistical analysis of a six-model ensemble. *Boreal Environment Research*, 15, 453–479.

- Nicholls R.J., Wong P.P., Burkett V.R., Codignotto J.O., Hay J.E., McLean R.F., Ragoonaden S., Woodroffe C.D. 2007. Coastal systems and low-lying areas. *Climate Change 2007: Impacts, Adaptation and Vulnerability. Contribution of Working Group II to the Fourth Assessment Report of the Intergovernmental Panel on Climate Change*. Parry M.L., Canziani O.F., Palutikof J.P., van der Linden P.J., Hanson C.E. (eds.), Cambridge University Press, Cambridge, UK, 315–356.
- Nilsson E., Rutgersson A., Dingwell A., Björkqvist J.V., Pettersson H., Axell L., Nyberg J., Stromstedt E. 2019. Characterization of wave energy potential for the Baltic Sea with focus on the Swedish Exclusive Economic Zone. *Energies*, 12(5), Art. No. 793, doi: 10.3390/en12050793.
- Orviku K. 2005. Seashore needs better protection (Mererand vajab paremat kaitset). In: *Year-book of the Estonian Geographical Society (Eesti Geograafia Seltsi aastaraamat)*, 35, 111–129, 2005, [In Estonian, with English summary].
- Orviku K. 2018. Rannad ja rannikud (Beaches and coasts). TLÜ kirjastus. Tallinn. [In Estonian].
- Orviku K., Granö O. 1992. Contemporary coasts. In *Geology of the Gulf of Finland*, Raukas, A. and Hyvärinen, H., (eds.), Tallinn, Valgus, 219–238 [in Russian].
- Orviku K., Jaagus J., Kont A., Ratas U., Rivis R. 2003. Increasing activity of coastal processes associated with climate change in Estonia. *Journal of Coastal Research*, 19(2), 364–375.
- Pellikka H., Leijala U., Johansson M.M., Leinonen K., Kahma K. 2018. Future probabilities of coastal floods in Finland. *Continental Shelf Research*, 157, 32–42, doi: 10.1016/j.csr.2018.02.006.
- Pilkey O.H., Davis T.W. 1987. An analysis of coastal recession models: North Carolina coast. In: Nummedal D., Pilkey O.H., Howard J. (eds.), *Sea-level Fluctuations and Coastal Evolution*, Tucson, Arizona: SEPM. Special Publication, 41, 59–68.
- Pindsoo K., Soomere T. 2015. Contribution of wave set-up into the total water level in the Tallinn area. *Proceedings of the Estonian Academy of Sciences*, 64(3S), 338–348, doi: 10.3176/proc.2015.3S.03.
- Pindsoo K., Soomere T. 2020. Spatial variability in trends in water level extremes in the Baltic Sea. *Continental Shelf Research*, 115, 53–64, doi: 10.1016/j.csr.2019.104029.
- Post P., Kõuts T. 2014. Characteristics of cyclones causing extreme sea levels in the northern Baltic Sea. *Oceanologia*, 56, 241–258.
- Pranzini E., Williams A. 2013. *Coastal Erosion and Protection in Europe*. Routledge, Taylor and Francis, Abingdon-New York, 457 pp.
- Ranasinghe R. 2016. Assessing climate change impacts on open sandy coasts: A review. *Earth-Science Reviews*, 160, 320–332, doi.org/10.1016/j.earscirev.2016.07.011.
- Ranasinghe R., Wu C.S., Conallin J., Duong T.M., Anthony E.J. 2019. Disentangling the relative impacts of climate change and human activities on fluvial sediment supply to the coast by the world's large rivers: Pearl River Basin, China. *Scientific Reports*, 9, Art. No. 9236, doi: 10.1038/s41598-019-45442-2.
- Rangel-Buitrago N.G., Anfuso G., Williams A.T. 2015. Coastal erosion along the Caribbean coast of Colombia: Magnitudes, causes and management. *Ocean & Coastal Management*, 114, 129–144, doi: 10.1016/j.ocecoaman.2015.06.024.

- Rangel-Buitrago N.G., Williams A.T., Anfuso G. 2018. Hard protection structures as a principal coastal erosion management strategy along the Caribbean coast of Colombia. A chronicle of pitfalls. *Ocean & Coastal Management*, 156, 58–75, doi: 10.1016/j.ocecoaman.2017.04.006.
- Ribeiro A., Barbosa S.M., Scotto M.G., Donner R.V. 2014. Changes in extreme sea-levels in the Baltic Sea. *Tellus A*, 66, Art. No. 20921.
- Rimkus E., Briede A., Jaagus J., Stonevicius E., Kilpys J., Viru B. 2018. Snow cover regime and its changes in Lithuania, Latvia, and Estonia. *Boreal Environment Research*, 23, 193–208.
- Rodríguez-Ramírez A., Morales J.A., Delgado I., Cantano M. 2008. The impact of man on the morphodynamics of the Huelva coast (SW Spain). *Journal of Iberian Geology*, 34(2), 313–327.
- Roelvink D., Reniers A. 2011. A Guide to Modeling Coastal Morphology. Advances in Ocean Engineering, World Scientific, Singapore, 292 pp, doi: 10.1142/7712.
- Rosati J.D., Dean R.G., Walton T.L. 2013. The modified Bruun Rule extended for landward transport. *Marine Geology*, 340, 71–81, doi: 10.1016/j.margeo.2013.04.018.
- Rosentau A., Meyer M., Harff J., Dietrich R., Richter A. 2007. Relative sea level change in the Baltic Sea since the littorina transgression. *Zeitschrift für Geologische Wissenschaften*, 35(1/2), 3–16.
- Rusu C., Soares G. 2012. Wave energy assessments in the Azores islands. *Renewable Energy*, 45, 183–196, doi.org/10.1016/j.renene.2012.02.027.
- Räämet A., Soomere T. 2010. The wave climate and its seasonal variability in the northeastern Baltic Sea. *Estonian Journal of Earth Sciences*, 59, 100–113, doi: 10.3176/earth.2010.1.08.
- Ryabchuk D., Spiridonov M., Zhamoida V., Nesterova E., Sergeev A. 2012. Long term and short term coastal line changes of the Eastern Gulf of Finland. Problems of coastal erosion. *Journal of Coastal Conservation*, 16, 233–242, doi: 10.1007/s11852-010-0105-4.
- Ryabchuk D., Leontyev I., Sergeev A., Nesterova E., Sukhacheva L., Zhamoida V. 2011. The morphology of sand spits and the genesis of longshore sand waves on the coast of the eastern Gulf of Finland. *Baltica*, 24(1), 13–24.
- Sergeev A., Ryabchuk D., Zhamoida V., Leont'yev I., Kolesov A., Kovaleva O., Orviku K. 2018. Coastal dynamics of the eastern Gulf of Finland, the Baltic Sea: toward a quantitative assessment. *Baltica*, 31(1), 49–62, doi:10.5200/baltica.2018.31.05.
- Schmager G., Fröhle P., Schrader D., Weisse R., Müller-Navarra S. 2008. Sea state, tides. In: Feistel R., Nausch G., Wasmund N. (eds.), *State and Evolution of the Baltic Sea 1952–2005*. Wiley, Hoboken, NJ, 143–198.
- Seifert T., Tauber F., Kayser B. 2001. A high resolution spherical grid topography of the Baltic Sea, (2nd ed.), Baltic Sea Science Congress, Stockholm 25–29 November 2001, Poster #147, available at: <https://www.io-warnemuende.de/topography-of-the-baltic-sea.html>.
- Short A.D., Jackson D.W.T. 2013. Beach morphodynamics. In: Shroder J.F. (ed.), *Treatise in Geomorphology*, 10, Academic Press, San Diego, 106–129, doi: 10.1016/B978-0-12-374739-6.00275-X.

- Smith R.K., Bryan K.R. 2007. Monitoring beach face volume with a combination of intermittent profiling and video imagery. *Journal of Coastal Research*, 23, 4, 892–898, doi: 10.2112/04-0287.1.
- Soomere T. 2001. Extreme wind speeds and spatially uniform wind events in the Baltic Proper, *Proceedings of the Estonian Academy of Sciences, Engineering*, 7(3), 195–211.
- Soomere T. 2003. Anisotropy of wind and wave regimes in the Baltic Proper. *Journal of Sea Research*, 49, 305–316.
- Soomere T. 2005. Wind wave statistics in Tallinn Bay. *Boreal Environment Research*, 10, 103–118.
- Soomere T. 2016. Extremes and decadal variations in the Baltic Sea wave conditions. In: Pelinovsky E., Kharif C. (eds.), *Extreme Ocean Waves*, Springer, 107–140, doi: 10.1007/978-1-4020-8314-3_8.
- Soomere T., Healy T. 2011. On the dynamics of “almost equilibrium” beaches in semi-sheltered bays along the southern coast of the Gulf of Finland. In: Harff J., Björck S., Hoth P. (eds.). *The Baltic Sea Basin. Central and Eastern European Development Studies*, Part 5, Springer, Heidelberg, Dordrecht, 255–279.
- Soomere T., Keevallik S. 2003. Directional and extreme wind properties in the Gulf of Finland. *Proceedings of the Estonian Academy of Sciences. Engineering*, 9(2), 73–90.
- Soomere T., Räämet A. 2011. Spatial patterns of the wave climate in the Baltic Proper and the Gulf of Finland. *Oceanologia*, 53(1), 335–371, doi: 10.5697/oc.53-1-Tl.335.
- Soomere T., Viška M. 2014. Simulated sediment transport along the eastern coast of the Baltic Sea. *Journal of Marine Systems*, 129, 96–105. doi: 10.1016/j.jmarsys.2013.02.001.
- Soomere T., Pindsoo K. 2016. Spatial variability in the trends in extreme storm surges and weekly-scale high water levels in the eastern Baltic Sea. *Continental Shelf Research*, 115, 53–64, doi: 10.1016/j.csr.2015.12.016.
- Soomere T., Weisse R., Behrens A. 2012. Wave climate in the Arkona Basin, the Baltic Sea. *Ocean Science*, 8(2), 287–300, doi: 10.5194/os-8-287-2012.
- Soomere T., Eelsalu M., Pindsoo K. 2018. Variations in parameters of extreme value distributions of water level along the eastern Baltic Sea coast. *Estuarine, Coastal and Shelf Science*, 215, 59–68, doi: 10.1016/j.ecss.2018.10.010.
- Soomere T., Kask A., Kask J., Nerman R. 2007. Transport and distribution of bottom sediments at Pirita Beach. *Estonian Journal of Earth Sciences*, 56, 233–254, <http://dx.doi.org/10.3176/earth.2007.04>.
- Soomere T., Kask A., Kask J., Healy T. 2008. Modelling of wave climate and sediment transport patterns at a tideless embayed beach, Pirita Beach, Estonia. *Journal of Marine Systems*, 74, S133–S146.
- Soomere T., Viška M., Lapinskis J., Räämet A. 2011. Linking wave loads with the intensity of erosion along the coasts of Latvia. *Estonian Journal of Engineering*, 17(4), 359–374, doi:10.3176/eng.2011.4.06.
- Soomere T., Zaitseva-Pärnaste I., Räämet A., Kurennoy D. 2010. О пространственно-временной изменчивости полей волнения Финского залива (Spatio-temporal variations of wave fields in the Gulf of Finland), *Фундаментальная и прикладная гидрофизика (Fundamental and Applied Hydrophysics)*, 4(10), 90–101 [In Russian, with English summary].

- Soomere T., Pindsoo K., Bishop S.R., Käär A., Valdmann A. 2013. Mapping wave set-up near a complex geometric urban coastline. *Natural Hazards and Earth System Sciences*, 13(11), 3049–3061, doi: 10.5194/nhess-13-3049-2013.
- Soomere T., Männikus R., Pindsoo K., Kudryavtseva N., Eelsalu M. 2017a. Modification of closure depths by synchronisation of severe seas and high water levels. *Geo-Marine Letters*, 37(1), 35–46, doi: 10.1007/s00367-016-0471-5.
- Soomere T., Viška M., Pindsoo K. 2017b. Retrieving the signal of climate change from numerically simulated sediment transport along the eastern Baltic Sea Coast. In: Harff J., Furmańczyk K., von Storch H. (eds.), *Coastline Changes of the Baltic Sea from South to East: Past and Future Projection*, Springer, Coastal Research Library, 19, 327–361, doi: 10.1007/978-3-319-49894-2_15.
- Stive M.J.F. 2004. How important is global warming for coastal regions? An editorial comment. *Climatic Change*, 64, 27–39.
- Stopa J.E., Filipot J.F., Li N., Cheung K.F., Chen Y.L., Vega L. 2013. Wave energy resources along the Hawaiian Island chain. *Renewable Energy*, 55, 305–321, doi: 10.1016/j.renene.2012.12.030.
- Suursaar Ü., Sooäär S. 2007. Decadal variations in mean and extreme sea level values along the Estonian coast of the Baltic Sea. *Tellus A*, 59, 249–260.
- Suursaar Ü., Kullas T., Otsmann M. 2002. A model study of the sea level variations in the Gulf of Riga and the Vainameri Sea. *Journal of Continental Shelf Research*, 22, 2001–2019, doi: 10.1016/S0278-4343(02)00046-8.
- Suursaar Ü., Kullas T., Otsmann M., Saaremäe I., Kuik J., Merilain M. 2006. Cyclone Gudrun in January 2005 and modelling its hydrodynamic consequences in the Estonian coastal waters. *Boreal Environment Research*, 11(2), 143–159.
- Särkkä J., Kahma K.K., Kamarainen M., Johansson M.M., Saku S. 2017. Simulated extreme sea levels at Helsinki. *Boreal Environment Research*, 22, 299–315.
- Torres A., Brandt J., Lear K., Liu J. 2017. A looming tragedy of the sand commons. *Science*, 357, 970, doi: 10.1126/science.aao0503.
- Tuomi L., Kahma K.K., Pettersson H. 2011. Wave hindcast statistics in the seasonally ice-covered Baltic Sea. *Boreal Environment Research*, 16(6), 451–472.
- Tõnisson H., Suursaar Ü., Kont A., Orviku K., Rivis R., Szava-Kovats R., Vilumaa K., Aarna T., Eelsalu M., Pindsoo K., Palginõmm V., Ratav U. 2014. Field experiments with different fractions of painted sediments to study material transport in three coastal sites in Estonia. *Journal of Coastal Research*, Special Issue 70, 229–234, doi:10.2112/SI70-039.1
- [USACE] 2002. Coastal Engineering Manual. Department of the Army. U.S. Army Corps of Engineers. Manual No. 1110-2-1100.
- Vaidya A.M., Kori S.K., Kudale M.D. 2015. Shoreline response to coastal structures. *Aquatic Procedia*, 4, 333–340, doi: 10.1016/j.aqpro.2015.02.045.
- Vann Jones E.C., Rosser N.J., Brain M.J. 2018. Alongshore variability in wave energy transfer to coastal cliffs. *Geomorphology*, 322, 1–14, doi: 10.1016/j.geomorph.2018.08.019.
- Vestøl O., Ågren J., Steffen H., Kier H., Tarasov L. 2019. NKG2016LU: a new land uplift model for Fennoscandia and the Baltic Region. *Journal of Geodesy*, 93, 1759–1779. doi: 10.1007/s00190-019-01280-8

- Viška M., Soomere T. 2012. Hindcast of sediment flow along the Curonian Spit under different wave climates. In: Proceedings of the IEEE/OES Baltic 2012 International Symposium "Ocean: Past, Present and Future. Climate Change Research, Ocean Observation & Advanced Technologies for Regional Sustainability," May 8–11, Klaipėda, Lithuania. IEEE Conference Publications, 7 pp., doi: 10.1109/BALTIC.2012.6249195.
- Vos K., Harley M.D., Splinter K.D., Simmons J.A., Turner I.L. 2019a. Sub-annual to multi-decadal shoreline variability from publicly available satellite imagery. *Coastal Engineering*, 150, 160–174, doi: 10.1016/j.coastaleng.2019.04.004.
- Vos K., Splinter K.D., Harley M.D., Simmons J.A., Turner I.L. 2019b. Coast Sat: a Google Earth Engine-enabled Python toolkit to extract shorelines from publicly available satellite imagery. *Environmental Modelling and Software*, 122, 104528. doi:10.1016/j.envsoft.2019.104528.
- Vousdoukas M.I., Ranasinghe R., Mentaschi L., Plomaritis T.A., Athanasiou P., Luijendijk A., Feyen L. 2020. Sandy coastlines under threat of erosion. *Nature Climate Change*, 10, 260–263, doi: 10.1038/s41558-020-0697-0.
- Wright L.D., Nichols C. (eds.). 2018. *Tomorrow's Coasts: Complex and Impermanent*. Springer, 374 pp., doi: 10.1007/978-3-319-75453-6.
- Žaromskis R., Gulbinskas S. 2010. Main patterns of coastal zone development of the Curonian Spit, Lithuania. *Baltica*, 23(2), 149–156.

Acknowledgements

My deepest gratitude is for my supervisor Prof. Tarmo Soomere for the advice, shared knowledge and kindness throughout my studies. I'm truly grateful for this unique opportunity to develop and work under his guidance and support. I also would like to thank my co-supervisor Prof. Artu Ellmann for the help provided.

I'm grateful to my dear friends and colleagues Dr Katri Pindsoo, Dr. Andrea Giudici and Dr. Maija Viška for their friendship and shared joyful moments. I would like to thank great people from the Laboratory of Wave Engineering: Dr. Nicole Delpeche-Ellmann, Prof. Kevin Parnell, Dr. Nadezhda Kudryavtseva, Rain Männikus, Dr. Artem Rodin, Dr. Bert Viikmäe, Dr. Andrus Räämet, Margus Rätsep, Fatemeh Najafzadeh and Kalev Julge for their valuable advice, assistance and company.

My sincerest thank go to my family, to my dearest daughters Adeele and Isabel Pantoja Eelsalu and to Camilo A. Pantoja Viveros for their love, unfailing support and encouragement. I also would like to thank my parents Ene and Olev Eelsalu, my brother Edvard Eelsalu and my sister-in-law Geidi Steinberg for provided help and support.

I thank the Estonian Land Board for providing ALS data and the Swedish Meteorological and Hydrological Institute for providing the Rossby Centre Ocean water level data.

Abstract

Quantification of the reaction of Estonian beaches to changing wave loads

This thesis addresses properties of the drivers responsible (wave impact and course of the water level) for the biggest changes to Baltic Sea beaches as well as methods to quantify the sediment budget during the slow evolution phase of the beaches in the eastern Baltic Sea.

The main properties and spatio-temporal variability of the onshore wave energy flux is evaluated for the eastern Baltic Sea shore from the Bay of Gdańsk to the eastern Gulf of Finland based on numerically reconstructed wave fields for the period 1970–2007, with a spatial resolution of 3 nautical miles, using the third generation wave model WAM. The average wave energy flux over the 38 years varies from 0.5 kW/m to 2.55 kW/m along the coast. The total theoretical wave energy resource from the Sambian Peninsula until the Estonian–Russian border is about 1.5 GW. The Bay of Gdańsk and the interior of the eastern part of the Gulf of Finland may add up to 450 MW. Wave fields with a significant wave height of 2–4 m and a peak period of 6–9 s transport the largest amount of energy to the coast. The wave energy flux is highly intermittent. The most severe wave conditions provide by two orders of magnitude larger than average energy flux. About 30% of the annual energy that arrives at the coast in 3–4 days whereas the approximately 100 calmest days provide only 1% of the annual energy flux.

An ensemble approach is applied to estimate the frequency of the occurrence of extreme water levels for four locations along the coast of Estonia. The ensemble involves projections based on water level observations from Tallinn, Pärnu, Ristna and Narva-Jõesuu and nearby offshore modelled water level data extracted from the Rossby Centre Ocean (RCO) model for 1961–2005. None of the commonly used extreme value distributions is able to fully replicate the water level records. The ensemble average provides a sensible projection for estimations of high water levels and their return periods at three locations while the coastal site Ristna (open to the Baltic proper) exhibits a significant contribution of local effects (apparently wave set-up) to the high water levels.

A simple method is introduced for splitting the locally measured or modelled time series of water level into proxies of local storm surges and the water volume of the entire Baltic Sea. The residual of the running average over 8.25 days follows an exponential distribution for a large range of storm surge heights. Its exponent is used for the quantification of different coastal sections with respect to the probability of coastal flooding.

A technique for the estimate of the sand budget and a detailed three-dimensional analysis of beach evolution is developed by combining terrestrial and airborne laser scanning techniques. It is and applied to quantify changes on the central section of Piritä Beach in Tallinn Bay. Changes to the underwater sand volume, evaluated using the classical concept of the equilibrium beach profile and an inverse Bruun Rule, show that the changes on the underwater part of the beach are almost certainly much larger than the changes on the subaerial part.

Lühikokkuvõte

Eesti rannikute reaktsioon muutuvatele lainekoormustele

Analüüsitakse Läänemere idaranniku liiva- ja kruusarandade arengut kujundavate kesksete tegurite (lainetus ja veetase) omadusi ning võimalusi mõõta või muul moel kvantifitseerida randade reaktsiooni.

Randa jõudev laineenergia voog määrab suuresti rannikuprotsesside intensiivsuse ja piki randa kulgeva settetranspordi mahu. Selle suuruse, suuna ning ajalis-ruumilise muutlikkuse analüüs Läänemere idaosas tugineb kolmanda põlvkonna spektraalse lainemudeli WAM abil rekonstrueeritud lainetuse andmestikule ajavahemikul 1970–2007 ruumilise lahutusvõimega 3 meremiili. Laineenergia summaarne pikaajaline keskmine voog (lainetuse poolt ajaühikus randa toodav energia) ca 1400 km pikkusel rannalõigul (sh Liivi laht) on ligikaudu 1,5 GW. Gdański lahes ja Soome lahe idaosas lisandub sellele kokku ca 450 MW. Kõige energiarikkamad on lained kõrgusega 2–4 m ja perioodiga 6–9 s.

Pikaajaline keskmine laineenergia voog varieerub piki kõnesolevat rannikut viis korda, vahemikus 0,5 kuni 2,5 kW/m. Üksikuid kohti, kuhu jõuab naaberpiirkondadega võrreldes märksa rohkem laineenergiat ning kus võib olla mõttekas seda kasutada, leidub nii Gdański lahes kui ka Soome lahe idaosas.

Laineenergia voog varieerub ajas palju rohkem. Tugevates tormides võib randa jõudev laineenergia voog ületada pikaajalist keskmist võimsust enam kui 100 korda. Kolme kuni nelja kõige tormisema päeva lained toovad randa ligikaudu 30% aastasest energiast ning ligikaudu 100 kõige vaiksema päeva lained kokku vaid 1% aastasest energiast.

Eesti rannavete ekstreemsete veetasemete tõenäosuse ja korduvuse hindamiseks rakendati ansamblipõhist lähenemist. Modelleeritud ja mõõdetud andmete alusel konstrueeritud projektsioonid on Narva-Jõesuus, Tallinnas ja Pärnus jaotunud suhteliselt ühtlaselt ning see lähenemine annab kooskõlalise tulemuse. Ristna näitel selgus, et ansamblipõhine lähenemine võimaldab identifitseerida kohad, kus lokaalsed tegurid (nt laineaju ehk lainetuse tõttu lisanduv täiendav veetõus) moodustavad märkimisväärse osa kõrgest veeseisust.

Näidati, et kohalik tormiaju ja kogu Läänemere veetaseme muutuste panust veetasemete kujunemisse saab eristada, keskmistades veetaseme hektväärtusi üle 8 päeva. Läänemere keskmist veetaset kirjeldab 8 päeva keskmine, mis järgib hästi normaaljaotust. Tormiajude esinemist (kogu veetase miinus 8 päeva keskmine) kirjeldab eksponentsiaaljaotus. Selle astmenäitaja iseloomustab tormiaju riski konkreetses kohas.

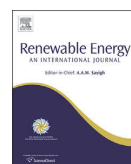
Muutusi rannaliiva hulgas ja liiva ümberjaotumist aastate lõikes analüüsiti, kombineerides lennukilt ja lokaalselt teostatud laserskaneerimise tulemusi Piritä ranna keskosa näitel. Suured muutused üksikute aastate tasakaalustuvad pikema aja vältel. Veealusel rannaprofiilil paikneva liiva hulka veepiirist sulgemissügavuseni hinnati kaudselt tasakaalulise rannaprofiili teooria alusel, rakendades Bruuni pöördreeglit veepiiri nihkumisele. Kuigi see meetod on hinnanguline ja ebatäpne, näitab selle rakendamine, et veealused mahumuutused on ligikaudu kaks korda suuremad kui muutused kuival rannaosas.

Appendix: Papers constituting the thesis



Paper I

Soomere T., Eelsalu M. 2014. On the wave energy potential along the eastern Baltic Sea coast. *Renewable Energy*, 71, 221–233, doi: 10.1016/j.renene.2014.05.025.



On the wave energy potential along the eastern Baltic Sea coast



Tarmo Soomere^{a, b, *}, Maris Eelsalu^a

^a Wave Engineering Laboratory, Institute of Cybernetics at Tallinn University of Technology, Akadeemia tee 21, 12618 Tallinn, Estonia

^b Estonian Academy of Sciences, Kohtu 6, 10130 Tallinn, Estonia

ARTICLE INFO

Article history:

Received 7 September 2013

Accepted 13 May 2014

Available online 10 June 2014

Keywords:

Wave energy

Semi-sheltered sea

Baltic Sea

Wave climate

Marine protected areas

ABSTRACT

We analyse the wave energy resource theoretically and practically available in a semi-sheltered shelf sea of moderate depth and with relatively severe but highly intermittent wave climate on the example of the Baltic Sea. The wave properties along the entire eastern Baltic Sea coast, from the Sambian (Samland) Peninsula to the eastern Gulf of Finland, are reconstructed numerically for 1970–2007 with a spatial resolution of 3 nautical miles (5.5 km) and temporal resolution of 1 h using the third generation wave model WAM. Owing to the shallowness of the sea (54 m on average) the finite-depth dispersion relation is used in the estimates of the wave energy resources in the nearshore, at depths of 7–48 m where the WAM model provides adequate results. The average wave energy flux (wave power) over the 38 years in question is about 1.5 kW/m (at selected locations up to 2.55 kW/m) in the nearshore regions of the eastern Baltic Proper but much smaller, about 0.7 kW/m, in the interior of the Gulf of Finland and the Gulf of Riga. The total theoretical wave energy resource in the entire study area is about 1.5 GW. The existing and proposed marine protected areas limit the available wave energy resource down to ~840 MW. The production of grid energy is complicated because of extremely high intermittency and strong seasonal variation of the wave properties and frequent presence of sea ice. Although the wave energy resources are of obvious interest at some locations, their use for supplying power into the grid is questionable and probably not feasible in the conceivable future.

© 2014 Elsevier Ltd. All rights reserved.

1. Introduction

The gradually growing consumption of electricity and obvious impossibility of covering it solely by increasing the burning of fossil fuels call for the analysis of prospective sources of renewable energy. A feasible potential energy source is the field of ocean waves [1]. The wave energy potential in the entire World Ocean is comparable to the total energy consumption today. Wave energy has clear potential even in countries with extremely high energy consumption per capita such as the United States where the theoretical ocean wave energy resource exceeds 50% of the annual domestic energy demand [2].

In addition to the high energy density of ocean waves, many realistic sources of energy are located in the nearshore regions close to coastal population centres. The coastal region is indeed the fourth most intense energy conversion zone on the Earth after volcanic eruptions, earthquakes and asteroid impacts. The physics

behind this feature is that the water surface is an almost perfect waveguide for non-breaking waves. Thus, part of the energy supplied to the water surface by wind and small-scale fluctuations of the air pressure over an extensive impact area is converted into waves that propagate over large distances with almost no loss of energy and finally bring their energy into a coastal zone. As a result, wave energy is in places more consistent and predictable than some other renewable technologies.

Similarly to the fossil energy sources, the wave energy levels are highly variable along the coasts of the World Ocean [3]. According to recent estimates, two per cent of the world's coastal waters have densities of the wave energy flux (wave power) that are great enough for extracting wave energy. The resources in these areas equate to 480 GW of power output or 4200 TWh/yr of electricity generation [4]. Many countries have evaluated their regional- and national-scale [5,6] wave energy resources in the recent past. The driving forces for such evaluations have been diverse, from attempts to ensure energy self-sufficiency of single islands [7–13] or regions [14–19] to economically-oriented national-scale evaluations [2,20] (see Ref. [5] for a detailed list of literature). The most visionary authors suggest that a feasible number of renewable plants extracting energy from wind, water and sunlight could fully power the entire world, including hydrogen production for all

* Corresponding author. Wave Engineering Laboratory, Institute of Cybernetics at Tallinn University of Technology, Akadeemia tee 21, 12618 Tallinn, Estonia. Tel.: +372 6204176.

E-mail address: soomere@cs.ioc.ee (T. Soomere).

purposes, already in 2030, with the energy cost similar to that of today [21].

The Baltic Sea (Fig. 1) has relatively limited wave energy resources. Its small size restricts the amount of atmospheric energy that can be converted into wave energy. This sea has, however, clear potential for exemplifying efforts and challenges in the use of wave energy in semi-sheltered water bodies of small depth where the use of the deep-water interpretation of the wave energy flux is no more valid. Similarly to other parts of the World Ocean, proper evaluation of the power present in waves in the Baltic Sea is a challenge owing to the scarcity of wave measurements and the relatively short length of the existing records. A feasible solution is to use numerically reproduced wave time series [22–24]. An overview of recent efforts using such basinwide simulated wave fields is presented in Ref. [25].

The first studies into the wave energy potential in the Baltic Sea date back to the 1980s [26,27]. Earlier attempts at its estimation were limited to either the western gateway of the sea [28] or to wave simulations over short time intervals [29,30]. Nevertheless, they have provided a rough insight of the basic levels of wave energy which is valuable today. While in many sections of the open ocean the onshore wave energy flux exceeds 50 kW/m [1], its typical values are 1.5–2.5 kW/m in coastal stretches open to the Baltic Proper (Fig. 1) and below 1 kW/m in sub-basins and partially sheltered bays of the Baltic Sea [31]. The most favourable locations are outside the main body of the Baltic Sea, in the nearshore of the Kattegat and Skagerrak (Fig. 1) where the average wave energy flux ranges from 2.4 to 5.2 kW/m [28]. The largest problem in this area is the intermittency of the wave climate: some 80% of the annual energy is found in wave conditions with a higher than average energy flux. The interior of the Baltic Sea has clearly lower wave energy: its typical level is around 2 kW/m [26].

Unlike from wind energy flux, wave energy and its flux are two-dimensional phenomena. If wave energy has once been absorbed

by an array of converters, it takes a long time (or, equivalently, a large distance) for the wave field to regain its energy. Therefore, estimates of the available wave energy based on spatial distributions of wave properties [29] may be misleading for small water bodies, whose dimensions are much shorter than the saturation fetch length. The wave fields in such water bodies are usually fetch-limited. Their properties are largely dictated by the size of the water body and it is normally possible to use the energy of storm waves only once on their way from the generation area to the coast. For this reason the wave energy issues in small seas are treated differently than in the open ocean conditions where large-scale wind systems (such as monsoons, trade winds or air flow in the “roaring forties”) have an extension much larger than the fetch length necessary for the creation of high and long waves.

An implicit conjecture from this observation is that the best location for the wave energy converters in smaller water bodies is the “downwind” nearshore area where the wave energy flux usually reaches its maximum. Both the wind and wave climate of the Baltic Sea are strongly anisotropic. The predominant winds blow from the south-west or north-north-west [32] and normally give rise to larger and longer waves in the eastern regions of the sea [33–36]. This feature together with estimates in Ref. [30] suggests that the eastern Baltic Proper has the highest concentration of wave energy resource in the entire Baltic Sea.

The purpose of this paper is to systematically analyse the potential for the wave energy production along the eastern Baltic Sea coast from the viewpoint of theoretically available total wave power for the entire region. The focus is on an almost 1400 km long nearshore stretch from the Sambian (Samland) Peninsula (Kaliningrad District) to the eastern end of the Gulf of Finland, including the Gulf of Riga (Fig. 2). This stretch is divided into 222 sections with a length of about 6 km. Following many similar studies (see references above), we rely on numerically simulated wave time series in these sections. Although such simulations do not exactly restore the real wave properties and may suffer from certain biases, they replicate these key features of wave fields that severely restrict the use of common types of wave energy converters in this and similar basins and provide challenges to new technologies.

The time series of wave properties (significant wave height, peak period, propagation direction) are first calculated for each of the 222 sections in question for 38 years (1970–2007) with a temporal resolution of 1 h and in deep enough areas where the hindcast of wave properties is adequate. The resulting 333,096 single values of wave characteristics are used to evaluate the instantaneous onshore wave energy flux (wave power) in each 1-h interval during these 38 years. The resulting hourly values of this flux represent the theoretically available wave energy resource in each segment. These values are used to calculate the total energy resource in the study area and in its certain segments. Finally, the temporal and spatial variability of the instantaneous wave energy flux in each section and in certain longer parts of the nearshore are analysed from the viewpoint of practical usability of this energy resource.

The paper is organised as follows. Section 2 provides an insight into the wave calculations, the results of which are used for the estimates of the wave energy resource. Section 3 presents the approach used for these estimates in our study area. Section 4 describes the main results of the analysis and Section 5 summarises the outcome and discusses several implications of the research.

2. Wave data

The Baltic Sea wave climate is, on average, relatively mild compared to the wave climates of the North Sea or the North Atlantic. The typical long-term significant wave heights H_5 are

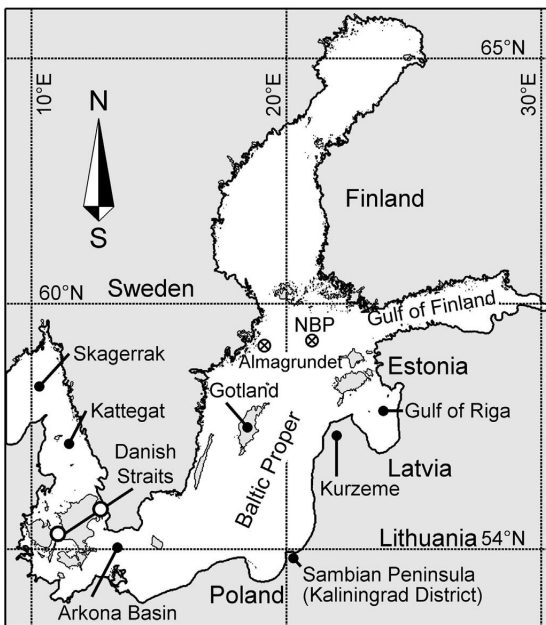


Fig. 1. Scheme of the Baltic Sea and the area covered by the wave model grid. NBP stands for a wave measurement buoy in the northern Baltic Proper.



Fig. 2. Nearshore grid cells of the wave model along the converter line in the eastern Baltic Sea coast and in the Gulf of Riga. Four cells (Nos 24, 73, 147 and 197, marked by red rectangles) are used to characterise wave energy resources at single locations. A colour version of the figure is available in the online version of this manuscript.

about 1 m in the Baltic Proper [33–39], 0.6–0.8 m in the open parts of its larger sub-basins such as the Gulf of Finland [39] or Arkona Basin [40] (Fig. 1) and well below 0.5 m in relatively large semi-sheltered bays such as Tallinn Bay [34]. These values are by 10–20% lower in the nearshore regions [41–43]. The most frequent wave heights are also about 20% lower than the long-term average wave height. The waves are relatively short: the common wave periods are 3–5 s in the offshore and 2–4 s in coastal areas [44]. The majority of the combinations of wave heights and periods roughly correspond to saturated wave fields in the northern Baltic Proper. The properties of the roughest seas, however, usually match a JONSWAP spectrum that corresponds to fetch-limited seas. Strong swells are infrequent in all parts of the Baltic Sea [36,44].

The wave climate of the Baltic Sea is highly intermittent. Although the average wave heights are quite small, this sea occasionally hosts furious wave storms. Numerical simulations indicate that the significant wave height may exceed 9.5 m in the northern Baltic Proper and at the entrance to the Gulf of Finland [35,39,45]. A

hot spot of wave energy with significant wave heights at times reaching almost 10 m evidently exists somewhere west of the Latvian coast [35]. The largest instrumentally measured values are $H_S = 8.2$ m obtained in the northern Baltic Proper (NBP in Fig. 1) on 22 December 2004 [39] and $H_S = 7.82$ m recorded at Almagrundet on 13/14 January 1984 (Fig. 1; an alternative estimate from the wave spectrum for the latter value is $H_S = 7.28$ m [37]). The maximum wave height in the Gulf of Finland was 5.2 m on 15 November 2005 (the highest individual wave 9 m [39]). Rough seas occurred also on 30 November 2012 when the single wave height reached even 9.4 m (http://www.itameriportaali.fi/en/tietoa/veden_liikkeet/en_GB/aaltoennatyksia/). The significant wave height may have exceeded 6 m in the Gulf of Finland in January 2005 [45].

The described features signal that using simplified semi-empirical wave models and especially one-point wind data [41,43] is not justified for evaluation of spatio-temporal variability of wave properties and associated wave energy flux. For this reason, in this paper we use the instantaneous wave fields that were calculated using the third-generation spectral wave model WAM [46]. This model describes the evolution of a two-dimensional wave spectrum and thus provides adequate information about all major wave properties, including the wave propagation direction. It systematically includes the main effects affecting the wave generation and dissipation as well as non-linear interactions between the wave harmonics: the coastline of the basin, bathymetric effects (shoaling, refraction), spatial and temporal variation of wind properties, wave propagation on the sea surface, quadruplet interactions between wave harmonics, whitecapping and wave dissipation in shallow areas due to bottom friction, and interaction of waves and stationary currents. A thorough discussion of the physics, underlying equations and approximations and the overall implementation is presented in Ref. [46]. The application of the model for the Baltic Sea is discussed in Refs. [34,39].

For this study, the time series of wave properties were estimated for the time interval of 38 years (1970–2007). The model was run in the finite-depth mode for the entire Baltic Sea to the east of the Danish straits (Fig. 1) on a regular rectangular grid with a spatial resolution of $3'$ along latitudes and $6'$ along longitudes (about 3×3 nautical miles, 5.5 km, 11,545 sea points) [47]. The wave energy flux from the North Sea through the Danish straits is very small [33,34] and was ignored in the calculations.

The wave model was forced with near-surface wind at the 10 m level constructed from the Swedish Meteorological and Hydrological Institute geostrophic wind database with a spatial and temporal resolution of $1^\circ \times 1^\circ$ and 3 h, respectively (6 h before September 1977). The geostrophic wind speed was multiplied by 0.6 and the wind direction was turned counterclockwise by 15° [47]. This approximation, although neglecting several details of the wind fields, is used in many studies in the Baltic Sea region (e.g., [48,49]). The presence of ice is ignored in the calculations. This is generally acceptable for the southern part of the study area but may substantially overestimate the overall wave energy resource in the northern Baltic Proper and especially in the Gulf of Riga and Gulf of Finland. This feature, however, does not change the key messages of the analysis.

The directional resolution of calculations was 15° (24 equally spaced directions). The lowest frequency was 0.042 Hz (wave period 23.9 s) as in the standard set-up of the WAM model for open ocean conditions [46]. The frequencies of wave components were arranged in a geometrical progression with an increment of 1.1. Differently from the standard configuration of the WAM model, the calculations were performed in an extended frequency range up to about 2 Hz using 42 frequency bins reflecting wave periods down to 0.5 s. Such an extension ensures realistic wave growth rates in low wind conditions after calm situations [31] and an adequate reproduction of the high-frequency part of the wave fields [40]. The

output, saved once an hour, comprised 333,096 single values of wave height, period and direction at each grid cell in 1970–2007.

The accuracy and reliability of the wave calculations, performed with the above-described wave model and forcing, are discussed in a number of recent papers ([36,50] and references therein). A comparison of the modelled data with historical visual observations from the eastern coast of the Baltic Sea suggests that the model probably underestimates the long-term average wave height by about 10% [50]. As no long-term instrumentally measured wave data are available near the study area [36], a detailed comparison of the results of wave modelling was performed against wave data measured at Almagrundet and in the northern Baltic Proper (NBP in Fig. 1) [50,51]. The main statistical properties of modelled wave fields (e.g., seasonal patterns of wave intensity, distributions of the occurrence of wave conditions with different heights and periods, short-term (1–3 years) interannual variability in the wave heights) satisfactorily match the measured data [50].

The model acceptably represents the wave properties in average wind and wave conditions (when $H_s \sim 1$ m) and catches important strong wave events and their duration in most cases. The largest discrepancies from the measured data occur during single extreme storms [47]. The model tends to underestimate the wave height in some short storms. For example, for a sequence of seven strong but short storms in October 2000, with measured H_s up to 4 m at Almagrundet, the bias and root mean square deviation were 0.47 and 0.72 m, respectively [51]. Similarly, in January 2005 (when H_s up to 7.2 m was recorded in the northern Baltic Proper), the model bias was 0.46 m. A probable reason for the bias (similarly to the open ocean conditions [52]) is the low temporal resolution of the forcing data (3–6 h). In relatively short storms wind time series with this resolution often do not reflect the course of wind in a sufficiently detailed manner. Such mismatches of the measured and modelled wave properties are common in contemporary efforts to model wave conditions in the Baltic Sea [38] where many storms are short and not fully replicated by atmospheric models. As will be demonstrated below, the possible underestimation of wave heights in some short storms and the above-described bias do not change the basic outcome of our research.

3. Calculation of wave power

Our aim is to evaluate the entire theoretical resource of wave power approaching the nearshore of the eastern Baltic Sea in terms of the wave energy flux. First, we consider the optimum location of wave converters for onshore-propagating wave fields, describe a sample (piecewise straight) line for such converters at a certain distance from the coast (depending on the geographical locations of available wave data) and discuss shortly the extremes and reliability of the wave data at this line. Next we introduce an appropriate way of the evaluation of the onshore wave energy flux based on the modelled wave data, water depth along this line and geometry of each straight section of this line and, finally, describe how the seasonal or regional values of the total wave power resource can be obtained.

3.1. Location of the maximum of wave power

As the wave fields of the Baltic Sea are usually fetch-limited (see above), their energy flux in many occasions continues to grow almost until the coast. The average depth of this sea is only 54 m and the average depth of its largest basin, the Gotland Sea, is 71 m [53]. It is therefore not rational to limit the study to the truly deep-water areas (in which the water depth is at least half the wave length) because the maximum of the wave energy flux is often reached at smaller depths. It is well known that waves lose their

energy in shallow water and their energy flux rapidly decreases with the decrease in the water depth [54]. Therefore, the largest wave energy resource is available in reasonably deep nearshore regions where interactions with the seabed do not yet considerably reduce the wave energy. A reasonable depth (equivalently, the optimum location of wave energy converters) can be estimated, to a first approximation, based on the linear wave theory and common properties of approaching waves in the study area.

The typical wave periods are much shorter in the Baltic Sea than in the open ocean [35]. This feature has important consequences on the intensity of wave–bottom interactions in this water body. The implications can be expressed in the linear wave theory in terms of the parameter kd , where k is the wave number and d is the water depth. The finite-depth dispersion relation for water waves is $\omega = \sqrt{gk \tanh(kd)}$, where $\omega = 2\pi/T$ is the angular frequency, T is the wave period and g is acceleration due to gravity. Comparatively long Baltic Sea waves with quite a long period of $T = 7$ s for this sea correspond to the same value of this parameter $kd \approx 1.5$ at a depth of $d = 16.5$ m as relatively common ocean swells with a period of $T = 12$ s at a depth of $d = 50$ m.

This difference can be further exemplified in terms of the maximum near-bottom orbital velocity that roughly characterises the intensity of wave–bottom interactions and potential loss of wave energy. Open ocean swells with periods of T equalling 12–15 s lose part of their energy starting from a depth of 50–60 m [54]. It follows from the linear wave theory that a typical Baltic Sea wave with the same height but with a period of $T = 5.5$ s develops the same near-bottom orbital velocity as the above swells at a much smaller depth (about 17 m). Therefore, the Baltic Sea wave fields are much less impacted by the seabed than their sisters in the open ocean [54]. This observation explains why the WAM model (that performs well for depths >50 m along the open ocean coasts [54]) works equally well until depths of 10–15 m for the wave fields that are common in the Baltic Sea.

The presented arguments suggest that wave energy losses owing to wave–bottom interactions are minor in the Baltic Sea until a depth of about 15 m. The water depth, wave energy and its flux (wave power) usually rapidly decrease further onshore [54]. Therefore, it can be assumed that the energy resource of onshore-propagating storm waves reaches its maximum approximately at this depth.

3.2. Waves at the converter line

Following this conjecture, we evaluate the entire onshore wave power along a line drawn through selected grid cells of the wave model that are located at a distance of a few kilometres from the eastern coast of the Baltic Sea. The water depth at these grid cells is 18 m on average and varies in the range of 7–48 m. The above arguments suggest that (1) the loss of wave energy owing to wave–bottom interaction is generally minor at this line and (2) the used wave model performs well at this line for the typical wave conditions; thus it is appropriate to directly use the above-described modelled wave data.

This line, called the converter line in this paper, is chosen as a piecewise straight line consisting of 222 about 6 km long sections in the eastern Baltic Sea (Fig. 2). It starts from the Sambian Peninsula (20° E, 55° N), covers the entire nearshore of Lithuania, Latvia (including the Gulf of Riga) and Estonia, and extends to the eastern part of the Gulf of Finland, to Kurgolovo in Russia (28° E, 59° 51' N). Its total length is about 950 km (154 sections) in the Baltic Proper and the Gulf of Finland and about 450 km (68 sections) in the Gulf of Riga. Sections 1–154 are numbered from the Sambian Peninsula to the eastern Gulf of Finland and Sections 155–222 counter-clockwise along the coast of the Gulf of Riga (Fig. 2).

The converter line connects the mid-points of edges of wave model grid cells (numbered similarly to the sections above) that are located exactly to the north, south, east or west of each other. In certain cases (e.g. cell 73 in Fig. 3) it may match one of the edges. To properly evaluate the wave energy flux over the entire study area, it is necessary to account for the length L_j of each section. The length of its sections oriented in the north–south direction equals the size of the grid cell (3 nautical miles or about 5.5 km). Differently oriented segments of this line may be longer (Fig. 3). If the neighbouring cells only touch each other at their corners, the relevant section of the converter line is by $\sqrt{2}$ times or by $\sqrt{5}/2$ times longer than the grid size (Fig. 3). The length of sections oriented in the east–west direction also varies to some extent. The largest difference is between the east–west oriented converter line segments of the Sambian Peninsula at a latitude of 55° N and similar sections in the Gulf of Finland close to a latitude of 60° N. The length of each section was calculated using the ArcMap software from the exact locations of the corners and mid-points of the edges of the grid cells of the wave model (Fig. 3).

The wave properties used for the evaluation of the wave energy resource (significant wave height $H_{S,ij}$, peak period T_{ij} , wave propagation direction) during the i -th sequential hourly interval in 1970–2007 ($1 \leq i \leq 333,096$) along the j -th section ($1 \leq j \leq 222$) of the converter line are extracted directly from the WAM model at these model cells where the j -th section is located (Figs. 2 and 3). Doing so accounts for the generation of wave energy and its transformation (incl. changes in the wave height and group velocity due to shallow-water effects) on its way from the open sea to the optimum location of the wave energy converters in the best possible manner. The overall wave height maximum along the entire study area (10.7 m, Fig. 4) exceeds to some extent the maxima estimated for the offshore conditions in extreme storms in the open Baltic Sea (9.6–9.7 m [39,45]). The single maxima at selected sections of the converter line may be still realistic owing to refraction-driven wave energy focussing [34,55,56]. The maximum significant wave heights for the Gulf of Finland and for the Gulf of

Riga (over 8 m) seem to be overestimated. There is, however, evidence in older literature that single waves with a height of around 10 m have occurred in the southern part of the Gulf of Riga during extreme north–north–western storms. The number of such modelled wave conditions is very small. The threshold for wave heights occurring with a frequency of 0.1% is well below 4 m for the Gulf of Riga, varies between 4 and 5 m in the nearshore of the eastern Baltic Proper and is around 3 m in the Gulf of Finland. Therefore, the overestimation of extreme wave heights on a few occasions has a negligible effect on the estimates of the long-term wave energy flux, which are based on 333,096 hourly values of wave height, period and direction for each section.

3.3. Onshore wave energy flux

For elementary sinusoidal waves the total energy density, averaged over either a wave length or period, is

$$E = \frac{1}{8} \rho g H^2, \quad (1)$$

where ρ is the water density and H is the wave height. This expression cannot be applied directly to most natural situations. On the one hand, ocean wave fields typically consist of a large number of superimposed components with different heights and periods, the total energy of which is equal to that of a sine wave with the root-mean-square wave height H_{rms} . On the other hand, ocean wave fields are commonly characterised using the significant wave height H_S . These two measures are related in a simple manner for narrow-banded wave fields, for which the heights of single waves defined from a zero-crossing method obey a Rayleigh distribution and $H_S = \sqrt{2} H_{rms}$ [57]. Therefore, the wave power, calculated using Eq. (1), is often much higher than the one derived from the full wave spectrum [5]. An acceptable representation of the energy density of commonly occurring ocean wave fields, characterised using significant wave height and employed in this paper, is

$$E = \frac{1}{16} \rho g H_S^2. \quad (2)$$

The wave energy propagates with the group velocity \vec{c}_g . This quantity is a vector, which length (group speed c_g) is a function of the local water depth and wave period. For narrow-banded wave fields it is customary to associate this speed with the group speed of the most energetic waves, equivalently, with the waves with a period corresponding to the modelled peak period. An even better quantity for this purpose is the so-called energy period that unfortunately was not saved in wave calculations used in this paper [50]. Following these considerations, the magnitude of the energy flux (wave power) P_{ij} of an instantaneous wave field approaching the j -th section of the converter line during the i -th hourly interval

$$P_{ij} = E_{ij} c_{g,ij} = \frac{1}{16} \rho g H_{S,ij}^2 c_{g,ij}, \quad (3)$$

where $c_{g,ij}$ is the group speed of such waves, is equal to the energy flux of elementary (sine) waves with the height of $H_{S,ij}/\sqrt{2}$ and with the period equal to the modelled peak period.

As the Baltic Sea is relatively shallow, the use of the deep-water group speed would severely overestimate the wave energy potential for the largest and longest waves in many sections of the converter line. It is correct to employ the wave properties (wave number) and the group speed

$$c_g = \frac{\omega}{2k} \left(1 + \frac{2kd}{\sinh 2kd} \right), \quad (4)$$

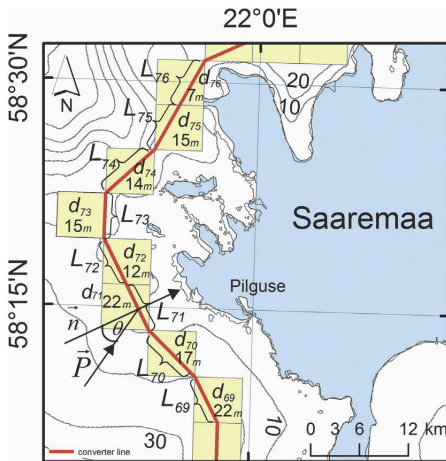


Fig. 3. Scheme of the location of the converter line (red) through the selected wave model grid cells (yellow rectangles), lengths L_j of its straight sections and depths d_j used in the wave model in the vicinity of the western tip of the island of Saaremaa (cells 69–76). The schematic representation of the wave energy flux vector \vec{P} , the onshore normal of the converter line \vec{n} and the approach angle θ (subscripts omitted for clarity of the image) are presented for cell 71. The manor of Pilguse was the home of Fabian Gottlieb von Bellingshausen (1778–1852) who discovered Antarctica. A colour version of the figure is available in the online version of this manuscript.

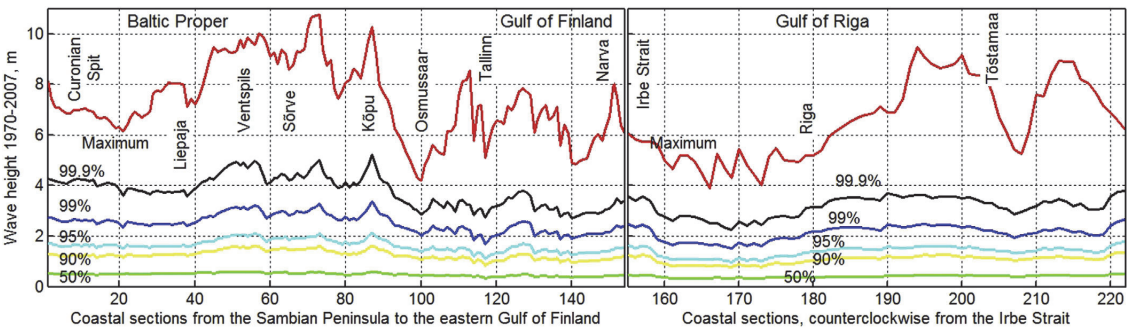


Fig. 4. Modelled significant wave height (overall maximum over the years of simulation and thresholds for various quantiles) in the nearshore of the eastern Baltic Proper, Gulf of Finland and Gulf of Riga in 1970–2007.

using the finite-depth dispersion relation $\omega = \sqrt{gk \tanh(kd)}$. The dispersion relation was solved accurately (with about 7 correct decimal digits, which is the precision of replication of decimal numbers in a 32-bit computer) for the wave number k_{ij} for each section of the converter line (using the water depth d_j in the relevant cell of the wave model, Fig. 3) for each modelled value of the wave period $T_{ij} = 2\pi/\omega_{ij}$. The resulting values of k_{ij} were used to calculate the group speed $c_{g,ij}$ of waves after Eq. (4).

The wave energy flux over the sea surface is a vector $\vec{P} = E \vec{c}_g$ aligned with the wave propagation direction (see Fig. 3 for an example). For narrow-banded wave fields this direction is taken equal to the modelled wave direction. Although keeping the core information about directionality, this approximation discards the equally important information about the directional spreading of the wave components [22]. Even if we adjust a directional wave energy converter into the best orientation, the resulting expression for the wave power provides a higher than truth value [22]. The difference may be relatively small for regular ocean swells but is evidently large in areas such as the Baltic Sea that host mostly young windseas with high directionality.

The waves usually approach the open ocean coast almost incidentally [57] and thus the wave energy flux is typically propagating nearly directly onshore. This is different in the Baltic Sea basin where waves often approach the coast under very large angles [58] and may (e.g. at some headlands) propagate along the coast or even in the offshore direction. Therefore, wave energy flux may approach a particular segment of the chosen converter line under virtually any angle. The associated wave energy resource for each section of the converter line obviously depends on the approach angle of waves. The theoretically available (onshore-propagating) wave energy resource is equal to the onshore wave energy flux through the converter line, equivalently, to the component of the wave energy flux normal to the relevant segment of the coastline. The density of this flux P_{ijn} (per unit of length of the converter line) is

$$P_{ijn} = P_{ij} \cos \theta_{ij} \text{ [W/m]}, \tag{5}$$

where θ_{ij} is the angle between the wave energy flux vector approaching the j -th segment of the converter line and its onshore-directed normal within the i -th hourly time interval (Fig. 3). We assume that the energy of waves propagating along the converter line or to the offshore is not exploitable; thus we set $P_{ijn} = 0$ when $\theta_{ij} \geq 90^\circ$.

3.4. Wave energy resource

The total instantaneous onshore wave energy flux P_{ij}^h , theoretically available for the real converters mounted along a particular (j -

th) section of the converter line of a length of L_j (Fig. 3) during the i -th hourly time interval, is

$$P_{ij}^h = P_{ijn} L_j \text{ [W]}. \tag{6}$$

The modelled wave properties (significant height, propagation direction and wave period) are available once an hour. It is natural to assume that they represent the average wave conditions during the relevant interval $\Delta t = 1 \text{ h}$. Then the product

$$P_{ij}^{Wh} = P_{ijn} L_j \Delta t \text{ [W} \cdot \text{h]} \tag{7}$$

expresses the total amount of theoretically available wave energy along each section of the converter line within such an 1-h interval.

The average wave energy resource over the entire study area is found in a classical manner, by means of summing first all values of P_{ij}^{Wh} over all sections ($1 \leq j \leq 222$) to obtain the total onshore wave energy flux $P_i^{\text{tot}} = \sum_{j=1}^{222} P_{ij}^{Wh}$ within each considered 1-h interval, and taking then an average of P_i^{tot} over all 1-h intervals in 1970–2007 ($1 \leq i \leq 333,096$). To highlight spatial variations of the wave energy resource, similar operations are performed for selected sets of sections of the converter line, for example, for the Gulf of Riga that is covered by cells $154 \leq j \leq 222$. To highlight temporal variations of the potentially available wave energy flux, we analyse time series of P_{ij}^{Wh} for selected sections $j = 24, 73, 147, 197$ that are characteristic for some larger nearshore areas. Finally, certain elements of spatio-temporal variations of the theoretically available wave energy flux are addressed by means of considering total or average wave energy flux for certain time intervals (e.g., single months) or longer sections of coastline (Table 1) by means of summing or averaging the values of P_{ij}^{Wh} over the relevant sets of indices i, j .

Table 1
Long-term average onshore energy flux (theoretically available wave power, MW) along the eastern Baltic Sea coast. Kurzeme stands for the entire coastline of the Kaliningrad District, Lithuania and the Latvian Baltic Proper coast, from 20° E, 55° N to 21°50' E, 57°45' N (grid cells 1–61 in Fig. 2). The Gulf of Finland is represented by grid cells 101–154 located to the north-east of 23°20' E, 59°12' N. Cells 62–100 between Kurzeme and Gulf of Finland are denoted as Western Estonia. The Gulf of Riga is covered by cells 154–222.

	Eastern Baltic	Kurzeme	Gulf of Riga	Estonia	Western Estonia	Gulf of Finland
Entire coastline	1491	596	283	611	391	220
Areas with no restrictions	839	245	149	446	297	149

4. Results

4.1. Bulk wave energy resource

In this paper we are mostly interested in the energy resource in terms of the annual average wave power for the entire study area and to a lesser extent in its spatio-temporal variations. We do not discuss the characteristics of the possible wave energy converters to be used, but focus on the analysis of the power theoretically available in the given area. The data and approach described in the previous sections evidently provide an adequate first guess of the available wave energy resource and its variations in space and time, although uncertainties in the wave data may give rise to certain deviations of the resulting estimates from their true values.

The entire eastern Baltic Sea can, on average, supply about 1.5 GW of the wave energy flux at the converter line. As this line is set along the locations where the energy flux of onshore waves reaches its maximum and the presence of ice is ignored, this estimate and similar estimates below should be interpreted as theoretical limiting values of the relevant quantities under the existing climatic conditions.

In order to understand the regional variations and proportions of the wave energy resources, we divide the study area into four stretches: Kurzeme, Western Estonia, Gulf of Riga and Gulf of Finland (see Table 1 for their description and for the relevant set of the numbers of segments of the converter line in Eq. (7)). The largest resources occur along the Kurzeme Peninsula and the western coast of the Estonian archipelago (about 600 MW each). The resources in the Gulf of Riga and the Gulf of Finland are considerably smaller. The entire Gulf of Riga can provide about 280 MW and the southern coast of the Gulf of Finland about 220 MW. The total resource of the Gulf of Finland is much greater because the predominant winds blow here from the south-west and the wave heights (especially the higher quantiles of wave conditions) are, on average, somewhat larger in the northern part of this gulf [59].

The long-term average wave energy flux per unit length of the converter line varies markedly along the eastern Baltic Sea (Fig. 5). It is not unexpected that the energy flux is the largest (typically in the range of 1.5–2.5 kW/m) in the eastern Baltic Proper and considerably smaller in the Gulf of Finland (at best around 0.5 kW/m) and in the eastern Gulf of Riga (about 1 kW/m). Although the modelled extreme wave heights in the Gulf of Riga are almost the same as in the Baltic Proper, high waves are infrequent in this gulf. The average energy flux in this gulf is also much smaller than in the open part of the Baltic Sea. Part of this difference stems from relatively short wave periods in both the Gulf of Riga and the Gulf of Finland. Interestingly, the alongshore variation in the average wave energy flux is much larger in these gulfs than in the Baltic Proper. This feature is apparently related to the two-peak structure of predominant winds [32] and to the similar structure of predominant approach directions of the highest waves.

The average wave energy flux (up to 2.55 kW/m, Fig. 5) is largest in the nearshore of the island of Saaremaa (Fig. 2). Similar values have been hindcast also in the northern part of the Kurzeme Peninsula (to the north of 57° N), in the nearshore of the Sõrve Peninsula (the southernmost part of Saaremaa) and in the south-western and western nearshore of the island of Hiiumaa (Fig. 2). The average energy flux is somewhat smaller, in the range of 1.5–2 kW/m, along the entire coastline of the Kaliningrad District and Lithuania and along the southern part of the Latvian coastline. This distribution only partially matches the similar distribution for the average wave heights in the Baltic Sea [36]. The average wave energy flux decreases rapidly to the east of the Kõpu Peninsula (the

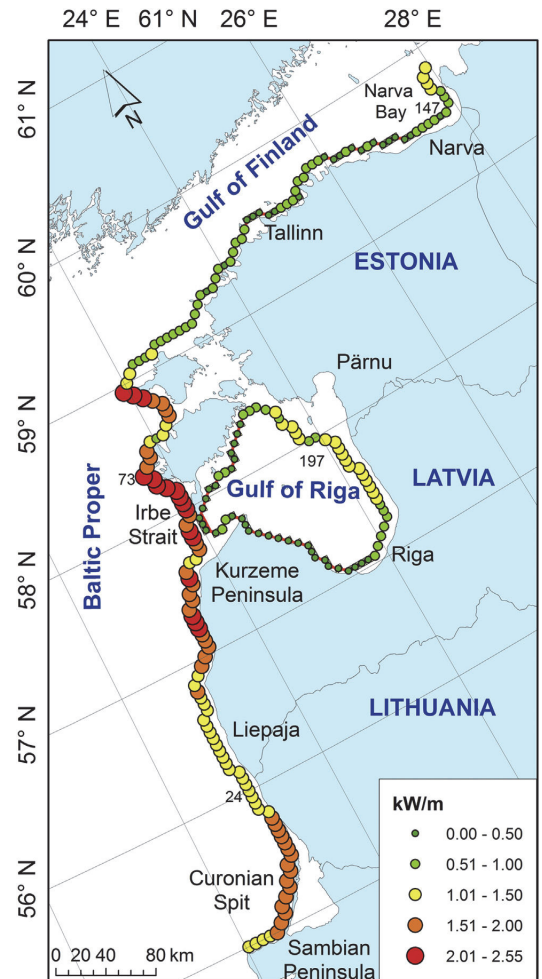


Fig. 5. Long-term average wave energy flux along the coasts of the eastern Baltic Proper, Gulf of Finland and Gulf of Riga in 1970–2007. A colour version of the figure is available in the online version of this manuscript.

westernmost part of Hiiumaa) and is mostly well below 1 kW/m in the interior of the Gulf of Finland. The largest levels of the wave energy flux in this gulf occur along the eastern coast of Narva Bay where they reach 1 kW/m in a section that is completely open to the west.

The spatial distribution of the wave energy flux is substantially anisotropic in the Gulf of Riga, with values over 1 kW/m along its eastern coast and below 0.5 kW/m along its western coast. This feature obviously mirrors the well-known anisotropy of the moderate and strong winds in the northern Baltic Proper: most of these winds blow from the south-west or north-north-west [32]. Although the north-north-western winds may be the strongest, they are relatively infrequent and the statistics of south-western winds governs the distribution of wave energy in the Gulf of Riga. This anisotropy *inter alia* means that the wave energy flux along the eastern (Swedish) coast of the Baltic Proper [26,27] is evidently much smaller than the values given here for the coasts of Latvia and western Estonia.

4.2. Temporal variability of the wave energy flux

The wave energy flux is usually much more intermittent in semi-sheltered seas than at the open ocean coasts. The reason is that intense remote swells (that give a considerable amount of the total wave energy resource in the open ocean [3]) are practically absent in sheltered water bodies. This feature is particularly strongly expressed in the Baltic Sea. Although this sea may host almost as high waves as the Mediterranean Sea, its limited size dictates that both the reaction (saturation) time of wave fields and the memory of wave fields after the wind has ceased are relatively short, from a few hours to maximally one day [31,32]. As the wave energy flux behaves roughly as H_S^2 in shallow waters, even modest variations in the wave height may lead to substantial variations in the energy flux. The onshore component of the wave energy flux may be additionally modified in single cells by possible turns in the wind direction.

The basic features of the variability of the wave energy flux are highlighted below based on the analysis of the temporal course of wave power at four locations. These locations are representative for the four stretches defined above (eastern Gulf of Riga, eastern Gulf of Finland, Western Estonia and the Baltic Proper coast of Latvia, Lithuania and the Kaliningrad District, denoted together as Kurzeme) and represent substantially different wave energy resources. The chosen locations are (i) at the border of Lithuania and Latvia (cell 24 in Fig. 2), (ii) to the west of Saaremaa at the location that provides the largest wave energy resource in the entire study area (cell 73), (iii) at the southern coast of Narva Bay (cell 147) and (iv) in the eastern Gulf of Riga (cell 197).

The maximum values of p_{ij}^{Wh} frequently exceed its average levels by at least two orders of magnitude at each of these locations ($j = 24, 73, 147, 197$; Fig. 6). The peak wave power values reached 680 kW/m during a furious storm in the north-eastern Baltic Proper (near the Western Estonian archipelago) and almost 470 kW/m in the eastern part of the Gulf of Riga. Such high energy fluxes were exceptional in the Gulf of Riga. The all-time peak of wave power was about 286 kW/m in the south-eastern Baltic Proper and much smaller, slightly exceeding 100 kW/m, at the southern coast of Narva Bay in the eastern Gulf of Finland.

High variability becomes also evident in joint distributions of the occurrence of wave fields with different heights and periods (scatter diagrams). These diagrams usually express the counts of wave fields with a certain height and period (numbers in panels of Fig. 7). This count is amended by an estimate of the bulk wave energy resource (calculated as described above) that is contained, on average, each year in all wave fields with a fixed height and period (colour scale). Different roles of waves with different heights and periods in the wave energy budget are exemplified through isolines that indicate the instantaneous wave energy flux for such waves. As typical of sheltered seas, the maximum counts of wave fields with a certain height and period in Fig. 7 are concentrated around a combination of wave fields roughly corresponding to either a Pierson–Moskowitz spectrum or to fetch-limited wave fields with a JONSWAP spectrum. As higher and longer waves provide much larger energy fluxes than short and low waves, the maxima of bulk wave energy resource are provided by wave conditions that are relatively rare. The greatest contribution to the wave power at all four sites represented in Fig. 7 is provided by

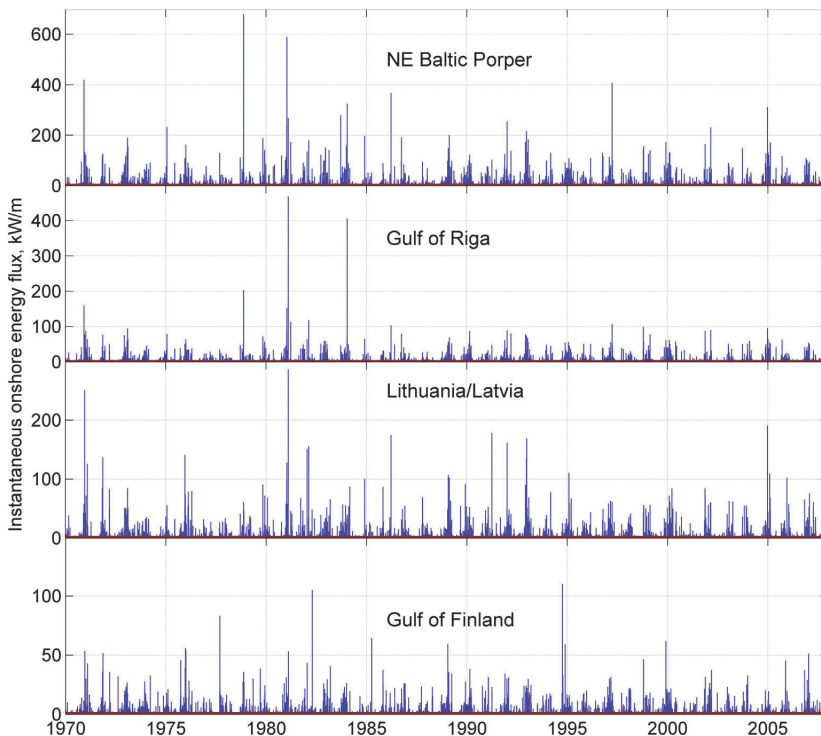


Fig. 6. Instantaneous onshore wave energy flux at four selected grid cells (see Fig. 2) in the nearshore of Saaremaa in the north-eastern Baltic Proper, in the eastern Gulf of Riga, at the border of Latvia and Lithuania in the south-eastern Baltic Proper and in the eastern Gulf of Finland in 1970–2007. The red horizontal line indicates the average wave energy flux for each location. A colour version of the figure is available in the online version of this manuscript.

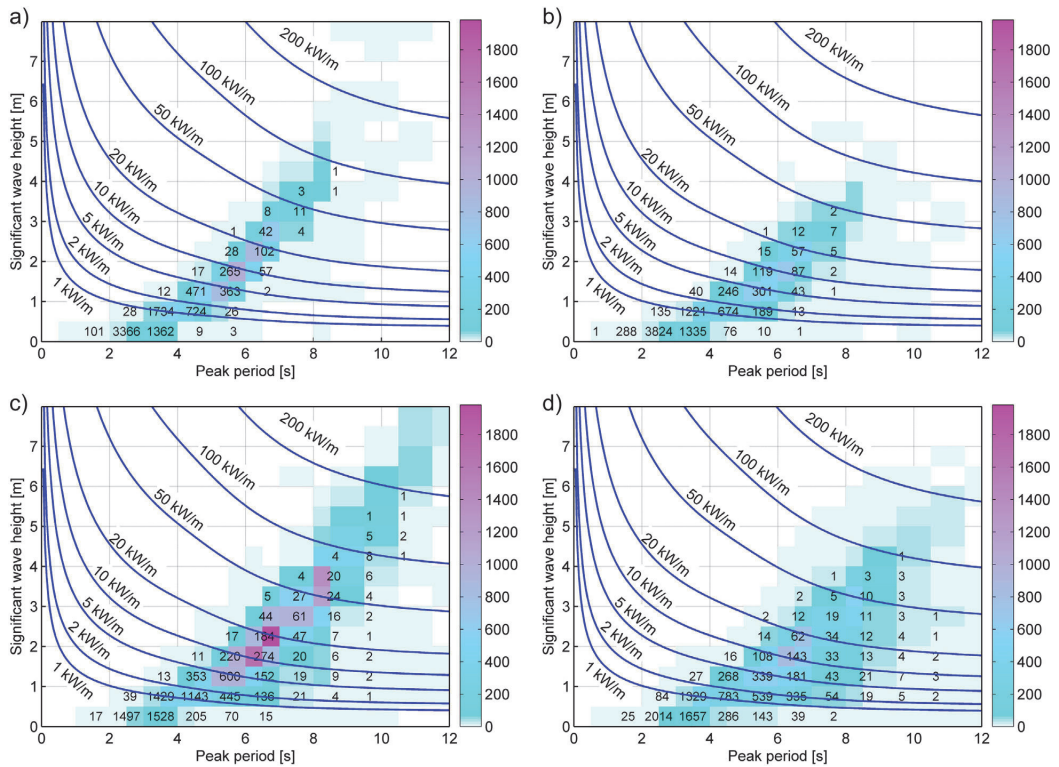


Fig. 7. Combined scatter and energy diagram for four selected wave model grid cells: (a) cell 197 in Fig. 2 in the Gulf of Riga, (b) cell 147 in the eastern Gulf of Finland, (c) cell 73 near Saaremaa, (d) cell 24 at the border of Latvia and Lithuania. The numbers show the annual average of hours with the relevant wave conditions with a resolution of 0.5 m in wave heights and 1 s in wave periods for 1970–2007. The colour scale shows the annual bulk energy resource [kW·h/m] carried onshore by wave fields with the relevant wave properties with a resolution of 0.5 m in wave heights and 0.5 s for waves with periods less than 7 s and 1 s for waves with periods longer than 7 s. Solid blue lines present the instantaneous energy flux for different combinations of the significant wave height and peak period for the water depth in the selected grid cell. A colour version of the figure is available in the online version of this manuscript.

wave conditions with the significant wave height of 1.5–2.5 m and the peak period of 5–7 s. The typical energy flux of such waves is on the order of 10 kW/m. It is therefore rational to use wave energy converters designed for these wave parameters in the study area. Although much higher levels of instantaneous wave energy flux may occur at these sites, such waves are infrequent. The wave energy flux exceeded 100 kW/m on very few occasions. Their average duration was below 1 h/yr in the Gulf of Finland, Gulf of Riga and in the southern Baltic Proper and reached about 15 h/yr near Saaremaa.

Not unexpectedly, the strongest cyclic variations in the wave energy flux $P_{ij}^{w/h}$ reflect the seasonal course of wind speed in the study area. The intermittency of the wave energy flux becomes vividly evident from the comparison of its monthly mean values with the standard deviation of its single values for these months in different years (Fig. 8). This intermittency is present both at individual locations (not shown) and in the values calculated over longer coastal stretches. The standard deviation of the hourly values of the energy flux normally exceeds the relevant monthly average by 8–10 times, whereas the difference is smaller in summer and larger in winter.

Almost half of the wave energy flux crosses the converter line in winter (December–January–February) and only 7% in summer (June–July–August) (Fig. 9). This proportion is roughly the same along the entire study area. Interestingly, the distribution of the

wave energy flux between seasons varies considerably in different years (Fig. 10). In some years (e.g., 1986) the wintertime wave energy flux forms only 20% of the annual energy flux but reaches up to 60% during the most severe winters. The relative variation (from 10% to 60% of the annual flux) in the energy flux is largest in autumn. Spring and summer together usually provide less than 25% of the annual flux. This pattern simply reflects a strong seasonal variation in the wind speed [32] and wave climate [47] in this region, with the calmest time in late spring and summer and the windiest time in autumn and winter. As the energy flux in shallow water is roughly proportional to $H_s^{2.5}$, these variations are particularly pronounced in the seasonal course of the wave energy resources. Interestingly, interannual variations in the seasonal wave energy resource are highly coherent over different coastal stretches (Kurzeme, Western Estonia, Gulf of Riga, Gulf of Finland): the deviations from the relevant values in single years (not shown) differ from those calculated for the entire study area by only a few per cent.

4.3. The role of heavy storms

The discussed features of the wave energy flux vividly reflect the basic properties of the Baltic Sea wave fields such as the highly intermittent wave regime, the presence of mostly fresh, young windseas, almost total absence of intense remote swells, short reaction time of the wave field to changing wind conditions and short

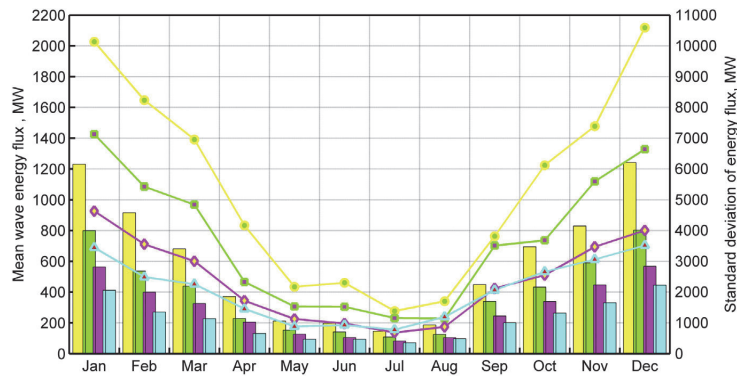


Fig. 8. Seasonal course of the monthly onshore wave energy flux (bars) and the monthly standard deviation (lines) summarised for the coastal stretches from the Sambian Peninsula to the Irbe Strait (Kurzeme, yellow), Western Estonia (green), Gulf of Riga (magenta) and the Gulf of Finland (cyan). A colour version of the figure is available in the online version of this manuscript.

memory of the wave field after the end of a storm. These features largely stem from the small size of the water body. A natural conjecture is that a substantial amount of the wave energy flux is concentrated in short time intervals even in domains that are fully open to the Baltic Proper and thus affected by waves generated in storms elsewhere in the Baltic Sea. This conjecture is analysed by sorting all 333,096 single hourly values of the wave energy flux p_{ij}^{Wh} ($1 \leq i \leq 333,096$) in each section of the converter line (fixed values of j) in ascending order and subsequent evaluation of the contribution of the hourly intervals with the lowest and highest values of p_{ij}^{Wh} . The results, therefore, represent the formal proportion of the calmest and windiest conditions in a year notwithstanding their sequence of occurrence.

The total duration of calm events and episodes during which no onshore energy flux is available is at least 25% of the entire year at the four selected locations (Fig. 11), varying to some extent along the coast. It was, on average, 93.8 days/yr in the southern Baltic and 102.7 days/yr in the nearshore of Saaremaa in 1970–2007. In semi-sheltered sub-basins of the Baltic Sea this duration is as long as about 1/3 of the year (118 days/yr in the eastern Gulf of Finland and 118.6 days/yr in the eastern Gulf of Riga). The calmer half-year (understood as the set of 1-h intervals with the smallest onshore

wave energy flux each year; see above) provides only 1% of the total annual energy flux (Fig. 11). Most of the energy flux is concentrated in a relatively small number of wave events. About 90% of the entire annual wave energy flux arrives within about three months (1/4 of the time), 75% of it arrives in five weeks and almost 60% within 18 days. While there is some variation in the duration of relatively calm episodes in different locations, the proportion of the roughest seas in the total annual energy flux is practically the same for the entire study area (insert in Fig. 11). A few strongest wave storms, with a total duration of about two days, produce about 20% of the annual wave energy flux.

4.4. Wave energy and marine protected areas

The above estimates reflect the theoretically available wave energy flux towards the eastern Baltic Sea coasts. Although some systems of wave energy converters are claimed to be able to catch as much as 80% of the bulk wave energy, losses in the conversion process and the unusable part of wave motion are still considerable. The realistic output into the electricity grid would hardly exceed 50% of the theoretically available energy [29]. Therefore, even if the entire study area would be covered with the very best existing

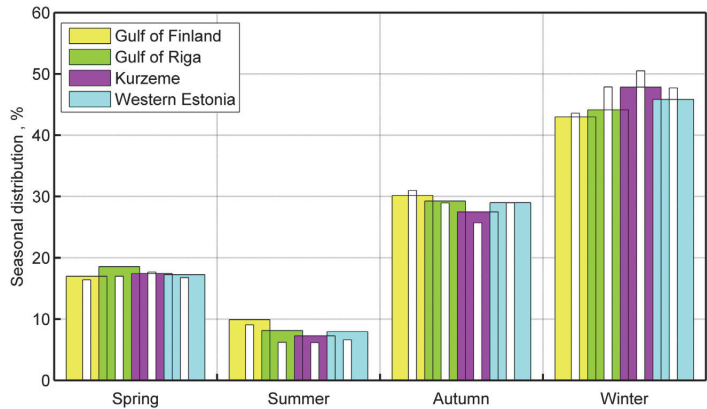


Fig. 9. The proportion of the average wave energy flux in different seasons from the annual average integrated over longer coastal stretches (wide bars) and in grid cells Nos 24, 73, 147 and 197 in Fig. 2 (narrow white bars).

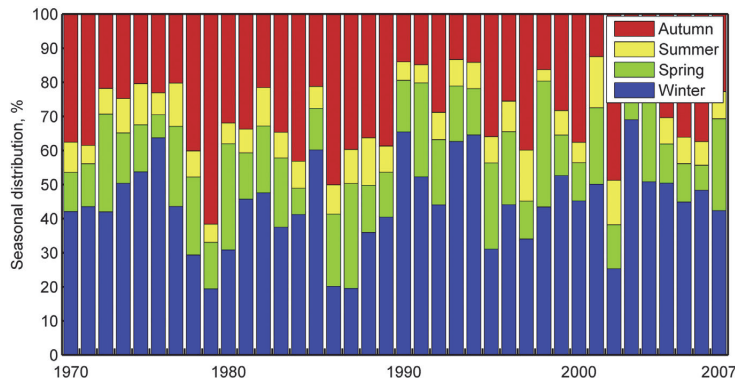


Fig. 10. The proportion of wave energy approaching the entire study area in different seasons in single years. The similar distributions for shorter coastal stretches (Kurzeme, Western Estonia, Gulf of Riga, Gulf of Finland) are almost identical with the presented distribution.

converters, their theoretical contribution to the grid would probably not exceed 700 MW.

There are, however, other constraints that severely limit the energy production. While fairways to the harbours can be easily kept open by smart distribution of the converters, energy production is highly questionable in the vicinity of marine protected areas (MPA). The existing and planned MPAs, incl. the Natura 2000 areas, cover about 46% of the study area (Fig. 12). Recalculating the wave energy resources for the rest of the converter line (summing only over those values of p_{ij}^{wh} that correspond to the sections of the converter line that do not overlap with the existing or planned MPAs) shows that the unprotected areas provide only 56% (42–73% for different coastal stretches in Table 1) of the theoretically available bulk wave energy flux. The wave energy production would hardly be possible in the nearshore of Latvia and Lithuania if all the planned marine protected areas were designated. Moreover, it is not clear how wave energy extraction in areas adjacent to the MPAs would affect the ecosystem in the MPAs. It is natural to assume that energy production will not be allowed, at least in the part of the “transit” regions through which waves approach the MPAs. Together with the limitations of the existing converters, the discussed needs for the protection of marine and coastal environment would probably reduce the theoretical maximum wave energy

contribution the grid to the level of 300–400 MW for the entire study area.

5. Conclusions and discussion

The wave energy potential of the eastern Baltic Sea is definitely appreciable. The best location for wave energy converters is in the nearshore at water depths of 15–20 m. On average, the wave energy flux is about 1.5 kW/m and reaches up to 2.55 kW/m in selected locations of the north-eastern Baltic Proper. The wave energy resources are much smaller, normally around 0.6–0.7 kW/m, in the interior of the Gulf of Finland and in the Gulf of Riga. The total theoretical wave energy resource is about 1.5 GW for the entire nearshore of the eastern Baltic Sea, from which the Gulf of Finland and Gulf of Riga together form about 0.5 GW.

The existing and proposed marine protected areas limit severely the available wave energy resource down to about 840 MW in the eastern Baltic Sea and to about 500 MW along the eastern coast of the Baltic Proper. Given a realistic utility factor of 30% for the Baltic Sea [29], the total wave energy resource is ~200 MW for all three Baltic countries (Estonia, Latvia, Lithuania) and the Kaliningrad District (Russia) together. This amount forms about 6% of the current electricity consumption in that region (<http://www.kpmg.com/EE/et/IssuesAndInsights/ArticlesPublications/Documents/KPMG-energia-analys-web.pdf>). Although this amount will probably never play any decisive role in the grid energy production in this region, it could still be valuable for certain coastal domains.

The major limiting factors affecting the production of grid energy are the high intermittency and strong seasonal variation in the wave properties. These two aspects severely complicate the relevant technical solutions. For example, about half of the annual wave energy flux arrives within several strongest storms with a total duration of about two weeks. This is the time interval when also the wind energy production is at its maximum. Moreover, it is probably necessary to switch off the wave energy converters or to pack them to the seabed during extreme storms. Technically, this problem is similar to the issues related to hurricanes and typhoons [10]. Another major issue is the regular presence of ice in both the wave generation domain (that reduces the available wave energy) and potential locations of wave energy converters [53]. Given also the high cost of the connections between many feasible locations of wave energy plants and the existing grid, it is not likely that wave energy production in the coastal waters of the Baltic Sea will become economically justified in the conceivable future, similarly to the

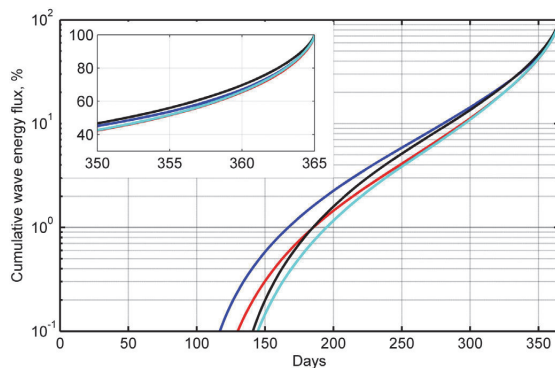


Fig. 11. Cumulative energy flux at the four selected cells Nos 24, 73, 147 and 197 in Fig. 2 (blue: the border between Latvia and Lithuania, red: western coast of Saaremaa, black: eastern Gulf of Finland, cyan: eastern Gulf of Riga) on annual average. The inset reflects the contribution of the most intense wave fields during 360 h (15 days) a year. A colour version of the figure is available in the online version of this manuscript.

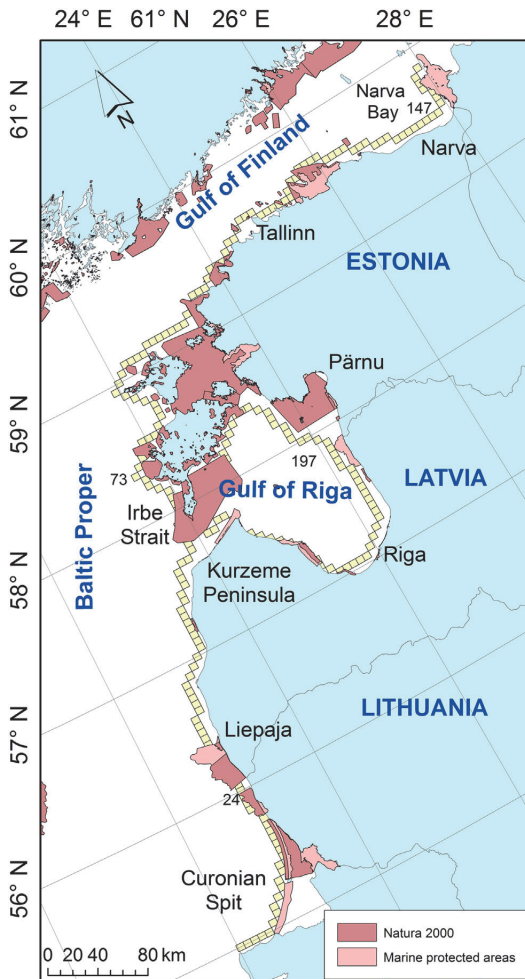


Fig. 12. The existing and proposed Baltic Sea protected areas and Natura 2000 areas along the eastern coast of the Baltic Sea. Data courtesy of HELCOM: http://www.helcom.fi/environment2/biodiv/en_GB/bspas/ (March 2013). A colour version of the figure is available in the online version of this manuscript.

situation in several more advanced regions in terms of wave energy such as the eastern coast of the Mediterranean Sea [20].

This of course does not mean that the wave energy resource is a principally unusable asset in the Baltic Sea region. It would definitely be of some use for remote locations that are not connected to the main grid. In some locations arrays of wave energy converters may serve as a perfect substitute for breakwaters or “soft” measures of coastal protection. Such arrays may be used as portable constructions to slow down the littoral flow near vulnerable coastal sections and to fill with sediment the coastal stretches that currently suffer from erosion. The intermittent nature of the wave energy flux does not prevent its use for the heating or pumping of water, hydrogen production, etc. Finally, the intermittent nature of the Baltic Sea wave fields could be interpreted as a challenge to new and creative solutions for wave energy converters.

Acknowledgements

This study was a part of the project “Science-based forecast and quantification of risks to properly and timely react to hazards impacting Estonian mainland, air space, water bodies and coasts” (TERIKVANT), supported by the European Union (European Regional Development Fund, ERDF) and managed by the Estonian Research Council in the framework of the Environmental Technology R&D Programme KESTA. The research was partially supported by the targeted financing of the Estonian Ministry of Education and Research (grant SF0140007s11), by the Estonian Science Foundation (grant No. 9125) and through support of the ERDF to the Centre of Excellence in Non-linear Studies CENS. The authors are deeply grateful to Andrus Räämet for providing the simulated wave data and to Maija Viska for her help in the design of maps.

References

- [1] Cruz J. Ocean wave energy, current status and future perspectives (green energy and technology). Springer; 2008. p. 461.
- [2] Previsic M, Epler J, Hand M, Heimiller D, Short W, Eurek K. The future potential of wave power in the United States. Prepared by RE Vision Consulting on behalf of the U.S. Department of Energy; 2012. p. 122.
- [3] Arinaga RA, Cheung KF. Atlas of global wave energy from 10 years of reanalysis and hindcast data. *Renew Energy* 2013;39:49–64.
- [4] Jacobson MZ. Review of solutions to global warming, air pollution, and energy security. *Energy Environ Sci* 2009;2:148–73.
- [5] Defne Z, Haas KA, Fritz HM. Wave power potential along the Atlantic coast of the southeastern USA. *Renew Energy* 2009;34:2197–205.
- [6] Hughes MG, Heap AD. National-scale wave energy resource assessment for Australia. *Renew Energy* 2010;35:1783–91.
- [7] Stopa JE, Cheung KF, Chen Y-L. Assessment of wave energy resources in Hawaii. *Renew Energy* 2011;36:554–67.
- [8] Iglesias G, Carballo R. Wave resource in El Hierro—an island towards energy self-sufficiency. *Renew Energy* 2011;36:689–98.
- [9] Rusu L, Guedes Soares C. Wave energy assessments in the Azores islands. *Renew Energy* 2012;45:183–96.
- [10] Chiu F-C, Huang W-Y, Tiao W-C. The spatial and temporal characteristics of the wave energy resources around Taiwan. *Renew Energy* 2013;52:218–21.
- [11] Stopa JE, Filipot J-F, Li N, Cheung KF, Chen Y-L, Vega L. Wave energy resources along the Hawaiian Island chain. *Renew Energy* 2013;55:305–21.
- [12] Sierra JP, González-Marco D, Sospedra J, Gironella X, Mössö C, Sánchez-Arcilla A. Wave energy resource assessment in Lanzarote (Spain). *Renew Energy* 2013;55:480–9.
- [13] Vicinanza D, Contestabile P. Wave energy potential in the north-west of Sardinia (Italy). *Renew Energy* 2013;50:506–21.
- [14] Folley M, Whittaker TJT. Analysis of the nearshore wave energy resource. *Renew Energy* 2009;34:1709–15.
- [15] Rusu E, Guedes Soares C. Numerical modelling to estimate the spatial distribution of the wave energy in the Portuguese nearshore. *Renew Energy* 2009;34:1501–16.
- [16] Iglesias G, Carballo R. Wave energy resource in the Estaca de Bares area (Spain). *Renew Energy* 2010;35:1574–84.
- [17] Iglesias G, López M, Carballo R, Castro A, Frigaard P. Wave energy potential in Galicia (NW Spain). *Renew Energy* 2009;34:2323–33.
- [18] Kim G, Jeong WM, Lee KS, Jun K, Lee ME. Offshore and nearshore wave energy assessment around the Korean peninsula. *Renew Energy* 2011;36:1460–9.
- [19] Saket A, Etemad-Shahidi A. Wave energy potential along the northern coasts of the Gulf of Oman, Iran. *Renew Energy* 2012;40:90–7.
- [20] Aoun NS, Harajli HA, Queffeuilou P. Preliminary appraisal of wave power prospects in Lebanon. *Renew Energy* 2013;53:165–73.
- [21] Jacobson MZ, Delucchi MA. Providing all global energy with wind, water, and solar power, Part I: technologies, energy resources, quantities and areas of infrastructure, and materials. *Energy Policy* 2011;39:1154–69.
- [22] Portilla J, Sosa J, Cavaleri L. Wave energy resources: wave climate and exploitation. *Renew Energy* 2013;57:594–605.
- [23] Liang B, Fan F, Yin Z, Shi H, Lee D. Numerical modelling of the nearshore wave energy resources of Shandong peninsula, China. *Renew Energy* 2013;57:330–8.
- [24] Ortega S, Osorio AF, Agudelo P. Estimation of the wave power resource in the Caribbean Sea in areas with scarce instrumentation. Case study: Isla Fuerte, Colombia. *Renew Energy* 2013;57:240–8.
- [25] Aydoğan B, Ayat B, Yüksel Y. Black Sea wave energy atlas from 13 years hindcasted wave data. *Renew Energy* 2013;57:436–47.
- [26] Martensson M, Bergdahl L. On the wave climate of the southern Baltic. Report Series A:15, Department of Hydraulics. Sweden: Chalmers University of Technology; 1987.
- [27] Söderberg P. The Swedish coastal wave climate. SSPA Research Report No. 104. Gothenburg, Sweden: SSPA; 1987.

- [28] Waters R, Engström J, Isberg J, Leijon M. Wave climate off the Swedish west coast. *Renew Energy* 2009;34:1600–6.
- [29] Bernhoff H, Sjøstedt E, Leijon M. Wave energy resources in sheltered sea areas: a case study of the Baltic Sea. *Renew Energy* 2006;31:2164–70.
- [30] Henfridsson U, Neimane V, Strand K, Kapper R, Bernhoff H, Danielsson O, et al. Wave energy potential in the Baltic Sea and the Danish part of the North Sea, with reflections on the Skagerrak. *Renew Energy* 2007;32:2069–84.
- [31] Soomere T. Wind wave statistics in Tallinn Bay. *Boreal Environ Res* 2005;10:103–18.
- [32] Soomere T, Keevallik S. Anisotropy of moderate and strong winds in the Baltic Proper. *Proc Estonian Acad Sci Eng* 7; 2001. pp. 35–49.
- [33] Jönsson A, Broman B, Rahm L. Variations in the Baltic Sea wave fields. *Ocean Eng* 2003;30:107–26.
- [34] Soomere T. Anisotropy of wind and wave regimes in the Baltic Proper. *J Sea Res* 2003;49:305–16.
- [35] Schmager G, Fröhle P, Schrader D, Weisse R, Müller-Navarra S. Sea state, tides. In: Feistel R, Nausch G, Wasmund N, editors. *State and evolution of the Baltic sea 1952–2005*. Hoboken NJ: Wiley; 2008. pp. 143–98.
- [36] Soomere T, Räämet A. Spatial patterns of the wave climate in the Baltic Proper and the Gulf of Finland. *Oceanologia* 2011;53(1-TI):335–71.
- [37] Broman B, Hammarklint T, Rannat K, Soomere T, Valdmann A. Trends and extremes of wave fields in the north–eastern part of the Baltic Proper. *Oceanologia* 2006;48:165–84.
- [38] Cieslikiewicz W, Paplińska-Swercel BA. 44-year hindcast of wind wave fields over the Baltic Sea. *Coast Eng* 2008;55:894–905.
- [39] Tuomi L, Kahma KK, Pettersson H. Wave hindcast statistics in the seasonally ice-covered Baltic Sea. *Boreal Environ Res* 2011;16:451–72.
- [40] Soomere T, Weisse R, Behrens A. Wave climate in the Arkona Basin, the Baltic Sea. *Ocean Sci* 2012;8:287–300.
- [41] Suursaar Ü, Kullas T. Decadal variations in wave heights off Cape Kelba, Saaremaa Island, and their relationships with changes in wind climate. *Oceanologia* 2009;51:39–61.
- [42] Suursaar Ü, Kullas T. Decadal changes in wave climate and sea level regime: the main causes of the recent intensification of coastal geomorphic processes along the coasts of Western Estonia?. In: *WIT transactions on ecology and environment* 126; 2009. pp. 105–16.
- [43] Suursaar Ü. Waves, currents and sea level variations along the Letipea–Sillamäe coastal section of the southern Gulf of Finland. *Oceanologia* 2010;52:391–416.
- [44] Soomere T. Extremes and decadal variations of the northern Baltic Sea wave conditions. In: Pelinovsky E, Kharif C, editors. *Extreme ocean waves*. Springer; 2008. pp. 139–57.
- [45] Soomere T, Behrens A, Tuomi L, Nielsen JW. Wave conditions in the Baltic Proper and in the Gulf of Finland during windstorm Gudrun. *Nat Hazards Earth Syst Sci* 2008;8:37–46.
- [46] Komen GJ, Cavaleri L, Donelan M, Hasselmann K, Hasselmann S, Janssen PAEM. *Dynamics and modelling of ocean waves*. Cambridge University Press; 1994. p. 532.
- [47] Räämet A, Soomere T. The wave climate and its seasonal variability in the northeastern Baltic Sea. *Est J Earth Sci* 2010;59:100–13.
- [48] Myrberg K, Ryabchenko V, Isaev A, Vankevich R, Andrejev O, Bendtsen J, et al. Validation of three-dimensional hydrodynamic models in the Gulf of Finland based on a statistical analysis of a six-model ensemble. *Boreal Environ Res* 2010;15:453–79.
- [49] Höglund A, Meier HEM. Environmentally safe areas and routes in the Baltic Proper using Eulerian tracers. *Mar Pollut Bull* 2012;64:1375–85.
- [50] Räämet A. *Spatio-temporal variability of the Baltic Sea wave fields*. PhD thesis. Tallinn, Estonia: Tallinn University of Technology; 2010. p. 169, <http://digi.lib.ttu.ee/j/7500>.
- [51] Räämet A, Suursaar Ü, Kullas T, Soomere T. Reconsidering uncertainties of wave conditions in the coastal areas of the northern Baltic Sea. *J Coast Res* 2009;Special Issue 56:257–61.
- [52] Ching-Piao T, Ching-Her H, Chien H, Hao-Yuan C. Study on the wave climate variation to the renewable wave energy assessment. *Renew Energy* 2012;38:50–61.
- [53] Leppäranta M, Myrberg K. *Physical oceanography of the Baltic Sea*. Berlin Heidelberg New York: Springer Praxis; 2009. p. 378.
- [54] Ardhuin F, O'Reilly WC, Herbers THC, Jessen PF. Swell transformation across the continental shelf. Part I: attenuation and directional broadening. *J Phys Oceanogr* 2003;33:1921–39.
- [55] Liu PC, Chen HS, Doong D-J, Kao CC, Hsu Y-JG. Monstrous ocean waves during typhoon Krosa. *Ann Geophys* 2008;26:1327–9.
- [56] Babanin AV, Hsu T-W, Roland A, Ou S-H, Doong D-J, Kao CC. Spectral wave modelling of Typhoon Krosa. *Nat Hazards Earth Syst Sci* 2011;11:501–11.
- [57] Massel SR. *Ocean surface waves: their physics and prediction*. New Jersey: World Scientific; 1996. p. 491.
- [58] Viška M, Soomere T. Simulated and observed reversals of wave-driven alongshore sediment transport at the eastern Baltic Sea coast. *Baltica* 2013;26:145–56.
- [59] Soomere T, Zaitseva-Pärnaste I, Räämet A, Kurennoy D. Spatio-temporal variations of wave fields in the Gulf of Finland. *Fund Appl Hydrophys* 2010;4(10):90–101 [in Russian].



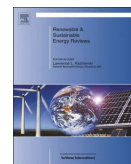
Paper II

Kovaleva O., Eelsalu M., Soomere T. 2013. Hot-spots of large wave energy resources in relatively sheltered sections of the Baltic Sea coast. *Renewable and Sustainable Energy Reviews*, 74, 424–437, doi: 10.1016/j.rser.2017.02.033.



Contents lists available at ScienceDirect

Renewable and Sustainable Energy Reviews

journal homepage: www.elsevier.com/locate/rser

Hot-spots of large wave energy resources in relatively sheltered sections of the Baltic Sea coast

Olga Kovaleva^{a,b,*}, Maris Eelsalu^b, Tarmo Soomere^{b,c}^a Immanuel Kant Baltic Federal University, Nevskogo str., 14, 238300 Kaliningrad, Russia^b Institute of Cybernetics at Tallinn University of Technology, Akadeemia tee 21, 12618 Tallinn, Estonia^c Estonian Academy of Sciences, Kohtu 6, 10130 Tallinn, Estonia

ARTICLE INFO

Keywords:

Wave power
Wave modelling
Baltic Sea
Gulf of Finland
Bay of Gdańsk

ABSTRACT

Even though semi-sheltered sea areas usually have limited wave energy resources, some regions of such basins may still be suitable for wave energy production. We provide a review of the existing wave energy studies in the Baltic Sea basin and discuss specific features and limitations for wave energy production in this water body and possible types of small-scale wave energy converters. We also extend the numerical analysis of wave energy resources in the Baltic Sea to some semi-sheltered nearshore sections that may host large levels of wave energy flux because of a specific combination of the wind regime and geometry of the sea. The test areas are located in the vicinity of the Bay of Gdańsk and in the eastern Gulf of Finland. The estimates of wave energy flux rely on numerically reconstructed time series of wave properties with a spatial resolution of 5.5 km along a > 200 km long coastal section. The average wave energy resource in the test areas is much lower than at the open eastern Baltic Sea coast. However, several sections of the test regions have wave energy potential comparable to fully-open nearshore areas. The onshore wave energy flux reaches 1.79 kW/m at the coast of the Sambian (Samland) Peninsula and 1.61 kW/m in selected sections of the north-eastern Gulf of Finland. These levels provide reasonable options for local wave energy production.

1. Introduction

Ocean waves are one of the most feasible sources of renewable energy [1]. While certain quantities of wave energy reach each coastal area, some locations are presently not favourable for (grid) energy production for various reasons, frequently due to the limitations of existing wave energy converters (WECs) [2]. Although the most promising parts of nearshore waters cover only 2% of the ocean shoreline, they may provide up to 480 GW of power output or 4200 TWh/yr of electricity generation [3]. This energy is fully renewable because it stems from solar power. The wind fields serve as a mediator and the water surface serves as a waveguide that channels the energy to the production site. Therefore, wave energy harvesting is associated with very low levels of pollution and CO₂ release and side effects (e.g., shifting of ship navigation routes or an increase in military importance of an area [4]) are minor.

Wave energy resources (per meter of coastline) are generally less beneficial in semi-sheltered water bodies such as the Mediterranean Sea [5,6], Black Sea [7] or the Baltic Sea [8,9]. Even though semi-sheltered sea areas usually have limited wave energy resources even on the European scale [10], some regions of such basins may still be

suitable for wave energy production [11]. For example, some coastal segments may have large waves arriving from neighbouring open sea domains under certain wind directions [12]. Wave refraction in shallow areas may systematically lead to large concentrations of wave energy in the nearshore [13] and to the formation of unexpectedly rough wave conditions [14]. In some occasions it is possible to harvest wave energy from large areas [8] or to substantially reduce the energy cost using co-located wind and wave farms [15]. Wave energy harvesting at these locations (and sometimes even in relatively mild wave climates) may serve as an economically efficient way for the protection of certain structures [16,17]. The presence of systematic wind anisotropy may lead to reasonable wave energy resources in some coastal areas where long and high waves occur relatively frequently. In the Baltic Sea such areas are found in the nearshore of the north-western and south-western Baltic Proper [18].

Consideration of these matters together with emerging new technical solutions and small-scale devices that are able to accommodate steep waves and intermittent wave conditions [19] (see also <http://www.earthtimes.org/energy/wave-power-generator-tested-black-sea-storm/2011/>) reinforces the interest in wave energy potential in semi-sheltered sea areas. This potential has been studied in some detail for

* Corresponding author at: Immanuel Kant Baltic Federal University, Nevskogo str., 14, 238300 Kaliningrad, Russia.

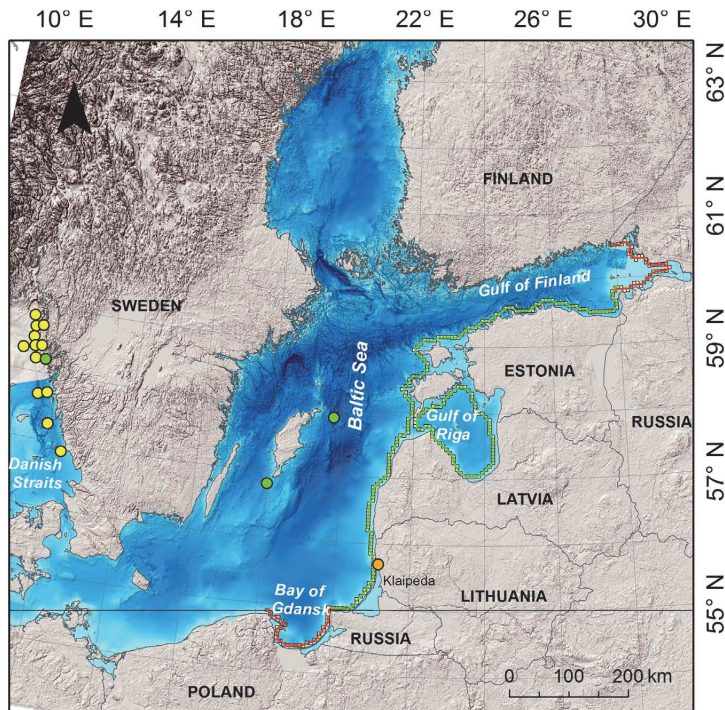


Fig. 1. Location scheme of the Baltic Sea areas for which the wave energy potential has been addressed in the literature. Small green squares cover the domain considered in [9]. Circles indicate localized study areas (orange [20], green [36], yellow [37]). The analysis for the Bay of Gdańsk and the eastern part of the Gulf of Finland (small red squares) is performed in this paper. (For interpretation of the references to color in this figure legend, the reader is referred to the web version of this article.).

the open eastern coast of the Baltic Proper and for some sections of the nearshore of the Gulf of Riga and southern Gulf of Finland based on numerical simulations [9] and long-term time series of visual wave observations [20].

In this paper we provide a review of the outcome of the existing wave energy studies in the Baltic Sea basin (Fig. 1). The focus is on the identification of locations (hot-spots) where wave energy flux is at levels favourable for wave energy production in the future. These areas are also the most vulnerable in terms of coastal erosion. As an important side effect of wave energy production, erosion prone locations may be partially protected against high waves by (chains or arrays of) WECs. We specifically explore the wave properties and prospective for wave energy production in two regions at the eastern coast of the Baltic Sea – the Bay of Gdańsk and the eastern part of the Gulf of Finland (Fig. 2) using the technique developed in [9]. We also discuss prospective designs of small-scale WECs and feasible ways for practical use of wave energy in the Baltic Sea conditions.

The paper is structured as follows. A review of the basic features of the Baltic Sea wave climate, the core quantities used to characterise the wave energy potential, the outcome of wave energy studies in this region and an insight into feasible designs of WECs are presented in Section 2. Section 3 describes the technique of evaluation of wave energy resource along longer coastal stretches from time series of wave height, period and propagation direction. It also gives a brief insight into the implementation of the wave model WAM, the output of which is used in the calculations. Section 4 describes the results of the evaluation of the wave energy potential and discusses the similarities and differences of the wave energy potential in the test areas (the Bay of Gdańsk and the eastern Gulf of Finland). Section 5 presents a short discussion of the outcome and Section 6 formulates the conclusions.

2. Wave energy potential in the Baltic Sea

2.1. Wave climate in the Baltic Sea basin

The core features of the Baltic Sea wave climate from the viewpoint of wave energy harvesting are: (i) relatively mild overall wave regime, (ii) predominance of comparatively short waves, (iii) marked anisotropy and (iv) high intermittency of wave fields, and (v) occasional presence of very rough seas.

The wave climate of the Baltic Sea is, on average, relatively mild [21]. The long-term significant wave height H_s slightly exceeds 1 m in the open part of the Baltic Proper. Wave heights are somewhat less between Gotland and the Swedish mainland and in the Bay of Bothnia. The wave climate is even milder, with H_s around 0.6–0.8 m in semi-sheltered sub-basins such as the Gulf of Finland, Gulf of Riga or Arkona Basin [21,22].

While regular swells are usually the best wave conditions for energy harvesting [1], strong long-period swells are infrequent in all parts of the Baltic Sea [18,23]. As characteristic to semi-sheltered water bodies, the predominant wave periods are considerably shorter in the Baltic Sea than in the neighbouring North Sea or the North Atlantic. Usually waves with periods of 4–6 s predominate in the Baltic Proper (where periods up to 7–8 s also often occur). The typical periods are even smaller, about 3–4 s in the more sheltered and coastal regions [21]. This means that WECs for this region should be designed for relatively steep waves.

The wave regime of the Baltic Sea is markedly anisotropic. This feature is caused by the presence of a two-peak directional structure of marine winds: strong winds predominantly blow from the south-west and north-north-west [24]. This anisotropic wind pattern leads to considerable wave energy concentration along the eastern coasts of the



Fig. 2. Study areas of possible hot spots of wave energy resources in the eastern Baltic Sea. The red line indicates the stretches addressed in this study. The wave energy resource along the stretch from the Sambian Peninsula to Narva Bay (green line) is explored in [9] and in the area near Klaipėda (Lithuania) in [20]. (For interpretation of the references to color in this figure legend, the reader is referred to the web version of this article.).

sea [18,25]. Accordingly, the highest and longest waves are usually found in the eastern regions of all sub-basins of the sea [18,25]. Hot-spots of wave energy should therefore occur at the entrance to the Gulf of Riga and in some locations to the west of the Latvian coast [22]. The properties of wave energy flux in these two nearshore segments are addressed in [9].

The situation in the Baltic Sea offers major technical challenges for wave energy harvesting [9]. Most importantly, the wave heights and periods are highly intermittent both in time and space at various scales [18]. Moreover, the Baltic Sea wave climate exhibits significant seasonal variations. For example, the probability of significant wave height exceeding 1 m varies from about 90% in November to about 10% in May [18]. The highest wave activity occurs in January, and waves are almost as high from October to December [18].

Whilst most of the time the significant wave height is below 0.5 m, the Baltic Sea occasionally has very strong wave storms. The largest instrumentally measured significant wave height is $H_s = 8.2$ m in the

northern Baltic Proper [25]. Numerical simulations indicate that the significant wave height may reach almost 10 m in this region [26] and along some parts of the Latvian coast [22].

2.2. Wave energy flux from time series of wave properties

The fundamental quantity for wave energy harvesting is the wave energy flux. This measure characterises the amount of energy brought by waves to a certain location per unit of time and unit of the wave crest length [27]. The classic expression for the total (sum of kinetic and potential) average wave energy density E (per unit of sea area) of elementary (sinusoidal or Airy) waves is [28]

$$E = \frac{1}{8} \rho g H^2, \quad (1)$$

where ρ is the water density, g is acceleration due to gravity and H is the wave height. Wave systems with a constant height of all single crests are rare and natural wave fields are usually characterised by significant wave height H_s [29]. Their energy, strictly speaking, should be calculated from the full wave energy spectrum [30].

The wave energy flux is a vector $\vec{P} = E \vec{c}_g$ aligned with the wave propagation direction. Its length (and, therefore, the wave energy resource) depends on the group velocity \vec{c}_g . As the Baltic Sea is relatively shallow, it is necessary to employ the intermediate-depth dispersion relation $\omega = \sqrt{gk \tanh(kd)}$, where $\omega = 2\pi/T$ is the angular frequency, T is the wave period, $k = 2\pi/l$ is the wave number, l is the wave length and d is water depth. In this framework the group speed is expressed as

$$c_g = \frac{\omega}{2k} \left(1 + \frac{2kd}{\sinh 2kd} \right). \quad (2)$$

The group speed c_g explicitly depends on the wave length and implicitly on the wave period. The energy flux in each direction is generally a sum of fluxes provided by all harmonics of the wave system with different heights, periods and propagation speeds. Such a detailed description of wave fields is usually not available and the output of wave models and measurement devices normally comprises a few integral characteristics of wave properties.

The minimum amount of data necessary for the reproduction of wave energy fluxes contains the measured or modelled peak period (period of the highest waves in the field), significant wave height and average propagation direction. To a first approximation the energy flux of commonly occurring narrow-banded wave fields (typical for storm waves in which the distribution of single wave heights approximately follows a Rayleigh distribution) with limited directional spreading can be assumed to be equal to the energy flux of elementary (sine) waves with the height of $H_s/\sqrt{2}$, period equal to the modelled peak period and wave propagation direction equal to the modelled mean wave direction.

This approximation discards many details of the wave fields, most importantly, information about the directional spreading of the wave components and the associated energy flux. Although the main wave propagation direction can be identified for most of occasions, many components of natural wave fields normally propagate in a certain range of directions. Therefore, the resulting expression for the scalar value of the wave energy flux (also called wave power and usually estimated in kW/m)

$$P = E c_g \quad (3)$$

normally provides a higher than actual value for wave energy resource for any directional WEC [31]. The difference is evidently large in areas such as the Baltic Sea that often has sea (as opposed to swell) waves with a wide range of propagation directions.

2.3. Wave energy levels and limitations in the Baltic Sea

The first systematic instrumental measurements of the Baltic Sea wave properties started at the end of the 1970s specifically from the

viewpoint of the wave energy [32]. The focus was on the western gateway of the sea [33] that often received strong swells from the North Sea. The western part of the interior of the Baltic Sea was considered to be less favourable for industrial wave energy harvesting [34]. Even though the relevant measurements and simulations covered only short time intervals [35,36], they provided an adequate insight of the basic levels of wave energy in the target areas.

While in many sections of the open ocean the onshore wave energy flux exceeds 50 kW/m [1], these levels are at least by an order of magnitude lower in the Baltic Sea. The most favourable locations for wave energy production are in the nearshore of the Kattegat and Skagerrak (Fig. 1). These locations are outside the main body of the Baltic Sea and often affected by the North Sea wave fields. The average wave energy flux ranges from 2.4 to 5.2 kW/m in this domain [37]. The typical values of the wave energy flux are considerably lower, in the range of 1.5–2.5 kW/m [32] in coastal stretches of the interior of the Baltic Sea (Fig. 1) and below 1 kW/m in sub-basins and partially sheltered bays of the sea [38].

The largest problem faced by designers of WECs for this area is the intermittency of the wave climate: some 80% of the annual energy is found in wave conditions with a higher than average energy flux. An analysis of the related economic issues, including the degree of utilisation (the ratio of yearly produced energy in the installation and the installed power) led to the conjecture that relatively small units, possibly connected into large fields of devices, are the most beneficial in the Baltic Sea [39].

The northern regions of the sea are often covered by ice for periods of the year. Sea ice not only damps waves during a large part of the year [40] but also reduces the effective fetch length and thus the wave energy potential. As drifting ice fields may endanger WECs similarly to other coastal and offshore engineering structures [41], specific types of converters are necessary for the seasonally ice-covered seas [42].

In the past, instrumental wave measurements were only performed in the western and northern parts of the Baltic Sea [21]. For several decades visual observations from the coast served as the only available 'ground truth' of wave properties in the eastern part of the sea. The outcome of visual wave observations was employed in [20] to quantify the wave energy potential near Klaipėda (Lithuania) using a conventional method for calculating distributions of annual hydrologic variables. The annual average wave power flux varies in the range 0.4–1.6 kW/m. Therefore, the near-shore wave power potential along the Lithuanian coast is comparable with that of several other European semi-enclosed seas. The estimated potential of wave energy production along the coasts of Latvia is about 1000 GWh [43,44].

Long-term numerical reconstructions of wave properties shed further light to the eastern Baltic Sea wave energy potential and the associated wave energy resource. The entire onshore wave power was estimated in [9] for about 950 km long coastal stretch in the Baltic Proper from the Sambian (Samland) peninsula to the eastern Gulf of Finland and for about 450 km long stretch in the Gulf of Riga. The time series of basic wave properties (significant wave height, peak period and main wave direction) were calculated using the WAM wave model [29] with a spatial resolution of 3 nautical miles (about 5.5 km) and temporal resolution of 1 h for 1970–2007 [18].

The numerically reconstructed long-term average wave energy flux (per unit length of the shoreline) varies markedly along the eastern Baltic Sea coast. It is the largest (1.5–2.5 kW/m; with a maximum in the nearshore of the island of Saaremaa) in the eastern Baltic Proper and considerably smaller in the Gulf of Finland (around 0.5 kW/m). Consistent with the above-described anisotropy of moderate and strong winds, the wave energy flux exceeds 1 kW/m along the eastern coast of the Gulf of Riga but is <0.5 kW/m along its western coast. Its interannual variations are coherent over the entire study area and basically at the same level as established for the Klaipėda region [20]. The strong seasonal variation of the average wave energy flux reflects the seasonal course of wind speed in the Baltic Sea basin. The greatest

contribution to the wave power provide wave fields with the significant wave height of 1.5–2.5 m, the peak period of 5–7 s and the typical energy flux of about 10 kW/m. Even though such wave conditions are not very frequent, it is rational to use WECs designed for these wave parameters.

The total annual wave energy flux for the entire eastern part of the Baltic Sea (including the Gulf of Riga and the southern coast of the Gulf of Finland) is about 1.5 GW [9]. A large part of this resource (about 600 MW) approaches a relatively short segment of the coast that is most exposed to the predominant winds – the nearshore of the Kurzeme Peninsula and the western coast of the Estonian archipelago. An important limitation for the wave energy production is the presence of numerous existing and proposed marine protected areas that cover almost 50% of the shoreline [9].

Similarly to the western and central Baltic Sea, a critical limitation for the wave energy harvesting is that a great part of the energy flux is concentrated in a relatively small number of wave events. According to [9], about 90% of the annual wave energy flux arrives within three months and almost 60% within 18 days. The contribution of the roughest seas into the total annual energy flux is practically the same for the entire eastern Baltic Sea. This feature not only severely complicates the relevant technical solutions but also gives rise to the situation when about half of the annual wave energy flux arrives within several strong storms with a total duration of about two weeks, and about 30% of it within just a few days [9]. This is one of probable reasons why most of the existing devices have not been tested in the Baltic Sea environment [19].

2.4. Prospective designs of small-scale devices for wave energy harvesting in the Baltic Sea

More than 80 technologies for ocean wave energy harvesting have been proposed and/or tested by various authors and research teams [45]. Several significant overviews of the associated theoretical background [27] and fundamentals, working principles and main features of design of WECs [1,46,47] have been published within the two last decades. These synopses have been complemented by thorough overviews of the relevant technical solutions, experience with trial installations and parameters of industrial devices [45,48], necessary power-equipment and challenges connected with such devices [2], and foresight and insight into related socio-economic and legal aspects [49]. A detailed qualitative analysis of suitability of various kinds of devices in the Caspian Sea (that has fairly similar environmental conditions to those in the Baltic Sea) is presented in [45]. For this reason we discuss only the most recent aspects that are relevant to low-energy conditions and small-scale devices, and comment on few prospective options that have been proposed or tested for the conditions of semi-sheltered water bodies. In line with this viewpoint, we present in Table 1 only a few examples of working devices and comment on the main advantages and disadvantages of the relevant WEC designs in particular conditions of the Baltic Sea. The reader is referred to [45,49], for details and references.

The range of various wave energy converters (WEC) is often divided into as many as 12 different groups [46]. This classification uses three criteria: i) the oscillation modes (heave, surge, pitch) that are utilised, ii) the method of force reaction (against seabed or against another, differently oscillating, body) that is applied, and iii) the type of wave-oscillator interface (solid or flexible structure, or water-air interface of the oscillating-water column). In principle, all these types can be exploited in low-energy conditions. However, it is well known that some types of devices (e.g. Pelamis P1) produce the highest energy (and good economic returns) at high resource locations while other designs (e.g. Wave Star) also function well at sites with a lower resource [50]. This feature makes wave energy harvesting particularly sensitive with respect to potential climate change that may substantially affect wave regimes [51].

Table 1

Main features of different technologies for wave energy harvesting and examples of their realisation in field conditions. The classification mainly follows [47] but also includes the attenuator type of WEC as a separate class of devices [45] (notice a typo in captions of Table 1 and 2 in [45]).

Working principle	Examples of configuration and yield	Advantages	Disadvantages
Oscillating water column (OWC)			
Most widely used in the past; a typical example of so-called first generation of WECs	Offshore in shallow water: Pico 400 kW [70], floating in deeper water (> 40 m): Mighty Whale 110 kW [71], OceanLinx up to 1.5 MW [72]	Long-term experience with so-called first generation WECs Simplicity of the overall construction Locations can match hot spots of (offshore or nearshore) wave energy flux A feasible option for powering navigation buoys or certain vessels	The use of mainly potential energy of wave motion A specific (Wells type) air turbine or pump required Expensive mooring, cabling and maintenance Vulnerable to sea ice
	On-shore or in breakwater: LIMPET 500 kW [73], Sakata harbour (Japan) 60 kW [74], Mutriku (Spain) 16×16.5 kW [75]	Easier installation and maintenance Multi-purpose use for coastal protection Construction costs can be shared Less vulnerable to sea ice	Less energetic wave climate in prospective locations
Oscillating body			
Mostly used in offshore conditions; typically > 40 m depths. The devices largely represent so-called 3rd generation of WECs. Full-scale demonstrations are scarce.	Floating, using translation (heave): Prototype L-10: 10 kW [12], AquaBuoy 250 kW [76], Wavebob [77]	Locations can match hot spots of wave energy flux Suitable for powering navigation buoys or certain vessels Ease of the use of linear electrical generators (minimum moving parts) Easy to build arrays	More complex than OWC devices or other earlier designs Vulnerable to sea ice and extreme seas
	Offshore: SEAREV 500 kW [78]	The use of a wheel acting as pendulum No limitation for the stroke; Ease of mooring (just one cable) Works also in wave fields of medium height	Expensive mooring, cabling and maintenance Vulnerable to sea ice
	Submerged, using translation (heave): Archimedes Wave Spring (AWS) up to 2 MW maximum instantaneous power [79]	Easy to shelter at sea bottom against sea ice and extreme seas Ease of the use of linear electrical generators Less vulnerable to sea ice	Expensive mooring, cabling and maintenance
Attenuator [45]			
Attenuator WECs are designed so that the waves stimulate certain mechanical motions that are further converted into electricity.	Pelamis 750–1000 kW, first grid-connected farm of three devices in 2008 [47],	All the moving parts can be sheltered from the direct wave impact within a closed hull	Vulnerable to sea ice and extreme seas
	Wave Star up to 6 MW [80], Salter Duck (375 kW), Anaconda up to 1 MW [81]	A wheel can be used instead of pendulum with no limitations for the stroke Easy to build arrays (e.g. Wave Star)	
	Rotation: fully submerged WaveRoller [47], surface piercing Oyster 1: 315 kW [82], Oyster 800: 800 kW	Easy to shelter at sea bottom against sea ice and extreme seas	Less efficient for relatively short waves of semi-sheltered seas
Overtopping			
Captures the water that is close to the wave crest	Fixed structure at shoreline (with concentration of wave energy): Tapchan 350 kW [83], fixed in breakwater: SSG 40 kW [84]	Parts facing wave forces separated from the electricity generation Easier installation and maintenance Particularly suitable for very steep wave fields Large energy storage capacity Less vulnerable to sea ice	Relatively high waves required for efficient operation Less energetic wave climate in prospective locations Extensive construction works often needed to focus wave energy
	Floating: Wave Dragon 40 kW [85]	Locations can match hot spots of wave energy flux	Expensive mooring, cabling and maintenance; vulnerable to sea ice

As the wave properties in deep and intermediate water do not scale and in some locations the availability of energy is more important than the cost, the pragmatic approach is to choose or design a specific device

for each type of wave climate. This approach involves the need to match the own frequency of oscillation of the wave energy absorber with the frequency of incoming waves. It also sets severe restrictions on

dimensions of the devices and many WECs designed for relatively long-wave ocean climates have to be redesigned for smaller water bodies. The problem can be circumvented if many small buoys in a compact array are used [35,52].

Oscillating water column WECs make use of potential energy carried by ocean waves. They are the first [47] and until now one of the most popular types of WECs. Small-scale versions are also good wave absorbers for reducing wave reflection from vertical wall breakwaters, seawalls or other rigid structures [53]. These devices may provide an additional benefit by converting air kinetic energy into electric energy via an impulse turbine controlled by specific algorithms [54] in low energy seas like the Baltic Sea [53]. In such conditions it is particularly important to increase the efficiency of the devices. The presence of walls may increase power capture of heaving oscillating water column WECs and spar-buoy devices by up to 10–15% [55]. This effect is particularly favourable under low energy conditions near breakwaters or seawalls. The efficiency of the generator may be further increased by using latching control [56].

Several attempts have been made to construct small- and medium-scale WECs that would effectively cope with harsh properties of the Baltic Sea wave fields. The ideas and developments include, among others, a single heaving-buoy WEC operating and surviving ice interaction [42]. A new type of linear small-scale WEC was recently proposed specifically for low wave energy conditions [19]. Similar linear tubular devices tested for the Mediterranean [57] may also be a solution for the Baltic Sea. As the properties of wave fields in the Baltic Sea and Caspian Sea are quite similar, it is likely that point absorber WECs tested for the Caspian Sea [45] are the most appropriate devices for harvesting wave energy also in the Baltic Sea. As waves of the Baltic Sea are relatively steep, devices like SEAREV [58] that make use of the water surface inclination could work well in this sea.

Even though linear WECs that convert wave energy directly into electric power are still in the testing stage [47], such devices contain a minimum amount of moving details and are simple to control [59], and thus should be most reliable future technology. Specific designs of small-scale linear WEC-generators (exploiting pairs of permanent magnets and ferromagnetic cores between them) have been developed for basins of relatively low wave energy conditions and for various other purposes [19]. Other versions of such designs (e.g. Tubular Permanent Magnet Linear Generator, TPM-LiG) have been proposed for wave energy conversion for small sensorized buoys to be used, for example, in coral reef environments [60]. WECs with tubular linear generators have led to promising results in Italian coastal waters [61,62].

Oscillating bodies (both floating like Pelamis and submerged such as Oyster) can catch the energy of long-period swells that occur but are infrequent in the Baltic Sea [23]. The Finnish device WaveRoller [47]; see also <http://aw-energy.com/index.php/waveroller.html> makes use of the effect of wave shoaling (that leads to almost flat trajectories of water parcels in the nearshore) and is specifically designed for the Baltic Sea. Comparatively small devices that exploit wave overtopping (e.g., WaveCat [63],) may be suitable for relatively short and steep waves in semi-sheltered water bodies such as the Baltic Sea.

There are continuous new developments of WECs such as the Seaspoon device (that catches the kinetic energy of orbital motions ocean waves [64]), Eagle WEC [65], and the non-buoyant body type point absorbing WEC that uses a water filled container as a front end interface instead of a traditional buoyant buoy [66]. Trials of a full-scale Eagle WEC performed in 2012–2014 [65] indicated design problems but smaller-scale versions are likely more stable. Almost miniature pendulum-type wave energy harvesters have been tested for extending the operation time of underwater mooring platforms [67]. Apart from such innovative solutions, there seems still to be a market for simpler, robust mechanical devices (e.g. [68]) that survive in the extremely intermittent conditions of semi-sheltered seas (<http://www.earthtimes.org/energy/wave-power-generator-tested-black-sea-storm/>

2011/) and can serve as an alternative source of clean energy not only in developing countries [69] but also in regions where regular maintenance is complicated.

2.5. Potential locations of large wave energy flux

Even though the studies presented in [9] cover quite long coastal stretches, the geometry of the Baltic Sea (Fig. 1) suggests that several parts of the Baltic Sea nearshore may have even longer fetches for predominant wind directions and thus even more favourable wave energy harvesting conditions. These sections are primarily in the vicinity of the Bay of Gdańsk and the eastern Gulf of Finland (Fig. 2). These regions are geometrically sheltered from some of the strong wind directions. The Bay of Gdańsk is fully open to the north and to some extent to north-north-westerly winds. These winds may have been relatively infrequent before the 1980s when the storm cyclones were largely located to the west of Island [86] but have become the strongest (albeit less frequent than south-easterly winds) in the northern Baltic Proper during the last decades [24]. Some of the severest wave conditions of the Baltic Sea may appear in the vicinity of this bay.

The eastern Gulf of Finland often has waves that are excited by relatively frequent and strong west-south-westerly winds and further shaped by the so-called slanted fetch effect (that supports relatively long waves propagating along the gulf axis even if the wind blows obliquely across the gulf) [87]. It is therefore likely that certain locations in the eastern Gulf of Finland may host wave energy levels comparable to those in the nearshore of the Baltic Proper.

The study area in the Bay of Gdańsk contains a set of coastal sections with greatly different openness to the approaching waves. The sections along the shore of the Sambian Peninsula have one of the severest wave climates in the Baltic Sea while the sections in the western Bay of Gdańsk are almost completely sheltered from high waves. The wave regime in the open sections of this study area generally matches the overall properties of the wave climate of southern Baltic Sea [88,89]. This area is characterised by marked alongshore gradients of average and extreme wave properties. The energy fluxes computed for several points along the shore from Cape Taran to the Vistula River mouth show a significant decrease in both along-shore and cross-shore components of the wave energy flux from the north to the south [90]. This gradient eventually has substantial impact on the intensity and possibly also direction of wave-driven along- and cross-shore sediment transport and is also reflected in the intensity of coastal erosion [90]. As the nearshore deepens relatively rapidly, refraction of wave energy is minor and the direction of wave-driven transport is mostly determined by the deep-water wave approach direction [90].

The interior of the Bay of Gdańsk from the Hel Peninsula to approximately the middle of the Vistula Spit is markedly protected against high waves (at least from some directions) by the Hel Peninsula. The relevant coastal stretch is characterised by considerably lower typical wave heights than the western coast of the Sambian Peninsula or the northern shores of the Hel Peninsula. A comparison of wave heights in deep-water and the completely open (towards the Baltic Proper) location near Lubiato and another relatively deep-water location close to the Vistula river mouth indicates a difference of 45% in the wave heights during winter months and a somewhat smaller deviation (up to 33%) during summer months [91]. The impact of the sheltering effect of the peninsula is clearly present in geomorphological particularities of the shores of the Bay of Gdańsk. For example, differently from the delta of the Oder River [92], the delta of the Vistula River in the interior of the Bay of Gdańsk has a river-dominated nature [91] that is only weakly affected by wave action.

The wind and wave climates are more complicated in the Gulf of Finland. This water body has four significant wind directions and is at least partly ice-covered for several months each year [93]. The presence of long ice seasons can significantly influence energy fluxes during late

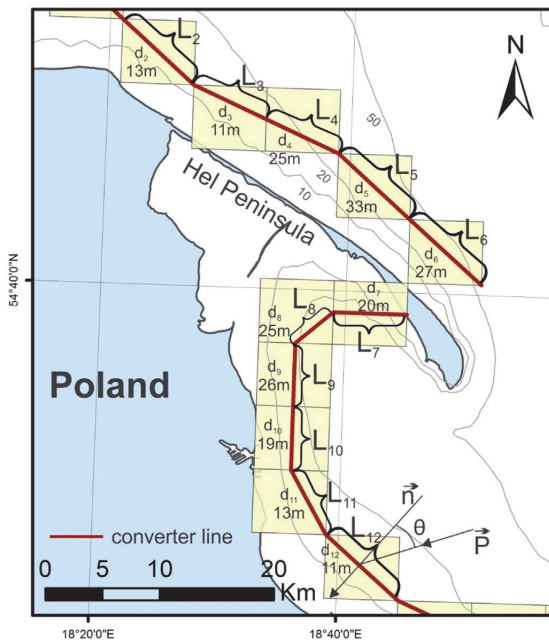


Fig. 3. Location of the lines (red, with length L_i and onshore normal vector \vec{n}) used for the calculation of the wave energy flux for each grid cell (yellow squares, model water depths d_i). The wave energy flux \vec{P} approaches the line in question under the (approach) angle θ between the wave propagation direction and \vec{n} . As the tip of the Hel Peninsula is not accurately represented in the particular implementation of the WAM model, cells 6 and 7 are disconnected in the image. (For interpretation of the references to color in this figure legend, the reader is referred to the web version of this article.)

autumn and winter [94] and may even make the common quantities for characterising the wave climate essentially meaningless [25]. The amount of days with protective ice cover has decreased during the last century by 5–7 days/yr on average for the Gulf of Finland [95,96]. This process has significantly contributed to the coastal evolution in the eastern part of the gulf [95].

Interannual and decadal variations in wind and wave properties are not as pronounced in the Gulf of Finland as they are in the Baltic Proper [18]. However, the anisotropy of wind and wave fields has much larger consequences in this water body. The southern coast of the gulf is relatively sheltered against high waves while the northern part is open to the predominant winds. Moreover, the phenomenon of slanted fetch frequently gives rise to long wave systems that propagate along the axis of the gulf [87]. These waves insignificantly impact the southern and northern coasts that are implicitly protected either by large peninsulas or by extensive archipelago. The resulting wave system may bring unexpectedly large amounts of wave energy to the eastern end of the gulf and may strongly contribute to quite rapid and significant coastal erosion in the north-eastern part of the gulf [95].

3. The search for hot-spots of wave energy: method and data

3.1. Modelled wave data

Similarly to [9], we employ for the calculation of wave energy flux (3) the time series of numerically replicated wave properties (significant wave height, peak period and mean wave direction) in the nearshore of the study areas. These time series are extracted from the output of the wave model WAM [29] that was run for 38 years (1970–2007) in the finite-depth mode for the entire Baltic Sea. The particular implementation of the WAM model and the quality of the

output has been discussed in several publications (see [18,21] and references therein) and we only briefly present their main features. As the basic wave data set is equivalent to the one used in [9], the presented results are directly comparable with those discussed in [9].

The model covers the Baltic Sea with a regular rectangular grid with a resolution of about 5.5 km [18]. The simulations use a directional resolution of 15° (24 equally spaced directions) and 42 frequency bins from 0.042 Hz in a geometrical progression with an increment of 1.1 up to about 2 Hz (periods down to 0.5 s). The inclusion of relatively small periods is necessary to capture wave growth rates in low wind conditions after calm periods [38] and to properly replicate the high-frequency part of the wave fields [97].

The wind forcing covered the time interval of 1970–2007 with a relatively low spatial and temporal resolution of 1°×1° and 3 h, respectively (6 h before September 1977) but represents essentially measured atmospheric data. That is, geostrophic wind speed from the Swedish Meteorological and Hydrological Institute database was multiplied by 0.6 and the wind direction was turned counterclockwise by 15° [18]. The ability of this approximation to reflect the actual wind data has discussed extensively in the literature. It does neglect many details of the wind fields but its use leads to a reasonable reproduction of wave statistics [9] and patterns of currents in the Baltic Sea [98]. A more substantial simplification is the ignoring of sea ice in wave calculations. This position is probably reasonable for the Bay of Gdańsk but may substantially overestimate the wave energy resource in the eastern Gulf of Finland. As will be seen below, this deviation from the natural conditions does not change the key outcome of the study.

The WAM model output comprised 333 096 hourly values of wave height, period and direction at each grid cell in 1970–2007. The modelled wave heights by about 10–15% underestimate the long-term average wave height [18,21], especially during strong storms. A part of the mismatch apparently stems from a limited temporal resolution of the wind information. The latter is a common problem whenever the weather system contains short violent storms and is present in wave energy assessments [99] and in the studies of wave properties in the Baltic Sea [88]. However, the main statistical properties of modelled wave fields (such as seasonal variations in the wave properties, the frequency of the occurrence of wave fields with specific heights and periods, and interannual variability in the wave heights) satisfactorily match the measured data [100]. Occasional deviations of the modelled wave properties from the measured ones do not change the basic conclusions of the analysis.

3.2. Evaluation of the onshore wave energy flux

The wave energy flux was calculated for a total of 75 nearshore sections (with a length of about 5.5 km, Fig. 3) of the eastern and southern Baltic Sea coast. Out of these, 36 sections are located along the Polish and Russian coasts of the Bay of Gdańsk and the Sambian Peninsula while 39 sections are in the nearshore of the Russian coast of the Gulf of Finland from Narva Bay to Vyborg Bay. These two focus areas are adjacent to the large stretch of the eastern Baltic Sea coast that was analysed from the wave energy viewpoint in [9]. The sections in Figs. 3 and 4 are numbered counterclockwise from the westernmost section of the study area near the coast of Poland.

Similarly to [9], the location of these sections matches the nearshore grid cells of the WAM model. As most of the Baltic Sea wave fields do not lose their energy at depths > 15 m [9], the grid cells are chosen at a reasonable distance from the coast in locations that are characterised by appropriate water depths (17 m on average over both areas). The maximal depths in these cells reach 39 m in the Bay of Gdańsk and 28 m in the eastern Gulf of Finland. The selected cells are located at a maximum distance of 13 km from the shoreline.

To produce results that are comparable with the existing research [9,20], we consider the onshore-directed part of the wave energy flux over the entire length of each coastal section. This approach char-

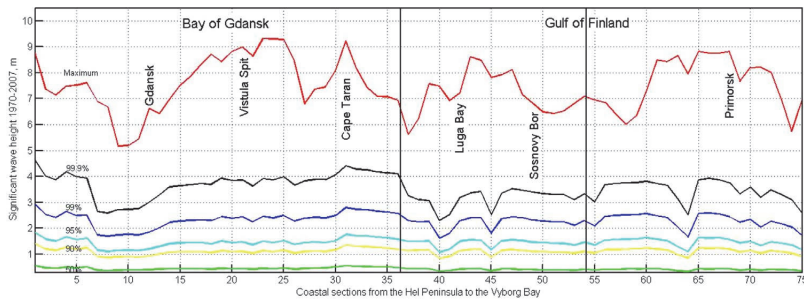


Fig. 4. Alongshore variation in different thresholds (50%-ile, 90%-ile, 95%-ile, 99%-ile, 99.9%-ile and the overall maximum) of wave heights in the study areas. See Figs. 2 and 3 for the location and numbering of coastal sections. The sections located at the southern and northern coasts of the Gulf of Finland are separated by a vertical line. The behaviour of these thresholds from Sambian Peninsula to Narva Bay is presented in [9], Fig. 4.

acterises the fraction of wave energy that could be extracted when a set of WECs would be placed into a particular grid cell along a line that is roughly parallel to the coast (Fig. 3). This fraction naturally depends on the mutual orientation of the wave propagation direction and such a line. As Eq. (3) represents energy flux per unit of wave crest, equivalently, per unit of length of such a line, the calculation of the total energy flux should take into account the lengths of these lines. Moreover, to quantify the entire available wave energy in a longer coastal stretch these lines should form a continuous chain (Fig. 3). Therefore, the lengths of such lines in single cells depend on the mutual location of the selected grid cells. They vary from 4.2 km (L_8 in Fig. 3) up to 8 km (e.g., L_5, L_6 and L_{12}) for the Bay of Gdańsk and 5.5–7.9 km for the eastern Gulf of Finland. The total length of the shoreline covered is 238 km and 235 km, respectively.

The wave energy flux $\vec{P} = E\vec{c}_g$ may approach the line defined in Fig. 3 under any angle. The density P_{ij} of the onshore wave energy flux per unit of length of this line in cell j ($1 \leq j \leq 35$ for the Bay of Gdańsk area, $1 \leq j \leq 39$ for the eastern Gulf of Finland, see above) at time instant i ($1 \leq i \leq 330\,096$ in 1970–2007) is

$$P_{ij} = E_{c_{gi}} \cos \theta_{ij} [W/m], \quad (4)$$

where $E_{c_{gi}}$ and θ_{ij} are the wave energy, group speed and approach angle for the relevant cell and time instant. This framework results in zero energy flux when the waves propagate offshore (under angles $\theta > 90^\circ$).

If the length of a particular (j -th) section is L_j , the onshore wave energy flux $P^{(ij)}$ (the total theoretically available wave energy) across the entire section is

$$P^{(ij)} = P_{ij} L_j [W] \quad (5)$$

The numerically reconstructed wave properties and thus the energy, group speed and propagation direction in Eq. (4) are available once an hour and thus represent the wave conditions during this 1-h time interval. Therefore, the resulting quantity also has the meaning of theoretical maximum energy production (in W-h) within the i -th one-hour-long time slice in 1970–2007 in the j -th coastal section. Based on this interpretation, all wave energy characteristics below have been evaluated by means of simply summing up or averaging certain sets of values of $P^{(ij)}$. For example, the total theoretical wave energy resource for a single section j during any time interval of interest (e.g. year) is simply the sum of $P^{(ij)}$ over all 1-h time slices within the interval of interest.

4. Results

4.1. Significant wave heights

A convenient way to highlight the differences between wave conditions in the two test areas and to compare those with similar

quantities in the rest of the eastern Baltic Sea is to consider the alongshore variation in the maxima and higher quantiles of the simulated wave heights (Fig. 4). It is not surprising that the maximum wave heights (9.4 m) for the simulation time interval 1970–2007 are almost the same as for the open eastern Baltic Sea coast [18]. The resulting maxima also match the estimates in [22].

Such high waves are evidently driven by strong northern winds in the Baltic Proper. The most frequent wind direction in the entire Baltic Sea is south-west and west. The fetch of these winds for the shores of the Sambian Peninsula is considerably shorter than the fetch for northern winds. Even though the strong north or north-western winds are less frequent, they may be even stronger in the northern Baltic Proper [24] and thus may give rise very large wave heights near the Sambian Peninsula and in the open part of the Bay of Gdańsk. The deep minimum in the higher quantiles of wave heights in the western sections of the Bay of Gdańsk is obviously caused by geometrical shelter by the Hel Peninsula. It is, however, not clear why maximum wave heights in some parts of the Sambian Peninsula and at the northern coast of the Hel Peninsula are lower than in the south-east of the Bay of Gdańsk. A possible reason may be wave refraction.

It is also natural that the maximum wave heights in the Bay of Gdańsk are bigger than in the eastern Gulf of Finland. It is, however, somewhat counter-intuitive that large sections of the north-eastern coast of the Gulf of Finland may have almost as high waves as the completely open coastal sections of the Bay of Gdańsk. Very large wave heights were also reconstructed near the eastern coast of the Luga Bay and near the entrance to the Vyborg Bay. These segments are exposed to the dominant winds and have long corresponding fetches. However, even though the fetch length for some sections of the eastern Gulf of Finland and for a narrow range of wind directions is basically as long as the extension of the entire Baltic Proper, natural directional spreading of wave energy should lead to much smaller wave heights at the ends of narrow water bodies compared to wide ones [101]. As the slanted fetch phenomenon is normally not fully resolved by the standard WAM model [87], some other mechanism should cause the formation of high waves in the eastern the Gulf of Finland.

Examination of higher quantiles of wave heights (Fig. 4) shows that extremely rough wave conditions occur relatively infrequently in both study areas. In terms of the 99% and 99.9% highest waves the northern coast of the Hel Peninsula and most of the Sambian Peninsula have clearly larger values than the eastern Gulf of Finland (where these thresholds are approximately 10% lower than in most of the Bay of Gdańsk, Fig. 4). Some fluctuations and small peaks or low values of these and other thresholds in Fig. 4 stem from the geometry and geomorphology of the study areas. Namely, some wave model cells and related coastal stretches are sheltered by capes (e.g. cells 40 and 44) or islands (cell 64).

Lower thresholds of wave properties such as the wave height median (the threshold for wave heights that occurs with a probability

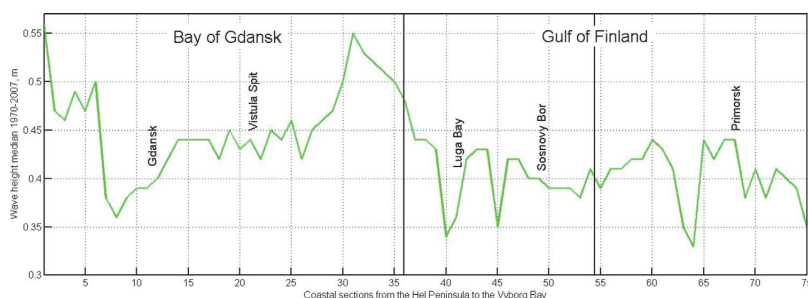


Fig. 5. Alongshore variation in the thresholds for 50% of the wave heights in the study areas. See Figs. 2 and 3 for the location and numbering of coastal sections. The sections located at the southern and northern coasts of the Gulf of Finland are separated by a vertical line.

of 50%, Fig. 5) provide an alternative description of the wave climate. These waves are usually only a little higher than the most probable wave heights. The alongshore variation of this quantity clearly indicates that those parts of the Bay of Gdańsk that are open to extreme waves whereas much more wave energy may reach the northern coast of the Hel Peninsula and the entire coastline of the Sambian Peninsula. Consistent with the above description of the spatial patterns of the Baltic Sea wave climate, the eastern Gulf of Finland receives much fewer occasions of such intermediate wave fields than the two peninsulas.

4.2. Average wave energy flux

The average densities of wave energy flux in the two areas are largely different and somewhat smaller than at the open Baltic Sea coast: about 1.2 kW/m in the Bay of Gdańsk region and 0.7 kW/m in the eastern Gulf of Finland. The total annual onshore wave energy flux in the Bay of Gdańsk (280 MW in 35 coastal sections) is almost twice as large as in the eastern Gulf of Finland (170 MW in 39 coastal sections). These numbers are commensurable with the wave energy resources for the entire Gulf of Riga (up to 280 MW) and for the southern coast of the Gulf of Finland (220 MW) [9]. The total wave energy resource in these two areas (about 460 MW) is about a third of the above-discussed quantity (1.5 GW) and thus by no means negligible. Therefore, even though some parts of the two study areas are sheltered against high waves, the total energy flux for these areas significantly contributes to the overall energy resource of the Baltic Sea.

Both areas in question exhibit very strong alongshore variation in the average wave energy flux. The largest levels of the energy flux reach 1.79 kW/m on the coast of the Sambian (Samland) Peninsula and 1.61 kW/m between Saint Petersburg and Vyborg. Both these values are somewhat smaller than the maxima for the open Baltic Sea coast (about 2.5 kW/m [9]) but still reasonable to be seriously considered for wave energy production. As expected, the biggest energy fluxes are found for coastal sections that are maximally open to waves approaching from the most frequent strong wind directions (sections No. 4, 31, 36, 62, 67, Fig. 6).

Interestingly, the alongshore variations in the average energy fluxes in the test areas do not follow any of the discussed distributions of various quantiles. This feature reflects the essential contribution of wave periods to the wave energy flux. The alongshore variations in this quantity are relatively smooth in the Bay of Gdańsk region where its level is approximately constant along the northern coast of the Hel Peninsula and the coast of the Sambian Peninsula and low levels are only found in the sheltered western Bay of Gdańsk.

Alongshore variations in the wave energy flux are much more complicated in the eastern Gulf of Finland. In the light of the above qualitative description of the wave climate it is natural that the southern coast of this study area (except for the westernmost section

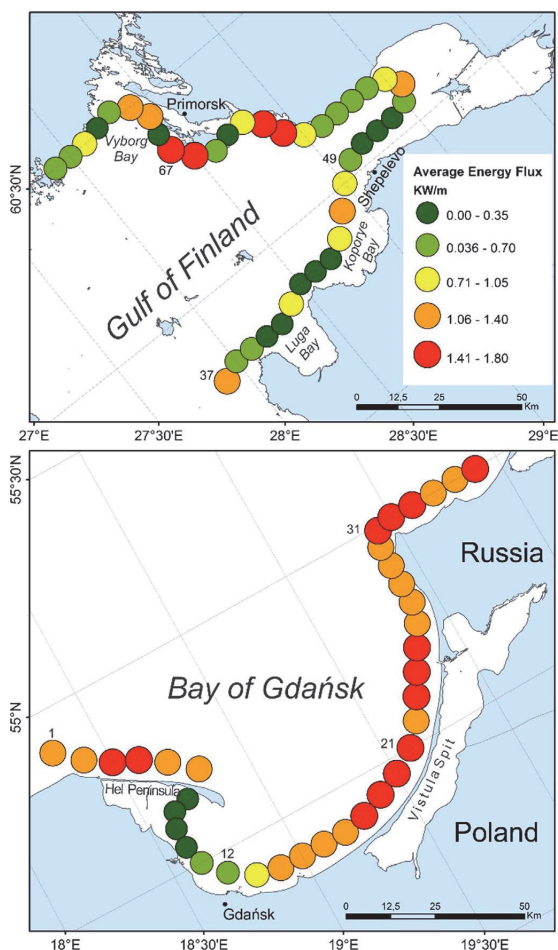


Fig. 6. Long-term average wave energy flux calculated for study areas.

that is open to the west) receives very limited amount of usable wave energy. However, substantial amounts of wave energy may penetrate to the vicinity of the Island of Kotlin for some wind directions. The most affected areas are two sections with a length of about 10 km on the north-eastern coast of the Gulf of Finland where the wave energy flux exceeds 1.4 kW/m (Fig. 6).

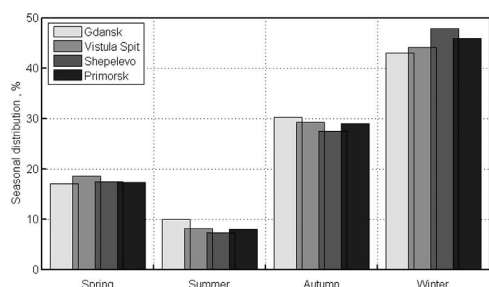


Fig. 7. Relative contribution of waves in different seasons into the annual energy flux in four selected coastal sections: Gdańsk (section 12 in Fig. 2), Vistula Spit (section 21), Shepelevo (section 49) and Primorsk (section 67).

4.3. Temporal variations and peaks in the wave energy flux

The seasonal variation in wave properties discussed above becomes evident in a more contrast way for the wave energy flux because higher waves tend to have larger periods and thus larger group speeds. The seasonal course in the wave energy flux is exemplified for four locations that are relatively favourable for wave energy harvesting (Figs. 7 and 8). Two of them are from the coast of the Bay of Gdańsk and two from the Gulf of Finland. The relevant shorelines have very different orientations and thus receive the largest levels of wave energy flux for winds from different directions.

During winter months (December–February) the study areas receive about 45% of the annual wave energy flux (Fig. 7). The autumn months (September–November) contribute about 30%, spring months (March–May) below 20% and summer months less than 10%. All these coastal sections receive more wave energy in December than in January and November (Fig. 8). Two of these (Shepelevo on the southern coast of the Gulf of Finland and near Gdańsk in a relatively sheltered area of the Bay of Gdańsk) are much calmer than the two other sites. The section near Primorsk is located in the semi-enclosed part of the Gulf of Finland but is one area open to predominant western and south-western storm events, with the longest fetch. Such events are one of the main deliverers of offshore wave energy. This difference signals the high sensitivity of different sections of these two study areas with respect to the anisotropic wind climate of the Baltic Sea where strong winds tend to blow from relatively narrow ranges of directions.

The monthly mean wave energy flux in December–January is almost an order of magnitude larger than the flux in May–June. The standard deviation of the monthly mean values exceeds by several times the average monthly values signalling extensive interannual variations in the usable wave energy resource. Similar to the rest of the eastern Baltic Sea coast [9] (not shown here), the highest variability

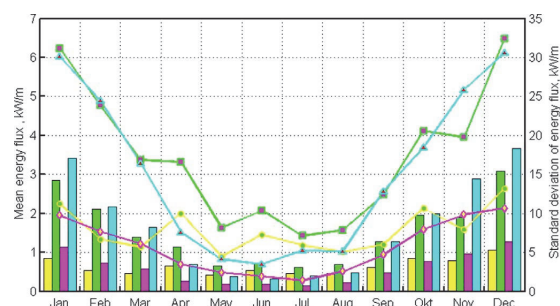


Fig. 8. Monthly mean energy flux and its standard deviation for four coastal sections: yellow: Gdańsk (section 12 in Fig. 2), green: Vistula Spit (section 21), magenta: Shepelevo (section 49), cyan: Primorsk (section 67). (For interpretation of the references to color in this figure legend, the reader is referred to the web version of this article.).

occurs during late autumn and early winter months but extensive variations may occur also in the energy flux in summer and spring seasons.

The most significant variations and remarkable peaks of the onshore wave energy flux occur during strong storms. The instantaneous energy flux may reach up to 300 kW/m in relatively open coastal sections (Fig. 9). Storms from different directions often bring markedly different amounts of wave energy to these two areas. For example, the storm on February 7, 1981 is clearly evident as a large peak in the energy flux in all four selected coastal sections (Fig. 9). The wind speed reached 20 m/s in the Gulf of Finland. The storm first blew from a southerly direction but later changed to the west. The sheltering effect of the Hel Peninsula is clearly evident in the difference in the energy flux near Gdańsk and in a more open section in the nearshore of the Vistula Spit. This storm also highlights the impact of wind anisotropy on the wave energy flux in the eastern Gulf of Finland. As waves in this storm approached the coast of Shepelevo at quite a large angle, the peak wave energy flux at Shepelevo was three times lower than in Primorsk.

The largest difference between the wave regimes in the two study areas becomes evident from the scatter diagrams of the contribution of various wave conditions into the total energy flux (Fig. 10). The combinations of wave properties in the eastern Gulf of Finland are concentrated into a narrow range of wave heights and periods. This means that WECs used in this area should be tuned to a particular wave height and period, for which they are most effective. On the contrary, the combinations of high-energy waves have substantial scatter in the nearshore of the Bay of Gdańsk. Thus, WECs in this area should be able to cope with very variable wave properties.

5. Discussion

This research extends the analysis of the wave energy resource performed in [9] for the open eastern Baltic Sea coast to the adjacent coastal stretches in the Bay of Gdańsk and in the eastern Gulf of Finland. The average onshore energy flux per unit length of the coastline is considerably smaller in these stretches that are usually characterised as semi-enclosed or semi-sheltered coastal regions. This flux, however, exhibits extensive alongshore variations. Importantly, several single sites in both study areas receive wave energy flux that is commensurable with a similar flux at the most energetic open coasts of the Baltic Proper. The two study areas may contribute about 1/3 (about 460 MW) to the total wave energy resource of the eastern Baltic Sea. This contribution, particularly for the eastern Gulf of Finland, is largely concentrated along short segments of the north-eastern coast of this water body and is thus relatively easily exploitable compared to the widely distributed wave energy resource along most of the eastern Baltic Sea coast.

Similar to the outcome of [9], the wave energy flux in both study areas exhibits strong temporal variation on interannual, annual, seasonal and monthly scales, and large variability in single storms. This feature together with the anisotropy of the most energetic wave fields (equivalently, the roughest wave conditions) has important implications for the understanding of coastal processes in the study areas. Long sections of both test areas suffer from coastal erosion and have high rates of alongshore sediment transport. The anisotropy of the wave fields may be one of the reasons why at times an inverse relationship between the wave energy and the evolution of a sea cliff in long-term scale is observed [102].

The situation is particularly complicated in the eastern Gulf of Finland where high waves may approach at large angles with respect to the coastline and give rise to instability of the entire coastal sediment system [103]. The presence of very large levels of wave energy in some locations (hot-spots) of this water body signals that much more intense coastal processes than previously thought based on the classic wave statistics may occur in the relevant coastal sections. In particular, this

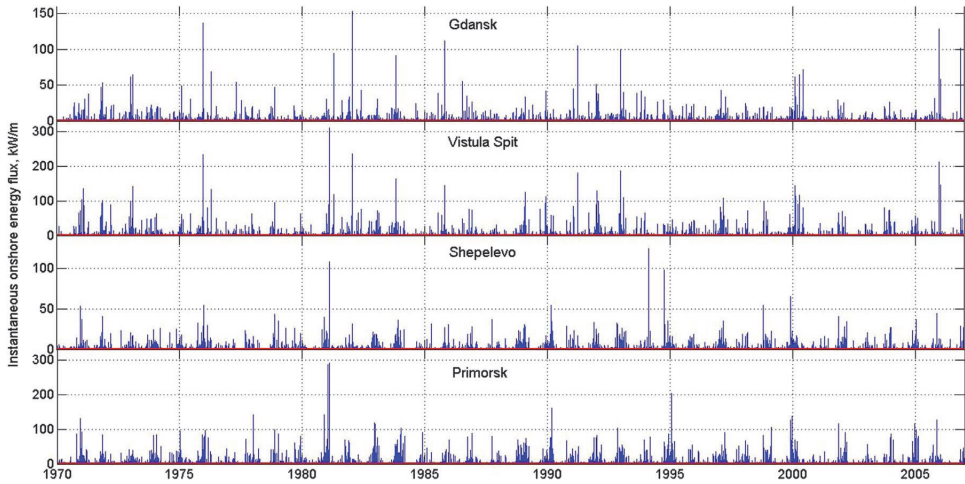


Fig. 9. Instantaneous onshore energy flux for the four selected grid cells.

feature naturally explains why some sections of the eastern Gulf of Finland nearshore and coast are almost totally stripped of fine sand deposits [104]. Even if wave energy harvesting is not beneficial

economically, the construction of energy farms can be a good preventive solution for environmental management of the affected coastal sections [16]. WECs will definitely catch some of wave energy and

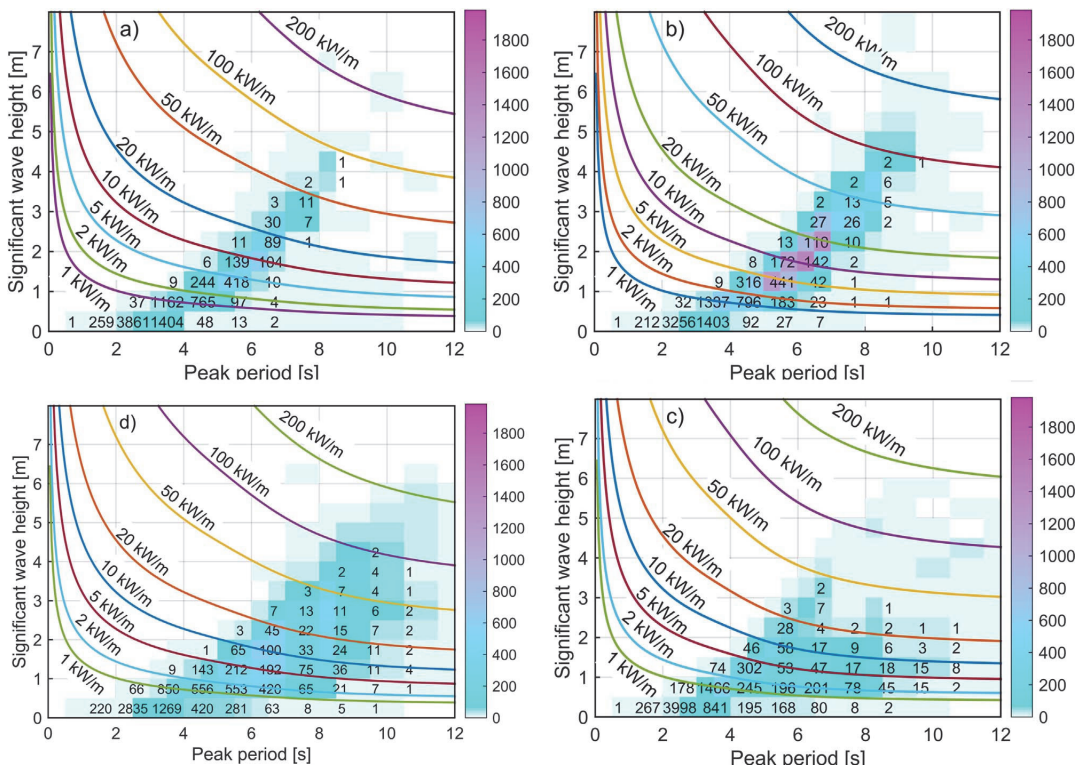


Fig. 10. Combined scatter and energy diagram for four wave model grid cells: (a, b) – cells 47 and 69, respectively, in the north-eastern part of the Bay of Gdańsk; The numbers show the annual average of hours with the relevant wave conditions with a resolution of 0.5 m in wave heights and 1 s in wave periods for 1970–2007. The colour scale shows the annual bulk energy resource [kW h/m] carried onshore by wave fields with the relevant wave properties with a resolution of 0.5 m in wave heights and 0.5 s for waves with periods less than 7 s and 1 s for waves with periods longer than 7 s. Solid lines present the instantaneous energy flux for different combinations of the significant wave height and peak period for the water depth in the selected grid cell. (For interpretation of the references to color in this figure legend, the reader is referred to the web version of this article.).

decrease heights of waves and their distractive forces along the affected coastal sections [17].

There exist several other options for the practical use of wave energy harvesting in the specific conditions of the Baltic Sea. For example, wide availability of wave energy, even if extremely intermittently distributed in time, can be used for environmental purposes. The deep waters of the Baltic Sea suffer from oxygen deficit and often exhibit anoxic conditions that are detrimental for the entire ecosystem of the sea [105]. The current strong stratification (that prevents oxygen penetration to the deeper layers) can be modified by pumping surface water into the deeper layers [106]. This kind of contemporary ocean engineering may considerably improve water quality of the Baltic Sea [107] and may successfully operate with the extremely intermittent wave climate and make use of independently working small distributed WECs of different types. It is likely that in long-term run this method of ocean engineering will have much better cost/benefit ratio compared, for example, to additional treatment of river water [106] and bring extensive ecological and environmental advantage. The occasional presence of sea ice in most of the Baltic Sea suggests that the design of such devices should involve an automatic option for diving of the devices for the winter period. This suggests that various WECs of point absorber type may be preferred.

Exploitation of wave energy in the Baltic Sea basin has generally similar benefits and drawbacks to those in other water bodies [4]. It has the potential to be both detrimental and beneficial to the environment [108]. The relevant evidence base, however, remains quite limited [109]. Rigid structures in the sea are (similarly to artificial reefs) often attractive to the fish and other kinds of life, and can be used as protection from predator. Also, fishing is questionable in the immediate vicinity of wave energy devices and it is unlikely that wave farms would be accepted near or within marine protected areas [9].

The major concerns are collision risks and habitat loss owing to noise and electromagnetic fields [108]. The Baltic Sea hosts extremely dense ship traffic and major ship routes should be clearly separated from the areas of wave energy extraction. As this sea is divided between countries with greatly different interpretation of democracy, wave farms may have certain military importance in this water body. Various electromagnetic fields from the converters and connecting cables may distract the behaviour of many marine animals [110], from eels to seals in the context of the Baltic Sea ecosystem, and evidence in this field is very scarce. Anthropogenic underwater noise has been only recently recognised as a worldwide problem [111]. This issue is particularly relevant in heavily exploited particularly sensitive sea areas such as the Baltic Sea.

Finally, the presented results indicate that the categories of “sheltered”, “semi-sheltered” or “semi-enclosed” basins may have substantially different meanings in terms of the classic wave climatology and in the light of the research into wave energy resource. These categories should be always considered together with the properties of the local wind climate such as the predominant of directions of strong winds, possibly multi-peak directional distributions of such winds and specific effects such as slanted fetch. The outcome of the analysis for the Gulf of Finland suggests that the match of some frequently occurring directions of strong winds with the particular geometry of some sea areas may lead to quite unexpected and nontrivial consequences in terms of the local wave regime.

6. Conclusions

The main conclusions from the presented material are as follows:

- The core features of the Baltic Sea wave climate from the viewpoint of wave energy harvesting are: (i) a relatively mild overall wave regime, (ii) predominance of comparatively short waves, (iii) marked anisotropy and (iv) high intermittency of wave fields, and (v) occasional presence of very rough seas.
- The wave energy resource (estimated as the onshore wave energy flux) has not only extensive spatial and seasonal variation but also extremely high temporal intermittency: about 30% of the annual energy flux arrives within a few days
- The variability in the wave energy resource requires new (possibly local, small-scale and able to cope with any wave approach direction [19]) technologies of wave energy harvesting that would survive in extremely rough seas, can cope with the occasional presence of ice and would also provide reasonable energy output in relatively mild wave conditions.
- Specific properties of the local wind climate, such as the predominant directions of strong winds, multi-peak directional distributions or specific effects such as slanted fetch may lead to the presence of short nearshore segments favourable for wave energy harvesting even along seemingly sheltered or low-energy coastal stretches.

Acknowledgements

The research was supported by institutional block grant IUT33-3 of the Estonian Ministry of Education and Research, grant 9125 by the Estonian Science Foundation and by the project “Sebastian Checkpoints – Lot 3 Baltic” of the call MARE/2014/09. The work was also partly financed by the Russian Science Foundation (Grant no. 14–37–00047) and the ERA-NET+ RUS project EXOSYSTEM (Grant No. ETAG16014), and strongly stimulated by discussions of potential targets of the Flag-ERA JTC2016 proposal FuturICT2.0. The simulated wave time series were kindly provided by Dr. A. Räämet. OK acknowledges the support of the DoRa scheme and the entire team is grateful to Prof. Kevin Parnell for valuable suggestions.

References

- [1] Cruz J. Ocean wave energy, current status and future perspectives (green energy and technology). Springer; 2008. p. 461.
- [2] López I, Andreu J, Ceballos S, Martínez de Alegría I, Kortabarria I. Review of wave energy technologies and the necessary power-equipment. *Renew Sustain Energy Rev* 2013;27:413–34.
- [3] Jacobson MZ. Review of solutions to global warming, air pollution, and energy security. *Energy Environ Sci* 2009;21:48–73.
- [4] Enerad E, Nazarpour D. Ocean's renewable power and review of technologies: case study waves. *New Dev Renew Energy* 2013;273–300. <http://dx.doi.org/10.5772/53806>.
- [5] Aoun NS, Harajli HA, Queffeuilou P. Preliminary appraisal of wave power prospects in Lebanon. *Renew Energy* 2013;53:165–73.
- [6] Arena F, Laface V, Malara G, Romolo A, Viviano A, Fiamma V, et al. Wave climate analysis for the design of wave energy harvesters in the Mediterranean Sea. *Renew Energy* 2015;77:125–41.
- [7] Aydoğan B, Ayat B, Yüksel Y. Black Sea wave energy atlas from 13 years hindcasted wave data. *Renew Energy* 2013;57:436–47.
- [8] Bernhoff H, Sjöstedt E, Leijon M. Wave energy resources in sheltered sea areas: a case study of the Baltic Sea. *Renew Energy* 2006;31:2164–70.
- [9] Soomere T, Eelsalu M. On the wave energy potential along the Eastern Baltic Sea coast. *Renew Energy* 2014;71:221–33.
- [10] Clément A, McCullen P, Falcao A, Fiorentino A, Gardner F, Hammarlund K, Lemonis G, Lewis T, Nielsen K, Petroncini S, Pontes MT, Schild P, Sjöström BO, Sørensen HC, Thorpe T. Wave energy in Europe: current status and perspective. *Renew Sustain Energy Rev* 2002;6:405–31.
- [11] Akpınar A, Kömürçü Mİ. Wave energy potential along the south-east coasts of the Black Sea. *Energy* 2012;42:289–302.
- [12] Waters R, Engström J, Isberg J, Leijon M. Wave climate off the Swedish west coast. *Renew Energy* 2009;34:1600–6.
- [13] Soomere T. Anisotropy of wind and wave regimes in the Baltic proper. *J Sea Res* 2003;49:305–16.
- [14] Babanin AV, Hsu TW, Roland A, Ou SH, Doong DJ, Kao CC. Spectral wave modelling of Typhoon Krosa. *Nat Hazard Earth Sys Sci* 2011;11:501–11.
- [15] Astariz S, Perez-Collazo C, Abanades J, Iglesias G. Co-located wave-wind farms: economic assessment as a function of layout. *Renew Energy* 2015;83:837–49.
- [16] Martinelli L. Wave energy converters under mild wave climates. In: OCEANS'11 MTS/IEEE KONA, 19–22 Sept 2011, Waikoloa, Hawaii, USA, IEEE; 2011. p. 1362–9.
- [17] Michailides C, Angelides DC. Optimization of a flexible floating structure for wave energy production and protection effectiveness. *Eng Struct* 2015;85:249–63. <http://dx.doi.org/10.1016/j.engstruct.2014.12.031>.
- [18] Soomere T, Räämet A. Spatial pattern of the wave climate in the Baltic Proper and the Gulf of Finland. *Oceanologia* 2011;53:335–71.
- [19] Blažauskas N, Pašilis A, Knolis A. Potential applications for small scale wave

- energy installations. *Renew Sustain Energy Rev* 2015;49:297–305.
- [20] Kasilis E, Punys P, Kofoed JP. Assessment of theoretical near-shore wave power potential along the Lithuanian coast of the Baltic Sea. *Renew Sustain Energy Rev* 2015;41:134–42.
- [21] Hünicke B, Zorita E, Soomere T, Madsen KS, Johansson M, Suursaar Ü. Recent change – sea level and wind waves. In: TheBACC II Author Team, editor. Second assessment of climate change for the Baltic Sea Basin, regional climate studies. Springer; 2015. p. 155–85.
- [22] Schmager G, Fröhle P, Schrader D, Weisse R, Müller-Navarra S. Sea state, tides. In: Feistel R, Nausch G, Wasmund N, editors. State and evolution of the Baltic Sea 1952–2005. Hoboken, NJ: Wiley; 2008. p. 143–98.
- [23] Soomere T. Extremes and decadal variations in the Baltic Sea wave conditions. In: Polinovsky E, Kharif C, editors. Extreme ocean waves. Springer; 2016. p. 107–40.
- [24] Soomere T. Extreme wind speeds and spatially uniform wind events in the Baltic proper. *Proc Est Acad Sci Eng* 2001;7:195–211.
- [25] Tuomi L, Kahma KK, Pettersson H. Wave hindcast statistics in the seasonally ice-covered Baltic Sea. *Boreal Environ Res* 2011;16:451–72.
- [26] Soomere T, Behrens A, Tuomi L, Nielsen JW. Wave conditions in the Baltic Proper and in the Gulf of Finland during windstorm Gudrun. *Nat Hazards Earth Syst Sci* 2008;8:37–46.
- [27] Falnes J. A review of wave-energy extraction. *Mar Struct* 2007;20(4):185–201. <http://dx.doi.org/10.1016/j.marstruc.2007.09.001>.
- [28] Massel SR. Ocean surface waves: their physics and prediction, 2nd ed. New Jersey: World Scientific; 2013. p. 692.
- [29] Komen GJ, Cavaleri L, Donelan M, Hasselmann K, Hasselmann S, Janssen PAEM. Dynamics and modelling of ocean waves. Cambridge University Press; 1994. p. 532.
- [30] Defne Z, Haas KA, Fritz HM. Wave power potential along the Atlantic coast of the southeastern USA. *Renew Energy* 2009;34:2197–205.
- [31] Portilla J, Sosa J, Cavaleri L. wave energy resources: wave climate and exploitation. *Renew Energy* 2013;57:594–605.
- [32] Falkemo C. Wave energy research in Sweden. Final report phase 4. Part II (V) Energy potential. Report GR:44. Gothenburg [In Swedish]; 1981.
- [33] Söderberg P. The Swedish coastal wave climate. SSPA Research Report No. 104. Gothenburg, Sweden: SSPA; 1987.
- [34] Mårtensson M, Bergdahl L. On the wave climate of the southern Baltic. Report Series A:15, Department of Hydraulics. Sweden: Chalmers University of Technology; 1987.
- [35] Bernhoff H, Sjøstedt E, Leijon M. Wave energy resources in sheltered sea areas: a case study of the Baltic sea. *Renew Energy* 2006;31:2164–70.
- [36] Henfridsson U, Neimane V, Strand K, Kapper R, Bernhoff H, Danielsson O, Leijon M, Sundberg J, Thorburn K, Ericsson E, Bergman K. Wave energy potential in the Baltic Sea and the Danish part of the North Sea, with reflections on the Skagerrak. *Renew Energy* 2007;32:2069–84.
- [37] Waters R, Engström J, Isberg J, Leijon M. Wave climate off the Swedish west coast. *Renew Energy* 2009;34:1600–6.
- [38] Soomere T. Wind wave statistics in Tallinn Bay. *Boreal Environ Res* 2005;10:103–18.
- [39] Leijon M, Bernhoff H, Berg M, Ågren O. Economical considerations of renewable electric energy production-especially development of wave energy. *Renew Energy* 2003;8:1201–9.
- [40] Vihma T, Haapala J. Geophysics of sea ice in the Baltic Sea – a review. *Progr Oceanogr* 2009;80:129–48.
- [41] Leppäranta M. Land–ice interaction in the Baltic Sea. *Est J Earth Sci* 2013;62:2–14.
- [42] Strömstedt E, Savin A, Heino H, Antbrams K, Haikonen K, Götschl T. Project WESA (wave energy for a sustainable archipelago) – a single heaving buoy wave energy converter operating and surviving ice interaction in the Baltic Sea. In: Proceedings of the 10th European wave and tidal energy conference (EWTEC). Aalborg, Denmark; September 2–5 2013.
- [43] Beringš Janis, Beringš Juris. Wave energy factors and development perspective analysis in Latvia. In: Proceedings of the 56th international scientific conference on power and electrical engineering of Riga Technical University RTUCON; 2015. p. 6.
- [44] Beringš Janis, Beringš Juris, Kalnačs J, Kalnačs A. Wave energy potential in the Latvian EEZ. *Latv J Phys Techn Sci* 2016;53(3):22–33. <http://dx.doi.org/10.1515/lpts-2016-0018>.
- [45] Alamian R, Shafagh R, Miri SJ, Yazdanshenas N, Shakeri M. Evaluation of technologies for harvesting wave energy in Caspian Sea. *Renew Sustain Energy Rev* 2014;32:468–76.
- [46] Hagerman G. Wave power. In: Bisio A, Boots SG, editors. Encyclopedia of energy technology and the environment... New York: Wiley; 1995. p. 2859–907.
- [47] Falcão AFO. Wave energy utilization: a review of the technologies. *Renew Sustain Energy Rev* 2010;14:899–918. <http://dx.doi.org/10.1016/j.rser.2009.11.003>.
- [48] Tiron R, Mallon F, Dias F, Reynaud EG. The challenging life of wave energy devices at sea: a few points to consider. *Renew Sustain Energy Rev* 2015;43:1263–72.
- [49] Uihlein A, Magagna D. Wave and tidal current energy – a review of the current state of research beyond technology. *Renew Sustain Energy Rev* 2016;58:1070–81. <http://dx.doi.org/10.1016/j.rser.2015.12.284>.
- [50] O'Connor M, Lewis T, Dalton G. Techno-economic performance of the Pelamis P1 and Wavestar at different ratings and various locations in Europe. *Renew Energy* 2013;50:889–900. <http://dx.doi.org/10.1016/j.renene.2012.08.009>.
- [51] Harrison GP, Wallace AR. Sensitivity of wave energy to climate change. *IEEE Trans Energy Convers* 2005;20(4):870–7. <http://dx.doi.org/10.1109/TEC.2005.853753>.
- [52] Garnaud X, Mei CC. Wave-power extraction by a compact array of buoys. *J Fluid Mech* 2009;635:389–413. <http://dx.doi.org/10.1017/S0022112009007411>.
- [53] Viviano A, Natsi S, Foti E, Bruce T, Allsop W, Vicinanza D. Large-scale experiments on the behaviour of a generalised oscillating water column under random waves. *Renew Energy* 2016;99:875–87. <http://dx.doi.org/10.1016/j.renene.2016.07.067>.
- [54] Song SK, Park JB. Control strategy of an impulse turbine for an oscillating water column-wave energy converter in time-domain using Lyapunov stability method. *Appl Sci Basel* 2016;6(10). <http://dx.doi.org/10.3390/app6100281>.
- [55] Gomes RPF, Henriques JCC, Gato LMC, Falcão AFO. Wave power extraction of a heaving floating oscillating water column in a wave channel. *Renew Energy* 2016;99:1262–75. <http://dx.doi.org/10.1016/j.renene.2016.08.012>.
- [56] Henriques JCC, Gato LMC, Falcão AFO, Robles E, Fay FX. Latching control of a floating oscillating-wave-column wave energy converter. *Renew Energy* 2016;90:229–41. <http://dx.doi.org/10.1016/j.renene.2015.12.065>.
- [57] Bracco G, Giorelli E, Mattiazzi G, Marignetti F, Carbone S, Attaianesi C. Design and experiments of linear tubular generators for the Inertial Sea Wave Energy Converter. *IEEE Energy Convers Congr Expo (ECCE)* 2011:3864–71. <http://dx.doi.org/10.1109/ECCE.2011.6064294>.
- [58] Cordonnier J, Gorintin F, de Cagny A, Clément AH, Baharit A. SEAREV: case study of the development of a wave energy converter. *Renew Energy* 2015;80:40–52.
- [59] Bozzetto A, Tedeschi E. Wave power extraction with constrained power take-off: Single capture vs. double capture point absorbers. In: Proceedings of the ninth international conference on ecological vehicles and renewable energies (EVER), Monte-Carlo, Monaco; 25–27 March 2014, 2015. p. 603–9.
- [60] Piri A, Grimaccia F, Mussetta M, Zich RE, Johnstone R, Palaniswami M, Rajasegarar S. Optimization of an energy harvesting buoy for coral reef monitoring. In: Proceedings of 2013 IEEE Congress on Evolutionary Computation (CEC), June 20–23, 2013, Cancun, Mexico. IEEE; 2013. p. 629–34.
- [61] Bozzi S, Miquel AM, Scarpa F, Antonini A, Archetti R, Passoni G, Grusso G. Wave energy production in Italian offshore: Preliminary design of a point absorber with tubular linear generator. In: Proceedings of the 4th International Conference on Clean Electrical Power: Renewable Energy Resources Impact, ICCPE; 2013. p. 203–8.
- [62] Bizzozero F, Giassi M, Grusso G, Bozzi S, Passoni G. 2014. Dynamic model, parameter extraction, and analysis of two topologies of a tubular linear generator for seawave energy production. In: Proceedings of international symposium on power electronics, electrical drives, automation and motion (SPEEDAM), 18–20 June 2014, IEEE; 2014. p. 433–8 <http://dx.doi.org/10.1109/SPEEDAM.2014.6872083>.
- [63] Fernandez H, Iglesias G, Lopez I, Schimmels S. Wavecat wave energy converter modelling by means of a RANS of numerical model. In: Brinkmann B, Wriggers P (eds.), 5th International Conference on Computational Methods in Marine Engineering (MARINE 2013), May 29–31, Hamburg, Germany; 2013. p. 125–36.
- [64] Di Fresco L, Traverso A. The SEASPOON innovative wave energy converter. In: 2013 OCEANS, San Diego, Oceans-IEEE Xplore; 2013. p. 10.
- [65] Chen AJ, You YG, Sheng SW, Lin HJ, Ye Y, Huang S. Nonlinear analysis of the crashworthy component of an eagle wave energy converter in rotating-collision. *Ocean Eng* 2016;125:285–94. <http://dx.doi.org/10.1016/j.oceaneng.2016.08.025>.
- [66] Amarakith A, Sivakumar K. Investigation on modeling of non-buoyant body typed point absorbing wave energy converter using adaptive network-based fuzzy inference system. *Int J Mar Energ* 2016;13:157–68. <http://dx.doi.org/10.1016/j.jome.2016.01.004>.
- [67] Ding WJ, Song BW, Mao ZY, Wang KY. Experimental investigations on a low frequency horizontal pendulum ocean kinetic energy harvester for underwater mooring platforms. *J Mar Sci Technol* 2016;21(2):359–67. <http://dx.doi.org/10.1007/s00773-015-0357-7>.
- [68] Youssef J, Matar J, Rahme P, Bou-Mosleh C. A nearshore heaving-buoy sea wave energy converter for power production. *Procedia Eng* 2016;145:136–43. <http://dx.doi.org/10.1016/j.proeng.2016.04.032>.
- [69] Bou-Mosleh C, Rahme P, Beaino P, Mattar R, Nassif EA. Contribution to clean energy production using a novel wave energy converter: renewable energy. In: 2014 International Conference on Renewable Energies for Developing Countries (REDEC), Beirut, Lebanon, 26–27 Nov 2014. IEEE; 2014. p. 108–11.
- [70] Falcão AFO. The shoreline OWC wave power plant at the Azores. In: Proceedings of the 4th European Wave Energy Conference. Aalborg, Denmark; 2000. p. 42–7.
- [71] Washio Y, Osawa H, Nagata Y, Fujii F, Furuyama H, Fujita T. The offshore floating type wave power device Mighty Whale™: open sea tests. In: Proceedings of the 10th International Offshore and Polar Engineering Conference ISOPE. Seattle, USA; 2000. p. 373–80.
- [72] Oceanlinx. Available from: (<http://oceanlinx.com/>) [accessed 17.01.17].
- [73] Heath T, Whittaker T, Boake C. The design, construction and operation of the LIMPET wave energy converter (Islay, Scotland). In: Proceedings of the 4th European Wave Energy Conference. Aalborg, Denmark; 2000.
- [74] Ohneda H, Igarashi S, Shinbo O, Sekihara S, Suzuki K, Kubota H. et al. Construction procedure of a wave power extracting caisson breakwater. In: Proceedings of the 3rd Symposium on Ocean Energy Utilization; 1991.
- [75] Torre-Enciso Y, Ortubia I, López de Aguilera L, Marqués J. Mutriku wave power plant: from the thinking out to the reality. In: Proceedings of the 8th European wave and tidal energy conference. Uppsala, Sweden; 2009. p. 319–29.
- [76] Weinstein A, Fredriksson G, Parks MJ, Nielsen K. AquaBuoy™-the offshore wave energy converter numerical modeling and optimization. In: Proceedings of the Oceans '04MTTS/IEEE Techno-Ocean'04. Kobe, Japan; 2004. p.1854–9.
- [77] Weber J, Mouwen F, Parish A, Robertson D. Wavebob – research and develop-

- ment network and tools in the context of systems engineering. In: Proceedings of the 8th European wave and tidal energy conference. Uppsala, Sweden; 2009.
- [78] Ruellan M, Ben Ahmed H, Multon B, Josset C, Babarit A, Clement A. Design methodology for a SEAREV wave energy converter. *IEEE Trans Energy Convers* 2010;25:760–7.
- [79] Gardner FE. Learning experience of AWS pilot plant test offshore Portugal. In: Proceedings of the 6th European wave energy conference; 2005. p. 149–54.
- [80] Wave Star Energy. Available online at: (<http://www.wavestarenergy.com/>) [accessed 17.01.17].
- [81] Heller V, Chaplin J, Farley F, Hann M, Hearn G. Physical model tests of the wave energy converter Anaconda. In: Proceedings of the 1st European conference of IAHR, Edinburgh, Paper MREc; 2010. p. 1–6.
- [82] Whittaker T, Collier D, Folley M, Osterried M, Henry A, Crowley M. The development of Oyster—a shallow water surging wave energy converter. In: Proceedings of the 7th European wave tidal energy conference, Porto, Portugal; 2007.
- [83] Evans DV, Falcao AFO (eds). Hydrodynamics of ocean wave-energy utilization. IUTAM Symposium, Lisbon, Portugal. Springer, Berlin; 1985.
- [84] Vicinanza D, Margheritini L, Kofoed JP, Buccino M. The SSG wave energy converter: performance, status and recent developments. *Energies* 2012;5:193–226.
- [85] Kofoed JP, Frigaard P, Friis-Madsen E, Sørensen HC. Prototype testing of the wave energy converter wave dragon. *Renew Energy* 2006;31:181–9.
- [86] Lehmann A, Getzlaff K, Harlaß J. Detailed assessment of climate variability in the Baltic Sea area for the period 1958 to 2009. *Clim Res* 2011;46:185–96.
- [87] Pettersson H, Kahma KK, Tuomi L. Predicting wave directions in a narrow bay. *J Phys Oceanogr* 2010;40(1):155–69.
- [88] Cieřlikiewicz W, Paplińska-Swercel B. A 44-year hindcast of wind wave fields over the Baltic Sea. *Coast Eng* 2008;55:894–905.
- [89] Różyński G. Long-term evolution of Baltic Sea wave climate near a coastal segment in Poland; its drivers and impacts. *Ocean Eng* 2010;37:186–99.
- [90] Ostrowski R, Pruszk Z, Skaja M, Szmytkiewicz M. Variability of hydrodynamic and lithodynamic coastal processes in the east part of the Gulf of Gdańsk. *Arch Hydro-Eng Environ Mech* 2010;57(2):139–53.
- [91] Różyński G. Wave climate in the Gulf of Gdańsk vs. open Baltic Sea near Lubiatowo, Poland. *Arch Hydro-Eng Environ Mech* 2010;57(2):167–76.
- [92] Zhang W, Schneider R, Kolb J, Teichmann T, Dudzinska-Nowak J, Harff J, Hanebuth T. Land-sea interaction and morphogenesis of coastal foredunes – a modelling case study from the southern Baltic Sea coast. *Coast Eng* 2015;99:148–66.
- [93] Soomere T, Myrberg K, Leppäranta M, Nekrasov A. The progress in knowledge of physical oceanography of the Gulf of Finland: a review for 1997–2007. *Oceanologia* 2011;50:287–362.
- [94] Zaitseva-Pärnaste I, Soomere T. Interannual variations of ice cover and wave energy flux in the north-eastern Baltic Sea. *Ann Glaciol* 2013;54:175–82.
- [95] Ryabchuk D, Kolesov A, Chubarenko B, Spiridonov M, Kurennoy D, Soomere T. Coastal erosion processes in the eastern Gulf of Finland and their links with geological and hydrometeorological factors. *Boreal Environ Res* 2011;16(Suppl. A):117–37.
- [96] Sooäär J, Jaagus J. Long-term changes in the sea ice regime in the Baltic Sea near the Estonian coast. *Proc Estonian Acad Sci Eng* 2007;3:189–200.
- [97] Soomere T, Weisse R, Behrens A. Wave climate in the Arkona Basin, the Baltic Sea. *Ocean Sci* 2012;8:287–300.
- [98] Myrberg K, Ryabchenko V, Isaev A, Vankevich R, Andrejev O, Bendtsen J, Erichsen A, Funkquist L, Inkala A, Neelov I, Rasmus K, Rodriguez Medina M, Raudsepp U, Passenko J, Söderkvist J, Sokolov A, Kuosa H, Anderson TR, Lehmann A, Skogen MD. Validation of three-dimensional hydrodynamic models in the Gulf of Finland based on a statistical analysis of a six-model ensemble. *Boreal Environ Res* 2010;15:453–79.
- [99] Ching-Piao T, Ching-Her H, Chien H, Hao-Yuan C. Study on the wave climate variation to the renewable wave energy assessment. *Renew Energy* 2012;38:50–61.
- [100] Räämet A. Spatio-temporal variability of the Baltic Sea wave fields [PhD thesis]. Tallinn, Estonia: Tallinn University of Technology; 2010. p. 169 (<http://digi.lib.ttu.ee/i/?500>).
- [101] USACE (United States. Army. Corps of Engineers; Coastal Engineering Research Center). Shore protection manual. Dept. of the Army, Waterways Experiment Station, Corps of Engineers, Coastal Engineering Research Center, Vicksburg, Miss. & Washington, DC; 1984. p. 656.
- [102] Benumof BT, Storlazzi CD, Seymour RJ, Griggs GB. The relationship between incident wave energy and seacliff erosion rates: San Diego County, California. *J Coast Res* 2000;16:1162–78.
- [103] Ashton A, Murray A, Arnault O. Formation of coastline features by large-scale instabilities induced by high-angle waves. *Nature* 2001;414(6861):296–300.
- [104] Atlas of geological and environmental geological maps of the Russian area of the Baltic Sea (Petrov OV, ed). Saint Petersburg, VSEGEI; 2010. p. 78.
- [105] Diaz RJ, Rosenberg R. Spreading dead zones and consequences for marine ecosystems. *Science* 2008;321(5891):926–9. <http://dx.doi.org/10.1126/science.1156401>.
- [106] Forth M, Liljebladh B, Stigebrandt A, Hall POJ, Treusch AH. Effects of ecological engineered oxygenation on the bacterial community structure in an anoxic fjord in western Sweden. *ISME J* 2015;9(3):656–69. <http://dx.doi.org/10.1038/ismej.2014.172>.
- [107] Stigebrandt A, Gustafsson BG. Improvement of Baltic proper water quality using large-scale ecological engineering. *Ambio* 2007;36(2–3):280–6.
- [108] Inger R, Attrill MJ, Bearhop S, Broderick AC, Grecian WJ, Hodgson DJ, Mills C, Sheehan E, Votier SC, Witt MJ. Marine renewable energy: potential benefits to biodiversity? An urgent call for research. *J Appl Ecol* 2009;46:1145–53. <http://dx.doi.org/10.1111/j.1365-2664.2009.01697.x>.
- [109] Grecian WJ, Inger R, Attrill MJ, Bearhop S, Godley BJ, Witt MJ, Votier SC. Potential impacts of wave-powered marine renewable energy installations on marine birds. *IBIS* 2010;152(4):683–97. <http://dx.doi.org/10.1111/j.1474-919X.2010.01048.x>.
- [110] Gill AB, Gloyne-Philips I, Kimber J, Sigay P. Marine renewable energy, electromagnetic (EM) fields and EM-sensitive animals. In: Marine Renewable Energy Technology and Environmental Interactions (Shields MA, Payne AIL, eds), Humanity and the Sea, Springer, Dordrecht, The Netherlands; 2014. p. 61–79. http://dx.doi.org/10.1007/978-94-017-8002-5_6.
- [111] Williams R, Wright AJ, Ashe E, Blight LK, Brintjes R, Canessa R, Clark CW, Cullis-Suzuki S, Dakin DT, Erbe C, Hammond PS, Merchant ND, O'Hara PD, Purser J, Radford AN, Simpson SD, Thomas L, Wale MA. Impacts of anthropogenic noise on marine life: publication patterns, new discoveries, and future directions in research and management. *Ocean Coast Manag* 2015;115:17–24. <http://dx.doi.org/10.1016/j.ocecoaman.2015.05.021>.



Paper III

Eelsalu M., Soomere T., Pindsoo K., Lagemaa P. 2013. Ensemble approach for projections of return periods of extreme water levels in Estonian waters. *Continental Shelf Research*, 91, 201–210, [dx.doi.org/10.1016/j.csr.2014.09.012](https://doi.org/10.1016/j.csr.2014.09.012).



Contents lists available at ScienceDirect

Continental Shelf Research

journal homepage: www.elsevier.com/locate/csr

Research papers

Ensemble approach for projections of return periods of extreme water levels in Estonian waters

Maris Eelsalu^a, Tarmo Soomere^{a,*}, Katri Pindsoo^a, Priidik Lagemaa^b^a Institute of Cybernetics at Tallinn University of Technology, Akadeemia tee 21, 12618 Tallinn, Estonia^b Marine Systems Institute at Tallinn University of Technology, Akadeemia tee 15a, 12618 Tallinn, Estonia

ARTICLE INFO

Article history:

Received 22 June 2014

Received in revised form

30 August 2014

Accepted 24 September 2014

Available online 2 October 2014

Keywords:

Water level

Extreme value distributions

Ensemble approach

Baltic Sea

Block maxima method

Wave set-up

ABSTRACT

The contribution of various drivers to the water level in the eastern Baltic Sea and the presence of outliers in the time series of observed and hindcast water level lead to large spreading of projections of future extreme water levels. We explore the options for using an ensemble of projections to more reliably evaluate return periods of extreme water levels. An example of such an ensemble is constructed by means of fitting several sets of block maxima (annual maxima and stormy season maxima) with a Generalised Extreme Value, Gumbel and Weibull distribution. The ensemble involves projections based on two data sets (resolution of 6 h and 1 h) hindcast by the Rossby Centre Ocean model (RCO; Swedish Meteorological and Hydrological Institute) and observed data from four representative sites along the Estonian coast. The observed data are transferred into the grid cells of the RCO model using the HIROMB model and a linear regression. For coastal segments where the observations represent the offshore water level well, the overall appearance of the ensembles signals that the errors of single projections are randomly distributed and that the median of the ensemble provides a sensible projection. For locations where the observed water level involves local effects (e.g. wave set-up) the block maxima are split into clearly separated populations. The resulting ensemble consists of two distinct clusters, the difference between which can be interpreted as a measure of the impact of local features on the water level observations.

© 2014 Elsevier Ltd. All rights reserved.

1. Introduction

Flooding of low-lying nearshore areas is one of the largest threats for coastal countries. The associated risks are severely enhanced by the projected increase in the sea level. This increase will eventually over-ride the current postglacial uplift for all Estonian coasts (cf. Johansson et al., 2014). Some information about the changes may be extracted from long-term water level time series. This information, however, is of limited use because of extensive short-term climate variability (Weisse and von Storch, 2010) and associated flooding risks (Gaslikova et al., 2013). In other words, the properties of strong storms and associated surges may change aperiodically, often on a decadal scale, within quite a wide range. For the listed reasons estimates of extreme water levels and their return periods are often constructed using a combination of relatively short-term sets of recorded water level, numerical modelling and various statistical distributions of extreme values (van den Brink et al., 2005; Sterl et al., 2009,

among others). The estimates usually reveal extensive disparity depending on the particular method in use, set of underlying data and regional differences in the storm surge heights (Bardet et al., 2011). The discrepancies can be attributed to a number of reasons, from the shortness and inaccuracy of the observations up to the possible presence of a specific population of intense storms, properties of which do not obey the distribution of commonly occurring wind events (van den Brink et al., 2005; Suursaar and Sooäär, 2007).

The situation is particularly complicated in the Baltic Sea where such populations of extreme water levels in different sea areas are naturally created by the possibility of encountering relatively long-term aperiodic high water levels in the entire sea (Leppäranta and Myrberg, 2009). The predominance of westerly winds among strong wind events additionally modifies the course of water level in the eastern regions of this water body (Suursaar et al., 2006a; Averkiev and Klevanny, 2010). The distribution of deviations of the instantaneous water level from the long-term average is close to a normal distribution (Johansson et al., 2001; Suursaar and Sooäär, 2007). The difference from a Gaussian distribution is insignificant for moderate deviations of both signs. There are two important exceptions. Firstly, all extremely large deviations from the average level correspond to high water level events (Johansson et al., 2001). Secondly, the

* Corresponding author. Tel.: +372 6204176.

E-mail addresses: maris.eelsalu@ioc.ee (M. Eelsalu), soomere@cs.ioc.ee (T. Soomere), katrip@ioc.ee (K. Pindsoo), priidik.lagemaa@msi.ttu.ee (P. Lagemaa).<http://dx.doi.org/10.1016/j.csr.2014.09.012>

0278-4343/© 2014 Elsevier Ltd. All rights reserved.

distribution is not exactly symmetric: relatively high water levels are more probable equivalent low water levels. These properties reflect the well-known asymmetry of water level in the Estonian waters: while high water levels are usually short-living transient events, low water levels often persist for relatively long time. The largest mismatch between a normal distribution and measured or modelled values is evident for extreme surges (Johansson et al., 2001; Suursaar and Sooäär, 2007).

The described deviations of the water level anomalies from a Gaussian distribution are unimportant for applications that address commonly occurring water levels (Stramska, 2013), their spatial and seasonal variations and trends (Hünicke and Zorita, 2008; Hünicke, 2010; Scotto et al., 2009; Stramska et al., 2013), or certain quantiles (Barbosa, 2008; Donner et al., 2012). The non-Gaussian population, however, may substantially affect the results of calculations of exceedance probabilities of rare events in coastal engineering and projections of extreme water levels and their return periods (Suursaar and Sooäär, 2007; Johansson et al., 2011). Such projections are commonly done by using extreme value statistics. In essence, they rely on extrapolations of the water levels beyond the time interval and range of observations or model hindcasts (see, e.g., Mudsbach and Jensen (2009) for a discussion of such methods for the Baltic Sea).

Different methods of this type exploit similar statistical parameters of observed or modelled values of water level and basically differ only in how the existing values are accounted for in the implementation of the particular model. These methods implicitly rely on the assumption that the measured or modelled water levels at least approximately follow certain classical (e.g., a Gaussian or Weibull) distribution. If this assertion is true, other classical statistical methods (such as a Gumbel distribution) can be used for evaluation of their extreme values.

If the empirical distribution of water level time series at a particular location substantially deviates from a Gaussian one, or has a substantial number of outliers, its extreme values not necessarily obey any classical (Fréchet, Weibull or Gumbel, Coles, 2001) extreme-value statistics. It is therefore not surprising that slightly different methods can yield significantly different predictions of extreme water levels and their return periods (e.g., Sterl et al., 2009). Moreover, even the use of the same technique may lead to large spreading of the results owing to the use of various weights of the rare measured values or various options for (the evaluation of) the model parameters (Arns et al., 2013). For example, even the initial de-trending of water level, often applied as a background procedure, may modify the results of the projections of extreme events. The long-term course of water levels in many locations is far from linear (Donner et al., 2012). An obvious shift in the water level trend was observed in the Baltic Sea in the 20th century (Johansson et al., 2001, 2014; Dailidienė et al., 2006). The above-discussed skewness of the distribution of water levels additionally complicates the problem and leads to a much higher increase in the annual maximum water levels compared to the changes in the mean values (Jaagus and Suursaar, 2013). Suursaar and Sooäär (2007) even conclude that no single commonly used extreme value distribution is able to adequately describe or predict extreme water level events in some locations of Estonia.

This situation calls for alternative approaches for the evaluation of extreme water levels and their return periods. A possible first-order solution to improve the performance of the projections of rare water level events is to use an ensemble approach (Christiansen et al., 2010). This approach has become a standard way of addressing of forecasts and projections that are highly sensitive with respect to the initial conditions or certain model parameters (Araújo and New, 2006). The basic idea is that a (possibly weighted) average of a cluster of projections is often a much better forecast than any single model could provide (Cheung, 2001). This approach is usually employed for projections of extreme surges via the construction of an ensemble of models for water level time series (e.g., Sterl et al., 2009; Mel et al.,

2013). In the Baltic Sea conditions it has been also applied to project the local mean sea level rise (Johansson et al., 2014).

In this paper we explore a simple way to create an ensemble for estimates of extreme water levels and their return periods from a viewpoint that offers considerable reduction of computational loads. Namely, instead of re-running atmospheric and water level models, we use three independent data sets (one measured and two modelled), several methods for their handling and a few methods for the assessment of extreme values and their return periods. Doing so is equivalent to implicitly perturbing the “weight” of single block maxima (e.g., annual water level maxima) in the measured or modelled data by using different extreme value distributions rather than perturbing the initial data of simulations. The obvious drawback is that the estimates of errors and uncertainties are not straightforward. However, the simplicity and transparency of this easy-to-use approach evidently counterbalances a certain loss of rigorosity.

The analysis is performed for four coastal regions (Fig. 1) that are representative for a large part of the entire coastline of Estonia and have been extensively considered in earlier studies (Suursaar and Sooäär, 2007). The location near the island of Hiiumaa is characteristic to relatively straight coastal sections and headlands in the north-eastern Baltic Proper where the extreme water levels are comparatively limited. The site near Tallinn portrays coastal segments of semi-enclosed subbasins of the Baltic Sea with highly complicated geometry. A site in Narva Bay represents widely open bays that are vulnerable with respect to large-scale storm surges for almost all westerly wind events. Finally, Pärnu Bay is particularly vulnerable with respect to specific wind events from a narrow direction range and offers one of the largest ranges of water levels in the Baltic Sea basin (Suursaar and Sooäär, 2007). We intentionally selected the grid cells of the used circulation models at a distance of a few km from the observation sites in order to avoid possible distortions of the modelled water level because of insufficient spatial resolution of the local bathymetry and geometry.

Heuristically, the use of an average over an ensemble of projections is only justified if the errors of various projections are random. This property can be to some extent tested (but of course not proved) by looking at the appearance of the entire ensemble. It is natural to expect that projections containing random errors are distributed more or less uniformly within the entire range of projected values. This is usually not the case in dynamical projections of climate change and associated sea level rise (e.g., Johansson et al., 2014) but should be so for projections based on statistical concepts and consistent initial data. In this context, an important outcome of our analysis is the demonstration that the resulting ensemble of projections does not contain any obvious outliers for several representative locations of the Estonian coast in which the observations adequately reflect the open-sea water level. Similar ensembles, however, may exhibit clearly separated clusters for locations where the contribution of local factors to the observed water level is significant.

The paper is organized as follows. Section 2 provides information about the data sets, methods of their handling and statistical distributions used to build the projections of extreme water levels and their return periods. The ensembles of projections for the sites in question and their properties are presented in Section 3. Section 4 discusses the outcome of these projections and possibilities of the practical use of the presented approach.

2. Data and methods

2.1. Hindcast and observed data

The ‘ground truth’ is represented by water level measurements at the four sites that have been performed for many decades

(Suursaar and Sooäär, 2007). For example, the oldest water level records in Tallinn reach back to the year 1809 and regular monthly mean water level records start from the year 1842 (Suursaar et al., 2011). The monthly extreme values have been filed at these sites since the end of the 19th century (Table 1). Time series of regular observations are available from the middle of the 20th century (Table 1) two or four times a day (once in 12 or 6 h) and later on once an hour. As the observation intervals have changed in the course of time, none of the observed time series is completely homogeneous; however, it is likely that various sources of inhomogeneity of the time series do not significantly affect the monthly maxima.

The observed (or measured) values at these sites are presented in the official height system used in Estonia which is called the Baltic Height System BK77 with its reference zero-benchmark at

the Kronstadt near St. Petersburg. The Kronstadt zero is defined as the average water level in Kronstadt in 1825–1840 (Lazarenko, 1986).

Water level observations in three sites (Table 1) have performed in the same location for a long time while one station (Tallinn) has been relocated in 1996. For this reason the data for Tallinn stem from three different sources. The observations up to the year 1996 were performed by the Estonian Meteorological and Hydrological Institute (EMHI) in Tallinn Old Harbour. Since then the water level observations at this site by the EMHI were terminated due to the construction works and moved to Muuga Harbour. However, the Tallinn Harbour Enterprise continued the observations until the water level mooring buoy operated by Marine Systems Institute at Tallinn University of Technology (MSI) was installed. Therefore, a combined dataset from EMHI,

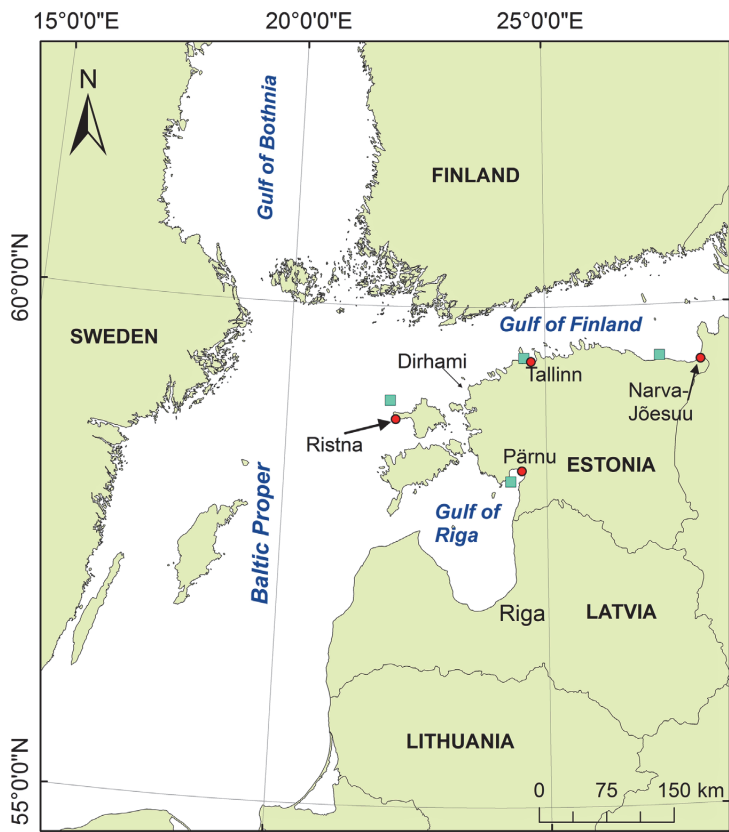


Fig. 1. Location scheme of the four sites used in this study. Red circles indicate the observation sites and green rectangles—the associated points of the circulation model (for interpretation of the references to colour in this figure legend, the reader is referred to the web version of this article).

Table 1
Co-ordinates of observation sites, centroids of the associated model grid cells in Fig. 1, model water depth at these cells and the mean water level in simulations. Years in brackets indicate the start of recording of monthly extreme values at a particular site.

Location	Observations since	Co-ordinates	RCO (6 h)	Model water depth (m)	Mean level (cm)	HIROMB	Mean level (cm)
Narva-Jõesuu	(1899) 01.10.1950	59°28'06"N 28°02'32"E	59.49°N 27.25°E	24	19.17	59.5°N 27.25°E	5.93
Tallinn	(1899) 01.01.1945	59°26'39"N 24°45'49"E	59.49°N 24.583°E	27	17.24	59.5°N 24.58°E	−0.81
Ristna	(1922) 01.01.1950	58°55'14"N 22°03'23"E	59.06°N 21.98°E	42	14.66	59.0°N 22.0°E	−2.95
Pärnu	(1893) 01.11.1949	58°23'12"N 24°29'33"E	58.26°N 24.32°E	6	18.14	59.25°N 24.3°E	5.21

Tallinn Harbour Enterprise and MSI (Lagemaa et al., 2013) is used in this study. To comply with the modelled data range, only observations from the interval 1961–2005 are used.

The water levels at the grid cells indicated in Table 1 were extracted from the output of two different circulation models. Water level data simulated using the Rossby Centre Ocean Model (RCO, Swedish Meteorological and Hydrological Institute) were used without any adjustment except for de-meaning. We employed data from two different model runs with the same basic setup but with slightly different starting instance and duration. One of these data sets has a temporal resolution of 6 h and the other 1 h.

The RCO model has been thoroughly described, e.g., in (Meier et al., 2003) and we present here only its key features. Its horizontal resolution is 2×2 nautical miles and it uses 41 vertical levels (thickness 3–12 m) in z -co-ordinates. The model follows boundary information in the northern Kattegat and is coupled to a sea ice model. The particular model runs for 1961–2005 (May 1961–May 2005 by the 6 h dataset; January 1961–December 2005 by the 1 h dataset) was forced with high-resolution meteorological information from a regionalization of the ERA-40 re-analysis over Europe with a horizontal resolution of 22 km in which the wind is adjusted using simulated gustiness to improve the wind statistics (Samuelsson et al., 2011). Details of the model set-up and an extensive validation of its output are provided in (Meier et al., 2003; Meier and Höglund, 2013). The results of the water level hindcast and forecast are analysed in detail in (Meier et al., 2004). The model generally acceptable represents the time series and statistics of water levels but has some problems with replication of storm surges in the western Baltic Sea.

The zero water level in the RCO model is defined by the topography, i.e., connected with the bedrock. The model uses information from so-called Warnemünde topography (Seifert et al., 2001). As several different open sea maps have been used to construct this information, it is not straightforward to associate the model water level with a particular height system. In particular, land uplift is neglected in the model implementation. The study area experiences weak uplift that has been almost compensated by the global sea level rise during the last decades. The sea level data used to drive the model at the open boundary in Kattegat are based upon the height system NH60 (Meier et al., 2004). It is natural to interpret the model output in this system. The model, however, works in spherical co-ordinates and thus neglects several other factors that affect the water level such as the ellipticity of the Earth or the shape of the geoid. The modelled sea surface level follows the geodetic solution with an accuracy of 2–3 cm (Ekman and Mäkinen, 1996). However, the implementation of the principle of volume conservation in ocean modelling means that the impact of variable salinity and temperature of sea water on water level is often neglected in the models. This may lead to substantial systematic deviations of the modelled water level from the measured ones. These differences reach 30–35 cm in low-salinity parts of the Gulf of Bothnia and Gulf of Finland (Ekman and Mäkinen, 1996). In the context of extreme water levels and their return periods such a basically constant difference between the modelled and measured values is immaterial as the modelled extreme values are counted (similarly to the measured extreme values) from the long-term mean water level. To a first approximation, we consider in this study the de-meaned values of modelled water levels and call them hindcast data.

Alternatively, a semi-synthetic data set was generated by merging measured water levels with a hindcast of a higher-resolution operational circulation model. For this purpose we used the output of the HIROMB (High-Resolution Operational Model for the Baltic Sea) model (Funkquist, 2001) operational BS01 setup with a resolution of 1 nautical mile (Lagemaa et al., 2011). This

water level forecasting system in Estonia is operational since 08.08.2005 (Lagemaa et al., 2011). The model belongs to the family of 3D circulation models originally developed by the Federal Maritime and Hydrographic Agency (BSH), Germany (Kleine, 1994), later implemented also at the SMHI and Danish Meteorological Institute and further developed for the Baltic Sea conditions by the HIROMB consortium. An earlier overview of different model versions and their set-up in the Gulf of Finland is presented in (Gästgifvars et al., 2008).

As the grid cells of the HIROMB model do not coincide with the locations of water level observations, it was necessary to transform the existing measurements at the four sites to the open-sea water level at the locations of the selected grid cells of this model. The observed time series were transferred using the HIROMB model and a linear regression to a distance of about 10 km in Tallinn, 15 km in Pärnu, 20 km in Ristna and 40 km in Narva-Jõesuu. The regression coefficients were calculated by matching the monthly maximum water levels at the nearest observation site with the water level output of the HIROMB model in 2006–2013. The very high values of Pearson correlation coefficients ($R > 0.99$ for all sites) confirmed the suitability of this method. For the purposes of our study it was sufficient to apply the regression model to the monthly maximum values of measured water level data. The resulting values are called observed data.

2.2. Extreme value distributions

An ensemble of projections of extreme water levels and their return periods was constructed based on the commonly used distributions of extreme values. These distributions are theoretical limiting distributions for maximums or minimums (extreme values) of the relevant samples of independent, identically distributed random variables, and are only reached when the sample size increases infinitely. The family of the limiting (extreme value) distributions consists of the Gumbel, Fréchet and Weibull distributions. They can be considered as particular cases of the Generalized Extreme Value (GEV) distribution

$$G(y) = \exp \left\{ - \left[1 + \xi \left(\frac{y - \mu}{\sigma} \right) \right]^{-1/\xi} \right\}. \quad (1)$$

Here y has the meaning of block maxima (e.g. annual maximum water levels) and μ , σ and ξ are called the location, scale and shape parameter (Coles, 2001). The return period $T(\hat{y})$ for a certain value \hat{y} is given by the $[1 - 1/T(\hat{y})]$ -th percentile of $G(y)$

$$T(\hat{y}) = \frac{1}{1 - G(\hat{y})}. \quad (2)$$

For $\xi \rightarrow 0$ the GEV distribution reduces to the Gumbel distribution $\Lambda(y) \sim \exp\{-\exp(-y)\}$, for $\xi < 0$ (which is frequent in oceanographic applications) it represents the Weibull distribution and for $\xi > 0$ (which is typical for finance market problems) the Fréchet distribution. The latter two distributions formally mirror each other but represent basically different physical situations. The Weibull distribution matches extremes of so-called light-tailed (very rapidly decaying) distributions while the Fréchet distribution is the limiting one of those which have polynomially (that is, relatively slowly) decaying tails. The Gumbel distribution is suitable for distributions possessing an exponential tail such as the Gaussian distribution.

The distributions of both modelled and measured water levels are typical for similar distributions in the north-eastern Baltic Sea (Johansson et al., 2001; Suursaar and Sooäär, 2007). They all resemble a Gaussian distribution but are usually skewed towards high water levels and thus have a maximum at or slightly below the long-term mean. For example, the distribution for the simulated water levels in the Tallinn Bay using the 6-h values from the RCO

model (Fig. 2) resembles a modified Gaussian distribution. It is moderately skewed (skewness 1.23). Its kurtosis (3.09, which is almost equal to the kurtosis of a Gaussian distribution) signals that the probability of very large values (either positive or negative water levels) insignificantly differs from their expectation for a Gaussian-distributed data set.

The distribution of measured water levels at Tallinn Old Harbour has a similar shape (Fig. 2). Its right-hand tail (extreme surges) is neither polynomial nor exponential. A typical feature of the coastal waters of Estonia (Suursaar et al., 2006a, b; Suursaar and Sooäär, 2007) and the entire north-eastern Baltic Sea (Johansson et al., 2001) is the presence of a few outliers. These are very high water levels (often regarded as values larger than the third quartile plus 1.5 times the difference between the first and third quartile) that are vividly represented in Fig. 2. This set may represent a specific population of water levels created by the interaction of sequences of storms that markedly increase the water volume of the Baltic Sea and a strong storm approaching when the entire Baltic Sea water level is unusually high (Suursaar and Sooäär, 2007).

The presence of a few such values (usually < 0.01% of the total water level recordings) insignificantly impacts the integral parameters of the overall (almost Gaussian-shaped) distribution. These values may still substantially affect the parameters of the associated extreme value distributions and projections of return periods of very large water levels (Suursaar and Sooäär, 2007). The use of a Gumbel distribution (which has an exponentially decreasing tail in semi-logarithmic co-ordinates) would eventually

underestimate the importance of positive outliers in Fig. 2 (and to lead to a certain underestimation of extremes). The use of a Weibull distribution would do the opposite because its tail decays as a power law in semi-logarithmic co-ordinates far to the right of the rightmost data depicted in Fig. 2. It is thus plausible to consider a set of various distributions for long-term projections.

To evaluate the parameters of the GEV, Gumbel and Weibull distributions we used *Hydrognomon*, a freely available general-purpose software tool for the processing and analysis of hydrological data (<http://hydrognomon.org/>). It is an open source application running on standard Microsoft Windows platforms, and also part of the openmeteo.org framework. This software employs typical hydrological applications, such as homogeneity tests, evapotranspiration modelling, stage-discharge analysis, areal integration of point data, of hydrometric data processing, and lumped hydrological modelling. We used only the statistical modules of *Hydrognomon* that provide numerical tools for data exploration, fitting of distribution functions, statistical prediction, Monte-Carlo simulation, determination of confidence limits, analysis of extremes, and construction of ombrian (intensity-duration-frequency) curves.

2.3. Projections based on block maxima

All constructed projections are built using so-called block maximum method (e.g., Arns et al., 2013). The monthly maximum values evidently cannot be assumed as uncorrelated because of substantial time lag between the impact of large-scale atmospheric patterns and the reaction of water level in terms of monthly means (Johansson et al., 2014). For this reason the hindcast and observed time series were divided into longer blocks of fixed length so that the maximum values within the blocks were uncorrelated. For each above-described data set we formed two sets of block maxima. Following the common practice in the Baltic Sea conditions (Lagemaa et al., 2013), the first set contained the extreme values in each calendar year.

In some cases, however, the obtained values may be correlated. For example, a maximum in December for one year and another in January of the subsequent year may reflect the impact of the same cluster of storms. The strong seasonal variation of water levels provides a natural way to construct an alternative set of block maxima of 1-yr intervals. Namely, stormy seasons (August–March) contain all annual highest water levels in the Estonian coastal waters and are clearly separated by calm spring seasons (Johansson et al., 2001; Suursaar et al., 2002; Jaagus and Suursaar, 2013). Therefore, the block maxima over such stormy seasons (equivalently, over the time intervals from a June until the subsequent May) are completely uncorrelated.

The two sets of block maxima generally differ insignificantly. The projections of extreme water levels and their return periods, however, show substantial differences (Fig. 3). For Estonian coastal waters the extreme water levels projected using the maxima of stormy seasons are usually higher than those based on the annual maxima. The differences are relatively large (about 20 cm for water levels that occur once in 200 yr) for the RCO data and somewhat smaller but still substantial (about 10 cm) for the observed data.

The above-discussed mismatch between the actual distributions of observed and hindcast water levels and a Gaussian one suggests that none of the extreme value distributions perfectly captures the extreme levels for longer return periods. The nature of deviations of the actual distributions from a Gaussian one is not known and thus the biases produced by the use of either of these distributions are also unknown. To resolve the problem at least to a first approximation it is reasonable to assume that the errors of each distribution are randomly distributed. This assumption is to

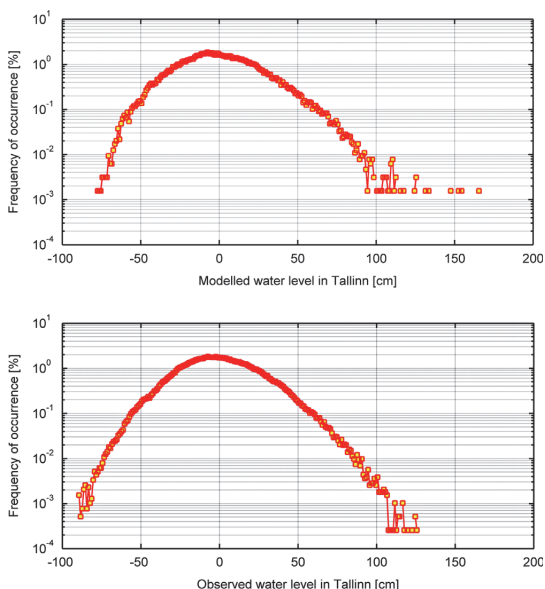


Fig. 2. Frequency of occurrence of deviations of the water level from the long-term mean in the RCO simulations (6-h values in 1961–2005, upper panel) and in measurements in Tallinn Harbour (1945–15.05.1995). As the measurement site was relocated from Tallinn Old Harbour to Muuga Harbour in 1996, the distribution of observed values does not contain the highest examples in the 2000 s (135 cm in 2001; 152 cm in 2005). The recordings of the largest values after the turn of the millennium raises the question whether the overall dynamics of the water level may have changed since 1996. A similar change has been found in the statistics of wave-driven setup in the vicinity of Tallinn for 1981–2012. All the highest waves have occurred after 1995 but the highest set-up apparently occurred in many locations before 1995 (Soomere et al., 2013). A probable reason is a change in the wind direction in strongest storms, with obvious changes to the local water level dynamics.

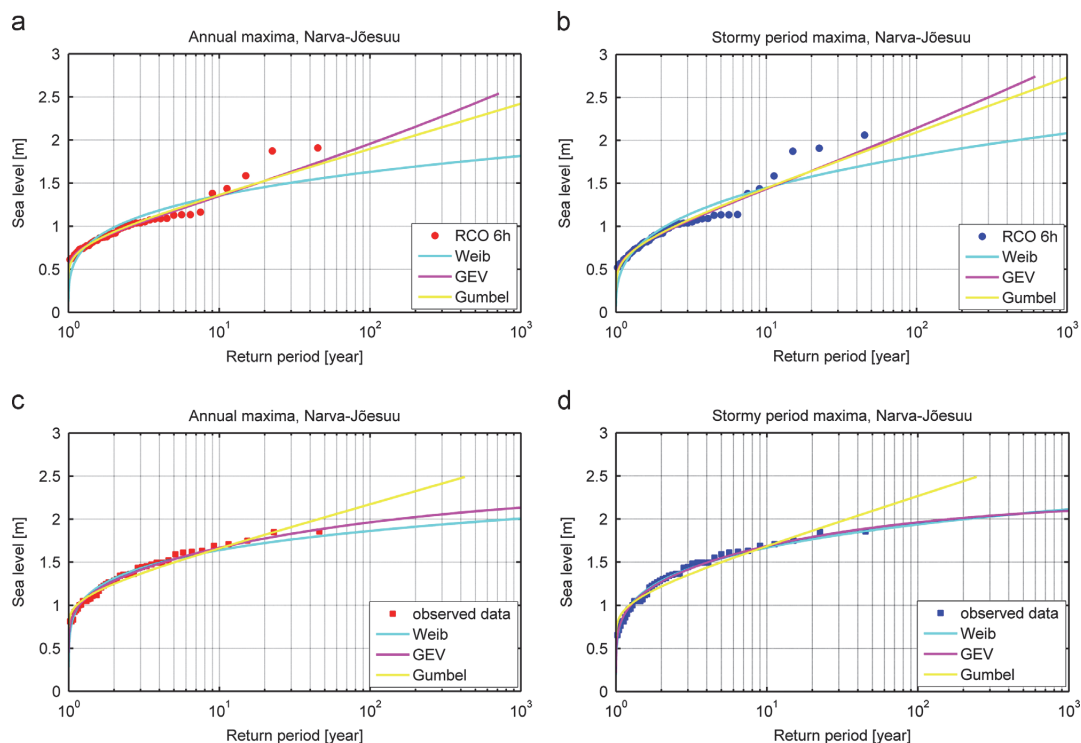


Fig. 3. Return periods of extreme water levels at Narva-Jõesuu according to the results of the 6-h RCO data (upper panels) and the observed data set (lower panels). Note that the latter data is actually a semi-synthetic data set obtained based on actual observations and the output of HIROMB as explained above. The panels at left correspond to projections based on annual maxima, the panels at right—to projections based on maxima over stormy seasons. Single markers represent the set of block maxima in the relevant data sets. Magenta line: the projection based on the GEV distribution, cyan line: Weibull distribution, yellow line: Gumbel distribution (for interpretation of the references to colour in this figure legend, the reader is referred to the web version of this article).

some extent supported by the appearance of the projections using different distributions (Fig. 3). For example, if the 6-h RCO data are used, the GEV distribution projects the largest extreme water levels that largely match the projection using a Gumbel distribution. If, however, the observed data is used, the GEV distribution projects the smallest values that almost coincide with the outcome of a Weibull distribution.

Given such an extensive variability of different projections, a feasible solution is the concurrent use of all these distributions. The average of such an ensemble of projections eventually provides a reasonable estimate of the true value. Following this conjecture, we include results obtained using the Gumbel and Weibull distributions into the ensemble of projections along with the outcome of the GEV distribution. Although the projections made using the GEV distribution often outperform the other approaches (Lowe et al., 2001; Wroblewski, 2001; van den Brink et al., 2005), the spreading of all three projections provides valuable additional information about their possible bias. Interestingly, the spreading of all four versions of projections of extreme water levels once in 200+ yr is almost the same.

3. Results

The empirical estimates of extreme water levels up to once in 45 yr from the hindcast and observed data differ markedly. The difference of these values for Tallinn (Fig. 4) is relatively small but still is about 20 cm for water levels once in 5–10 yr and reaches

30 cm for water levels once in 22 yr. In spite of these deviations, the different projections are located much closer to each other. They spread only by 25 cm for water levels once in 20 yr, by about 50 cm for water levels once in 100 yr and about 80 cm for water levels once in 1000 yr. This range is quite small compared to many other similar exercises (Sterl et al., 2009) and signals good consistency of the underlying data. Importantly, different projections are almost uniformly distributed within the entire ‘corridor’ formed by the largest and smallest projected extreme water level. Also, the lines corresponding to different projections often cross each other. These features suggest that the assumption of randomness of the error of each projection is not explicitly violated and that the median (or average value) of the ensemble of projections is a good estimate for the extreme water levels and return periods at this location.

The severest storm surges at Pärnu (2.75 m in 2005, 2.53 m in 1967) are extremely high in the context of the Baltic Sea. The total range of variations is as large as 4 m at Pärnu. The nature of such surges has been extensively discussed in the literature (Suursaar et al., 2006a; Suursaar and Sooäär, 2007, among others). The common opinion is that these values cannot be fit into any of the existing theoretical extreme value distributions. Fig. 5 suggests that the presence of these values markedly affects the appearance of the GEV and Gumbel fit (cf. Suursaar and Sooäär, 2007) while the Weibull fit seems to be largely governed by the rest of the block maxima.

The different sets of block maxima in Fig. 5 also deviate typically by 20 cm for return periods less than 15 yr but up to 60–70 cm for

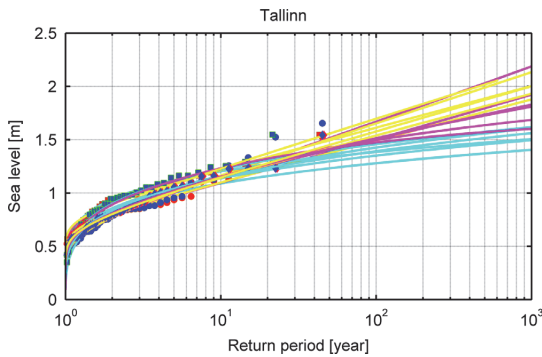


Fig. 4. Return periods of extreme water levels according to different projections at Tallinn. Block maxima: red circles—annual maxima of the RCO 6-h data, blue circles—stormy season maxima of the RCO 6-h data; red rhombi—annual maxima of the RCO 1-h data, blue rhombi—stormy season maxima of the RCO 1-h data; red squares—annual maxima of the observed data set; blue squares—stormy season maxima of the observed data set. The markers showing the block maxima derived from the 1-h RCO data almost coincide with those for the RCO 6-h data set. Yellow lines: projections using the Gumbel distribution, magenta—GEV distribution; cyan—Weibull distribution. Note that the difference between the observed and hindcast block maxima corresponding to the calendar years (red) or to stormy seasons (blue) does not become evident in the scale of the image but considerably impacts the relevant projections starting from return periods of about 20 yr (for interpretation of the references to colour in this figure legend, the reader is referred to the web version of this article).

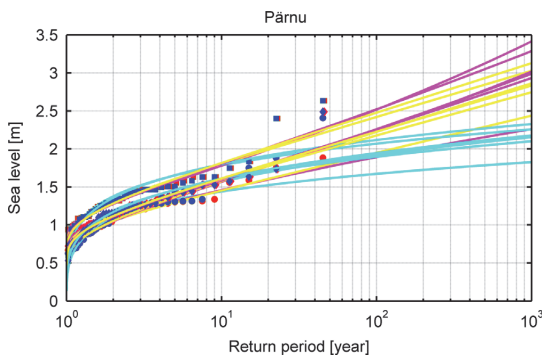


Fig. 5. Return periods of extreme water levels according to different projections at Pärnu. Notations are the same as for Fig. 4. As the RCO set does not cover the entire 2005 year, the surge in January 2005 is not reflected in the set of annual maxima of this data set.

return periods of 22 and 45 yr. This span is reflected in a somewhat larger spread of various projections than in Fig. 4. The spread is 40–50 cm for return periods of 10–20 yr and increases to 80 cm for return periods of 100 yr and to 150 cm for return period of 500 yr. Although the spread of the block maximum data is much larger for Pärnu than for Tallinn, the lines corresponding to different projections are relatively uniformly distributed within the corridor of all projections.

The deviations between the different values of block maxima for relatively short return periods (2–10 yr) are quite large at Narva-Jõesuu (Fig. 6). The observed values exceed the hindcast ones typically by up to 50 cm. The difference diminishes for the largest block maxima and the overall maxima of all three data sets only differ by less than 20 cm. The differences for the return periods of 2–10 yr evidently reflect local features of the measurement site. The observations were made using a staff mounted in the harbour located ca 200 m upstream of River Narva (Fig. 7). The river flow is occasionally blocked by a sand bar at the river mouth.

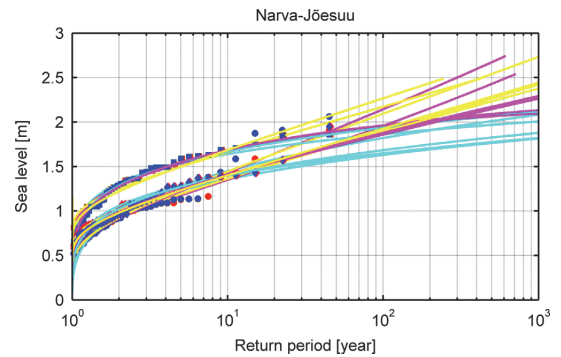


Fig. 6. Return periods of extreme water levels according to different projections at Narva-Jõesuu. Notations are the same as for Fig. 4.

The water depth at the sill usually varies in the range of 2–3 m (Laaneau et al., 2007). The gently sloping sandy seabed is favourable for the formation of relatively high local wind-driven surge and wave-induced set-up. These features are not resolved by the circulation models with a moderate spatial resolution like the RCO model. The entire river mouth area is open to the predominant wave propagation direction. It is thus likely that local wind-driven surge (similarly to Pärnu, Suursaar and Sooäär, 2007) and wave set-up (Dean and Bender, 2006) often substantially contribute to the observed water levels. The sill is gradually eroded by large discharge in spring and restored by wave-driven alongshore sand transport in late summer and autumn (Laaneau et al., 2007). Its dynamics may thus add considerable seasonality into the difference between the (hindcast) open sea level and the observed water level.

Under described circumstances it is not unexpected that the hindcast and measured block maxima form two distinct populations (Fig. 6). These populations, however, have almost matching values for the water level once in 45 yr. The presence of the two populations gives rise to two clusters of projections. These clusters are clearly separated for return periods of less than 20 yr but largely merge for longer return periods. Starting from return periods of about 30 yr they are more or less uniformly distributed between the largest and lowest projected water levels. The joint spread of the two sets of projections is about 40 cm for return periods of 20 yr, increases to about 60 cm for return periods of 100 yr and is close to 100 cm for return periods of about 500 yr. These values are comparable to those for Pärnu.

The situation is completely different at Ristna (Fig. 8). The measured and hindcast block maxima differ radically, from 30 cm for as short return periods as 2 yr up to almost 90 cm for the return period of 45 yr. Even if the overall highest observed value (209 cm, January 2005) is considered as not representative (Suursaar et al., 2006b; Suursaar and Sooäär, 2007), the deviations between the hindcast and observed block maxima are massive. Accordingly, the projections form two clearly separated clusters that do not overlap even for return periods of 1000 yr. The spreading of the projections within each cluster is fairly limited (below 10 cm) until return periods of about 25 yr and increases to 25–30 cm for return periods of 100 yr and to 40–60 cm for return periods of 500 yr. This modest spreading signals that both data sets (observed and hindcast) are internally consistent and that the all-time highest measured value (209 cm) is a valid member of the data set.

The described substantial deviation of the hindcast and observed data sets and associated projections signals that local features play a decisive role in the formation of the observed water level at Ristna.



Fig. 7. Location of the water level observation peel (green circle) in Narva-Jõesuu at the left bank of the River Narva. The white line to the east of the observation site indicates the border between Estonia and Russia. The right bank of the river is blurred by the image provider. Source: Estonian Land Board, www.maaamet.ee (for interpretation of the references to colour in this figure legend, the reader is referred to the web version of this article).

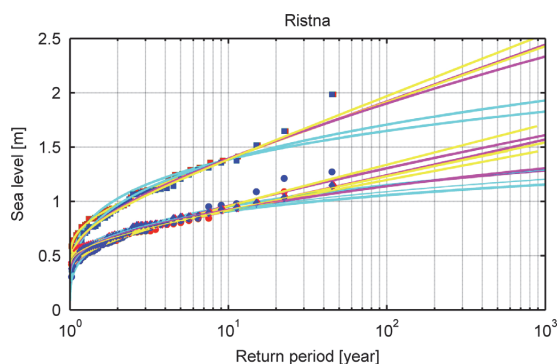


Fig. 8. Return periods of extreme water levels according to different projections at Ristna. Notations are the same as for Fig. 4.

The site is located in a small harbour of Kalana at the southern coast of the Kõpu Peninsula (Hiiumaa). The coastline is fully open to the predominant south-western winds and evidently to the largest waves that may reach the coasts of Hiiumaa. The geometry of the harbour (Fig. 9) is favourable for the formation of higher water levels in its interior under southern and south-western winds and by waves approaching from south-west. The seabed deepens relatively rapidly. It reaches a depth of 5 m at a distance of 150–200 m from the coast and 10 m at a distance of 300 m from the coast. Therefore, quite large waves may reach the immediate vicinity of the harbour and to produce substantial set-up. It is not uncommon that significant wave heights over 4 m reach this area (Tuomi et al., 2011). Such waves usually approach the coast from the south-west, that is, almost incidentally to the shoreline, and thus may create set-up heights up to 1 m in ideal conditions (Dean and Bender, 2006).

4. Conclusions and discussion

The analysis of the frequency of occurrence of various water levels along the Estonian coast suggests that none of the commonly used extreme value distributions (Generalised Extreme Value, Gumbel,

Weibull) is able to perfectly replicate the observed and hindcast extreme water levels. The Gumbel fit tends to produce larger projections of extreme levels for longer return periods than the Weibull fit. The GEV fit usually gives certain intermediate values but may match either Gumbel or Weibull fit, depending on the location and the method of building the block maxima. The typical spreading of the projections that employ six different sets of block maxima as the input to a particular distribution is fairly limited (below 10 cm) until return periods of about 25 yr. It increases to 25–30 cm for return periods of 100 yr and to 40–60 cm for return periods of 500 yr. The discrepancy apparently reflects the presence of a population of water levels that do not fit the general statistics and correspond to specific dynamically driven situations such as a high surge after a sequence of strong storms that have already increased the volume of the water in the Baltic Sea.

As hypothesized above, a feasible way to take into account the presence of this population is to employ the ensemble approach. If single projections of the extreme water levels are more or less uniformly distributed, a reasonable projection can be obtained as a median, average or weighted average of the ensemble members. This perception is largely met for coastal segments where the water level measurements or observations (that have been usually performed from certain coastal engineering structures) properly reflect the open-sea water level. This is the case for two substantially different locations such as Tallinn and Pärnu, to a lesser extent for Narva-Jõesuu but completely different for Ristna. For the first three locations, the spreading of the entire ensemble is < 50 cm for about 20 yr return periods and increases to 75 cm for about 100 yr and 125 cm for about 500 yr return period. Importantly, no clear outliers exist among predictions for these sites in the sense that no prediction is clearly above or below the cluster of other predictions. All projections of extreme water levels in the ensemble are generally homogeneously spread between the highest and the lowest one. Moreover, no prediction fits well the ensemble average. This appearance of the ensembles signals that the assumption of random distributions of errors of single projections is sensible. The median of the ensemble for 1 in 100 yr event corresponds almost exactly with the highest measured or hindcast water levels at Tallinn, Narva and Ristna. The two highest surges in Pärnu are 1 in 300–500 yr events (Suursaar and Sooäär, 2007).



Fig. 9. Location of the water level observation peel (green circle) in Ristna (Kalana Harbour). Source: Estonian Land Board, www.maaamet.ee (for interpretation of the references to colour in this figure legend, the reader is referred to the web version of this article).

It is likely that the described difference in the appearance of the ensembles of projections is associated with different contribution of local effects into the observed water levels. The observation site in Tallinn is located at the entrance to Tallinn Old Harbour. The water depth in its vicinity is > 10 m and the reading evidently reflects well the open-sea water level. The observation site at Pärnu is located a little bit upstream of the River Pärnu, in an ancient city moat. The depth of the River Pärnu mouth is kept at the level of about 5 m, which is comparable with the water depth in the entire Pärnu Bay. Therefore, wave set-up and local (near-shore) surge are both immaterial at the observation site. The observed water level reflects well the situation at the end of about 1 km long jetties that prevent the river mouth from silting. The water level at this location is reasonably reflected by contemporary circulation models. The observed water level data for Narva-Jõesuu evidently contain a certain contribution from the local effects (local surge, wave set-up, seasonally varying sill at the river mouth). Their impact is still moderate in the sense that the ensemble of projections for longer return periods has the same basic features as those for Tallinn and Pärnu.

The situation in Ristna is completely different. It is likely that local effects (first of all wave-induced set-up) substantially contribute to the formation of the observed block maxima. Fig. 8 suggest that their contribution is about 1/3 of the total water level. This estimate is supported by the large difference in the maximum water levels in January 2005 between Ristna (207 cm) and Dirhami (134 cm, Suursaar et al., 2006b) located about 80 km to the north-east (downwind for this storm) at the entrance of the Gulf of Finland (Fig. 1). This value is also consistent with the widely used rule of thumb for the open ocean coasts where wave set-up often provides 1/3 of the maximum surge at the waterline (Dean and Bender, 2006). It is likely that this locally induced contribution varies substantially along the coast of the Kõpu Peninsula already on scales of a few km depending on the orientation of the coast (cf. Soomere et al., 2013). This feature greatly complicates the analysis and projections of extreme water levels and their return periods compared to other coastal segments of Estonia.

Although extensive and rapid local changes in the water level are possible in the Gulf of Finland, strong spatial correlation of water level recordings extends to at least 150–200 km (Raudsepp

et al., 1999; Johansson et al., 2001). The typical de-correlation time is about two weeks (Raudsepp et al. 1999). These features suggest that the proposed ensemble approach is likely usable for the entire Gulf of Finland. In particular, the analysis of the Narva-Jõesuu data set advocates that it makes sense to approximate the observed extreme values in this gulf over a distance of tens of km to match them with the output of contemporary circulation models such as HIRLAM in studies of water levels in future climates. It is also likely that similar properties are valid for the eastern Gulf of Riga that has relatively regular geometry and bathymetry.

The extensive mismatch between the (offshore) hindcast and (coastal) observed water level data at Ristna not only renders the entire idea of building an ensemble of projections inoperable but possibly even misleading for locations of this type. More importantly, it emphasizes that numerically simulated water levels and associated projections of extreme surges and their return periods may completely overlook such essential components of storm surges as wave set-up and calls for much more detailed analysis of their possible role.

Another aspect is that the population of (positive) outliers in the water level time series may have several sources (cf. Haigh et al., 2014). The relatively well-known contributor to these is the possibility of pumping large volumes of water into the Baltic Sea by a sequence of strong storms (see Leppäranta and Myrberg, 2009 and references therein). Although it often provides 40–50% of the total storm surge, its contribution is commonly not singled out from the water level time series although the impact of this aperiodic mechanism not necessarily has a Gaussian-type distribution. The impact of local sources of extremely high water levels along the coast is often discussed but in a very few occasions separated from the total water level. It is unclear how to quantify their contribution even in statistical sense. A part of this contribution apparently mirrors the distribution of wind speeds from a particular unfavourable direction. While the overall distribution of all wind speeds commonly matches well a Rayleigh distribution in the north-western Europe (Troen and Petersen, 1989), similar distributions for single directions often deviate from the Rayleigh one (Soomere, 2001). Furthermore, the largest corrections to the water level (e.g. the highest wave set-up) is not necessarily synchronised with the course of the highest open-sea levels.

Acknowledgements

The research was a part of the project TERIKVANT (managed by the Estonian Research Council in the framework of the Environmental Technology R&D Programme KESTA and financed by the ERDF). The work was additionally supported by targeted financing SF0140007s11 of the Estonian Ministry of Education and Research, Grant 9125 by the Estonian Science Foundation and through support of the ERDF to the Centre of Excellence in Non-linear Studies CENS. The simulated hydrographic data were kindly provided by the Swedish Meteorological and Hydrological Institute in the framework of the BONUS BalticWay cooperation (Soomere et al., 2014).

References

- Arns, A., Wahl, T., Haigh, I.D., Jensen, J., Pattiaratchi, C., 2013. Estimating extreme water level probabilities: a comparison of the direct methods and recommendations for best practise. *Coast. Eng.* 81, 51–66.
- Araújo, M.B., New, M., 2006. Ensemble forecasting of species distributions. *Trends Ecol. Evol.* 22, 42–47.
- Averkjev, A.S., Klevanny, K.A., 2010. A case study of the impact of cyclonic trajectories on sea-level extremes in the Gulf of Finland. *Cont. Shelf Res.* 30, 707–714.
- Barbosa, S.M., 2008. Quantile trends in Baltic Sea level. *Geophys. Res. Lett.*, 35 (Art. No. L22704).
- Bardet, L., Duluc, C.-M., Rebou, V., L'Her, J., 2011. Regional frequency analysis of extreme storm surges along the French coast. *Nat. Hazards Earth Syst. Sci.* 11, 1627–1639.
- Cheung, K.K.W., 2001. A review of ensemble forecasting techniques with a focus on tropical cyclone forecasting. *Meteorol. Appl.* 8, 315–332.
- Christiansen, B., Schmith, T., Thejil, P., 2010. A surrogate ensemble study of sea level reconstructions. *J. Clim.* 23, 4306–4326.
- Coles, S., 2001. An Introduction to Statistical Modeling of Extreme Values. Springer, London.
- Dalidienė, I., Davulienė, L., Tilickis, B., Stankevičius, A., Myrberg, K., 2006. Sea level variability at the Lithuanian coast of the Baltic Sea. *Boreal Environ. Res.* 11, 109–121.
- Dean, R.G., Bender, C.J., 2006. Static wave set-up with emphasis on damping effects by vegetation and bottom friction. *Coast. Eng.* 53, 149–165.
- Donner, R.V., Ehrcke, R., Barbosa, S.M., Wagner, J., Donges, J.F., Kurths, J., 2012. Spatial patterns of linear and nonparametric long-term trends in Baltic sea-level variability. *Nonlinear Process. Geophys.* 19, 95–111.
- Ekman, M., Mäkinen, J., 1996. Mean sea surface topography in the Baltic Sea and its transition area to the North Sea: a geodetic solution and comparisons with oceanographic models. *J. Geophys. Res.–Oceans* 101 (C5), 11993–11999.
- Funkquist, L., 2001. HIROMB, an operational eddy-resolving model for the Baltic Sea. *Bull. Mar. Inst. (Gdańsk)* 28, 7–16.
- Gästgärf, M., Müller-Navarra, S., Funkquist, L., Huess, V., 2008. Performance of operational systems with respect to water level forecasts in the Gulf of Finland. *Ocean Dyn.* 58, 139–153.
- Gaslikova, L., Grabemann, I., Groll, N., 2013. Changes in North Sea storm surge conditions for four transient future climate realizations. *Nat. Hazard.* 66, 1501–1518.
- Haigh, I.D., Wijeratne, E.M.S., MacPherson, L.R., Pattiaratchi, C.B., Mason, M.S., Crompton, R.P., George, S., 2014. Estimating present day extreme water level exceedance probabilities around the coastline of Australia: tides, extra-tropical storm surges and mean sea level. *Clim. Dyn.* 42, 121–138. <http://dx.doi.org/10.1007/s00382-012-1652-1>.
- Hünicke, B., 2010. Contribution of regional climate drivers to future winter sea-level changes in the Baltic Sea estimated by statistical methods and simulations of climate models. *Int. J. Earth Sci.* 99, 1721–1730.
- Hünicke, B., Zorita, E., 2008. Trends in the amplitude of Baltic Sea level annual cycle. *Tellus A* 60, 154–164.
- Jaagus, J., Suursaar, Ü., 2013. Long-term storminess and sea level variations on the Estonian coast of the Baltic Sea in relation to large-scale atmospheric circulation. *Estonian J. Earth Sci.* 62, 73–92.
- Johansson, M., Boman, H., Kahma, K.K., Launinen, J., 2001. Trends in sea level variability in the Baltic Sea. *Boreal Environ. Res.* 6, 159–179.
- Johansson, M., Kahma, K., Pellikka, H., 2011. Sea level scenarios and extreme events on the Finnish coast. *VTT Tied. Valt. Tek. Tutk.* 2571, 570–578.
- Johansson, M.M., Pellikka, H., Kahma, K.K., Ruosteenoja, K., 2014. Global sea level rise scenarios adapted to the Finnish coast. *J. Mar. Syst.* 129, 35–46.
- Kleine, E., 1994. Das operationelle Modell des BSH für Nordsee und Ostsee. Konzeption und Übersicht. Bundesamt für Seeschifffahrt und Hydrographie.
- Laanearu, J., Koppel, T., Soomere, T., Davies, P.A., 2007. Joint influence of river stream, water level and wind waves on the height of sand bar in a river mouth. *Nordic Hydrol.* 38, 287–302.
- Lagemaa, P., Elken, J., Kõuts, T., 2011. Operational sea level forecasting in Estonia. *Estonian J. Eng.* 17, 301–331.
- Lagemaa, P., Raudsepp, U., Kõuts, T., Allik, A., Elken, J., 2013. Tallinna linna Haabersti, Põhja-Tallinna ja Kakumäe linnaosade meretasemete stsenaariumite modelleerimine (Modelling of water level scenarios for City of Tallinn). Research report, Marine Systems Institute at Tallinn University of Technology, Tallinn (29 pp.).
- Lazarenko, N.N., 1986. Variations of mean level and water volume of the Baltic Sea. In: *Proceedings of the Water Balance of the Baltic Sea Environment*, 16, pp. 64–80.
- Lowe, J.A., Gregory, J.M., Flather, R.A., 2001. Changes in the occurrence of storm surges around the United Kingdom under a future climate scenario using a dynamic storm surge model driven by the Hadley Centre climate models. *Clim. Dyn.* 18, 179–188.
- Leppäranta, M., Myrberg, K., 2009. *Physical Oceanography of the Baltic Sea*. Springer, Berlin, pp. 378.
- Meier, H.E.M., Höglund, A., 2013. Studying the Baltic Sea circulation with Eulerian tracers. In: Soomere, T., Quak, E. (Eds.), *Preventive Methods for Coastal Protection*. Springer, Cham Heidelberg, pp. 101–130.
- Meier, H.E.M., Döschner, R., Faxén, T., 2003. A multiprocessor coupled ice-ocean model for the Baltic Sea: application to salt inflow. *J. Geophys. Res.–Oceans* 108 (C8), 32–73.
- Meier, H.E.M., Broman, B., Kjellström, E., 2004. Simulated sea level in past and future climates of the Baltic Sea. *Clim. Res.*, 59–75.
- Mel, R., Sterl, A., Lionello, P., 2013. High resolution climate projection of storm surge at the Venetian coast. *Nat. Hazards Earth Syst. Sci.* 13, 1135–1142.
- Mudersbach, C., Jensen, J., 2009. Extreme value statistical analysis of historical, observed and modeled water levels on the German Baltic Sea coast [Extremwertstatistische Analyse von Historischen, Beobachteten und Modellierten Wasserständen an der Deutschen Ostseeküste]. *Küste* 75, 131–161.
- Raudsepp, U., Toompua, A., Kõuts, T., 1999. A stochastic model for the sea level in the Estonian coastal area. *J. Mar. Syst.* 22, 69–87.
- Samuelsson, P., Jones, C.G., Willén, U., Ullerstig, A., Gollvik, S., Hansson, U., Jansson, C., Kjellström, E., Nikulin, G., Wyser, K., 2011. The Rossby Centre Regional Climate Model RCA3: Model description and performance. *Tellus A* 63, 4–23.
- Seifert, J., Tauber, F., Kayser, B., November 25–29, 2001. A high resolution spherical grid topography of the Baltic Sea, revised edition. In: *Baltic Sea Science Congress*. Poster #147, Stockholm (www.iowarnemunde.de/iowtopo_resampling.html).
- Scotto, M.G., Barbosa, S.M., Alonso, A.M., 2009. Model-based clustering of Baltic sea-level. *Appl. Ocean Res.* 31, 4–11.
- Soomere, T., 2001. Extreme wind speeds and spatially uniform wind events in the Baltic Proper. *Proc. Estonian Acad. Sci. Eng.* 7, 195–211.
- Soomere, T., Pindsoo, K., Bishop, R.R., Käär, A., Valdmann, A., 2013. Mapping wave set-up near a complex geometric urban coastline. *Nat. Hazards Earth Syst. Sci.* 13, 3049–3061.
- Soomere, T., Döös, K., Lehmann, A., Meier, H.E.M., Murawski, J., Myrberg, K., Stanev, E., 2014. The potential of current- and wind-driven transport for environmental management of the Baltic Sea. *Ambio* 43, 94–104.
- Sterl, A., van den Brink, H., de Vries, H., Haarsma, R., van Meijgaard, E., 2009. An ensemble study of extreme storm surge related water levels in the North Sea in a changing climate. *Ocean Sci.* 5, 369–378.
- Stramska, M., 2013. Temporal variability of the Baltic Sea level based on satellite observations. *Estuar. Coast. Shelf Sci.* 133, 244–250.
- Stramska, M., Kowalewska-Kalkowska, H., Świrgoń, M., 2013. Seasonal variability in the Baltic Sea level. *Oceanologia* 55, 787–807.
- Suursaar, Ü., Soõäär, J., 2007. Decadal variations in mean and extreme sea level values along the Estonian coast of the Baltic Sea. *Tellus A* 59, 249–260.
- Suursaar, Ü., Kullas, T., Ottsmann, M., 2002. A model study of the sea level variations in the Gulf of Riga and the Vainameri Sea. *Cont. Shelf Res.* 22, 2001–2019.
- Suursaar, Ü., Jaagus, J., Kullas, T., 2006a. Past and future changes in sea level near the Estonian coast in relation to changes in wind climate. *Boreal Environ. Res.* 11, 123–142.
- Suursaar, Ü., Kullas, T., Ottsmann, M., Saaremäe, I., Kuik, J., Merilain, M., 2006b. Cyclone Gudrun in January 2005 and modelling its hydrodynamic consequences in the Estonian coastal waters. *Boreal Environ. Res.* 11, 143–159.
- Suursaar, Ü., Jaagus, J., Kullas, T., Tõnison, H., 2011. Estimation of sea level rise and storm surge risks along the coast of Estonia, Baltic Sea—a tool for coastal management. *Littoral* 2010, 12005.
- Troen, I., Petersen, E.L., 1989. *European Wind Atlas*. Risø National Laboratory, Roskilde, Denmark.
- Tuomi, I., Kahma, K.K., Pettersson, H., 2011. Wave hindcast statistics in the seasonally ice-covered Baltic Sea. *Boreal Environ. Res.* 16, 451–472.
- van den Brink, H.W., Konnen, G.P., Opsteegh, J.D., 2005. Uncertainties in extreme surge level estimates from observational records. *Phil. Trans. Roy. Soc. A* 363 (1831), 1377–1386.
- Weisse, R., von Storch, H., 2010. *Marine Climate and Climate Change. Storms, Wind Waves and Storm Surges*. Springer, Berlin, Heidelberg (220 pp.).
- Wroblewski, A., 2001. A probabilistic approach to sea level rise up to the year 2100 at Kolobrzeg. *Pol. Clim. Res.* 18, 25–30.



Paper IV

Soomere T., Eelsalu M., Kurkin A., Rybin A. 2015. Separation of the Baltic Sea water level into daily and multi-weekly components. *Continental Shelf Research*, 103, 23–32, doi: 10.1016/j.csr.2015.04.018.



Separation of the Baltic Sea water level into daily and multi-weekly components



Tarmo Soomere^{a,b,*}, Maris Eelsalu^a, Andrey Kurkin^c, Artem Rybin^c

^a Institute of Cybernetics at Tallinn University of Technology, Akadeemia tee 21, 12618 Tallinn, Estonia

^b Estonian Academy of Sciences, Kohtu 6, 10130 Tallinn, Estonia

^c Nizhny Novgorod State Technical University n.a. R.E. Alekseev, 24 Minin street, 603950 Nizhny Novgorod, Russia

ARTICLE INFO

Article history:

Received 22 October 2014

Received in revised form

18 April 2015

Accepted 22 April 2015

Available online 24 April 2015

Keywords:

Water level

Subtidal scale

Statistical analysis

Exponential distribution

Poisson processes

Baltic Sea

ABSTRACT

Storm surges and changes in the water volume of the entire sea, with typical time scales about a day and a few weeks, respectively, are the largest contributors to the water level variations at the eastern Baltic Sea coasts. Our analysis employs time series of sea levels numerically reconstructed using the RCO (Rossby Center, Swedish Meteorological and Hydrological Institute) ocean model for 1961–2005. The distribution for the weekly-scale water level, defined as a running average over a certain time interval, has an almost Gaussian shape. For the 8-day average the distribution of the residual, interpreted as the frequency of occurrence of local storm surges of different height, almost exactly matches the exponential distribution that can be considered as reflecting the time between events of the underlying Poisson process. The distribution of the total water level contains a few outliers that often do not match the classical statistics. All extreme values (outliers) of water level are a part of the exponential distribution of storm surges for averaging intervals longer than about 3 days. Such separation of phenomena on different temporal scales is universal for the entire eastern Baltic Sea coast. The slopes of the exponential distribution for low and high water levels are different, vary markedly along the study area and provide a useful quantification of different coastal sections with respect to the probability of coastal flooding.

© 2015 Elsevier Ltd. All rights reserved.

1. Introduction

Coastal flooding is one of the most devastating natural hazards. Although no clear trend has been recorded in its intensity and frequency over the last decades (Weisse et al., 2014), its projections show a rapid increase in the related losses (Hallegatte et al., 2013). The combination of the global sea level rise (Cazenave et al., 2014), increase in the storminess (Alexandersson et al., 2000; Jaagus et al., 2008) or properties of cyclones (Sepp et al., 2005; Sepp, 2009) in the Baltic Sea region has reinforced the need for better understanding of how the water masses react to such changes.

The total water level in a serious flood event is normally the joint result of the impact of several drivers. The largest contributions usually stem from tides and low atmospheric pressure (inverted barometric effect), wind-driven surge and wave-induced set-up. The resulting values may be to some extent modified by meteorologically driven long waves such as meteorological

tsunamis (Monserrat et al., 2006; Pattiaratchi and Wijeratne 2014; Pellikka et al., 2014) [also called squall line waves in the USA (Sallenger et al., 1995) and baric waves in some studies of the Baltic Sea (Wisniewski and Wolski, 2011)], seiches, tide–surge interactions (Batstone et al., 2013; Olbert et al., 2013) and other site-specific phenomena.

It is usually assumed that contributions from different mechanisms to the resulting water level are basically independent. This assumption makes it possible to single out the signal of each mechanism from the overall course of water level and to analyse separately its progression, timing and contribution to the flooding (e.g., Losada et al., 2013). It also allows in-depth analysis of gradual changes in the averages and extremes caused by a single driver (e.g., Howard et al., 2014; Weiss et al., 2014) and finally constructing a projection of joint changes in mean and extreme water levels and return periods of dangerous events.

This approach is a standard tool in areas where local water level is driven by changes in the long-term mean, properties of storms and tidal activity (Pugh and Vassie, 1978, 1980). In such cases it is customary to decompose the water level time series into periodic (or dynamic) and random components, and to analyse their contribution separately (Haigh et al., 2010).

The situation is more complicated in locations exhibiting

* Corresponding author at: Institute of Cybernetics at Tallinn University of Technology, Akadeemia tee 21, 12618 Tallinn, Estonia.

E-mail addresses: soomere@cs.ioc.ee (T. Soomere),

maris.eelsalu@ioc.ee (M. Eelsalu), aakurkin@gmail.com (A. Kurkin).

<http://dx.doi.org/10.1016/j.csr.2015.04.018>

0278-4343/© 2015 Elsevier Ltd. All rights reserved.

substantial aperiodic variations in sea level at daily to monthly scales (called subtidal water level variability, Buschman et al., 2009). This component may be significant along the open ocean coast (e.g., near Crescent City, California) (Percival and Mojfeld, 1997) where it is driven by atmospheric pressure patterns. It is often much more pronounced in semi-enclosed estuaries and basins such as the Delaware estuary (Wong and Moses-Hall, 1998), Galveston Bay (Guannel et al., 2001), Tampa Bay (Wilson et al., 2014) or the Baltic Sea (Leppäranta and Myrberg, 2009), where it is associated with changes in the overall volume of water in the basin.

The fundamentally aperiodic components have a typical time scale of a few weeks in the Baltic Sea. This is due to the impact of sequences of storm cyclones (Post and Kõuts, 2014) that may bring substantial amounts of water into the sea and lead to a 1 m increase in its water level (Johansson et al., 2001) similarly to Chesapeake Bay (Bosley and Hess, 2001). This value is comparable or even larger than the all-time maximum height of the local storm surge in the eastern Baltic Sea measured from the average water level in the entire sea. The local impact of storms (the classical storm surge) develops on the background of this (elevated or depressed) water level. For example, in north-western Estonia the all-time highest total water level is about 1.5 m (1.48 m at Dirhami, 1.52 m or 1.55 m at Tallinn according Suursaar et al., 2006b and Averkiov and Klevanny, 2010, respectively), whereas the magnitude of the local storm surge is about half of it. For this reason the most devastating surges occur in the eastern part of the Baltic Sea when a strong storm approaches after a sequence of previous storms has considerably increased the overall water volume of the Baltic Sea (Johansson et al., 2001).

The presence of this large-amplitude aperiodic component leads to a major problem in the construction of projections of future extreme Baltic Sea water levels. The total water level time series contains a few very large positive outliers in many locations. Their presence not only deviates from the predictions of the classical statistical distributions but may also substantially affect the properties of the “tail” of these distributions and render the standard methods for the evaluation of return periods of high water levels essentially meaningless (Suursaar et al., 2006a, 2015). This situation calls for more detailed studies of the mechanisms behind such outliers and of the possibilities of their separation into a specific population of events.

Previous attempts to separate sea level variations on different scales in the Baltic Sea largely focus on establishing long-term trends in mean and extreme water levels (Barbosa, 2008; Johansson et al., 2011) and on distinguishing tidal, annual and semi-annual (Ekman, 1996; Stramska, 2013) phenomena and the so-called pole tide or Chandler peak (about 14.3 months, Ekman, 1996; Medvedev et al., 2014). Long-term changes in water level along the Estonian coasts are usually separated into two parts: the joint impact of global sea-level rise and postglacial land uplift (called external impacts, Suursaar et al., 2006a) and changes driven by atmospheric forcing. The external impacts led to the total (annual mean) sea level rise in the range of 7.5–15.3 cm at different locations in 1950–2002.

The strongest periodic signal in the water level time series is the annual variation in sea level (Johansson et al., 2001). It ranges between 20 and 25 cm in the Gulf of Finland (Raudsepp et al., 1999) and has increased by about 5 cm in Pärnu and Narva-Jõesuu (Suursaar et al., 2006a, 2015). This variation is usually less than 10% of the total range of water level variations (Suursaar et al., 2006a) and about 50% of the typical (annual) standard deviation of the instantaneous water level recordings (Johansson et al., 2001; Suursaar et al., 2006a). The contribution from diurnal tides is usually a few centimetres, reaching 10 cm in selected locations of the Gulf of Finland (Leppäranta and Myrberg, 2009) and 17–19 cm

in the easternmost region of this gulf (Neva Bay, Medvedev et al., 2013).

Several drivers with different temporal and spatial scales may contribute to subtidal variations in the water level. Although intra-seasonal variations in freshwater inflow may add a few centimetres to the water level in the neighbourhood of large river mouths (Leppäranta and Myrberg, 2009), subtidal variations in the Baltic Sea mostly result from atmospheric pressure and direct wind impact. Storm surges have a typical time scale of 1 day. The above-mentioned sequences of storms (Post and Kõuts, 2014) may add up to 1 m to the level of the entire sea over a typical time scale of a few weeks (Feistel et al., 2008; Leppäranta and Myrberg, 2009).

Therefore, even if various harmonic components have been singled out, as has been done in common models of water level (e.g., Raudsepp et al., 1999), the residual signal is a mixture of reactions of water level to at least two strong drivers (single storms and subtidal variations) with different temporal scales and contains a substantial aperiodic component.

In this paper we make an attempt to separate the major components of the course of water level based on the difference of their typical time scales. The problem would be relatively simple if we had at our disposal the correct time series of the overall water volume of the Baltic Sea and a necessary correction procedure to calculate the associated values for the idealised calm water level (e.g., taking account of the spatial distribution of air pressure or changes in salinity) at each site of interest. These data are usually not available. Our aim is to develop a meaningful and easy-to-use method for such a separation based on local (measured or modelled) time series of water level.

As the subtidal and storm-driven components of water level are fundamentally aperiodic in the Baltic Sea basin, the application of Fourier analysis is problematic because a very large number of harmonics are usually necessary to properly describe the properties of an aperiodic signal. We rely on the classical technique of the running average of water level time series with a properly designed length of the averaging interval. Interestingly, for a particular choice of this length the distribution of the frequency of occurrence of local storm surges of different height becomes the exponential distribution with the probability density function $\sim \exp(-\lambda x)$. Such distributions describe inter alia the time between events in a Poisson process (in which events occur continuously and independently at a constant average rate). This property opens a way to systematically characterise the exposedness of different sections of the coast to local storm surges using just one parameter – the exponent of this distribution, equivalently, the rate parameter λ (or, more conveniently, the associated scale parameter $1/\lambda$) of the exponential distribution.

The paper is structured as follows. Section 2 provides a short overview of the circulation model, the output of which is used in the analysis, and describes the spectral composition of the water level time series. Section 3 introduces the scheme used for the separation of short-term (surge-driven) and weekly-scale (associated with the volumetric changes of the entire Baltic Sea) variations in water level. An estimate of the proper length of the averaging interval that allows for meaningful separation of the processes is provided in Section 4 and an overview of spatial variations in the scale parameter of the resulting exponential distribution is available in Section 5.

2. Material and method

The analysis relies on numerically simulated water levels sampled once in 6 h at nearshore locations along the eastern Baltic Sea coast. These locations (Fig. 1) were chosen as the closest grid

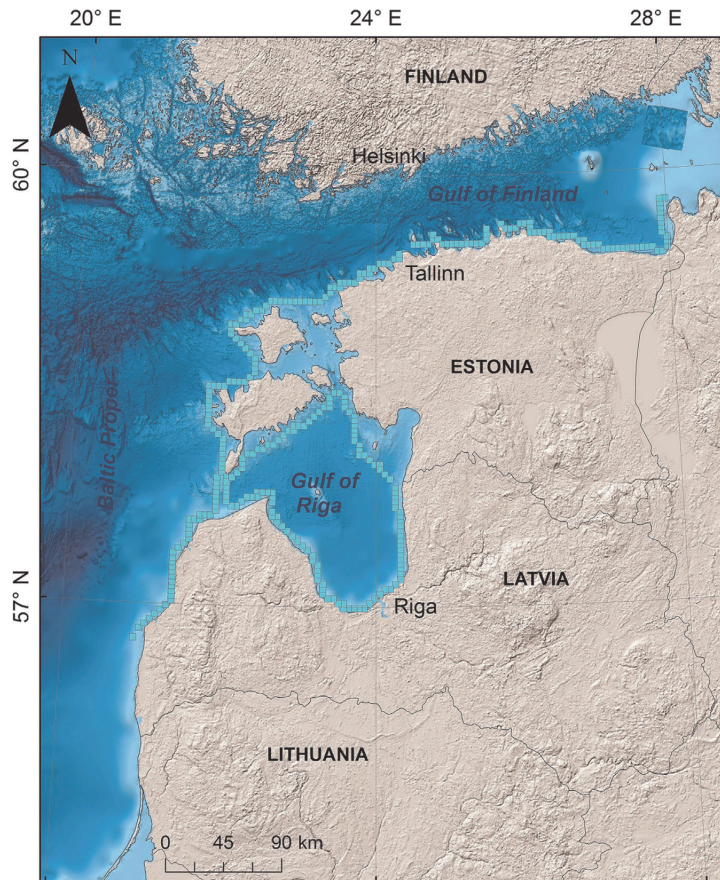


Fig. 1. Selected RCO model grid cells in the eastern Baltic Sea.

cells to the model coastline in the depth range of 6–30 m. The water levels were extracted from the output of the Rossby Centre Ocean Model (RCO, Swedish Meteorological and Hydrological Institute) and were used without any adjustment except for de-meaning (understood here as removing the 44-year mean).

The RCO model has been thoroughly described in the scientific literature (e.g., Meier et al., 2003; Meier and Höglund, 2013). Its horizontal and vertical resolutions are 2×2 nautical miles (about 3.7 km) and 3–12 m, respectively. The model run for May 1961–May 2005 is coupled to a sea ice model and uses boundary information in the northern Kattegat and a meteorological data set with a horizontal resolution of 22 km produced from the ERA-40 re-analysis (Samuelsson et al., 2011). Generally the model represents well both the time series and statistics of water levels but shows a certain mismatch for storm surges in the western Baltic Sea (Meier et al., 2004). A possible reason for the mismatches may be the ignoring of wave-induced set-up (Eelsalu et al., 2014).

The water level in the RCO model relies on the relevant data at the open boundary in Kattegat that are based upon the height system NH60 (Meier et al., 2004). The zero water levels in the rest of the model domain are connected with the bedrock through the so-called Warnemünde topography (Seifert et al., 2001). This data set incorporates open sea maps based on various height systems. The model neglects land uplift in the northern parts of the Baltic Sea. The impact of variable salinity and temperature of sea water

on water level is also neglected due to the principle of volume conservation; however, both the thermosteric and halosteric effects are small in shallow seas like the Baltic Sea. The RCO model suggests that about half of the sea level gradient between the Kattegat and the northern Bothnian Bay (about 35 cm, Ekman and Mäkinen, 1996) is explained by the mean zonal wind speed and the remaining part is explained by the baroclinic motion due to the horizontal salinity gradient (Meier et al., 2004). As we focus on the separation of the variability of water level at daily and weekly scales and consider the de-measured values of model output, small systematic deviations of the modelled water levels from the actual ones are immaterial in the context of this study. It is still straightforward to connect the obtained results with reality as they reflect the statistical parameters of deviations of water level from its long-term value.

In this study we use the time series of water level sampled once in 6 h. The total number of single values during the period of 29 May 1961–31 May 2005 is 64,293. The power spectrum of the modelled water level time series between the frequencies of diurnal tides and annual and semi-annual cycles contains a wide range of harmonics and has no distinct peak (Fig. 2). Therefore, the largest excursions of water level and especially of extreme water levels are almost entirely governed by aperiodic components with a wide spectrum. This feature, however, does not mean that the water level time series in the eastern Baltic Sea has a fully random

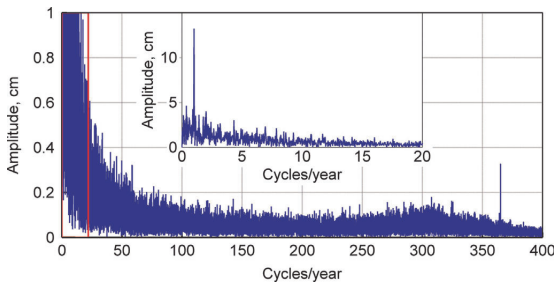


Fig. 2. Amplitude spectrum of de-measured values of simulated sea levels near Tallinn in 1961–2005. The inset presents low-frequency variations with periods exceeding 18 days indicated by the red box in the main panel. (For interpretation of the references to colour in this figure legend, the reader is referred to the web version of this article.)

nature. Although extensive and rapid local changes in the water level are possible, strong spatial correlation of water level recordings extends to 150–200 nautical miles, that is, over the entire Gulf of Finland. The typical de-correlation time is about two weeks (Raudsepp et al., 1999). The autocorrelation function vanishes for much longer lags of 60–90 days, signalling the importance of seasonal-scale processes.

Fig. 2 shows that there is no typical period of water level variations in the Gulf of Finland. As is common for such variations in the eastern Baltic Sea, only the annual peak and a smaller peak corresponding to the tidal cycle are clearly distinguishable. The rest of the spectrum of amplitudes is extremely wide. It has no obvious gap that could be used for the design of a proper high-pass or low-pass filter (so that the spectrum of shorter-period water level fluctuations would remain undistorted) for a formal separation of short-term variations from longer-term ones. Attempts to remove the annual cycle (cf. Raudsepp et al., 1999) have not improved the situation.

The shape of the spectrum in Fig. 2 suggests that the amplitudes of Fourier components with periods shorter than about 3 weeks decay rapidly. The components with periods less than 5–7 days (~ 50 cycles/yr) have amplitudes about 1/10 of the typical values of the components with periods of one month. Therefore it is eventually possible to adequately distinguish the variations longer than about a week from faster ones. The presence of a wide spectrum signals that the use of classical spectral filters may lead to substantial leakage of energy to some harmonics and may distort the appearance of both components in question. A feasible solution is to apply a certain smoothing operator to the water level time series to single out the weekly-scale component (that evidently reflects most of the fluctuations of the entire Baltic Sea water volume). The calculation of a residual (the total water level minus the weekly-scale component) is essentially a simple high-pass filter and its result evidently represents well the range of single-storm-driven local water level variations.

To a first approximation, we explore the ability of a simple running mean to separate the variations at different scales. The key question is the proper choice of the averaging interval T_A . This issue can be illustrated on the example of the simulated water level time series for January 1993 (Fig. 3). Water was continuously pushed into the Baltic Sea by a sequence of storms on 09–19 January 1993. This process continued from 21 January and reached saturation on 22–26 January 1993, after which the entire Baltic Sea level started to decrease. The time series on 10–26 January may contain a certain level of 1-day seiches (so-called harbour mode) in the Gulf of Finland (Jönsson et al., 2008). As the selected grid cell is close to the nodal point of these seiches, their amplitude should be quite limited.

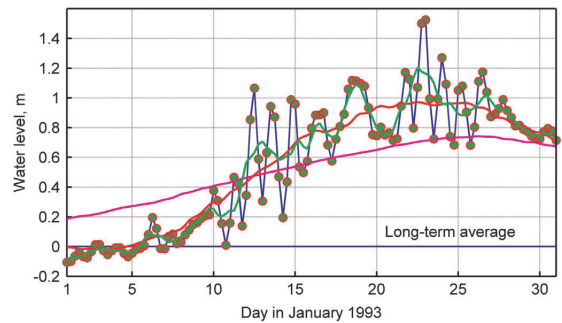


Fig. 3. Simulated water level (circles connected with a blue line), its 18-h (green), 8-day (red) and 20-day (magenta) running mean near Tallinn (Fig. 1). (For interpretation of the references to colour in this figure legend, the reader is referred to the web version of this article.)

On the one hand, for short averaging intervals ($T_A = 1$ –2 days) the resulting running average incorporates a substantial part of short-term variations, especially when several storms arrive in a sequence (Fig. 3). The result considerably overestimates the background water level of the entire Baltic Sea and thus is not a proper proxy for the volumetric changes of the sea. The residual (total water level minus the running average) contains negative relative surges up to 45 cm. On the other hand, longer averaging intervals ($T_A > 3$ weeks) evidently smooth out a large part of volumetric changes.

For the sequence of storms represented in Fig. 3 a reasonable averaging length seems to be about one week. This choice provides sensible separation of single events from the total time series. As typical of high-pass filters, the procedure of the calculation of the residual (storm-driven) variations effectively removes long-time correlations. The formal de-correlation time $\tau_0 = -\tau/\ln r_1$ can be approximately estimated from the lag length τ (interval between subsequent water level recordings) and lag-1 autocorrelation coefficient r_1 (von Storch and Zwiers, 1999). For example, while the total water level de-correlation time is approximately 14 days, it is less than one day for the residual (storm-driven) variations if $T_A = 8$ days. The autocorrelation function of storm-driven variations (Fig. 4) contains a relatively deep negative lobe (with a minimum about -0.2) for time lags of about 3 days. Its presence signals that this procedure does not perfectly remove short-term (a few days) correlations from the existing water level variations. However, given the above-discussed nature of the water level time series, it is unlikely that more elaborate methods (e.g., higher-order binomial, possibly variable weight running average) would considerably improve the result.

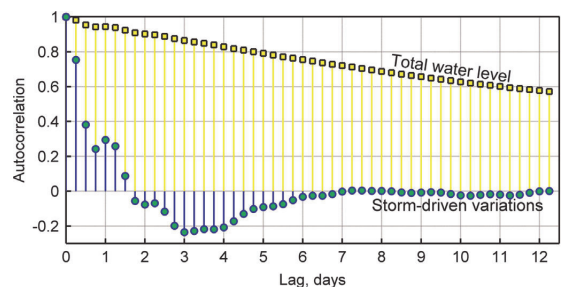


Fig. 4. Autocorrelation function of time series of the total water level and of the residual reflecting storm-driven variations for the averaging interval of 8 days.

3. Separation of outliers and short- and long-term variations

The distribution of the frequency of occurrence of total water level values considered above resembles, as typical of the eastern Baltic Sea (Johansson et al., 2001), a modified Gaussian distribution. It usually contains several very large positive outliers – extremely high water levels – for most locations along the Estonian and Latvian coasts. For a location near Tallinn (Fig. 1), it is moderately skewed (skewness 1.22, the mode located at a small negative value). The frequencies of occurrence of different water levels are thus not exactly symmetric and high water levels are more probable than equal values of low water levels (Fig. 5). The kurtosis of this distribution is 3.05, which is almost equal to the kurtosis of a Gaussian distribution. Therefore, the probability of outliers (either positive or negative) insignificantly differs from their expectation for a Gaussian-distributed data set. In other words, the presence of a few outliers in water level recordings almost does not impact the integral parameters of the overall Gaussian-like distribution.

A specific problem in the analysis and forecast of water levels in the eastern Baltic Sea is the frequent presence of outliers in water level records, which may substantially modify the projections of future extreme water levels and associated return periods (Suur- saar and Sooäär, 2007; Eelsalu et al., 2014). The proposed separation sheds some light on this problem by showing from where the outliers stem. It is natural that an increase in T_A leads to a decrease in the frequency of very large average water levels. For T_A up to about 2 days the distributions of the running average contain a few weak positive outliers (Fig. 5a), however, such outliers are not present for $T_A > 3$ days. Although the shape of the distribution of the running average is somewhat irregular for $T_A > 10$ days, the statistics of their values seems to approximately follow the Gaussian one and classical statistical methods (such as a Gumbel distribution or a Generalised Extreme Value distribution) can be used to evaluate their extreme values and return periods with high accuracy and small uncertainty.

The distribution of the time series of the residual variations considerably differs from a Gaussian one. This residual mostly reflects local storm-driven variations although for T_A longer than 3–4 days it may contain a certain contribution from the changes in the Baltic Sea water volume. As expected, its distribution is centred at zero. Its overall shape and the number of outliers substantially depend on the averaging interval. For relatively short T_A this distribution is almost symmetric. For very small averaging intervals ($T_A < 1.5$ days) this time series tends to follow the instantaneous values of the total water level. Interestingly, for such short averaging intervals the residual time series does not contain any outliers. This feature probably reflects the short duration of extremely high water level events and suggests that these are separated by at least a few days.

For averaging intervals in the range of 2–4 days the time series of storm-driven variations contain outliers of moderate amplitude (50–70 cm) of both signs (Fig. 5a). This property simply reflects the presence of large almost symmetric variations in water level with respect to the short-term mean (Fig. 3) and definitely does not indicate a symmetry of low and high water levels. A further increase in T_A causes a gradual shift in the positioning of the outliers. The negative outliers disappear and all positive outliers of the total water level are shifted into the distribution of residuals. This process starts from about $T_A \approx 2.5$ days, and for T_A longer than 3–4 days the entire population of outliers has been shifted into the time series of the residual (Fig. 5b).

The largest values of the running average water level for the above-discussed value $T_A = 8$ days reach 1 m, that is, about 60% of the largest outliers. This reflects the well-known fact that the changes in the entire Baltic Sea water volume substantially

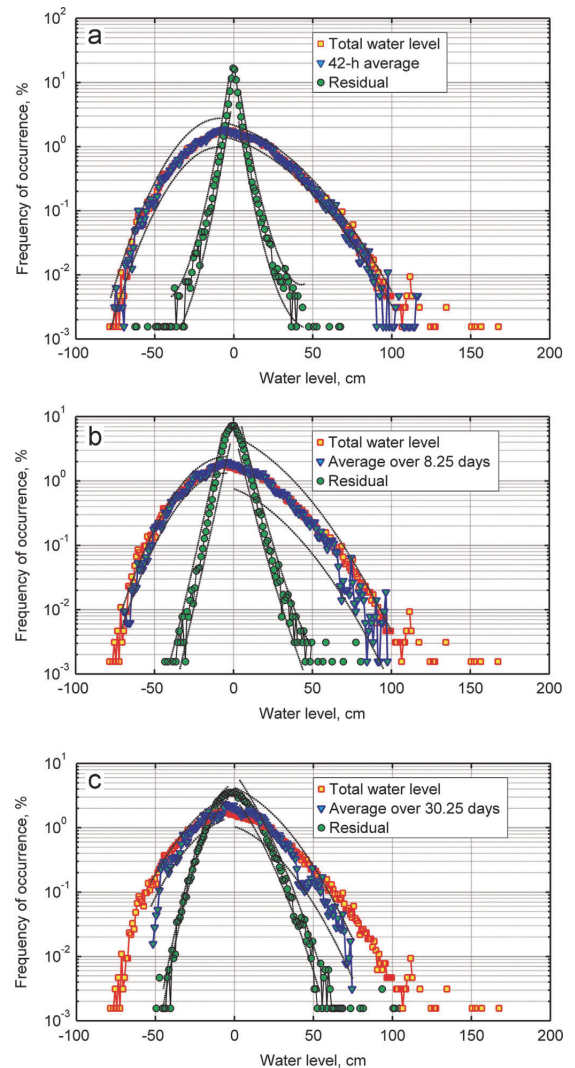


Fig. 5. Frequency of occurrence of water levels near Tallinn for different lengths of the averaging interval T_A : (a) $T_A = 42$ h, (b) $T_A = 192$ h (8.25 days), (c) $T_A = 726$ h (30.25 days). Dashed black curves indicate 95% confidence levels of the approximation of positive and negative surges and their components (from ± 3 cm until the first water level with a zero occurrence) using a quadratic function. The confidence levels are indicated in panel (a) for the distribution of the total water level and in panels (b, c) for the average over 8.25 and 30.25 days, respectively. The minimum level of frequency of occurrence $1.5554 \times 10^{-3}\%$ reflects just one occasion out of 64,293 hourly values. Several markers at this level may correspond to the same positive or negative surge event with a duration of ≥ 6 h.

contribute to the extreme water levels. The quasi-Gaussian appearance of the distribution of this water level component suggests that its contribution to the extremes can be adequately quantified using classical extreme value distributions, even though it contains a certain proportion of storm-driven variations (cf. Fig. 3).

Interestingly, the proposed separation positions all water level outliers in the residual signal. This indicates that storm-driven variations, although they formally contribute only $< 40\%$ to the maximum water level in the selected grid cell, play the governing

role in the most dangerous situations. In particular, they have a substantial role in all extremely high (> 130 cm) cases. A strong skewness of the distribution of the residual for T_A about a week (3.8 for $T_A = 8$ days) reflects extensive asymmetry of high and low water levels in such variations. Its particularly large kurtosis (about 17 in this case) shows that this quantity has a much larger probability for positive outliers than a similar Gaussian-distributed variable. Therefore, its extreme values not necessarily obey the classical (Fréchet, Weibull or Gumbel) statistics.

4. Exponential distribution of the frequency of occurrence of storm-driven component of the water level

The above discussion shows that the values of T_A on the order of one week lead to a satisfactory separation of storm surges from variations reflecting the entire Baltic Sea water volume. A more justified estimate of the proper length of T_A can be identified from the shape of the probability distribution of the residual time series.

The shapes of the distributions of the averaged and residual time series (Fig. 5) obviously depend on the length T_A of the averaging interval. For shorter values of T_A (up to a few days) the distribution of the time series of the running average almost exactly matches the distribution of total water levels (Fig. 5a). The difference is largest for the highest surges, the maximum values of which are levelled off in the averaging process. More importantly, for averaging intervals below a week both branches of this distribution (for negative and positive surges) are concave curves in the log-linear plot. They can be reasonably approximated using a quadratic function with a positive coefficient at the leading term. On the contrary, for longer averaging intervals (over 10 days) the relevant graph is convex and the leading term of the quadratic function is negative. In both occasions the relevant distributions belong to the general family of exponential distributions.

The most interesting particular case happens for $T_A \approx 8$ days when the coefficient at the leading term of such an approximation vanishes (Fig. 6). In this case the probabilities for both low and high storm-driven water levels decay linearly in the log-linear plot (Fig. 5b). The resulting exponential distributions with the probability density functions $\sim \exp(-\lambda x)$ are known to describe the time between events in a Poisson process. Unlike a Poisson process (in which single events occur continuously and independently at a constant average rate) and a Poisson distribution (a discrete probability distribution that expresses the probability of a given number of events occurring in a fixed interval of time and/or space), the exponential distribution is the continuous analogue of the geometric distribution.

The averaging interval for which the storm-driven variations follow the exponential distribution can be interpreted as a natural

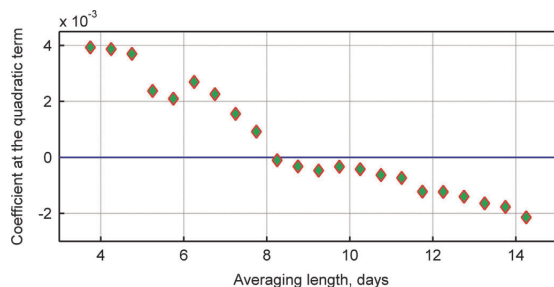


Fig. 6. The dependence of the coefficient at the quadratic term in the exponent of the distribution of the positive residual water level variations (positive storm-driven surges) on the length of the averaging interval. The data are the same as in Fig. 5. The quadratic equation is fitted to the interval from 3% down to 0.01%.

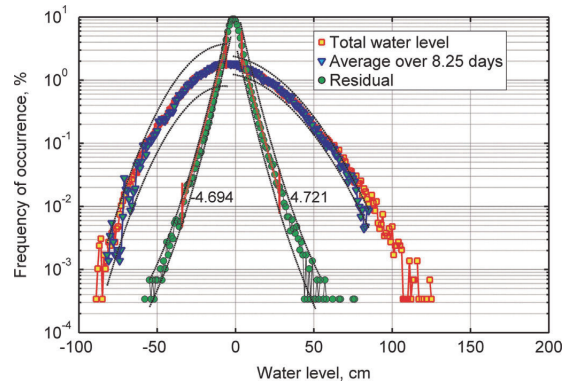


Fig. 7. Frequency of occurrence of hourly observed water levels at Tallinn Harbour in 1961–1995 for the averaging interval of 192 h (8.25 days). Red vertical lines indicate the range of water levels that are taken into account in the calculation of the linear approximation of the occurrence of residuals. Numbers at black lines indicate the scale parameter $-1/\lambda$. Dashed black curves indicate 95% confidence level of the approximation of positive and negative surges (from ± 3 cm until the first water level with a zero occurrence) using a quadratic function for the residual and for the average over 8.25 days. Notice that the number of single observations is much larger than the number of samples of modelled water level time series in Figs. 5 and 8 and that the all-time highest observed water levels in 2001 and 2005 are not present in the observed data set because of the relocation of the measurement site (Suursaar and Sooäär, 2007). (For interpretation of the references to colour in this figure legend, the reader is referred to the web version of this article.)

scale for the separation of short-term (daily scale) fluctuations of water level from similar variations that are caused by global (in the context of the Baltic Sea) processes. This scale roughly (8 days or about 45 cycles/yr) corresponds to the frequency at which the amplitude spectrum of de-measured values of simulated sea levels starts to increase rapidly towards longer-period components (Fig. 2).

This separation is equally valid for the observed water level time series (Fig. 7). Here the exponential distribution adequately describes an even wider range of the frequencies of occurrence of residuals than for the modelled water levels.

The described separation and the properties of the distributions of both water level components are valid for the entire eastern Baltic Sea. The distribution of the running averages always resembles a (modified) Gaussian distribution and does not contain any outliers for $T_A > 4$ days. Therefore, it is likely that probabilities of a substantial contribution of this component to the total water level can be reasonably quantified using the classical Gaussian statistics.

The distribution of storm-driven variations matches well an exponential distribution for the averaging interval of about 8 days. This feature makes it possible to adequately quantify the probability of having high local storm surges for any location of the study area in a straightforward manner using just one parameter – the slope $\lambda > 0$ of the graph of the exponential distribution $\sim \exp(-\lambda x)$, equivalently, the exponent of this distribution. It is convenient to use the associated scale parameter $-1/\lambda$, because high surges are much more likely as for sites characterised by its large values than for sites with its small values. The choice of the sign links the low water levels (negative surges) with negative values of the scale parameter. Note that this quantification ignores the presence of outliers and is thus only applicable to a limited range of upper quantiles of the total water level.

5. Spatial variations in the scale parameter of the exponential distribution

The slopes of the exponential distributions of modelled water

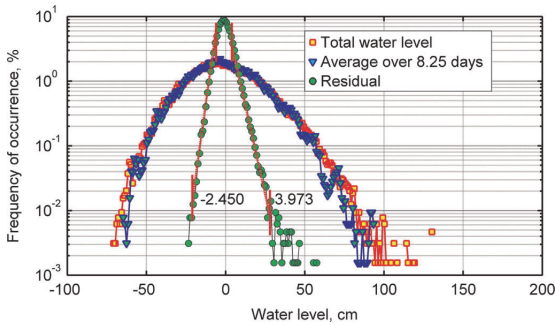


Fig. 8. Scheme of the linear approximation (red lines) of the distribution of residual water level fluctuations at a location at the shore of the open Baltic Proper. Red vertical lines indicate the range of water levels that are taken into account in the calculation of the linear approximation of the occurrence of residuals. Numbers at black lines indicate the scale parameter. (For interpretation of the references to colour in this figure legend, the reader is referred to the web version of this article.)

levels were evaluated by the approximation of the relevant sections of the graph with a linear function (Figs. 7 and 8). The graphs were almost linear in the range from 3–6% down to 0.01–0.02%, that is, over more than two orders of magnitude. The distribution of negative surges was mostly approximately linear in this

representation down to the smallest modelled values. The percentages of the largest positive values (that usually corresponded to outliers) varied considerably.

The scale parameters of the positive and negative branches of exponential distributions (Fig. 8) varied largely (by a factor of almost 3) along the eastern Baltic Sea coast (Fig. 9). The smallest absolute values of residual (storm-driven) low water levels (2.1–2.5) occurred in the open Baltic Proper along the western coast of the Estonian archipelago and Latvia (Fig. 9). The absolute values were somewhat larger (~ 3) at the entrance to the Gulf of Riga and Gulf of Finland and much larger (~ 5) in the interiors of these gulfs. This variation is consistent with the common perception that low water levels predominate in semi-enclosed areas in the easternmost domain of the Baltic Sea, whereas below-average water levels are modest and less frequent along the open Baltic Proper coast.

The scale parameters of the distribution of storm-driven (positive) surges have a matching pattern but are generally larger (also in terms of absolute values) and slightly less variable along the shores of the study area (Fig. 10). This mismatch of the quantity $-1/\lambda$, characterising negative and positive surges, makes it possible to systematically quantify the asymmetry of high and low water levels in different coastal sections of the Baltic Sea basin (Johansson et al., 2001, 2014; Suursaar and Sooäär, 2007). The smallest scale parameters (3–4) are found at the open Baltic

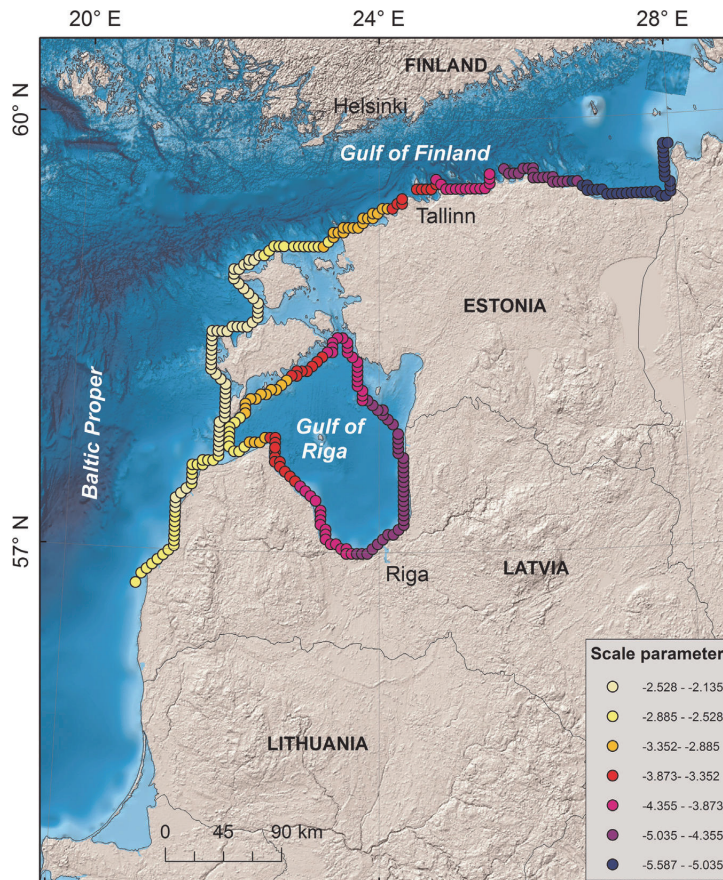


Fig. 9. The scale parameter of the exponential distribution of the frequency of occurrence of storm-driven low water levels in the eastern Baltic Sea.

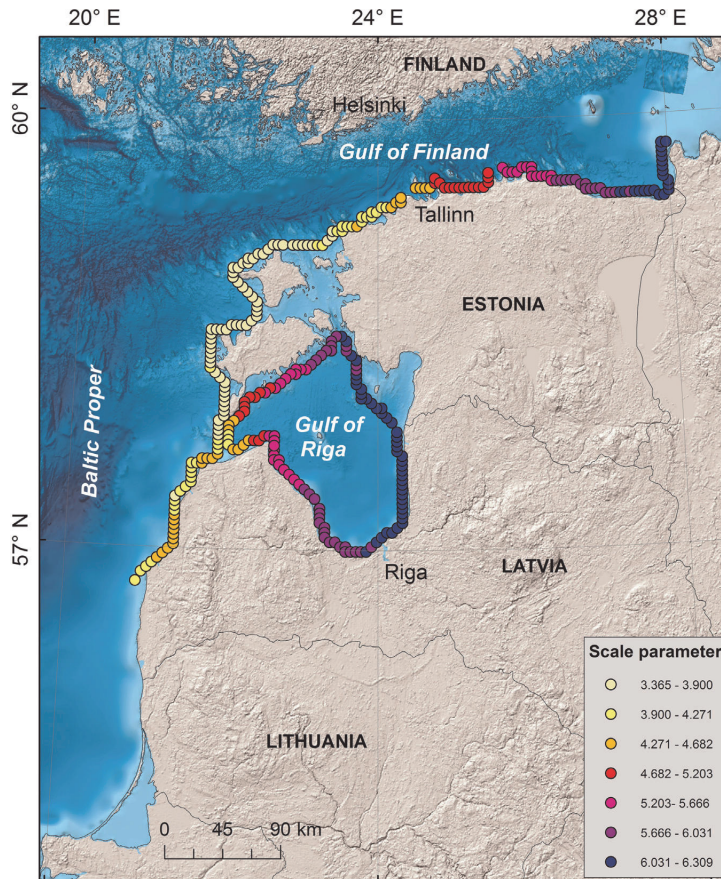


Fig. 10. The scale parameter of the exponential distribution of the frequency of occurrence of positive storm-driven surges in the eastern Baltic Sea.

Proper coasts. The values of $-1/\lambda$ are about 5 at the entrance to and in the range of 5.5–6.3 in the interiors of the Gulf of Riga and Gulf of Finland.

6. Conclusions and discussion

A core problem addressed in this paper, relevant to the analysis, forecast and future projections of the Baltic Sea water level, is how to separate the local (wind- and air pressure-driven) short-term reaction of the water masses from variations in the background level of the entire Baltic Sea or its sub-basins. Each of these components may account for about half of the total water level at extreme occasions and cannot be neglected in virtually any part of the sea. The presented analysis suggests that a natural, straightforward and rich in content separation can be produced by means of a surprisingly simple operation of the running average. The distribution of the resulting weekly-scale average water level has, as expected, an almost Gaussian shape. The distribution of the residual (equivalently, the frequency of occurrence of local storm surges of different height) contains all outliers of the water level time series for averaging intervals longer than about 3 days and almost exactly matches an exponential distribution for the 8-day average. The slopes of the positive and negative branches of this distribution for low and high water levels provide a useful

quantification of different coastal sections with respect to the probability of coastal flooding.

The success of this approach is based on the considerable difference between typical time scales of these two major processes. While storm surges usually last less than one day, changes to the water volume of the entire Baltic Sea (and associated variations in the local water level) are driven on (multi-)weekly scales as a joint impact of a sequence of storms (Post and Kõuts, 2014).

A weak point of this approach is that the weekly-scale water level, obtained as a simple running average of water level time series, incorporates a substantial part of storm surges and thus cannot be directly used as a proxy for volumetric changes of the Baltic Sea. This problem can be partly circumvented by using advanced filtering techniques but will eventually persist to some extent because of relatively small difference in temporal scales of the two processes. Although the operation of averaging largely smoothens out short-term variations, the distribution of this weekly-scale component has an almost Gaussian shape for any reasonable averaging length.

The distribution of the residual, interpreted as the frequency of occurrence of local storm surges of different height, commonly follows a general exponential distribution. Interestingly, it almost exactly matches an exponential distribution $\sim \exp(-\lambda x)$ if the above averaging is performed over 8 days. This feature may open new ways for the evaluation of extreme water levels, their trends and

return periods in the Baltic Sea basin. For this particular averaging length the variations in the total water level can be, at least formally, separated into processes obeying classical statistical distributions. In short, the proposed approach allows the description of the total water level as a superposition of an almost Gaussian process of a certain measure of background water levels with a Poisson process mimicking the contribution of short-term storm-driven variations. The exponential distribution can be interpreted as describing the time intervals between events of the Poisson process. Thus, a proper statistics of water levels could be constructed using bivariate distributions of these two components that obey different statistics. Such separation of phenomena on different temporal scales is universal for the entire eastern Baltic Sea coast. To clearly highlight this outcome, we have deliberately kept the averaging method as simple and basic as possible.

The variations in the amount of water in the Baltic Sea have an obvious seasonal cycle and, more importantly, several evident limiters for its magnitude. The sequence of storms that “feed” the Baltic Sea with water cannot be long. An approximation to their statistics can apparently be extracted from measured or modelled water level variations in the central Baltic. The resulting Baltic Sea water level has a limiting value, for which the storm-driven water inflow through the Danish straits is balanced by the outflow in the deeper layers of these straits. This limit under existing and changing climate conditions can be eventually modelled using a sequence of real or synthetic storms, similarly to Averkiev and Klevanny (2010).

The proposed separation of the water level components sheds some light on the problems associated with the projections of extreme water levels and their return periods by means of showing from where the outliers in the Baltic Sea water level stem. Importantly, the short-term variations with the exponential distribution (and apparently reflecting the underlying Poisson process) contain all outliers of the total water level starting from a certain length of averaging, thus offering a possibility of associating water level outliers with a clearly defined population of events. This outcome, although noteworthy, does not yet provide any practical improvement of estimations of the probabilities of extreme water levels.

The proposed approach is evidently applicable to other basins hosting a wide spectrum of different processes affecting the water level variations. The key precondition is the possibility of the separation of water level into components driven by processes at different time scales. For example, in estuaries with relatively large discharge and a sill at the entrance even relatively modest wind speed is able to block the outflow (Lehmann et al., 2011) and water level may rapidly increase because of river discharge.

Acknowledgements

The research was supported by institutional financing of the Estonian Ministry of Education and Research IUT33-3, the Estonian Science Foundation (Grant 9125) and through support of the ERDF to the Centre of Excellence in Non-linear Studies CENS. The simulated hydrographic data were kindly provided by the Swedish Meteorological and Hydrological Institute in the framework of the BONUS BalticWay cooperation (Soomere et al., 2014).

References

Alexanderson, H., Tuomenvirta, H., Schmith, T., Iden, K., 2000. Trends of storms in NW Europe derived from an updated pressure data set. *Clim. Res.* 14, 71–73.
Averkiev, A.S., Klevanny, K.A., 2010. A case study of the impact of cyclonic trajectories on sea-level extremes in the Gulf of Finland. *Cont. Shelf Res.* 30, 707–714.

Barbosa, S.M., 2008. Quantile trends in Baltic Sea level. *Geophys. Res. Lett.* 35, Art. No. L22704: 6 pp.
Batstone, C., Lawless, M., Tawn, J., Horsburgh, K., Blackman, D., McMillan, A., Worth, D., Lager, S., Hunt, T., 2013. A UK best-practice approach for extreme sea-level analysis along complex topographic coastlines. *Ocean Eng.* 71, 28–39.
Bosley, K.T., Hess, K.W., 2001. Comparison of statistical and model-based hindcasts of subtidal water levels in Chesapeake Bay. *J. Geophys. Res.–Oceans* 106 (C8), 16869–16885.
Buschman, F.A., Hoitink, A.J.F., van der Vegt, M., Hoekstra, P., 2009. Subtidal water level variation controlled by river flow and tides. *Water Resour. Res.* 45, W10420. <http://dx.doi.org/10.1029/2009WR008167>.
Cazenave, A., Dieng, B., Meyssignac, B., von Schuckmann, K., Decharme, B., Berthier, E., 2014. The rate of sea-level rise. *Nat. Clim. Chang.* 4, 358–361.
Elsalou, M., Soomere, T., Pindsoo, K., Lagemaa, P., 2014. Ensemble approach for projections of return periods of extreme water levels in Estonian waters. *Cont. Shelf Res.* 91, 201–210.
Ekman, M., 1996. A common pattern for interannual and periodical sea level variations in the Baltic Sea and adjacent waters. *Geophysica* 32, 261–272.
Ekman, M., Mäkinen, J., 1996. Mean sea surface topography in the Baltic Sea and its transition area to the North Sea: a geodetic solution and comparisons with oceanographic models. *J. Geophys. Res.–Oceans* 101 (C5), 11993–11999.
Feistel, R., Nausch, G., Wasmund, N. (eds.), 2008. State and evolution of the Baltic Sea 1952–2005. Wiley, Hoboken, New Jersey.
Guannel, G., Tissot, P., Cox, D.T., Michaud, P., 2001. Local and remote forcing of subtidal water level and setup fluctuations in coastal and estuarine environments. In: *Proceedings of the 4th Conference on Coastal Dynamics*. 11–15 June 2001, Lund, Sweden, pp. 443–452.
Haigh, I.D., Nicholls, R., Wells, N., 2010. A comparison of the main methods for estimating probabilities of extreme still water levels. *Coast. Eng.* 57, 838–849.
Hallegatte, S., Green, C., Nicholls, R.J., Corfee-Morlot, J., 2013. Future flood losses in major coastal cities. *Nat. Clim. Chang.* 3, 802–806.
Howard, T., Pardaens, A.K., Bamber, J.L., Ridley, J., Spada, G.L., Hurkmans, R.T.W., Lowe, J.A., Vaughan, D., 2014. Sources of 21st century regional sea-level rise along the coast of northwest Europe. *Ocean Sci.* 10, 473–483.
Jaagus, J., Post, P., Tomingas, O., 2008. Changes in storminess on the western coast of Estonia in relation to large-scale atmospheric circulation. *Clim. Res.* 36, 29–40.
Johansson, M., Boman, H., Kahma, K., Launinen, J., 2001. Trends in sea level variability in the Baltic Sea. *Boreal Environ. Res.* 6, 159–179.
Johansson, M., Kahma, K., Pellikka, H., 2011. Sea level scenarios and extreme events on the Finnish coast. *VTT Tied. Val. Tek. Tutk.* 2571, 570–578.
Johansson, M.M., Pellikka, H., Kahma, K., Ruosteenoja, K., 2014. Global sea level rise scenarios adapted to the Finnish coast. *J. Mar. Syst.* 129, 35–46.
Jönsson, B., Döös, K., Nycander, J., Lundberg, P., 2008. Standing waves in the Gulf of Finland and their relationship to the basin-wide Baltic seiches. *J. Geophys. Res.–Oceans* 113 (C3), C03004.
Lehmann, A., Getzlaff, K., Harlaß, J., 2011. Detailed assessment of climate variability in the Baltic Sea area for the period 1958 to 2009. *Clim. Res.* 46, 185–196.
Leppäranta, M., Myrberg, K., 2009. *Physical Oceanography of the Baltic Sea*. Springer, Berlin, p. 378.
Losada, I.J., Reguero, B.G., Méndez, F.J., Castaneda, S., Abascal, A.J., Mínguez, R., 2013. Long-term changes in sea-level components in Latin America and the Caribbean. *Global Planet. Change.* 104, 34–50.
Medvedev, I.P., Rabinovich, A.B., Kulikov, E.A., 2013. Tidal oscillations in the Baltic Sea. *Oceanology* 53, 526–538.
Medvedev, I.P., Rabinovich, A.B., Kulikov, E.A., 2014. Pole tide in the Baltic Sea. *Oceanology* 54, 121–131.
Meier, H.E.M., Höglund, A., 2013. Studying the Baltic Sea circulation with Eulerian tracers. In: Soomere, T., Quak, E. (Eds.), *Preventive Methods for Coastal Protection*. Springer, Cham Heidelberg, pp. 101–130.
Meier, H.E.M., Döschner, R., Faxén, T., 2003. A multiprocessor coupled ice-ocean model for the Baltic Sea: application to salt inflow. *J. Geophys. Res.–Oceans* 108 (C8), 32–73.
Meier, H.E.M., Broman, B., Kjellström, E., 2004. Simulated sea level in past and future climates of the Baltic Sea. *Clim. Res.* 27, 59–75.
Monserrat, S., Vilibić, I., Rabinovich, A.B., 2006. Meteotsunamis: atmospherically induced destructive ocean waves in the tsunami frequency band. *Nat. Hazards Earth Syst. Sci.* 6, 1035–1051.
Olbert, A.L., Nash, S., Cunnane, C., Hartnett, M., 2013. Tide-surge interactions and their effects on total sea levels in Irish coastal waters. *Ocean Dyn.* 63, 599–614.
Pattiaratchi, C., Wijeratne, M.S., 2014. Observations of meteorological tsunamis along the south-west Australian coast. *Nat. Hazards* 74, 281–303.
Pellikka, H., Rauhala, J., Kahma, K.K., Stipa, T., Boman, H., Kangaset, A., 2014. Recent observations of meteotsunamis on the Finnish coast. *Nat. Hazards* 74, 197–215. <http://dx.doi.org/10.1007/s11069-014-1150-3>.
Percival, D.B., Mofjeld, H.O., 1997. Analysis of subtidal coastal sea level fluctuations using wavelets. *J. Am. Stat. Assoc.* 92, 868–880.
Post, P., Kõuts, T., 2014. Characteristics of cyclones causing extreme sea levels in the northern Baltic Sea. *Oceanologia* 56, 241–258.
Pugh, D., Vassie, J., 1978. Extreme sea-levels from tide and surge probability. In: *Proceedings of the 16th Coastal Engineering Conference (Hamburg)*. ASCE, New York, vol. 1, pp. 911–930.
Pugh, D., Vassie, J., 1980. Applications of the joint probability method for extreme sea-level computations. *Proc. Inst. Civ. Eng.* 69, 959–975.
Raudsepp, U., Toompuu, A., Kõuts, T., 1999. A stochastic model for the sea level in the Estonian coastal area. *J. Mar. Syst.* 22, 69–87.

- Sallenger Jr, A.H., List, J.H., Gelfenbaum, G., Stumpf, R.P., Hansen, M., 1995. Large wave at Daytona Beach, Florida, explained as a squall-line surge. *J. Coast. Res.* 11, 1383–1388.
- Samuelsson, P., Jones, C.G., Willén, U., Ullerstig, A., Gollovik, S., Hansson, U., Jansson, C., Kjellström, E., Nikulin, G., Wyser, K., 2011. The Rossby Centre Regional Climate Model RCA3: model description and performance. *Tellus A* 63, 4–23.
- Seifert, T., Tauber, F., Kayser, B., 2001. A high resolution spherical grid topography of the Baltic Sea, revised edition. In: *Baltic Sea Science Congress*, 25–29 November 2001, Stockholm, Poster #147, (www.iowarnemuende.de/iowtopo_resampling.html).
- Sepp, M., 2009. Changes in frequency of Baltic Sea cyclones and their relationships with NAO and climate in Estonia. *Boreal Environ. Res.* 14, 143–151.
- Sepp, M., Post, P., Jaagus, J., 2005. Long-term changes in the frequency of cyclones and their trajectories in Central and Northern Europe. *Nord. Hydrol.* 36, 297–309.
- Soomere, T., Döös, K., Lehmann, A., Meier, H.E.M., Murawski, J., Myrberg, K., Stanev, E., 2014. The potential of current- and wind-driven transport for environmental management of the Baltic Sea. *Ambio* 43, 94–104.
- Stramska, M., 2013. Temporal variability of the Baltic Sea level based on satellite observations. *Estuar. Coast. Shelf Sci.* 133, 244–250.
- Suursaar, Ü., Sooäär, J., 2007. Decadal variations in mean and extreme sea level values along the Estonian coast of the Baltic Sea. *Tellus A* 59, 249–260.
- Suursaar, Ü., Jaagus, J., Kullas, T., 2006a. Past and future changes in sea level near the Estonian coast in relation to changes in wind climate. *Boreal Environ. Res.* 11, 123–142.
- Suursaar, Ü., Kullas, T., Otsmann, M., Saaremäe, I., Kuik, J., Merilain, M., 2006b. Cyclone Gudrun in January 2005 and modelling its hydrodynamic consequences in the Estonian coastal waters. *Boreal Environ. Res.* 11, 143–159.
- Suursaar, Ü., Jaagus, J., Tõnisson, H., 2015. How to quantify long-term changes in coastal sea storminess? *Estuar. Coast. Shelf Sci.* 156, 31–41. <http://dx.doi.org/10.1016/j.ecss.2014.08.2001>.
- von Storch, H., Zwiers, F.W., 1999. *Statistical Analysis in Climate Research*. Cambridge University Press, Cambridge, p. 484.
- Weisse, R., Bellafiore, D., Menéndez, M., Méndez, F., Nicholls, R.J., Umgiesser, G., Willems, P., 2014. Changing extreme sea levels along European coasts. *Coast. Eng.* 87, 4–14.
- Wilson, M., Meyers, S.D., Luther, M.E., 2014. Synoptic volumetric variations and flushing of the Tampa Bay estuary. *Clim. Dyn.* 42, 1587–1594.
- Wisniewski, B., Wolski, T., 2011. Physical aspects of extreme storm surges and falls on the Polish coast. *Oceanologia* 53 (1–II), 373–390.
- Wong, K.-C., Moses-Hall, J.E., 1998. On the relative importance of the remote and local wind effects to the subtidal variability in a coastal plain estuary. *J. Geophys. Res.–Oceans* 103 (C9), 18393–18404.

Paper V

Julge K., Eelsalu M., Grünthal E., Talvik S., Ellmann A., Soomere T., Tõnisson H. 2014. Combining airborne and terrestrial laser scanning to monitor coastal processes. 2014 IEEE/OES Baltic International Symposium “Measuring and Modelling of Multi-Scale Interactions in the Marine Environment”, May 26–29, 2014, Tallinn, Estonia. IEEE Conference Proceedings, 10 pp., doi: 10.1109/BALTIC.2014.6887874.

Combining Airborne and Terrestrial Laser Scanning to Monitor Coastal Processes

K. Julge¹, M. Eelsalu², E. Grünthal^{1,4}, S. Talvik¹, A. Ellmann¹, T. Soomere², H. Tõnisson³

¹ Department of Road Engineering, Tallinn University of Technology, Ehitajate tee 5, 19086 Tallinn, Estonia

² Institute of Cybernetics at Tallinn University of Technology, Akadeemia tee 21, 12618 Tallinn, Estonia

³ Institute of Ecology, Tallinn University, Uus-Sadama 5, 10120 Tallinn, Estonia

⁴ Estonian Land Board, Mustamäe tee 51, 10621 Tallinn, Estonia

Abstract—This study explores the potential of joint use of terrestrial (TLS) and airborne laser scanning (ALS) to quantify rapid and spatially inhomogeneous changes to the subaerial beach and to characterize the intensity of coastal processes. This remote sensing technology that uses scanning laser pulses for acquiring high-resolution three-dimensional surface of the measured object is applied to beach segment of the Pirita Beach (Tallinn Bay, the Baltic Sea). The extent and distribution of erosion and accumulation spots are analyzed by means of creating and comparing two digital terrain models of these areas from scanning point clouds obtained in different seasons. After elimination of systematic errors the ALS/TLS combination yields sub-decimeter accuracy for height determination of the beach. The analysis reveals not only the corresponding volume changes in the study area but also several features of internal dynamics of the beach across and along the waterline that are overlooked by classical monitoring methods. The benefits and shortcomings of combining the two laser scanning methods for monitoring coastal processes and the accuracy of the results are also discussed.

I. INTRODUCTION

The beaches of the Baltic Sea (Fig. 1) develop in relatively rare conditions of a large, relatively young and shallow, micro-tidal, seasonally ice-covered water body of extremely complicated shape [1]. Their key driving mechanism is a highly intermittent wave regime that is accompanied by aperiodic variations of the water level, seasonal ice cover [2], and frequent presence of conditions favorable for unexpectedly high run-up [3] and set-up [4]. The most interesting coastal segment in this respect is the southern coast of the Gulf of Finland where the beaches mostly overlie ancient dunes in deeply indented bays that are geometrically sheltered from a large part of the directions of strong winds. The volume of sediment and the magnitude of littoral drift are modest here and the entire coast in question generally suffers from sediment deficit [5],[6]. The beaches are to some extent stabilized by relatively rapid postglacial uplift (up to 2 mm/year) [7].

A specific feature of this coast is that the strongest storms tend to blow from directions from which winds are not very frequent [8]. Thus, differently from the classical examples of bay beaches [9], the bayhead beaches here are only partially sheltered from intense waves. This uplift combined with relatively low but intermittent hydrodynamic activity and limited supply of sand has led to a specific type of “almost equilibrium” beaches [10]. They often reveal step-like evolution: slow evolution is interspersed with rare but rapid

events that take place when high waves from an unusual direction occur simultaneously with high water levels before or after the ice season [11],[12].

A significant challenge in the understanding of the functioning of such beaches is to characterize and quantify the changes during the stages of their slow evolution. The key question is whether these beaches (or sections) gain or lose sediment in these stages. As the depth of mobilization of sediments frequently is fairly shallow and only a thin veneer of unconsolidated material may become mobile during these stages [9], the accuracy and spatial resolution of standard profiling of beaches is not sufficient to resolve the resulting changes, in particular, to recognize whether the middle parts of the beach show a healthy (concave) or problematic (convex) shape.

This contribution investigates the suitability of novel remote sensing methods like terrestrial (TLS) and airborne laser scanning (ALS) for monitoring coastal processes. ALS datasets are often used for different modelling and engineering



Figure 1. The Baltic Sea and the Gulf of Finland. The box indicates the study area in Tallinn Bay (see Fig. 2).

applications such as quantification of sediment volume transported by a major debris flow event [13] or assessments of riverbank erosion [14]. In particular, one of the well-known applications of ALS technique is forming Digital Elevation Models (DEM). The ALS equipment is mounted in an aircraft. The altitudes of surveying routes could reach up to a few kilometers, thus resulting in comparatively sparse data ($\sim 0.1\text{--}4$ points/m²). Repeated ALS measurements over the same area makes possible the creation of exact surface models for different time epochs and therefore enables the detection of inter-epoch volume and mass changes.

The laser scanning technique is capable of gathering accurate and high-resolution 3D data which covers the entire surface area of the beach. The advantage is that the entire area of interest can be included in the analysis while only changes along single profiles can be identified using classical methods of coastal monitoring. Thus, the ALS enables more accurate determination of the exact location and volumes of erosion and accumulation. In many countries nation-wide ALS campaigns have commenced, including Estonia [15]. Therefore ALS data of various vintages may already be accessible for regions of interest. Monitoring of coastal processes using ALS data has already been carried out, e.g. along the Baltic Sea shoreline by [16],[17].

This study attempts to widen the applicability and enhance the quality of standard ALS data products by using in situ TLS data for minimizing systematic errors between ALS and TLS datasets from different epochs. Combining TLS and ALS has been used, for example, to quantify the sediment volume transported by a major debris flow event in the Austrian Alps [13]. We explore the potential of the joint use of the TLS (mounted on a tripod) and ALS to quantify spatial changes to the subaerial beach. The goal is to characterize not only the overall intensity of coastal processes but also to shed light to the changes in the internal structure of the beach, in particular to identify whether the most representative parts of the beach gain or lose sediment.

We start from the description of the basic features of the ALS technique and the set-up of the terrestrial laser scanner. A case study is carried over a test area in Pirita Beach (Tallinn Bay, the Baltic Sea). The means of elimination of systematic and random errors of the ALS and TLS, creating and comparing of the resulting Digital Terrain Models (DTM) of test areas from scanning point clouds are discussed next. The main message is that the proposed technique is accurate enough to adequately recognize not only the overall volume changes but also to highlight local spots of accumulation and erosion and, most importantly, relatively small but systematic changes in the shapes of the coastal profiles.

II. LASER SCANNING

Laser scanning is a remote sensing method which utilizes laser pulses to measure distances to objects. Based on these distances and the angles of laser beams, the coordinates of measured points are calculated. This results in a 3D point

cloud of measured objects. The scanning device can be mounted on different platforms, i.e. a tripod (TLS), an aircraft (ALS) or a ground vehicle (mobile laser scanning).

1. Terrestrial laser scanning

TLS is used to acquire high-resolution accurate spatial data about objects such as buildings, bridges, statues, road surfaces or other structures. With TLS it is possible to gather data with an accuracy of about 1 cm or even better [18] and at a resolution up to a few mm. However, in order to save time and decrease the file sizes, the resolution is usually set at a few cm, depending also on the complexity of the measured object and the desired result.

Theoretically, TLS can be used for surveying surfaces within a 300 m range. However, in practice the maximum reasonable distance to a vertical surface is about 50–100 m and to a horizontal surface about 25–50 m, varying according to the specific scanner and the characteristics of the surface. A laser beam has a tendency to diverge, yielding the laser “foot-print” to increase in size the further it travels. Therefore, using shorter ranges enables acquiring finer details.

2. Airborne laser scanning

In ALS the scanning device is placed on an aircraft, e.g., plane, helicopter or unmanned aerial vehicle. ALS is cost-effective in applications where large areas need to be covered, for example measuring ground surfaces for compilation of terrain models, infrastructure objects, etc. Generally, an ALS point cloud is much less dense than a TLS point cloud. It usually varies from 0.1–20 points/m² depending on many factors. Acquiring more high-resolution data requires more time, flight hours and therefore more funds.

In order to determine the position and orientation of the aircraft at any instant, a Global Navigation Satellite System (GNSS) receiver and an Inertial Measurement Unit (IMU) are used. GNSS receiver records the position and IMU the pitch, roll and yaw of the aircraft. Since the calculation involves many parameters, the accuracy of ALS is less than that of TLS, and usually estimated at 2–15 cm in favorable conditions [15][19].

As ALS is generally performed at an altitude of up to 6000 m, the divergence of the laser beam is much more pronounced and the beam can reach up to a meter in diameter in ground surface. This means that capturing very fine details is impossible and measurement errors are more likely to occur. The possible errors are still negligible in many applications and the excellent cost/benefit ratio makes this technique highly attractive.

3. Combining ALS and TLS

Combining the results from different TLS and ALS campaigns raises some problems. First of all, in applications where the desired accuracy and data resolution are that of characteristic to TLS, ALS does not meet the expected demands. Also given the relatively large differences in spatial resolution, the methods for data processing have to be slightly altered. These differences are especially pronounced while

using automatic filtering, segmenting and modelling algorithms that require the use of different parameters depending on the point cloud density.

Additionally, combining different laser scanning methods and campaigns raises problems of accuracy. The main issue is how to ensure that the datasets are aligned to each other and determine whether systematic errors are present between them. Such errors can be due to ALS and TLS campaigns using different reference benchmarks. Usually TLS is performed using geodetic points on the ground while ALS uses data from GNSS systems and IMU to calculate the position and orientation.

Unifying point clouds from different campaigns could be accomplished by finding distinguishable points in both point clouds and moving one of the clouds to the correct location. Unfortunately, ALS data is usually not dense enough to accurately determine the coordinates of a particular point. Therefore, it is necessary to detect and quantify the systematic errors by other means.

The systematic error of elevation can be determined by using horizontal surfaces that are present in all point clouds. Such reference surfaces (e.g., a nearby parking lot at Pirita Beach, see below) need to be changeless during all the campaigns. By comparing the elevation differences between the same surface measured by TLS and ALS campaigns, the extent of the systematic error can be determined. Points near the edge of the surface should be discarded to minimize the errors caused by shifts in the (x, y) -plane and the large size of the ALS laser beam footprint on the ground. For example, a part of the ALS pulse might reflect from a curbstone instead of the pavement. The larger the reference surface area the better is the accuracy and reliability of linking of the ALS and TLS measurements.[20].

III. STUDY AREA

The test area of this study, Pirita Beach at the south-eastern bayhead of Tallinn Bay, Estonia, is a typical small, embayed beach of the southern coast of the Gulf of Finland (Fig. 2). This beach is one of the most popular recreational areas of the City of Tallinn, located next to the venue of the 1980 Olympic sailing regatta and hosting more than 3000 visitors daily on warm summer days. The beach is aligned between the northern mole of Pirita (Olympic) Harbor and a moraine scarp located about 400 m southwards from Merivälja jetty. The length of the sandy area is about 2 km and the dunes are relatively low: the maximum height of the scarp at the edge of the coastal forest is 1.5 m.

The stability of Pirita Beach has been discussed for several decades see [21],[22] and references therein). Prior to the mid-20th century, this beach was apparently stabilized by the postglacial uplift and natural sediment supplies but still suffered from a certain loss of sand [21]. Several attempts to refill the beach with material dredged from a neighboring harbor or transported from mainland quarries were undertaken in the 1970s. The entire subaerial beach from the waterline to



Figure 2. Location scheme of Pirita Beach in Tallinn Bay.

the scarp of the coastal forest was covered by an about 0.5 m thick sand layer. A total volume of 30 000 m³ with a typical grain size of 0.3 mm (which is considerably coarser than the native sand) was used to refill an about 1800 m long section. Additionally, finer sand was pumped to the southern (widest) section of the beach from the Pirita River mouth (see [23] and references therein). As the grain size of this sand volume was considerably smaller than the native sand, a large volume was probably relatively rapidly (in a few years) transported into deeper areas.

In recent decades, a gradual decrease of the beach width, recession of the scarp at the northern end of the beach, and extensive storm damage to the coastal forest have continued [22]. Although alterations of natural conditions such as an increase in storminess in the 1960s [24] may have caused increasing loads on Baltic beaches [11], a more probable reason for these changes at Pirita was the human intervention that has cut down the major natural sand supplies to the beach [10],[22]. For example, construction of Pirita Harbor substantially decreased the supply of river sand. The largest damage to the beach occurred in November 2001 and in January 2005 when high and long waves attacking the beach from northwest or west were accompanied with exceptionally high water level [22].

The recent status of the beach, a short overview of the local wave regime and the overall patterns of wave-induced sediment transport processes along the beach are presented in [22],[25]. The wave climate in the vicinity of the beach is relatively mild and the closure depth evaluated according to [26] is in the range of 2.4–2.6 m. The average net loss of sand from the entire beach was estimated to be in the range of 1000–1250 m³/yr in 1986–2006 based on the relocation of the waterline and the local uplift rate [27].

Southward transport dominates in the northern section of the beach whereas no prevailing transport direction exists in the southern sections. Consequently, different sections of the beach may have different level of erosion or accretion. Approximately 50% of Pirita Beach suffers from substantial

damage at times [25]. In the southern part, the width of the beach (up to 100 m, elevation up to 2 m above the mean water level) and the total sand volume has increased. This tendency is apparently long-term, since even the most violent storms in 2001 and 2005 have not affected the beach width in this relatively stable sector. The central part of the beach is in a near equilibrium state. The bluff at the back of the beach is at times eroded to some extent in strong storms but relatively intense aeolian sand transport into the dune forest [25] can be interpreted as an expression of an excess of sand and a generally healthy state of the beach.

Strong storms caused extensive regression of the bluff over an approximate 1 km long northern sector of the sandy beach in 1999–2005. The changes are marked northwards from the mouth of a small stream about 900 m to the north of Pirita Harbor (see its location in Fig. 4 below). The recession of the bluff was on average 1–2 m (at a few sections even 3–5 m) in 1999–2001. The most intense erosion occurred at the interface between the sandy and till coasts at the northern end of the beach.

Based on the described pattern of the alongshore sediment transport and erosion and deposition patterns, the central area of the beach in the vicinity of the above-mentioned stream mouth seems to be most sensitive with respect to changes in the hydrodynamic and meteorological forcing. Also, this area possibly has variable erosion and accumulation patterns and was selected as test region for this study.

IV. FIELD MEASUREMENTS AND DATA PROCESSING

The data set used in this study consists of both ALS and TLS data (Table I). The ALS data were gathered by the Estonian Land Board with a Leica ALS50-II airborne laser scanner. The Estonian Land Board also performed the ground filtering and classification of the measured points. In this

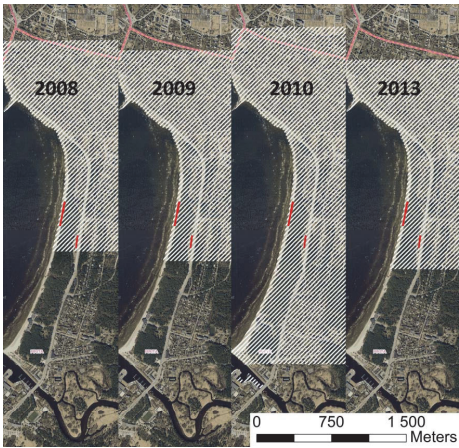


Figure 3. Flight corridors (hatch) of different ALS campaigns. Note a match between the location of the 2008, 2009 and 2013 flight corridors. The studied beach area and the parking lot used as a reference surface (Fig. 4) are marked in red.

analysis only the points classified as ‘ground’ were used. The test area is entirely located within a single flight corridor (Fig. 3), therefore the results are not affected by flight line matching errors.

TABLE I
AIRBORNE AND TERRESTRIAL SCANNING IN 2008–2013

Type of scanning	Day	Water level ^a , m	Flight height, m	Density of point cloud, points/m ²
ALS	6.05.2008	−0.18	2400	0.45
ALS	3.05.2009	−0.36	2400	0.45
ALS	4.06.2010	−0.04	3800	0.15
ALS	25.04.2013	−0.05 ^b	2400	0.45
TLS	18.12.2013	+0.35	-	2500

^a with respect to the long-term mean at Tallinn Harbor; ^b the same but measured at Pirita Harbor by the Estonian Environmental Agency, cf. Fig. 2.

The TLS survey was conducted with a pulse-based Leica ScanStation C10 with an average spatial resolution of ~2500 points/m² (2 × 2 cm). The beach survey was performed from six scanning stations (Fig. 4). For future surveys, nine reference points were established near the beach (Fig. 4) and coordinated by total station measurements from GNSS determined base lines (see Fig. 4). The heights of the points were determined with respect to a nearby located levelling benchmark.

To reduce systematic elevation differences between the

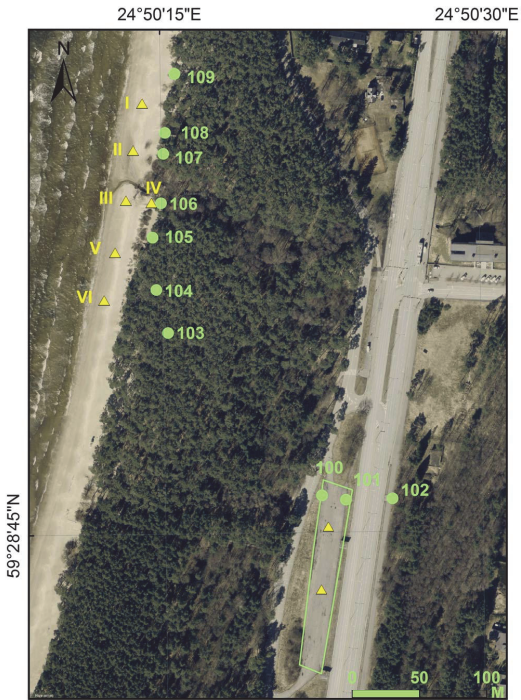


Figure 4. The reference points (numbered green circles) and TLS stations (yellow triangles). Reference points 100, 101, 102, 105 and 106 were measured with GNSS Reference point no. 106 also marks the beginning of a profile no. 3.

ALS and TLS data, we used the surface of a parking lot near the beach (Fig. 3) as a horizontal reference. This surface has been changeless (i.e. no repaving) since the first ALS flight in 2008. The reference surface was measured with TLS using reference points that were linked to points located at the beach.

All ALS surfaces were reduced to the TLS reference surface by applying elevation corrections (ΔH in Table II). Doing so improved the accuracy of the process of detection of deformations of the beach surface. These 1D corrections (ΔH) were derived from the average height differences of ground profiles of each ALS data-set from the TLS surface. The accuracy estimations are calculated from the TLS–ALS DEM differences for the reference parking lot. After elimination of the systematic errors the ALS/TLS combination yields sub-decimeter accuracy for height determination of the beach, cf. the last column in Table II.

TABLE II
HEIGHT CORRECTIONS APPLIED TO ALS DATA

Campaign	Elevation correction ΔH [m]	Average elevation difference from TLS measurements [m]	Standard deviation [m]
2008_ALS	0.036	0.030	0.024
2009_ALS	0.204	0.018	0.025
2010_ALS ^a	-0.176	-0.020	0.055
2013_ALS	0.010	0.004	0.022
2013_TLS	0	0	0

^a The 2010 ALS campaign was flown higher (cf. Table I) which affects the resolution and accuracy of the data.

The adjusted and aligned point clouds were used to form DTM's of the beach. Both raster based Digital Elevation Models and vector based Triangulated Irregular Network (TIN) models were used. The constructed DTMs were used to analyze and visualize the changes that had occurred through the years. The resulting DTMs constructed from ALS make it possible to highlight relatively long-term changes within 2008–2013 whereas a comparison of similar results from the ALS and TLS campaigns in 2013 allow for the identification of changes within one stormy season (this will be discussed elsewhere). Finally, the ALS data from different years enable us to recognize an interesting shift in the nature of changes to the beach around the year 2010.

V. LONG-TERM CHANGES

1. Single profiles

The study area is an about 250 m long strip in the central part of the beach (Fig. 5) where the earlier data and above discussion suggest a moderate loss of sand. This area contains one coastal profile (No. 3 in the relevant database) that is monitored regularly by the Geological Survey of Estonia in the framework of the national coastal monitoring programme [28]. Data for this profile, available for the years of 2003–2012 (Fig. 6), indicate the range of changes that can be identified using the classical methods of coastal monitoring. Although certain fluctuations occurred in the exact position of the beach surface and the zero-height line, none of these

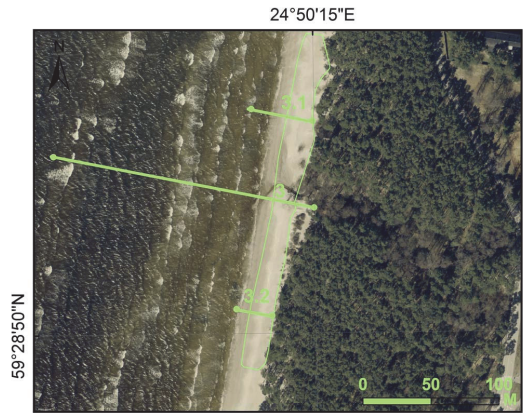


Figure 5. The study area in Pirita Beach and its cross-sections (profiles) used in Fig. 6 and 7. The profile in the centre of the test area matches profile No. 3 monitored by the Geological Survey of in the framework of the national coastal monitoring programme.

changes are systematic; in particular, and almost no changes to the sand volume of the dry beach have occurred during this decade. The data reveal much larger variations in the location and height of an underwater sand bar that seems to move onshore by about 4 m/yr.

To properly interpret the described data, it is important to note that this profile is located just next to the mouth of a small stream. Although this stream is evidently not capable of bringing substantial volumes of sand to the beach, even a small sediment supply may keep its immediate vicinity in an almost equilibrium on the background of a gradually eroding beach section. Also, the meandering of its mouth under bi-directional littoral flow [25] may to a certain extent affect the location of the waterline and the volume of sediment present exactly along the profile. However, making strong conclusions from the described behavior may not be justified.

The ALS and TLS data in 2008–2013 for this and neighbouring cross-sections located about 70 m to the south

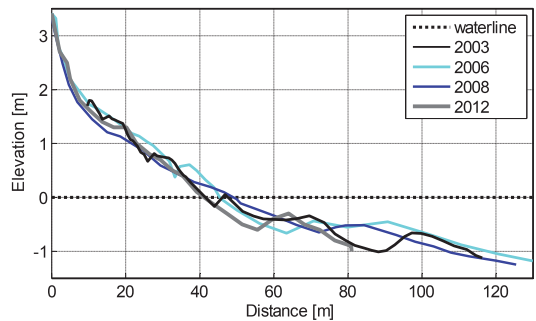


Figure 6. Beach profile No. 3 measured in 2003–2012. Data courtesy of the Geological Survey of Estonia.

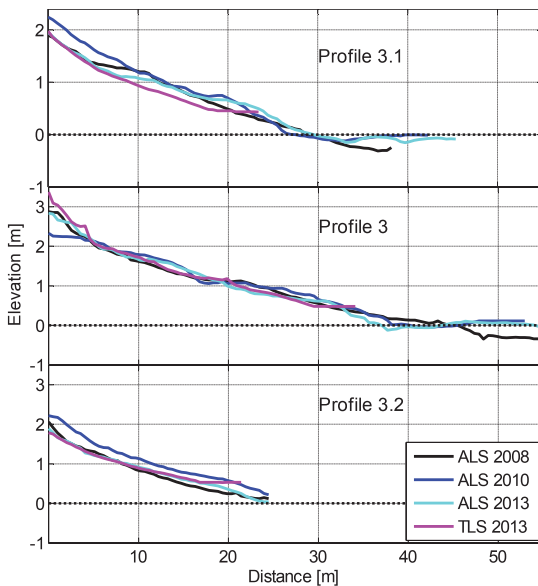


Figure 7. Beach profiles (see the location in Fig. 5) in 2008–2013 based on ALS and TLS data.

and about 60 m to the north of it (Fig. 5) add substantial information about the nature and course of the changes to the study area. Profile 3 in Fig. 7 matches the one routinely used in the national coastal monitoring programme [28] and portrayed in Fig. 6. The data at a distance of 0–10 m from the starting points of each profile are affected by the particular flying line and height of the plane carrying the ALS device. As the flying height in the ALS scan in 2010 (3800 m) was considerably higher than in the other years (2400 m), the relevant density of the point cloud was lower in 2010 and the scarp is evidently not properly reflected in the data. Therefore, the data at the beginning of the profiles (at a distance of 0–10 m in Fig. 7) are, at best, indicative. The end of the scanned profile depends on the instantaneous location of the waterline that may vary by 10–20 m depending on the water level during the scan.

Not surprisingly, the variation of the height of the beach surface along profile 3 measured by conventional means (Fig. 6) and using the ALS and TLS techniques (Fig. 7) largely coincide from the distance of 10–40 m from the beginning of the profile (reference point 106 in Fig. 4). This match *inter alia* once more confirms the reliability of the TLS and ALS data for changes to the subaerial beach.

The overall original shape of the beach in 2008 was moderately convex signaling a relatively healthy situation. The entire beach has undergone no substantial changes as noted also above. The volume of sand has increased at the waterline. The above discussion suggests that this may reflect either arriving of the underwater sand bar or local changes in the sediment volume caused by the small stream.

The ALS and TLS data for the other two profiles (3.1 and 3.2 in Fig. 5 and Fig. 7), however, indicate that substantial changes have occurred in the study area since 2008. These changes have clear structure along both profiles. As mentioned above, the changes at the distance of 0–10 m from their beginning may not be particularly reliable but still a certain loss of sand from the northern segment of the study areas characterized by this section of profile 3.1 is likely. Further down to the waterline, at a distance of 10–25 m from the beginning, the beach has kept its shape in 2008–2013 but has considerably lost sand in 2013. Its height has decreased by about 30 cm, which means the loss approximately 3 m^3 per meter of the coastline during this year. Although a part of this difference may stem from inexact match of the ALS and TLS data, it is likely that this section of the beach had negative sand budget in 2013. This loss has been only partially compensated by an accumulation in the vicinity of waterline (25–30 m from the beginning). Similarly to profile 3, considerable volume of sand has accumulated in shallow water to the offshore of the waterline. This match of accumulation with the one for profile 3 and with Fig. 6 suggests that a sand bar is gradually moving into the study area.

The evolution of the beach height along profile 3.2 suggests that changes to the southern segment of the study area were quite different from the above-described course. This profile demonstrates rapid changes along its entire subaerial length. The beach rapidly gained sand (about $5\text{--}6 \text{ m}^3$ per meter of coastline) in 2008–2010. This material was almost totally eroded in 2010–2013. A minor accumulating section in the TLS data in the immediate vicinity of the waterline may reflect the arrival of a sand bar (see the discussion above) but it may equally well reflect local and temporary wave-driven changes in the swash zone. The match of TLS and ALS for 2013 along this profile suggests that the differences between these data sets along profile 3.1 reflect changes to the beach and are not caused by uncertainties of the methods.

2. Spatial changes

As we are interested in the capacity of the ALS and TLS techniques to highlight and identify changes to beaches, we concentrate on the largest changes that occurred between the different measurement campaigns presented in Table I.

A comparison of the beach surface for 2008 and 2010 (both measured using the ALS technique) first demonstrates a rich spatial structure of changes superposed by substantial differences between the segments to the north and south of the stream mouth (Fig. 8). The entire study area gained sand with a total volume of about $500 \text{ m}^3/\text{yr}$ (Table III). Given the total scanned area of about 4500 m^2 , the used technique is thus capable of clearly identifying average changes on the order of a few cm. Erosion was observed only in a few spots (about 5% of the area; mostly around the mouth of the small stream; see the right panel of Fig. 8) that lost a few tens of m^3/yr altogether (less than 10% of the accumulation). Most likely, the related decrease in the height of the beach surface reflects

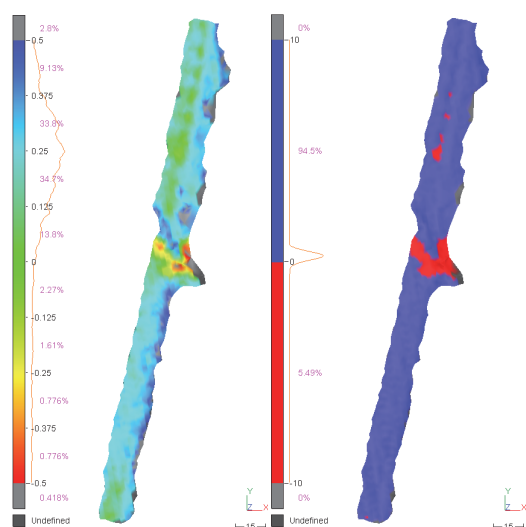


Figure 8. (left) Changes to the beach height from ALS in 2008 to 2010. The scale shows the extent of the differences (m) and the percentage of the scanned surface with a change rate within an interval of such rates; (right): the relevant erosion (red) and accumulation (blue) areas.

smoothing or relocation of local, small, temporary morphological features.

There were, however, considerable differences in the pattern of accumulation across the study area. The accumulation of sand was relatively rapid and homogeneous along and across the entire southern segment. The height of the beach typically increased by 20–30 cm (cf. profile 3.2 in Fig. 7). The accumulation in the northern segment, however, mostly occurred in the landward part of the beach. It is thus likely that most of the accumulation here was driven by aeolian transport. As mentioned above, a few areas of decrease in the height of the beach in the central part of the segment apparently reflect local smoothing of the beach surface.

Spatial changes in the beach height according to the above-discussed ALS survey in 2010 and a TLS survey in December 2013 (Fig. 9) revealed almost a totally opposite pattern. The entire study area lost sand. Only a small vicinity of the stream (8% of the entire surface) gained some sand. The total loss of sand over three years (2010–2013) was almost equal to the total gain in 2008–2010 (Table III). The amount of lost sand per meter of coastline was almost constant along the study area. Differently from the years 2008–2010, the changes to the beach height were distributed unevenly along the beach cross-section. The loss was largest in the landward part of the cross-section in the vicinity of the coastal scarp and somewhat smaller in the vicinity of the waterline. Although the ALS data may have relatively large uncertainty in the immediate vicinity of the coastal scarp near the forest, it is still likely that the loss of beach height was unevenly distributed across the beach.

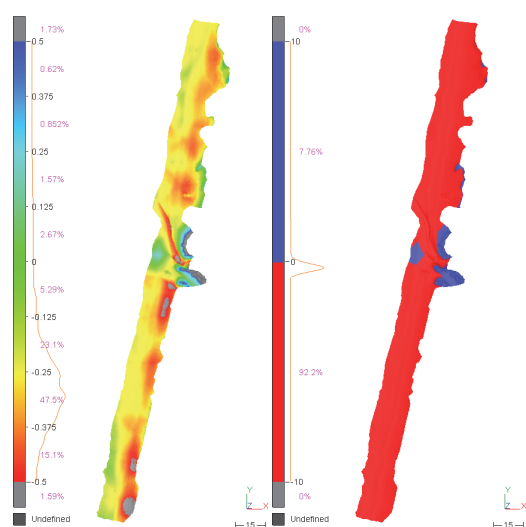


Figure 9. (left) Changes to the beach height from ALS in 2010 to TLS in 2013 (the scale shows the extent of the differences and the percentage falling between an interval); (right): the relevant erosion (red) and accumulation (blue) areas.

The described radical difference of the sign and spatial pattern of changes within the two discussed time intervals suggests that the properties of driving forces were likely quite different in these intervals. In terms of visually observed wave heights, the years 2009–2010 were relatively mild and the year 2011 relatively stormy. The annual mean for these years at Ventspils and Liepaja was by about 20% lower and for 2011 by about 10% larger than the long-term average [29],[30]. It is therefore likely that in 2008–2010 relatively mild wave conditions with a comparatively large proportion of swells (generated by typical south-westerly storms in the open Baltic Sea and the western Gulf of Finland) dominated the coastal processes in Pirita Beach and were favourable for recovery of the beach.

The stormy seasons of autumn and winter 2011/2012 were different. The autumn was stormy and the ice period started later than usual. Several strong wave storms affected not only the open Baltic Sea [31] but also the Gulf of Finland [32]. The autumn and winter of 2012/2013 were also comparatively stormy. For example, in November 2012 the all-time highest single wave in the Gulf of Finland was recorded near Helsinki in a storm that repeated the all-time highest significant wave height in this bay [29]. Although the latter storm blew from the east, it is likely that Pirita Beach was frequently impacted by severe and destructive wave conditions in 2010–2013.

This conjecture is supported by the spatial structure of measured changes. This structure is characteristic to severe wave conditions superposed with high local water level. In such situations waves erode unprotected sediment relatively far from the coastline (here in the vicinity of the coastal scarp). As the Baltic Sea storms are usually short, this

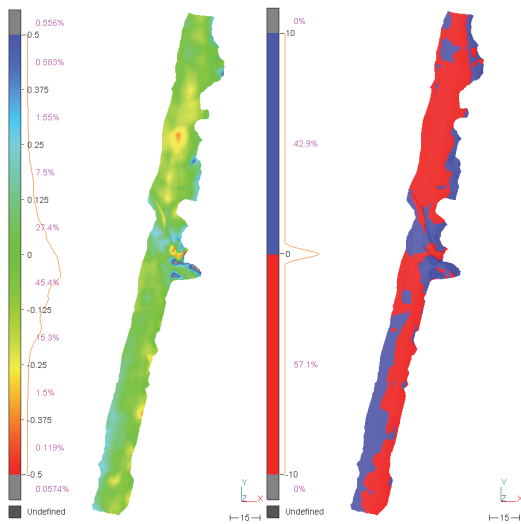


Figure 10. (left) Changes to the beach height from ALS in 2008 to TLS in 2013 (the scale shows the extent of the differences and the percentage falling between an interval); (right): the relevant erosion (red) and accumulation (blue) areas.

material is relocated to a relatively small distance along the coast and usually is deposited within the equilibrium beach profile for the particular storm and water level [33]. For the typical water levels and wave heights in storms that directly impact Pirita Beach [22][25], this means deposition mostly at depths from the waterline corresponding to the mean water level down to a depth of about 0.5 m. This material is often brought back to the seaward section of the subaerial beach by regular swells within a short period of time.

Based on the presented material and discussion, it is not unexpected that the changes to the study area during the five years 2008 (ALS)–December 2013 (TLS) are fairly minor (Table III) and have a variable spatial pattern (Fig. 10). The proportions of the eroding and accumulation regions are almost equal. The largest accumulation rates are in the vicinity of the mouth of the small stream but these apparently do not characterise properly the processes in other parts of the study area. These few small patches of accumulation around the stream are evidently connected with a relocation of the stream and filling the stream bed with sand from adjacent locations.

TABLE III
CHANGES IN THE SAND VOLUME IN THE 4567 M² TEST AREA

Interval	Accumulation [m ³]	Erosion [m ³]	Budget [m ³]
2008ALS–2009ALS	486	29	457
2009ALS–2010ALS	588	38	550
2008ALS–2010ALS	1046	38	1008
2008ALS–2013TLS	167	232	–65
2009ALS–2013TLS	63	653	–590
2010ALS–2013TLS	55	1164	–1109
2013ALS–2013TLS	139	258	119

An increase in the amount of sand is, however, noticeable in the vicinity of the waterline in the southernmost section of the experiment area while most of the northern part of the beach has lost sand. The local changes to the beach height are predominantly (73%) less than ± 12.5 cm. Only in a few locations in the middle of the northern segment has the beach lost almost 50 cm of height. As discussed above, areas of loss likely characterize local changes and are not representative of overall coastal processes.

The overall pattern of changes in the almost six years covered by the laser scanning data coincides with the common understanding of the nature of coastal processes and sand movement at Pirita Beach. As alongshore transport in the northern section of the beach is almost unidirectionally to the south [25] and sand sources in the north are quite limited, it is expected that the northern sections of the beach suffer more severely from sediment deficit and are more prone to erosion than the southern sections. Consistent with this conjecture, Fig. 10 reveals that in the northern segment of the test area the beach has mostly lost sand (predominantly from the central part of the strip, between the waterline and the scarp) while in the southern segment the losses are fairly minor and have occurred from the area relatively remote from the waterline and close to the scarp. This difference is also exemplified in profiles (Fig. 7).

VI. CONCLUSIONS AND DISCUSSION

The presented material suggests that the technology of repeated airborne and terrestrial laser scanning is accurate and reliable enough to recognize the internal structure of changes to the beach. Additional to the variations of the overall course of erosion and accumulation, the method in use is able to highlight changes in the beach profiles, local regions of accumulation and erosion and reveal relatively small changes in the shapes of the coastal profiles, and in this way better characterize the nature of the changes and to provide crucial information about whether the beach is losing sand or recovering.

The described major difference of the sign and spatial pattern of changes in 2008–2010 and 2010–2013 also vividly demonstrates one of the major shortcomings of classical coastal monitoring activities. As they largely rely on the observed changes along a few profiles, the credibility of the outcome crucially depends on the proper choice of the profiles. The presented material demonstrates that the beach height along profile No. 3 is governed by local processes, first of all by the impact of the small stream in the vicinity. Not only is this profile evidently able to replicate any essential changes to the adjacent segments of beach but in the discussed time intervals behaves almost oppositely to the real course of changes to the beach. The major advantage of both airborne and terrestrial laser scanning techniques is their ability to recognise a 'big picture' of the evolution of longer beach

sections and to avoid deceptive conclusions based on strongly localised data sets.

This feature suggests that the earlier estimates, both based on in situ observations [23] and on quite coarse modelling efforts [22] have led to valid conclusions about the spatial variations in the evolution of different parts of the beach. The numerical estimates in [22],[23], however, may reflect the intensity of sand loss in years when severe wave conditions directly impact Piritä Beach. As most of future climate projections suggest an increase in storminess and decrease in the length of the ice season, these estimates are evidently valid approximations of reality.

ACKNOWLEDGMENT

This study was a part of the projects ERMAS AR12052 and TERIKVANT, supported by the European Union (European Regional Development Fund, ERDF) and managed by the Estonian Research Council in the framework of the Environmental Technology R&D Programme KESTA. The ALS data used in this study was received from the Estonian Land Board under the license contract ST-A1-2422, 22/06/2012. The used Leica ScanStation C10 and licensed data processing software were acquired within frame of the Estonian Research Infrastructures Roadmap object Estonian Environmental Observatory (funding source 3.2.0304.11-0395, project No. AR12019). The research was partially supported by the targeted financing of the Estonian Ministry of Education and Research (grant SF0140007s11), by the Estonian Science Foundation (grant No. 9125) and through support of the ERDF to the Centre of Excellence in Non-linear Studies CENS.

REFERENCES

- [1] J. Harff, S. Björck, and P. Hoth, Eds., *The Baltic Sea Basin*, Central and Eastern European Development Studies. Heidelberg Dordrecht London New York: Springer, 2011, 449 pp.
- [2] M. Leppäranta and K. Myrberg, *The physical oceanography of the Baltic Sea*. Berlin Heidelberg: Springer, 2009.
- [3] I. Didenkulova, E. Pelinovsky, and T. Soomere, "Long surface wave dynamics along a convex bottom," *J. Geophys. Res.-Oceans*, vol. 114, art. No. C07006, 2009.
- [4] T. Soomere, K. Pindsoo, S.R. Bishop, A. Käär, and A. Valdmann, "Mapping wave set-up near a complex geometric urban coastline," *Nat. Hazards Earth Syst. Sci.*, vol. 13, pp. 3049-3061, 2013.
- [5] K. Orviku, *Estonian coasts*. Tallinn, 1974, 112 pp. [in Russian].
- [6] K. Orviku and O. Granö, "Contemporary coasts," in *Geology of the Gulf of Finland*, A. Raukas and H. Hyvärinen, Eds. Tallinn: Valgus, 1992, pp. 219-238 [in Russian].
- [7] T. Kall, T. Oja, and K. Tänavsuu, "Postglacial land uplift in Estonia based on four precise levelings," *Tectonophysics*, vol. 610, pp. 25-38, 2014.
- [8] T. Soomere and S. Keevallik, "Directional and extreme wind properties in the Gulf of Finland," *Proc. Estonian Acad. Sci. Eng.*, vol. 9, pp. 73-90, 2003.
- [9] K. F. Nordstrom, "Bay beaches," in *Encyclopedia of Coastal Science*, M. L. Schwartz, Ed. Dordrecht, The Netherlands: Springer, 2005, pp. 129-130.
- [10] T. Soomere and T. Healy, "On the dynamics of "almost equilibrium" beaches in semi-sheltered bays along the southern coast of the Gulf of Finland," in *The Baltic Sea Basin*, J. Harff, S. Björck, and P. Hoth, Eds. Central and Eastern European Development Studies, Part 5, Heidelberg Dordrecht London New York: Springer, 2011, pp. 255-279.
- [11] K. Orviku, J. Jaagus, A. Kont, U. Ratas, and R. Rivis, "Increasing activity of coastal processes associated with climate change in Estonia," *J. Coast. Res.*, vol. 19, pp. 364-375, 2003.
- [12] D. Ryabchuk, A. Kolesov, B. Chubarenko, M. Spiridonov, D. Kurennoy, and T. Soomere, "Coastal erosion processes in the eastern Gulf of Finland and their links with geological and hydrometeorological factors," *Boreal Environ. Res.*, vol. 16 (Suppl. A), 117-137, 2011.
- [13] D. P. Thoma, S.C. Gupta, M.E. Bauer, and C. Kirchoff, "Airborne laser scanning for riverbank erosion assessment," in *Remote Sensing of Environment*, vol. 95, pp. 493-501, 2005.
- [14] M. Bremer, O. Sass, "Combining airborne and terrestrial laser scanning for quantifying erosion and deposition by a debris flow event," *Geomorphology*, vol. 138, pp. 49-60, 2012.
- [15] A. Gruno, A. Liibus, A. Ellmann, T. Oja, A. Vain, and H. Jürgenson, "Determining sea surface heights using small footprint airborne laser scanning," in *Remote Sensing of the Ocean, Sea Ice, Coastal Waters, and Large Water Regions 2013 (Conference 8888)*, Dresden, Germany, 2013, C. Bostater, S. Mertikas, and X. Neyt, Eds. SPIE - International Society For Optical Engineering, 2013, pp. 88880R-1-88880R-13.
- [16] M. Viška, "Coastal erosion analysis using LiDAR data and field measurements in Zvejniekiems beach, east coast of the Gulf of Riga," in *5th International Student Conference [on] Biodiversity and Functioning of Aquatic Ecosystems in the Baltic Sea Region: Conference Proceedings*, October 6-8, 2010, Palanga, Lithuania, Klaipėda, 2010.
- [17] E. Grünthal, A. Gruno, and A. Ellmann, "Monitoring of coastal processes by using airborne laser scanning data," in *Proceedings Cygas, D. (Ed): Selected papers of the 9th International Conference on Environmental Engineering*, Vilnius, Lithuania, 22-23, May, 2014. Vilnius: Vilnius Gediminas Technical University Press, "Technika" (in press).
- [18] P. Dorninger, B. Szekely, A. Zamolyi, and A. Roncat, "Automated Detection and Interpretation of Geomorphic Features in LiDAR Point Clouds," *Vermessung & GeoInformation*, vol. 2, pp. 60-69, 2011.
- [19] E.J. Huising and L.M. Gomes Pereira, "Errors and accuracy estimates of laser data acquired by various laser scanning systems for topographic applications," *ISPRS Journal of Photogrammetry and Remote Sensing*, vol. 53, No. 5, pp. 245-261, 2004.
- [20] K. Julge and A. Ellmann, "Combining Airborne and Terrestrial Laser Scanning technologies for measuring complex structures," in *Selected papers of the 9th International Conference on Environmental Engineering*, Vilnius, Lithuania, 22-23, May, 2014. D. Cygas, Ed. Vilnius: Vilnius Gediminas Technical University Press "Technika" (in press).
- [21] K. Orviku, "Seashore needs better protection," in *Year-book of the Estonian Geographical Society*, vol. 35, pp. 111-129, 2005, [In Estonian, with English summary].
- [22] T. Soomere, A. Kask, J. Kask, and R. Nerman, "Transport and distribution of bottom sediments at Piritä Beach," *Estonian J. Earth Sci.*, vol. 56, pp. 233-254, 2007.
- [23] K. Orviku, and M. Veisson, "Lithodynamical investigations on the most important resort areas of Estonia and in the area of the Olympic Yachting Centre in Tallinn. Research report. Tallinn, Institute of Geology, 1979, 105 pp. [In Russian].
- [24] H. Alexandersson, T. Schmith, K. Iden, and H. Tuomenvirta, "Long-term variations of the storm climate over NW Europe," *Global Atmos. Ocean Syst.*, vol. 6, pp. 97-120, 1998.
- [25] T. Soomere, A. Kask, J. Kask, and T. Healy, "Modelling of wave climate and sediment transport patterns at a tideless embayed beach, Piritä Beach, Estonia," *J. Marine Syst.*, vol. 74, Suppl., pp. S133-S146, 2008.
- [26] W. A. Birkemeier, "Field data on seaward limit of profile change," *J. Waterw. Port Coastal Ocean Eng.* - ASCE, vol. 111, pp. 598-602, 1985.
- [27] A. Kask, T. Soomere, T. Healy, and N. Delpêche, "Sediment transport patterns and rapid estimates of net loss of sediments for "almost equilibrium" beaches," *J. Coast. Res.*, Special Issue 56, pp. 971-975, 2009.
- [28] S. Suuroja, A. Talpas, and K. Suuroja. 2004. *Mererannikute seire*. Report on activities on the subprogram "Monitoring of sea coasts of the state environmental monitoring in 2003. Part II: graphical attachments]. Manuscript, Estonian Geological Survey, Tallinn [in Estonian]; see also http://seire.keskkonnainfo.ee/index.php?option=com_content&view=article&id=2096&Itemid=409

- [29] I. Zaitseva-Pärnaste, *Wave climate and its decadal changes in the Baltic Sea derived from visual observations*. PhD thesis. Tallinn University of Technology, 173 pp., 2013.
- [30] B. Hünicke, T. Soomere, K.S Madsen, M. Johansson, Ü. Suursaar, and E. Zorita, Sea level and wind waves. Chapter 3.4.3 in The BACC Author Team. *Assessment of climate change for the Baltic Sea basin*. Springer, 2014, in press.
- [31] H. Tõnisson, Ü. Suursaar, R. Ravis, A. Kont, and K. Orviku, "Observation and analysis of coastal changes in the West Estonian Archipelago caused by storm Ulli (Emil) in January 2012," *J. Coast. Res.*, Special Issue 65, pp. 832-837, 2013.
- [32] H. Tõnisson, Ü. Suursaar, S. Suuroja, D. Ryabchuk, K. Orviku, A. Kont, Y. Sergeev, and R. Ravis, "Changes on coasts of western Estonia and Russian Gulf of Finland, caused by extreme storm Berit in November 2011," in *IEEE/OES Baltic 2012 International Symposium : May 8-11, 2012, Klaipeda, Lithuania, Proceedings: IEEE*, 2012, 1-7.
- [33] R.G. Dean and R.A. Dalrymple, *Coastal Processes with Engineering Applications*. Cambridge: Cambridge University Press, 2002.

Paper VI

Eelsalu M., Soomere T., Julge K. 2015. Quantification of changes in the beach volume by the application of an inverse of the Bruun Rule and laser scanning technology. *Proceedings of the Estonian Academy of Sciences*, 64(3), 240–248, doi: 10.3176/proc.2015.3.06.



Quantification of changes in the beach volume by the application of an inverse of the Bruun Rule and laser scanning technology

Maris Eelsalu^{a,*}, Tarmo Soomere^{a,b}, and Kalev Julge^c

^a Institute of Cybernetics at Tallinn University of Technology, Akadeemia tee 21, 12618 Tallinn, Estonia

^b Estonian Academy of Sciences, Kohtu 6, 10130 Tallinn, Estonia

^c Chair of Geodesy, Faculty of Civil Engineering, Tallinn University of Technology, Ehitajate tee 5, 19086 Tallinn, Estonia

Received 3 February 2015, accepted 25 April 2015, available online 20 August 2015

Abstract. We address the possibilities of combining terrestrial (TLS) and airborne laser scanning (ALS) techniques with the classical concept of equilibrium beach profile to quantify the changes in the total sand volume of slowly evolving sandy beaches. The changes in the subaerial beach are determined from a succession of ALS surveys that were reduced to the same absolute height using a TLS survey of a large horizontal surface of constant elevation. The changes in the underwater sand volume from the waterline down to the closure depth are evaluated using an inverse of the Bruun Rule. The relocation of the waterline is extracted from the ALS scanning of elevation isolines of 0.4–0.7 m. The method is applied to an about 200 m long test area in the central part of Pirita Beach (Tallinn Bay, north-eastern Baltic Sea). The sand volume in this area exhibits extensive interannual variations. The annual gain of sand in the entire beach was about 2000 m³/y in 2008–2010 and the annual loss was about 1100 m³/y in 2010–2014. The changes in the underwater part of the beach are by a factor of 2–2.5 larger than the changes in the subaerial part.

Key words: equilibrium beach profile, coastal processes, Bruun Rule, laser scanning, Pirita Beach.

1. INTRODUCTION

The nature and appearance of beaches of the Baltic Sea (Fig. 1) reflect several specific features of this large, relatively young and shallow water body of extremely complicated shape [21]. The conditions governing their evolution vary substantially depending on the location of the beach and particularly on the exposure of the beach to predominant wind directions [22]. The most important driver shaping the beaches here is the wind wave field. Its impact is at times amplified by large variations in the water level [21]. While the impact of tides is negligible in the interior of the Baltic Sea, seasonal ice cover may considerably modify the hydrodynamic activity in the northern parts of the sea over the course of a year.

Small sandy beaches on the southern coast of the Gulf of Finland form an interesting pool of seashores [13]. Much of the shoreline here is locally relatively

straight but follows the geometry of deeply indented bays cut into the limestone cliff [22]. Although many of these beaches overlie ancient dunes, the volume of the contemporary marine sand and the magnitude of the littoral drift are usually very modest [22,24]. The sea-shore is to some extent stabilized by the postglacial uplift (up to 2 mm/y) [18]. Most of these beaches suffer from sediment deficit [22,24] and are vulnerable to strong storms from certain directions.

Wave conditions in the Baltic Sea are highly variable with short but intense storms [15]. This feature is even more evident for the beaches in question. Although the entire southern coast of the Gulf of Finland is geometrically sheltered from one predominant direction of storms (south-west), large waves may approach from directions from which winds are not very frequent [30]. The described features have led to the development of ‘almost equilibrium’ beaches [29]. Their overall slow evolution is occasionally modified by rapid events when high waves approach from an unusual direction. If such waves are accompanied by a

* Corresponding author, maris.eelsalu@ioc.ee

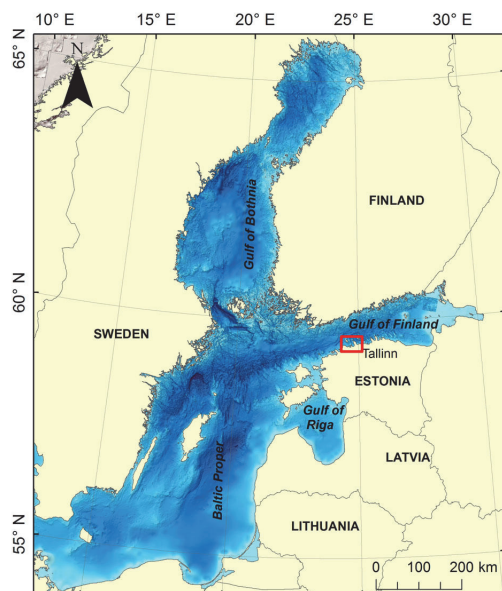


Fig. 1. The Baltic Sea and the Gulf of Finland. The box indicates the study area in Tallinn Bay in Fig. 2.

high water level and there is no protecting ice cover, substantial volumes of sand may be cut from the (fore)dunes relatively far from the usual waterline and distributed into the shallow nearshore [26,28].

The changes in sedimentary beaches are commonly evaluated using measurements of the beach or seabed height over a small number of selected profiles during a long time interval. The direction of sediment motion is added based on various morphological and geological features [7]. This approach is valid for long and mostly homogeneous (along the coastline) beaches. It may, however, easily overlook certain features of the evolution of relatively small beaches along which the impact of waves is not necessarily homogeneous and long-term changes are often masked by short-term variability of morphological elements or temporary shifts of the waterline. The situation is particularly complicated when local sources (e.g. river flow or erosion of single spots) contribute to the sediment budget. The quantification of the resulting volume changes over the subaerial beach requires high-resolution measurement techniques.

The morphology of the nearshore is usually more regular along the shoreline than the appearance of the dry beach. Waves generally smooth out seabed features on scales from ripples to sand bars. Strong storms tend to support a relatively homogeneous, often universal underwater beach profile down to the closure depth. Its idealized appearance is called the (Dean's) equilibrium beach profile (EBP) [6]. Its parameters basically depend

on the sediment texture (those that define the slope of the profile) and properties of the highest waves (those that define the closure depth, or equivalently, how deep the profile extends). The use of the concept of EBP makes it possible to roughly estimate the changes in the sediment volume in the nearshore based on a few parameters of sediment, wave climate, and relocation of the waterline [20]. This approach is particularly suitable for almost equilibrium beaches such as Pirita Beach [32] in Tallinn Bay or Valgerand Beach in Pärnu Bay [19] where only minor changes occur in the position of the waterline.

We address the possibilities of combining medium-range remote sensing methods such as terrestrial (TLS) and airborne laser scanning (ALS) [3] with the concept of the EBP to quantify the changes in the total sand volume of a typical almost equilibrium beach. High-resolution laser scanning data are used to build a sequence of Digital Terrain Models (DTM; in essence exact surface models of the study object or area) for different time instants (called epochs in the ALS literature) [17] and to detect inter-epoch volume changes. Depending on the altitudes of survey routes (often up to a few kilometres), the resulting spatial resolution ($\sim 0.1\text{--}4$ points/m²) is usually sufficient to adequately evaluate volume changes of sandy beaches [10,37].

The basic advantage of the ALS technique in coastal research is its ability to almost instantaneously gather accurate and high-resolution data over the entire surface of the beach [9,10,37]. Its limited spatial resolution compared to extremely high-resolution measurements over small areas can be complemented by the combined use of ALS and TLS data sets [16,17], which makes it possible to quantify the pattern of spatial changes in the subaerial beach.

In this paper we explore the potential of the laser scanning technique to quantify the total changes in the sand volume of an almost equilibrium beach during its slow evolution phase. The most significant limitation of this technique is that it normally does not recognize the underwater changes. This shortage can be to some extent circumvented using the concept of EBP and the Bruun Rule [4]. The basic idea is to evaluate the changes in the sand volume over the EBP using basic properties of the EBP, an inversion of the Bruun Rule [20], and the relocation of the waterline extracted from laser scanning data.

2. STUDY AREA

The test area – a section of Pirita Beach – is located on the southern coast of the Gulf of Finland at the south-eastern bayhead of Tallinn Bay. It is a typical small, embayed beach at the bayhead of a haven that extends deeply into the mainland of Estonia (Fig. 2). The sandy

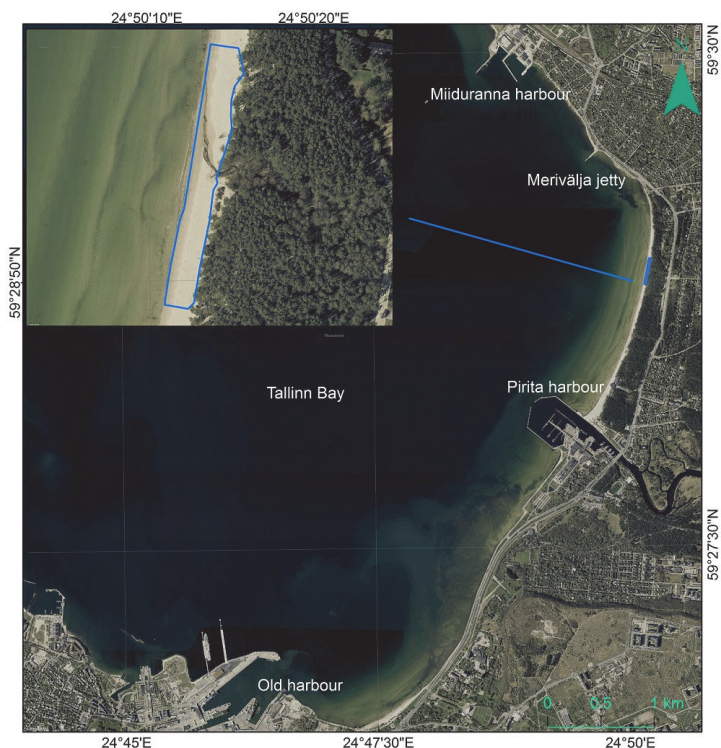


Fig. 2. The study area in Tallinn Bay.

beach with a total length of about 2 km stretches from the northern mole of Pirita (Olympic) Harbour until a moraine scarp located about 400 m southwards from Merivälja jetty. As is typical for beaches on the southern coast of the Gulf of Finland, the volume of the contemporary marine sand is quite limited, active foredunes are missing, and ancient dunes dominate the landscape inland. The overall intensity of coastal processes is low and the maximum height of the erosion scarp at the edge of the coastal forest is 1.5 m [31].

The coastal processes and the past and future of Pirita Beach have been the subject of discussions for decades [23,25,31]. The seashore is to some extent stabilized by the postglacial uplift (2.5 mm/y [18]) and by sediment supplies of the past. The stability of the beach is today threatened by a considerable decrease in the relative uplift rate and by the reduction of the natural sediment supplies [31]. The largest impact comes from the construction of Pirita Harbour, which has led to a substantial decrease in the supply of river sand to the beach.

Although the wave climate in the interior of Tallinn Bay is relatively mild and the closure depth along Pirita Beach is 2.4–2.6 m [33], single storms from unfavour-

able directions may cause severe destruction of the beach. The consequences of such storms in the 1970s have been mitigated by beach nourishment [23,25,31]. An increase in storminess in the second half of the 20th century [1] may have already overridden the stability of the eastern Baltic Sea beaches [26] and has caused severe sediment deficit on some beaches. Indeed, a gradual decrease in the beach width and recession of the coastal dune forest have continued in recent decades [17,31]. Approximately 50% of Pirita Beach, mostly its central and northern sections, suffers from damage at times [32]. The most significant damage to Pirita Beach in the recent past occurred in November 2001 and in January 2005 when high waves were accompanied with an exceptionally high water level [31].

The beach apparently lost, on average, 1000–1250 m³ of sand per year between 1986 and 2006 [20,32]. Its most vulnerable part is an approximately 1 km long northern section where an extensive regression of the bluff occurred between 1999 and 2005. The recession was up to 3–5 m in a few sections from 1999 to 2001 [17]. The most stable section is in the south where the width of the beach is up to 100 m and the sandy strip reaches an elevation up to 2 m above the

mean water level. The central part of the beach is in an almost equilibrium state.

The northern part of the beach has an almost unidirectional sand transport to the south whereas the transport direction is highly variable along other sections of the beach. The central area of the beach, selected as the test region for this study, is apparently the most sensitive with respect to changes in the hydrodynamic forcing and sediment supplies. Recent research has demonstrated that this area is extremely variable (both in time and space) with respect to erosion and accumulation [17]. The reader is referred to [31,32] for a detailed overview of the recent status of the beach, the local wave regime, and the properties of wave-induced sediment transport processes along the beach.

3. METHODS

3.1. Laser scanning techniques

Laser scanning technology has been suggested as an accurate and reliable method to quantify the coastal processes [9,10,37] and to evaluate the location of the shoreline [34]. The largest problem in using the ALS technique for the evaluation of sand volume is how to accurately determine and eliminate the systematic elevation errors between data sets measured from an aircraft in different surveys [9,17]. A combination of the TLS and ALS data sets makes it possible to remove the relevant bias, to reduce all the measured data sets to the one reference surface, and to accurately establish the absolute height of the sand surface in different scans [8,14]. Together with enhanced temporal resolution, this step is essential for an accurate evaluation of sand volume changes and for recognizing the internal structure of changes in the subaerial beach [17].

The elevation data of Pirita Beach from 2008 to 2013 were retrieved from the database of ALS measurements performed and pre-processed by the Estonian Land Board. Only points classified as ‘ground’ were used in this study. These ALS data sets, measured from an altitude of 2400 m and with an average density of 0.45 points/m², were complemented with TLS data with a much higher resolution of about 2 cm × 2 cm [17] gathered in 2013 and 2014.

All ALS surfaces were reduced to the reference surface using corrections derived from the exact elevation of a large car park near Pirita Beach. This area was measured using the TLS technology in December 2013 [17] and linked to the measurements at the beach. The resulting DTMs were suitable for estimating the changes in the absolute height of the beach and sediment volume along the beach. For technical details the reader is referred to [17]. During the TLS survey in 2013 the water level was relatively high (+0.4 m compared with the long-term mean). As the swash zone

covered a significant part of the subaerial beach, this data set was not suitable for estimations of shoreline changes. Another TLS survey was performed in late spring 2014 when the water level was relatively low (−0.2 m).

3.2. Bruun Rule

As the laser scanning technology is not able to measure the location of the seabed, a first approximation of the changes in the sand volume in the underwater part of a beach was obtained using the theory of the EBP [6]. An extension (inversion) of the Bruun Rule makes it possible to evaluate these changes from the associated shift $\Delta y(x)$ of the shoreline and closure depth $h^*(x)$. The change in the volume ΔV_Σ over the EBP can be expressed as [20]:

$$\Delta V_\Sigma = \int h^*(x) \Delta y(x) dx. \quad (1)$$

Here the x -axis is directed alongshore and the y -axis is perpendicular to the shoreline. In general, both closure depth and the shift of the waterline may vary along the shoreline. As the closure depth along the entire Pirita Beach varies insignificantly (2.4–2.6 m [2]), it can be considered as constant $h^*(x) = h^*$ in the short test area (Fig. 2). In this case the change in the sediment volume over the EBP is equal to the product of the closure depth and the total change of the dry land area. This approach ignores the sand volumes transported to deeper areas from the seaward end of the EBP and the relocation of sand in the immediate vicinity of the waterline. For small relocations of the waterline on gently sloping sandy beaches these amounts are usually minor compared to the total changes in the sand volume.

For simplicity we employ the most widely used shape of the EBP that corresponds to the uniform wave energy dissipation per unit water volume in the surf zone [7]. The water depth at the distance y from the waterline down to the closure depth is $h(y) = Ay^{2/3}$. The profile scale factor A (which depends on the predominant grain size) is immaterial for the quantification of volume changes in Eq. (1).

The Bruun Rule is valid for virtually any realistic coastal profile of sandy beaches where the overall cross-section is approximately linear. The existing observations and simulations [17,20,31,32] suggest that both the concept of EBP and the inversion of the Bruun Rule are applicable for Pirita Beach. Regular monitoring of beach profiles between 2003 and 2012 by the Geological Survey of Estonia [35] indicates that the height of underwater sandbars is modest (around 30 cm). Although the sandbars seem to move onshore by about 4 m/y [17], their presence introduces minor deviations of the real profiles from the EBP.

The implementation of Eq. (1) requires the knowledge of two parameters. The change in the waterline position can be estimated based on repeated ALS or TLS scanings as demonstrated below. Another key parameter is the closure depth h^* . Similarly to the EBP, it is a concept rather than a simply measurable quantity [2]. It is defined as the maximum depth at which the breaking waves effectively adjust the whole profile [11,12]. This definition suggests that the closure depth is a function of the wave climate and to some extent also of sediment texture. It is usually assumed that the closure depth is governed by the most severe wave conditions that persist for a reasonable time. In our context the conservative viewpoint is to use the values of closure depth from [33], which are evaluated on an annual basis [12]:

$$h^* = 1.75H_{s\,0.137\%} - 57.9 \frac{H_{s\,0.137\%}^2}{gT_s^2}, \quad (2)$$

where $H_{s\,0.137\%}$ is the significant wave height that is exceeded during 12 h/y (with a probability of 0.137%), T_s is the dominant peak period in such wave conditions, and g is acceleration due to gravity.

4. INTERANNUAL VARIABILITY OF THE SUBAERIAL BEACH

To demonstrate the capacity of the ALS and TLS techniques to quantify changes in the test area, we present a brief insight into the largest changes that occurred in 2008–2014. The rich spatial structure of the

sand accumulation between 2008 and 2010 (erosion was observed only in a few spots) was superposed by substantial differences between the northern and southern segments of the test area (Fig. 3a). The entire subaerial beach gained about 500 m³ of sand per year [17]. The height of the beach typically increased by 20–30 cm.

The changes had an almost totally opposite pattern between the ALS survey in 2010 and the TLS survey in May 2014 (Fig. 3b). The subaerial beach mostly lost sand in an amount almost equal to the total gain in 2008–2010. The changes in the beach height were distributed unevenly. The described features are coherent with the changing pattern of storms in 2008–2013 [17]. It is likely that in the period from 2008 to 2010 relatively mild wave conditions with a comparatively large proportion of swells, favourable for the recovery of the beach, dominated the coastal processes [17]. The autumn and winter of 2011/2012 and 2012/2013 were comparatively stormy [36] and Pirita Beach was frequently impacted by severe wave conditions.

These differences in wave properties are consistent with the spatial structure of the measured changes [17]. The overall pattern of changes matches the common ‘cut-and-fill’ cycle of sandy beaches. Under severe wave conditions and high water levels waves erode unprotected sediment from the upper part of the beach. As waves approach Pirita Beach almost incidentally, the eroded material is mostly deposited within the EBP [7]. This material is brought back into the vicinity of the waterline either by the onshore motion of sandbars or by regular swells. It is thus not surprising that the resulting

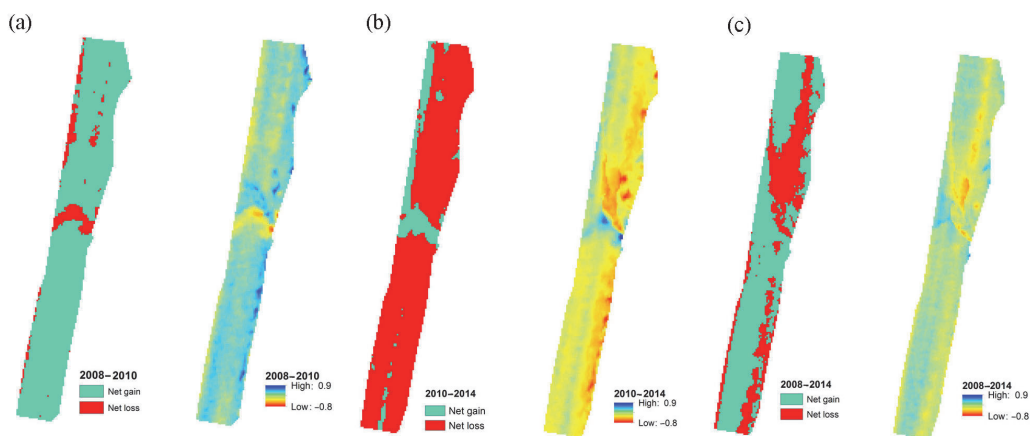


Fig. 3. Changes in the beach height: (a) in 2008–2010, (b) 2010–2014, (c) 2008–2014. The scale shows the differences in the beach height (m, right) and the relevant erosion (red) and accumulation (blue) areas.

changes in the sand volume of the subaerial beach during the six years from spring 2008 to spring 2014 were fairly minor (Fig. 3c). The only exception is the vicinity of the mouth of a small stream [17] where the changes are evidently connected with its relocation and are not representative of the processes in other parts of the study area.

The described technique is thus capable of highlighting fairly small changes (of the order of a few centimetres) in the sand surface height. The changes in the beach height in 2008–2014 are predominantly less than ± 12.5 cm (Fig. 3c). Consistently with the overall pattern of wave-driven sediment transport to the south in Pirita Beach [32], a certain amount of sand has been accumulated near the waterline in the southern part of the test area while almost the entire northern part of the beach has lost sand.

5. CHANGES IN THE UNDERWATER SAND VOLUME

Equation (1) suggests that the change in the underwater sediment volume over the EBP is, as a first approximation, proportional to the gain or loss of the dry beach area [20]. The shape of the beach in the vicinity of the waterline and the location of the waterline itself may be subject to rapid and essentially random variations (e.g. when a sandbar reaches the shoreline or when extensive cusps are formed) and thus are not always representative of the changes in the underwater sand volume. The appearance of a beach between the landward end of the swash zone and foredunes is often much more homogeneous. For this reason the position of the waterline is evaluated based on the shift of isolines of 0.3 m, 0.4 m, 0.5 m, 0.6 m, and 0.7 m on the dry beach (Table 1). These elevations are often impacted by waves during autumn storms and their relocation apparently follows the shift of the waterline.

Part of the estimates for the elevation heights of 0.3 m substantially deviates from the rest of the estimates, signalling that processes at this elevation may be considerably modified by local or short-term features such as the ‘beaching’ of a sandbar. The use of several

isolines allows uncertainty associated with the results to be reasonably evaluated. The relevant estimates for the elevation heights of 0.5 m and 0.6 m almost coincide (Fig. 4) and are highly coherent for all isolines of 0.4–0.7 m. Below we use the average of the relocation of these four isolines to represent the shift of the waterline. The largest deviation of the area change based on a single elevation from this average is 10% in 2008–2010 and 80% in 2010–2014.

The dry beach area therefore increased in the period from 2008 to 2010 and decreased to a lesser extent between 2010 and 2014. Consistent with the above analysis, the increase in the beach width is more pronounced (up to 7 m) in the southern part than in the northern part (up to 5 m) of the test area. The imbalance between the increase in 2008–2010 and the decrease in 2010–2014 (~25% of the entire pool of changes, Table 2) characterizes the uncertainty of the entire approach. Part of the widening of the beach is evidently connected with the decrease in the relative sea level owing to the postglacial uplift. This process apparently contributes about 1.5 m to the dry beach width [32], or equivalently, about 350 m² to the total dry beach area in 2008–2014.

Changes in the sand volume over the EBP (Table 2) are evaluated using Eq. (1), the average change in the dry beach area (Table 1), and the average closure depth $h^* = 2.5$ m for the study area [33]. Similarly to the subaerial beach, the underwater part of the beach also gained sand between 2008 and 2010 and lost sand between 2010 and 2014. The amount of sand gained and lost within these time intervals is almost equal (± 4000 m³). The relative uncertainty of the estimates (the imbalance of volumes for 2008–2010, 2010–2014, and 2008–2014) is obviously the same (about 25%) as for the changes of the dry beach area.

Interestingly, changes in the underwater sand volume are substantially (by a factor of up to 2.5) larger than over the dry beach. The annual gain of sand in the entire (subaerial and underwater) beach in the period from 2008 to 2010 is relatively rapid, about 2000 m³/y. The annual loss in the period from 2010 to 2014 is less intense, about 1100 m³/y. As these estimates are for only a short section of Pirita Beach, they are not directly

Table 1. Changes in the subaerial beach area (m²) based on the shift in the height isolines in 2008–2014

Time interval	Elevation height, m					
	0.3	0.4	0.5	0.6	0.7	Average for 0.4–0.7
	Surface change, m ²					
Spring 2008 to spring 2010	1055	1207	1259	1227	995	1172
Spring 2010 to spring 2014	–170	–698	–1020	–1041	–733	–873
Spring 2008 to spring 2014	840	749	513	509	551	581



Fig. 4. Changes in the position of the waterline (0.5 m and 0.6 m isolines) from 2008 to 2010.

Table 2. Changes in the sand volume (m^3) over the subaerial beach and down to the closure depth in the test area in 2008–2014

Time interval	Subaerial beach	Underwater profile	Total
Spring 2008 to spring 2010	1514	2930	4444
Spring 2010 to spring 2014	–1188	–2183	–3371
Spring 2008 to spring 2014	302	1453	1755

comparable with earlier estimates of sand deficit over the entire beach [32]. As the changes in question are much larger than similar changes for the subaerial beach, the uncertainty of the entire estimate mostly depends on the accuracy of the evaluation of the sand budget over the EBP.

6. DISCUSSION AND CONCLUSIONS

The presented results support the conjecture that it is possible to highlight quite subtle changes in the absolute height and appearance of slowly evolving sandy beaches by means of combining various laser scanning technologies [17]. We have further expanded the scope of the use of laser scanning techniques beyond its

classical limitations – towards the evaluation of the changes in the sand volume in the underwater part of the beach. The progress is achieved by means of the evaluation of the relocation of the waterline from the shift of a selection of isolines of the elevation of the sandy beach and the subsequent application of the theory of EBP and an inverse of the Bruun Rule. The major advantage of this approach is a small amount of data required for the analyses. To a first approximation, the changes in the underwater sediment volume can be estimated using a quantity derived from the local wave climate and changes in the position of the waterline.

The established synchronization of changes over the EBP and the subaerial beach is an unexpected feature of the test area. The conventional beach theory suggests that erosion on the upper profile (i.e. over the subaerial beach or from its upper part) during a stormy period is commonly accompanied by accumulation of sediment on the lower profile (e.g. in deeper sections of the EBP). This phase of the common cut-and-fill process is reversed during milder wave conditions, which bring sediment back from the deeper sections of the EBP to the shore and from where winds move it further to the upper beach. It is, though, unlikely that sand was added to the entire system in 2008–2010 and then removed in 2010–2014 because the seabed deepens relatively rapidly offshore from the closure depth and temporary deposition of large sand volumes in this part of the nearshore is not likely. It is more likely that, owing to the common large approach angles of storm waves in the Baltic Sea basin, sand was moved back and forth over the entire Pirita Beach. This conjecture is implicitly supported by the large variability in the simulated alongshore sand transport direction along this beach [32].

The results indicate that changes in the underwater part of the beach, from the waterline to the closure depth (about 2.5 m for the test area at Pirita Beach), are much larger (by a factor of 2–2.5) than similar changes in the subaerial part of the beach. Although this feature may reflect the small amount of the contemporary marine sand in the subaerial part of the study area, it suggests that underwater processes in the nearshore may predominate the evolution and fate of almost equilibrium beaches of the north-eastern Baltic Sea. Moreover, this proportion raises a serious question about the credibility of the estimates of the total changes in Table 2. In essence, the presented approach combines an extremely accurate way of measuring changes in the subaerial beach with a very coarse, almost conceptual application of the Bruun Rule and the equilibrium profile, both of which have been quite critically reviewed in the literature [5,27]. As the results based on the basically conceptually modelled data dominate the final outcome and there is no verification from another method, the quantitative outcome should be interpreted with care.

The variation in the course of coastal processes (intense accumulation in several years and almost equally intense erosion during several subsequent years) demonstrates that a comprehensive understanding of the functioning of beaches in this region requires long-term (at least on decadal scales) observations and simulations. The possibility of severe damages to beaches during extreme storms and changes in the duration of the ice season add complexity to the system and considerably reduce its predictability. Another source of uncertainties of the entire procedure stems from the nature of the concept of the EBP. This time-averaged property is applied here at relatively short (annual and intra-annual) scales at which the real profile may considerably deviate from the long-term average.

Even though the presented approach relies on the idealized concepts of the EBP and closure depth, the discussed results suggest that it may provide a feasible option for an inexpensive monitoring of almost equilibrium beaches over longer time intervals and for recognition of major changes that may impact the functioning of the entire beach system.

The concept implicitly relies on the separation of processes over the EBP and in deeper areas of the nearshore. Therefore, strictly speaking, it is directly applicable only in coastal segments where the EBP is clearly evident and the seabed rapidly deepens starting from the closure depth (as is the case in the deeper part of Pirita Beach [31]). We are looking forward to the validation of the outcome of this approach, for example in locations where the natural alongshore sediment transport has been blocked by a recent large coastal engineering structure.

ACKNOWLEDGEMENTS

The research was supported by the institutional financing of the Estonian Ministry of Education and Research (grant IUT33-3), by the Estonian Science Foundation (grant No. 9125), and through support of the European Regional Development Fund (ERDF) to the Centre of Excellence in Non-linear Studies CENS. The ALS data were received from the Estonian Land Board under the license contract ST-A1-2422, 22/06/2012. The used Leica ScanStation C10 and licensed data processing software were acquired within the frame of the Estonian Research Infrastructures Roadmap object Estonian Environmental Observatory (project No. AR12019).

REFERENCES

1. Alexandersson, H., Schmith, T., Iden, K., and Tuomenvirta, H. Long-term variations of the storm climate over NW Europe. *Global Atmos. Ocean Syst.*, 1998, **6**, 97–120.
2. Birkemeier, W. A. Field data on seaward limit of profile change. *J. Waterw. Port Coast. Ocean Eng.-ASCE*, 1985, **111**, 598–602.
3. Bremer, M. and Sass, O. Combining airborne and terrestrial laser scanning for quantifying erosion and deposition by a debris flow event. *Geomorphology*, 2010, **138**, 49–60.
4. Bruun, P. Sea level rise as a cause of erosion. *J. Waterway. Harbors Coastal Eng. Div. ASCE*, 1962, **88**, 117–133.
5. Cooper, J. A. G. and Pilkey, O. H. Sea-level rise and shoreline retreat: time to abandon the Bruun Rule. *Global Planet. Change*, 2004, **43**, 157–171.
6. Dean, R. G. Equilibrium beach profiles: characteristics and applications. *J. Coastal Res.*, 1991, **7**, 53–84.
7. Dean, R. G. and Dalrymple, R. A. *Coastal Processes with Engineering Applications*. Cambridge University Press, 2002.
8. Dorninger, P., Szekely, B., Zamolyi, A., and Roncat, A. Automated detection and interpretation of geomorphic features in LiDAR point clouds. *Vermessung & Geo-information*, 2011, **2**, 60–69.
9. Gruno, A., Liibus, A., Ellmann, A., Oja, T., Vain, A., and Jürgenson, H. Determining sea surface heights using small footprint airborne laser scanning. In *Remote Sensing of the Ocean, Sea Ice, Coastal Waters, and Large Water Regions 2013 (Conference 8888)*, Dresden, Germany, 2013 (Bostater, C., Mertikas, S., and Neyt, X., eds). SPIE, 2013, 88880R-1–88880R-13.
10. Grünthal, E., Gruno, A., and Ellmann, A. Monitoring of coastal processes by using airborne laser scanning data. In *Selected Papers of the 9th International Conference on Environmental Engineering, Vilnius, Lithuania, 22–23, May, 2014* (Cygas, D., ed.). Vilnius Gediminas Technical University Press “Technika”, Vilnius, 2014, 1–7.
11. Hallermeier, R. J. Uses for a calculated limit depth to beach erosion. In *Proceedings of the 16th International Conference on Coastal Engineering*. ASCE, Hamburg, 1978, 1493–1512.
12. Hallermeier, R. J. A profile zonation for seasonal sand beaches from wave climate. *Coast. Eng.*, 1981, **4**, 253–277.
13. Harff, J., Björck, S., and Hoth, P. (eds). *The Baltic Sea Basin*. Central and Eastern European Development Studies. Springer, Heidelberg, 2011.
14. Huising, E. J. and Gomes Pereira, L. M. Errors and accuracy estimates of laser data acquired by various laser scanning systems for topographic applications. *ISPRS J. Photogramm.*, 2004, **53**, 245–261.
15. Hünicke, B., Zorita, E., Soomere, T., Madsen, K. S., Johansson, M., and Suursaar, Ü. Recent change – sea level and wind waves. In *Assessment of Climate Change for the Baltic Sea Basin*. (The BACC Author Team). Regional Climate Studies. Springer, 2015, 155–185.
16. Julge, K. and Ellmann, A. Combining airborne and terrestrial laser scanning technologies for measuring complex structures. In *Selected Papers of the 9th International Conference on Environmental Engineering, Vilnius, Lithuania, 22–23, May, 2014* (Cygas, D., ed.). Vilnius Gediminas Technical University Press “Technika”, Vilnius, CD.
17. Julge, K., Eelsalu, M., Grünthal, E., Talvik, S., Ellmann, A., Soomere, T., and Tõnisson, H. Combining airborne and

- terrestrial laser scanning to monitor coastal processes. In *The 6th IEEE/OES Baltic Symposium 'Measuring and Modeling of Multi-Scale Interactions in the Marine Environment', May 26–29, Tallinn, Estonia*. IEEE Conference Publications, 2014, 1–9.
18. Kall, T., Oja, T., and Tänavsuu, K. Postglacial land uplift in Estonia based on four precise levelings. *Tectonophysics*, 2014, **610**, 25–38.
 19. Kartau, K., Soomere, T., and Tõnisson, H. Quantification of sediment loss from semi-sheltered beaches: a case study for Valgerand Beach, Pärnu Bay, the Baltic Sea. *J. Coastal Res.*, 2011, SI 64, 100–104.
 20. Kask, A., Soomere, T., Healy, T. R., and Delpeche, N. Rapid estimates of sediment loss for “almost equilibrium” beaches. *J. Coastal Res.*, 2009, SI 56, 971–975.
 21. Leppäranta, M. and Myrberg, K. *The Physical Oceanography of the Baltic Sea*. Springer, Berlin, 2009.
 22. Orviku, K. *Estonian Coasts*. Tallinn, 1974 [in Russian].
 23. Orviku, K. Seashore needs better protection. In *Year-Book of the Estonian Geographical Society*, 2005, **35**, 111–129 [in Estonian, with English summary].
 24. Orviku, K. and Granö, O. Contemporary coasts. In *Geology of the Gulf of Finland* (Raukas, A. and Hyvärinen, H., eds). Valgus, Tallinn, 1992, 219–238 [in Russian].
 25. Orviku, K. and Veisson, M. Lithodynamical investigations on the most important resort areas of Estonia and in the area of the Olympic Yachting Centre in Tallinn. Research report. Institute of Geology, Tallinn, 1979 [in Russian].
 26. Orviku, K., Jaagus, J., Kont, A., Ratas, U., and Ravis, R. Increasing activity of coastal processes associated with climate change in Estonia. *J. Coastal Res.*, 2003, **19**, 364–375.
 27. Pilkey, O., Young, R., and Cooper, A. Quantitative modeling of coastal processes: A boom or a bust for society? In *GSA Special Papers*, 2013, **502**, 135–144.
 28. Ryabchuk, D., Kolesov, A., Chubarenko, B., Spiridonov, M., Kurennoy, D., and Soomere, T. Coastal erosion processes in the eastern Gulf of Finland and their links with geological and hydrometeorological factors. *Boreal Environ. Res.*, 2011, **16**(Suppl. A), 117–137.
 29. Soomere, T. and Healy, T. On the dynamics of “almost equilibrium” beaches in semi-sheltered bays along the southern coast of the Gulf of Finland. In *The Baltic Sea Basin* (Harff, J., Björck, S., and Hoth, P., eds). Central and Eastern European Development Studies, Part 5. Springer, Heidelberg, 2011, 255–279.
 30. Soomere, T. and Keevallik, S. Directional and extreme wind properties in the Gulf of Finland. *Proc. Estonian Acad. Sci., Eng.*, 2003, **9**, 73–90.
 31. Soomere, T., Kask, A., Kask, J., and Nerman, R. Transport and distribution of bottom sediments at Pirita Beach. *Estonian J. Earth Sci.*, 2007, **56**, 233–254.
 32. Soomere, T., Kask, A., Kask, J., and Healy, T. Modelling of wave climate and sediment transport patterns at a tideless embayed beach, Pirita Beach, Estonia. *J. Marine Syst.*, 2008, **74**(Suppl.), S133–S146.
 33. Soomere, T., Viška, M., and Eelsalu, M. Spatial variations of wave loads and closure depth along the eastern Baltic Sea coast. *Estonian J. Eng.*, 2013, **19**, 93–109.
 34. Stockdon, H. F., Sallenger, A. H., Jr., List, J. H., and Holman, R. A. 2002. Estimation of shoreline position and change using airborne topographic lidar data. *J. Coastal Res.*, **18**, 502–513.
 35. Suuroja, S., Talpas, A., and Suuroja, K. Mererannikute seire. Report on activities on the subprogram “Monitoring of sea coasts of the state environmental monitoring in 2003. Part II: graphical attachments. Manuscript, Estonian Geological Survey, Tallinn, 2004 [in Estonian]. See also http://seire.keskkonnainfo.ee/index.php?option=com_content&view=article&id=2096&Itemid=409
 36. Tõnisson, H., Suursaar, Ü., Suuroja, S., Ryabchuk, D., Orviku, K., Kont, A., et al. Changes on coasts of western Estonia and Russian Gulf of Finland, caused by extreme storm Berit in November 2011. In *IEEE/OES Baltic 2012 International Symposium: May 8–11, 2012, Klaipeda, Lithuania, Proceedings*. IEEE, 2012, 1–7.
 37. Viška, M. Coastal erosion analysis using LiDAR data and field measurements in Zvejniekiems beach, east coast of the Gulf of Riga. In *5th International Student Conference [on] Biodiversity and Functioning of Aquatic Ecosystems in the Baltic Sea Region: October 6–8, 2010, Palanga, Lithuania, Klaipeda, Conference Proceedings*. 2010, 109–110.

Laserskaneerimise ja Bruuni pöördreegli kombineerimine rannaliiva mahu muutuste hindamiseks

Maris Eelsalu, Tarmo Soomere ja Kalev Julge

Liiva koguhulga muutusi aeglaselt arenevate randade veetalusel rannanõlval ja liivarannal hinnatakse erinevatel aegadel läbi viidud maapealse ning aerolaserskaneerimise andmetike kombineerimise kaudu klassikalise tasakaalulise profiili teooriaga. Muutused ajaveelal ja eelluidete piirkonnas tuvastatakse kord aastas tehtud aerolaserskaneerimise andmetikest, mis taandatakse samale absoluutkõrgusele muutumatu kõrgusega pinnal (parkimisplatsil) maapealse seadmega sooritatud täppismõõdistuste abil. Liiva mahu muutused veetalusel rannanõlval veepiirist kuni sulgemissügavuseni arvutatakse Bruuni pöördreegli alusel. Arvutuste aluseks on veepiiri nihkumine, mis leitakse erinevate aastate aerolaserskaneerimise andmetest 0,4–0,7 m samakõrgusjoonte ümberpaiknemise kaudu. Meetod on rakendatud ligikaudu 200 m pikkusele lõigule Pirita rannas. Liiva hulk testalal varieerub ulatuslikult aastate lõikes. Aastail 2008–2010 lisandus testalale ligikaudu 2000 m³ liiva aastas, samas vähenes seal liiva maht aastail 2010–2014 ligikaudu 1100 m³ võrra igaal aastal. Muutused veetalusel rannanõlval olid kuival rannaosal asetleidnud muutustest ligikaudu 2–2,5 korda suuremad.

Curriculum Vitae

Personal data

Name	Maris Eelsalu
Date and place of birth	20.10.1988, Virtsu, Estonia
Address	Akadeemia tee 21, 12618 Tallinn

Contact data

Phone	(+372) 559 333 09
E-mail	Maris.Eelsalu@taltech.ee

Education

Educational institution	Graduation year	Education (field of study / degree)
Tallinn University of Technology	2013	Earth Sciences / Master's Degree
Estonian Maritime Academy	2011	Hydrography / Applied higher education

Language competence/skills

Language	Level
Estonian	Native language
English	Fluent
Spanish	Basic skills

Special courses and further training

Period	Educational or other organisation
February 2016	Course <i>Process modelling of natural hazards</i> (Enschede, Netherlands)
August–September 2015	Visit to James Cook University in Australia, courses <i>Coastal and Catchment Geomorphology</i> and <i>Coastal management</i> (Townsville, Australia)
November 2014	Intense course <i>Wave dynamics and coastal processes</i> (Klaipėda, Lithuania)
November 2013	LIDAR data visualisation (Tallinn, Estonia)
September 2011	<i>Practical training course in Marine Science in Estonia and Finland</i> (Seili, Finland)

Professional employment

Period	Organisation	Position
Sept 2013–to date	Tallinn University of Technology, Institute / Department of Cybernetics	Early stage researcher
April 2012–Sept 2013	Tallinn University of Technology, Institute of Cybernetics	Technician

Research activity

Articles indexed by the Web of Science database (1.1):

Soomere T., **Eelsalu M.**, Pindsoo K. 2018. Variations in parameters of extreme value distributions of water level along the eastern Baltic Sea coast. *Estuarine, Coastal and Shelf Science*, 215, 59–68, doi:10.1016/j.ecss.2018.10.010.

Kovaleva O., **Eelsalu M.**, Soomere T. 2017. Hot-spots of large wave energy resources in relatively sheltered sections of the Baltic Sea coast. *Renewable and Sustainable Energy Reviews*, 74, 424–437, doi:10.1016/j.rser.2017.02.033.

Soomere T., Männikus R., Pindsoo K., Kudryavtseva N., **Eelsalu M.** 2017. Modification of closure depths by synchronisation of severe seas and high water levels. *Geo-Marine Letters*, 37(1), 35–46, doi:10.1007/s00367-016-0471-5.

Eelsalu M., Soomere T., Julge K. 2015. Quantification of changes in the beach volume by the application of an inverse of the Bruun Rule and laser scanning technology. *Proceedings of the Estonian Academy of Sciences*, 64(3), 240–248, doi: 10.3176/proc.2015.3.06.

Soomere T., **Eelsalu M.**, Kurkin A., Rybin A. 2015. Separation of the Baltic Sea water level into daily and multi-weekly components. *Continental Shelf Research*, 103, 23–32, doi: 10.1016/j.csr.2015.04.018.

Eelsalu M., Soomere T., Pindsoo K., Lagemaa P. 2014. Ensemble approach for projections of return periods of extreme water levels in Estonian waters. *Continental Shelf Research*, 91, 201–210, doi: 10.1016/j.csr.2014.09.012.

Tõnisson H., Suursaar Ü., Kont A., Orviku K., Rivis R., Szava-Kovats R., Vilumaa K., Aarna T., **Eelsalu M.**, Pindsoo K., Palginõmm V., Ratas U. 2014. Field experiments with different fractions of painted sediments to study material transport in three coastal sites in Estonia. *Journal of Coastal Research*, Special Issue 70, 229–234, doi: 10.2112/SI70-039.1.

Soomere T., **Eelsalu M.** 2014. On the wave energy potential along the eastern Baltic Sea coast. *Renewable Energy*, 71, 221–233, doi: 10.1016/j.renene.2014.05.025.

Soomere T., Viška M., **Eelsalu M.** 2013. Spatial variations of wave loads and closure depths along the coast of the eastern Baltic Sea. *Estonian Journal of Engineering*, 19(2), 93–109, doi: 10.3176/eng.2013.2.01.

Peer-reviewed articles in other international journals (1.2) and collections (3.1):

Kääd A., Valdmann A., **Eelsalu M.**, Pindsoo K., Männikus R., Soomere T. 2016. Preventive management of undesired changes in alongshore sediment transport in planning of waterfront infrastructure. In: Galiano-Garrigos A., Brebbia C.A. (eds.), *The Sustainable City XI: [Proceedings of the 11th International Conference on Urban Regeneration and Sustainability (SC 2016), Alicante, Spain]*. WIT Press, Ashurst Southampton, 419–430. (WIT Transactions on Ecology and the Environment; 204), doi: 10.2495/SC160361.

Pindsoo K., **Eelsalu M.**, Soomere T., Tõnisson H. 2014. An estimate of the impact of vessel wakes on coastal processes: a case study for Aegna, Estonia. 2014 In: *2014 IEEE/OES Baltic International Symposium, 26–29 May 2014, Tallinn, Estonia, Proceedings*, 9 pp., doi: 10.1109/BALTIC.2014.6887859.

Judge K., **Eelsalu M.**, Grünthal E., Talvik S., Ellmann A., Soomere T., Tõnisson H. 2014. Combining airborne and terrestrial laser scanning to monitor coastal processes. In: *2014 IEEE/OES Baltic International Symposium, 26–29 May 2014, Tallinn, Estonia, Proceedings*, 10 pp., doi: 10.1109/BALTIC.2014.6887874.

Eelsalu M., Org, M., Soomere T. 2014. Visually observed wave climate in the Gulf of Riga. In: *2014 IEEE/OES Baltic International Symposium, May 26–29.2014, Tallinn, Estonia*, 10 pp., doi: 10.1109/BALTIC.2014.6887829.

Articles published in other conference proceedings (3.4):

Eelsalu M., Pindsoo K., Soomere T. 2018. Interannual coastal processes in Estonia, Peraküla beach monitored by laser scanning technology. In: Köppen S., Reckermann M. (eds.), *2nd Baltic Earth Conference The Baltic Sea in Transition. Helsingør, Denmark, 11 to 15 June 2018, Conference Proceedings*. International Baltic Earth Secretariat Publication No 13, Geesthacht, Germany, 115–116.

Pindsoo K., **Eelsalu M.**, Soomere T. 2016. Spatial variation of statistical properties of extreme water levels along the eastern Baltic Sea. In: Reckermann M., Köppen S. (eds.), *1st Baltic Earth Conference Multiple drivers for Earth system changes in the Baltic Sea region: 13–17 June 2016, Nida, Curonian Spit, Lithuania; Conference Proceedings*. International Baltic Earth Secretariat Publication No 9, Geesthacht, Germany, 126–127.

Soomere T., **Eelsalu M.**, Pindsoo K. 2016. Water level extremes signal changes in the wind direction in the north-eastern Baltic Sea. In: Reckermann M., Köppen S. (eds.), *1st Baltic Earth Conference Multiple drivers for Earth system changes in the Baltic Sea region: 13–17 June 2016, Nida, Curonian Spit, Lithuania; Conference Proceedings*. International Baltic Earth Secretariat Publication No 9, Geesthacht, Germany, 132–133.

Soomere T., **Eelsalu M.**, Pindsoo K., Zujev M. 2013. Lessons from the almost seven decades of visual wave observations from the eastern Baltic Sea coast. In: Reckermann M., Köppen S. (eds.), *7th Study Conference on BALTEX: 10–14 June 2013, Borgholm, Island of Oland, Sweden, Conference Proceedings*, 91–92, (International BALTEX Secretariat Publication; 53).

Abstracts of conference presentations (5.2):

Eelsalu M., Männikus, R., Pindsoo, K., Soomere, T. 2018. In search for management options of shores of the City of Tallinn, Estonia. In: *7th IEEE/OES Baltic Symposium Clean and Safe Baltic Sea and Energy Security for the Baltic countries, 12–15 June 2018, Klaipėda, Lithuania, Abstract book*, 27.

Kovaleva O., Soomere T., **Eelsalu, M.** 2015. Comparison of the wave power for the open and sheltered segments of the Baltic Sea coast. *10th Baltic Sea Science Congress: Science and innovation for future of the Baltic and the European regional seas, 15–19 June 2015, Riga, Latvia, Abstract Book*, 210.

Kovaleva O., Soomere T., **Eelsalu M.**, Ryabchuk D. 2015. Determination of closure depths for sheltered areas of the eastern part of the Baltic Sea. *10th Baltic Sea Science Congress: Science and innovation for future of the Baltic and the European regional seas, 15–19 June 2015, Riga, Latvia, Abstract Book*, 233.

Eelsalu M., Soomere T., Pindsoo K., Lagemaa P. 2015. Ensemble approach for the projections of extreme water levels reveals bias in water level observations. *10th Baltic Sea Science Congress: Science and innovation for future of the Baltic and the European regional seas, 15–19 June 2015, Riga, Latvia, Abstract Book*, 85.

Pindsoo K., Soomere T., **Eelsalu M.**, Tõnisson H. 2015. Quantification of the impact of vessel wakes on a shingle-gravel beach. *10th Baltic Sea Science Congress: Science and innovation for future of the Baltic and the European regional seas, 15–19 June 2015, Riga, Latvia, Abstract Book*, 201.

Mingėlaitė T., **Eelsalu M.**, Pindsoo K., Soomere T., Dailidienė I. 2015. Return periods of extreme water levels along Lithuanian sea coast based on a simple ensemble of projections. *10th Baltic Sea Science Congress: Science and innovation for future of the Baltic and the European regional seas, 15–19 June 2015, Riga, Latvia, Abstract Book*, 238.

Pindsoo K., **Eelsalu M.**, Tõnisson H. 2014. An estimate of the impact of vessel wakes on coastal processes: a case study for Aegna, Estonia. *Measuring and Modeling of Multi-Scale Interactions in the Marine Environment: IEEE/OES Baltic Symposium 2014, May 26–29, 2014, Tallinn, Estonia, Abstract Book*, Tallinn, Tallinn University of Technology, 97.

Tõnisson H., Kont A., Suursaar Ü., Orviku K., **Eelsalu M.**, Pindsoo K., Suuroja S. 2014. Painted sediment experiments in studies of coastal processes. *The 12th Colloquium on Baltic Sea Marine Geology, Warnemünde, Germany, September 8–12, 2014*, 37.

Lagemaa P., **Eelsalu M.**, Pindsoo K., Soomere T. 2014. Properties of an ensemble of projections of extreme water levels near Tallinn. In: *Measuring and Modeling of Multi-Scale Interactions in the Marine Environment: IEEE/OES Baltic Symposium 2014, May 26–29, 2014, Tallinn, Estonia, Abstract Book*, Tallinn, Tallinn University of Technology, 64.

Pindsoo K., **Eelsalu M.**, Soomere T. 2014. Quantification of the impact of vessel wakes on the transport of coarse sediment. In: *Baltic Earth – Gulf of Finland Year 2014 Modelling Workshop “Modelling as a Tool to Ensure Sustainable Development of the Gulf of Finland-Baltic Sea Ecosystem”, Finnish Environment Institute, Helsinki 24–25 November 2014, Programme, Abstracts, Participants*. Geesthacht, Germany: Helmholtz-Zentrum Geesthacht, 16. (International Baltic Earth Secretariat Publication; 4).

Eelsalu M., Julge K., Grünthal E., Talvik S., Ellmann A., Soomere T., Tõnisson H. 2014. Combined laser scanning to monitor coastal processes. In: *MEME’2014: Mathematics and Engineering in Marine and Earth Problems, 22–25 July 2014, Aveiro, Portugal, Abstract Book*, 106–108.

Julge K., **Eelsalu M.**, Grünthal E., Talvik S., Ellmann A., Tõnisson H. 2014. Combining airborne and terrestrial laser scanning to monitor coastal processes. In: *Measuring and Modeling of Multi-Scale Interactions in the Marine Environment: IEEE/OES Baltic Symposium, May 26–29, 2014, Tallinn, Estonia*,

Eelsalu M., Soomere T. 2014. Intermittency of the wave energy flux in the eastern Baltic Sea. *MEME’2014: Mathematics and Engineering in Marine and Earth Problems, 22–25 July 2014, Aveiro, Portugal, Abstract Book*, 133–135.

Eelsalu M., Julge K., Grünthal E., Ellmann A., Soomere T. 2014. Laser scanning reveals detailed spatial structure of sandy beaches. In: *IUTAM Symposium on Complexity of Nonlinear Waves: 8–12 September 2014, Tallinn. Book of Abstracts*. Institute of Cybernetics at Tallinn University of Technology, 91.

Pindsoo K., Soomere T., **Eelsalu M.**, Tõnisson H. 2014. Vessel wakes effectively transport gravel, cobbles and pebbles. In: *MEME’2014: Mathematics and Engineering in Marine and Earth Problems, 22–25 July 2014, Aveiro, Portugal, Book of Abstracts*, 103–105.

Other creative activities (6.3; 6.7):

Eelsalu M., Soomere T. 2016. Laineenergia ja selle kasutamise varjukülgedest Läänemeres (Wave Energy and Associated Problems in the Baltic Sea). *Põlevad ja mittepõlevad energiaallikad (Combustible and non-combustible energy resources)*, 16–19 [Summary in English].

Eelsalu M., Ellmann A., Julge K., Märdla S., Soomere T. 2014. Rannaprotsesside anatoomia laserskaneerimise skalpelliga. In: Aan A., Narusk K. (eds.), *Kaugseire Eestis*, 47–58, Tallinn: Keskkonnaagentuur.

Soomere T., Pindsoo K., **Eelsalu M.** 2016. Veetasemete ekstreemumid ja korduvusperioodid Eesti rannikul. Research report [Tallinn]: Tallinna Tehnikaülikooli Küberneetika Instituut. [In Estonian].

Soomere T., **Eelsalu M.**, Pindsoo K. 2014. Rannasetete bilanss Miidurannast Tallinna Vanasadamani. Tallinn: Tallinna Tehnikaülikooli Küberneetika Instituut.

Soomere T., Pindsoo K., **Eelsalu M.** 2013. Kopli lahe suudmes esinevate kõrgete veetasemete tõenäosuse ja korduvuse hinnang, 30 pp. Tallinn: Tallinna Tehnikaülikooli Küberneetika Instituut.

Elulookirjeldus

Isikuandmed

Ees- ja perekonnanimi	Maris Eelsalu
Sünniaeg ja -koht	20.10.1988, Virtsu, Eesti
Adress	Akadeemia tee 21, 12618 Tallinn, Eesti

Kontaktandmed

Telefon	(+372) 559 333 09
E-mail	Maris.Eelsalu@taltech.ee

Hariduskäik

Õppeasutus	Lõpetamise aeg	Haridus (eriala / kraad)
Tallinna Tehnikaülikool	2013	Maateadused / magister
Eesti Mereakadeemia	2011	Hüdrograafia / rakenduskõrgharidus

Keelteoskus

Keel	Tase
eesti	emakeel
inglise	kõrgtase
hispaania	algtase

Täiendõpe

Õppimise aeg	Täiendõppe läbiviija nimetus
Veebruar 2016	Kursus <i>Process modelling of natural hazards</i> (Enschede, Holland)
August–September 2015	Kahekuuline visiit James Cooki Ülikooli Austraalias, kursused <i>Coastal and Catchment Geomorphology</i> ja <i>Coastal management</i> (Townsville, Austraalia)
November 2014	Intensiivkursus <i>Wave dynamics and coastal processes</i> (Klaipėda Ülikool, Leedu)
November 2013	LIDAR andmetöötlus kursus (Tallinn, Estonia)
September 2011	Rahvusvaheline suvekool <i>Practical training course in Marine science in Estonia and Finland</i> (Seili, Soome)

Teenistuskäik

Töötamise aeg	Tööandja nimetus	Ametikoht
September 2013–tänapäevani	Tallinna Tehnikaülikool, küberneetika instituut	Nooremteadur
Aprill 2012–September 2013	Tallinna Tehnikaülikooli Küberneetika Instituut	Tehnik

Teadustegevus

Avaldatud teadusartiklite ja konverentsiteeside ning peetud konverentsiettekannete loetelu on toodud ingliskeelse CV juures.